

**A Systems Approach to Characterize Drivers of Vaginal Microbiome Composition and Bacterial
Vaginosis Treatment Efficacy**

by

Christina Y. Lee

A dissertation submitted in partial fulfillment
of the requirements for the degree of
Doctor of Philosophy
(Biomedical Engineering)
in the University of Michigan
2023

Doctoral Committee:

Associate Professor Kelly Arnold, Chair
Associate Professor Sriram Chandrasekaran
Professor Denise Kirschner
Professor Xiaoxia Nina Lin
Professor Deepak Nagrath

Christina Y. Lee

chyylee@umich.edu

ORCID iD: 0000-0002-9393-2178

© Christina Y. Lee 2023

Acknowledgments

Special thanks to my committee and my advisor, Dr. Kelly Arnold, who provided thoughtful feedback and supported me throughout my time at the University of Michigan. I would also like to thank Dr. Amy Chung, whom I had the pleasure to work with on projects outside of my dissertation studies and who kept Melissa, Suzie, and me going in the early days of the COVID-19 pandemic. I would like to thank Kat for always being there since the beginning of our PhD journey, as well as Katy and Melissa who provided wonderful guidance during and after finishing their PhDs. Thank you to Suzie and Robbie, who always were happy to socialize in and outside of the lab and thank you to Sina and Kade who were fun additions to the group as I wrapped up my studies.

I would also like to thank my family, especially my mom and dad who have always encouraged me to pursue what I am passionate about and got me to this major milestone in my life. Thank you to my twin brother, Jason, who always knew how to keep perspective on this time in my life. Thank you to my partner, Kevin, who kept me grounded throughout my PhD and got me a puppy to keep me company as I had to work from home alone. Thank you to that puppy, Entei, for supervising the writing of this dissertation.

Lastly, thank you to the Rackham Graduate School for providing funding from the Rackham Merit Fellowship as well as providing funding for my internship through the Rackham Doctoral Intern Fellowship Program.

Table of Contents

Acknowledgments.....	ii
List of Tables	viii
List of Figures.....	ix
Abstract.....	xii
Chapter 1 Introduction	1
1.1 The Vaginal Microbiome	1
1.2 The Ecosystem of the Vaginal Microbiome.....	5
1.3 Therapies for Bacterial Vaginosis	9
1.4 Systems Biology and the VMB.....	12
1.5 Structure of Thesis.....	18
Chapter 2 Quantitative Modeling Predicts Mechanistic Links between Pre-treatment Microbiome Composition and Metronidazole Efficacy in Bacterial Vaginosis.....	21
2.1 Attributions.....	21
2.2 Abstract	21
2.3 Introduction	22
2.4 Results	24
2.4.1 The model predicts Lactobacillus MNZ sequestration influences efficacy	24
2.4.2 Model validation in Gv and Li co-cultures.....	28
2.4.3 Optimal MNZ doses are dependent on pre-treatment microbiome	30
2.4.4 Initial composition influences efficacy in more complex models.....	32
2.4.5 Pre-treatment composition is associated with clinical outcome.....	35

2.5 Discussion	38
2.6 Methods	42
2.6.1 Bacterial Strains and Culture Conditions	42
2.6.2 Metronidazole Quantification by Tandem Mass Spectrometry	42
2.6.3 Bacterial Quantification	43
2.6.4 Bacteria-MNZ experiments	44
2.6.5 ODE Models	44
2.6.6 Model Simulations and Validation	45
2.6.7 Generalized Models and Global Sensitivity Analysis	45
2.6.8 Software	50
2.6.9 Clinical data and study population	50
2.6.10 Analysis of Clinical Outcomes	51
2.7 Appendix	53
2.7.1 Supplementary Figures	53
2.7.2 Supplementary Tables	62
2.7.3 Supplementary Equations	64
Chapter 3 Evaluation of Vaginal Microbiome Equilibrium States Identifies Microbial Parameters Linked to Resilience after Menses and Antibiotic Therapy	66
3.1 Attributions	66
3.2 Abstract	66
3.3 Introduction	67
3.4 Results	71
3.4.1 The model reveals the potential for the VMB to exist in mono-stable or multi-stable states depending on microbial parameters that vary across individuals	71
3.4.2 Mono-stability is driven by specific interspecies interaction terms	75

3.4.3 Equilibrium subpopulations may explain variability in temporary vs. sustained CST switches observed from menses	77
3.4.4 BV clearance responses after antimicrobial therapy are associated with equilibrium behavior subtype.....	82
3.4.5 Combinatorial therapies and modified treatment duration demonstrate alternative strategies to treat BV	85
3.5 Discussion	87
3.6 Methods.....	91
3.6.1 Model Construction	91
3.6.2 Parameter Selection	92
3.6.3 Base in silico Population	93
3.6.4 Bifurcation Analyses	93
3.6.5 Perturbation Analyses.....	94
3.6.6 Clinical Datasets.....	95
3.6.7 Code and Data Availability	97
3.7 Appendix	98
3.7.1 Supplementary Figures.....	98
3.7.2 Supplementary Tables	103
3.7.3 Supplementary Text.....	105
Chapter 4 An <i>in silico</i> Framework for Rational Design of Vaginal Probiotic Therapy	107
4.1 Attributions.....	107
4.2 Abstract	107
4.3 Introduction	108
4.4 Results	110
4.4.1 Simulated probiotic strains result in variable response types across a virtual population	110

4.4.2 Sensitivity analyses reveal alternative probiotic characteristics that can improve probiotic strain efficacy	113
4.4.3 Combinatorial regimens can lower BV recurrence rates.....	116
4.4.4 Adjunctive antimicrobial therapy improves probiotic strain efficacy for underperforming strains.....	119
4.4.5 Lactin-V efficacy is moderately dependent on probiotic dosing frequency.....	122
4.5 Discussion	123
4.6 Methods.....	127
4.6.1 Model Construction	127
4.6.2 Virtual Population Development.....	128
4.6.3 BV Treatment Regimens	128
4.6.4 Local Sensitivity Analysis	129
4.6.5 Systematic Probiotic Strain Selection	130
4.6.6 Statistical Analyses.....	131
4.6.7 Code and Data Availability	131
4.7 Appendix	131
4.7.1 Supplementary Tables	131
4.7.2 Supplementary Figures.....	137
Chapter 5 Discussion and Conclusion	141
5.1 Concluding Remarks	141
5.1.1 Model Predicts Importance of Pre-treatment Composition on Treatment Efficacy... ..	141
5.1.2 Compositional States of VMB Demonstrate Mono- and Multi-Stability.....	144
5.1.3 Probiotic Strain Efficacy is Driven by Resident Community Characteristics.....	147
5.2 Future Work	149
5.2.1 Validation in Controlled Systems.....	150
5.2.2 Resolution of Interspecies Interactions	152

5.2.3 Incorporation of Vaginal Epithelium.....	157
5.2.4 Incorporation of Biofilms.....	160
Bibliography	162

List of Tables

Table 1.4.1 Comparison of microbiome characteristics	13
Table 2.7.1 Parameters for two species model.	62
Table 2.7.2 Parameter ranges used to simulate intra-species variability.	63
Table 2.7.3 Inter-species interaction terms.	63
Table 2.7.4 UMB-HMP cohort data.	63
Table 2.7.5 CONRAD BV cohort data.	64
Table 3.7.1 Description of LHS parameter ranges.	103
Table 3.7.2 Model CST centroids.	103
Table 3.7.3 Examples of how external factors can be simulated in the modeling framework. ..	104
Table 3.7.4 Digitized decay rates of BV associated bacteria treated with intravaginal metronidazole.....	104
Table 4.7.1 Explanation of LHS parameter ranges.	131
Table 4.7.2 Calculated antibiotic impact on BV-associated bacteria (nAB).	132
Table 4.7.3 Clinical probiotic regimens.....	133

List of Figures

Figure 1.1.1 Amsel criteria and relationship with vaginal microbiota. Modified from Coleman and Gaydos, 2018.....	4
Figure 1.4.1 Overview of systems biology techniques applied to the vaginal microbiome.	16
Figure 1.4.2. Vaginal microbiome ecological interactions translated to generalized Lotka-Volterra interspecies interaction terms.	18
Figure 2.4.1 Model schematic for bacterial growth dynamics in BV with MNZ treatment.	25
Figure 2.4.2 A higher initial Gv:Li ratio improves MNZ treatment efficacy.	27
Figure 2.4.3 Initial Gv:Li ratios dictate final microbial populations.	31
Figure 2.4.4 High pre-treatment BV:LB ratio is predicted to reduce MNZ efficacy in more complex microbial environments regardless of strain variability.	33
Figure 2.4.5 Increased initial BV:LB ratios associated with successful treatment of BV.....	36
Figure 2.7.1 Kinetic data for parameterization of MNZ interactions with <i>L. iners</i> and <i>G. vaginalis</i>	53
Figure 2.7.2 Model parameterization of growth dynamics with and without MNZ.	54
Figure 2.7.3 <i>L. iners</i> 1D sensitivity analysis.....	56
Figure 2.7.4 Comparison of model predictions with observed levels of MNZ and metabolites. .	57
Figure 2.7.5 <i>L. iners</i> susceptibility to MNZ does not influence Gv:Li ratio dependent MNZ efficacy.....	58
Figure 2.7.6 : BV:LB ratios influence endpoint BV-associated bacteria and <i>Lactobacillus</i> spp. abundances even with strain variation.	59
Figure 2.7.7 Uptake or Sequestration of <i>Lactobacillus</i> spp. with MNZ drives initial BV:LB ratio influence of MNZ efficacy.....	60
Figure 2.7.8 Initial relative abundance data for <i>L. iners</i> and <i>G. vaginalis</i> for clinical outcomes. 61	
Figure 3.4.1 Mathematical model of vaginal community state types.	72
Figure 3.4.2 Assessment of parameters that drive multi-stable vs mono-stable states.	76

Figure 3.4.3 Bifurcation analysis to explore menses-associated parameter alterations.....	78
Figure 3.4.4 Menses-associated compositional fluctuations in silico and in clinical samples.	80
Figure 3.4.5 Bifurcation analysis to explore the impact of antibiotics on nAB dominated communities.....	82
Figure 3.4.6 Predicted and clinically observed antibiotic response types.	83
Figure 3.4.7 Simulated antibiotic regimens.....	85
Figure 3.7.1 Analysis of Inter-species/Self-interaction Parameter Ranges.	98
Figure 3.7.2 Determination of Clinical Equilibrium Behavior Subtypes.	99
Figure 3.7.3 Generating matched in silico populations to clinical data.....	100
Figure 3.7.4 Menses simulations at varying degrees of simulated strength for oLB dominated states.....	101
Figure 3.7.5 Menses simulations at varying degrees of simulated strength for Li dominated states.....	102
Figure 4.4.1 Overview of probiotic strain modeling.....	111
Figure 4.4.2 Local sensitivity analysis of probiotic characteristics.....	114
Figure 4.4.3 Selection of optimal probiotics.....	115
Figure 4.4.4 Adjunctive antimicrobial therapy versus probiotic or antibiotic therapies in isolation.....	117
Figure 4.4.5 Drivers of population level composition alterations for a short-term regimen and Lactin-V regimen.....	120
Figure 4.4.6 Comparison of Lactin-V regimen with the short-term probiotic only regimen.	121
Figure 4.4.7 Impact of alternative dosing frequency on predicted BV recurrence rates.	122
Figure 4.7.1 Overview of analysis methodology.....	137
Figure 4.7.2 Four parameter local sensitivity analysis.	137
Figure 4.7.3 Lactin-V phase 2b clinical trial versus model simulations with increased antibiotic effect.	138
Figure 4.7.4 Parameter values for strains that could elicit consistent population-level compositional changes for a short-term regimen.....	139

Figure 4.7.5 Parameter values for strains that could elicit consistent population-level compositional changes with the Lactin-V regimen. 139

Figure 4.7.6 Comparison short-term probiotic only regimen top strains with Lactin-V regimen. 140

Figure 5.2.1 Comparison of gLV interspecies interaction term versus modeling with a chemically-mediated interaction for the competition for a growth limiting carbon source. 153

Abstract

The vaginal microbiome (VMB) is critical to female reproductive health, with *Lactobacillus* spp. dominance associated with health and a diverse, anaerobic community composition associated with a variety of adverse reproductive outcomes as well as increased susceptibility to sexually transmitted infections. This dysbiosis, known as bacterial vaginosis (BV), impacts nearly 30% of reproductive-age women. Therapies to treat this condition have largely remained the same over the last three decades despite the high frequency of recurrent cases. Difficulty in treating BV stems from several challenges such as there is not a single microbe causing the condition, complex ecological interactions between microbial species and the microenvironment dictate community composition and stability, and lack of adequate preclinical models to assess therapies. Ordinary differential equation (ODE)-based modeling can help capture these complexities and model the dynamics and stability of multi-species communities to better characterize key drivers of composition shifts to BV-associated communities and in response to therapies aimed to re-establish optimal composition.

Here, we established a series of mathematical models to help address key aspects of modeling the vaginal microbiome and the impact of BV therapies. In the first aim, a novel multi-species model was developed to replicate shifts between BV-associated bacteria and optimal composition (*Lactobacillus* spp. dominance) after treatment with a standard-of-care antibiotic, metronidazole. This model captured microbial metabolism by the target microbial species, *G. vaginalis*, and sequestration of metronidazole by the non-target species, *Lactobacillus iners*. Using this model, sensitivity analyses indicated that a key driver in antibiotic efficacy was the

pre-treatment ratio of *G. vaginalis* relative to *L. iners*. Counterintuitively, the model associated higher amounts of *L. iners* relative to *G. vaginalis* with worse treatment outcomes due to *L. iners* sequestering metronidazole to an extent that reduced the amount that could inhibit *G. vaginalis* growth. This association was validated with *in vitro* co-cultures and in two small clinical cohorts.

In the second aim, we used a model to understand the stability of VMB community state types and to identify specific microbial interactions that drive variability in stability. For this approach, we used a generalized Lotka-Volterra model, which predicts community composition as a function of pairwise interspecies interactions, microbial growth rates, and carrying capacities. Physiological parameter ranges were defined and used to generate virtual populations that predicted the frequency of mono- and multi-stable states observed across two clinical cohorts. Virtual populations were refined and then validated for community composition changes during and after menses and antibiotic therapies in separate clinical cohorts. The virtual population emphasized the importance of how BV-associated bacteria interact with *Lactobacillus* spp. for maintaining or reestablishing *Lactobacillus* spp. dominance.

Lastly, in aim 3 a similar approach using virtual populations was applied to the assessment of optimal probiotic characteristics for treating BV. The model explored two dosing regimens, an acute probiotic regimen and a regimen described for a phase 2b clinical trial of Lactin-V. Simulations supported that both resident *Lactobacillus* spp. and BV-associated bacteria interactions with probiotics could significantly impact probiotic efficacy, and thus should be an additional probiotic screening criterion. Model predictions exhibited similar population-level recurrence frequencies as observed in the Lactin-V trial and allowed for exploration of the relationship between probiotic strain characteristics and dosing regimens.

Overall, these three aims describe new frameworks to help explore and design new BV therapies that otherwise would be difficult to study *in vitro* or preclinically.

Chapter 1 Introduction

1.1 The Vaginal Microbiome

The vaginal microbiome (VMB) is centrally involved in female reproductive health, impacting fertility [1–3], pregnancy [4–9], pelvic inflammatory disease [1,10,11], as well as fungal, urinary, and sexually transmitted infections [12–17]. The VMB has also been implicated in heterogeneous drug efficacy, as certain VMB species metabolize therapeutic compounds to reduce bioavailability [18–20]. Despite these critical associations between the VMB and women's health, it has been challenging to identify mechanisms that link VMB composition and function to physiological outcomes due to the multitude of species that contribute to these conditions and the dynamic nature of the VMB. At a high level, an optimal composition is defined as having a *Lactobacillus* spp.-dominant homogenous community structure, whereas shifts to a polymicrobial anaerobic community structure are associated with negative reproductive outcomes and a common condition known as bacterial vaginosis (BV) [21,22].

Linking VMB composition with health outcomes was revolutionized by using a community grouping method that was first described by Ravel et al. (2011) called community state types (CST) [21]. The CST or the community grouping method helped simplify the hundreds of species in the VMB to five core compositional profiles, allowing VMB to be more easily associated with host characteristics and health outcomes [21]. CSTs were first determined using complete linkage hierarchical clustering, which is an unsupervised data-driven method that identified the five commonly accepted CSTs: CST-I (*L. crispatus* dominated), CST-II (*L. gasseri* dominated), CST-III (*L. iners* dominated), CST-IV (diverse group), and CST-V (*L. jensenii*

dominated). The observations that Ravel et al. reported with CSTs aligned with previous studies that analyzed a group of healthy Caucasian and Black women as well as with a study that characterized a group of Japanese women [23–25]. By stratifying patient populations with CSTs, VMB composition was linked with race/ethnicity, pH, and Nugent scores (assessment for clinical BV). Notably, healthy Hispanic and Black women tended to be overrepresented in the diverse CST group which is correlated with higher pH and BV-associated Nugent scores (an “unhealthy” VMB). This observation raised questions on the common assumption that *Lactobacillus* spp. dominated communities are required to be healthy.

CSTs have also been used to understand the relationship between the composition and temporal dynamics of the VMB [22]. One of the earliest studies that explored temporal variability in composition was Gajer et al. (2012) [22]. In this study, samples were collected twice weekly for 16 weeks (n = 32 women) and hierarchical clustering with silhouette values was used to classify each sample as a CST. This study then analyzed stability in terms of a normalized Jensen-Shannon divergence index as well as the frequency of transitions between CSTs across time points. The normalized Jensen-Shannon divergence index captured the differences between pairs of CSTs by calculating the median of Jensen-Shannon distances, with lower values indicating stability. Notably, the results supported two interesting findings: (1) the VMB could be stable and exhibit consistently high, BV-associated, Nugent scores and (2) the VMB could exhibit instability and have consistently low Nugent scores (healthy). These two findings suggested that variation in composition over time did not always equate to non-optimal VMB composition. When the data were analyzed by calculating the transitions between CSTs, CSTs associated with *L. crispatus* or *L. gasseri* dominance were most stable. In contrast, CSTs associated with *L. iners* dominance had more variable stability trends with some subjects stable

over time and others undergoing transitions to a variety of CSTs. To understand possible drivers of CST transitions a linear mixed effects model adjusted for several host factors was used, which revealed that bacterial communities tended to lack stability during menses and stability corresponded with estradiol and progesterone concentration.

Recently, there was a new methodology proposed to update how CSTs are determined so that it can be more consistently applied across different studies using a nearest centroid classification method [26]. Previously, CSTs were specific to each dataset due to the nature of hierarchical clustering, which depends on the relative similarity to the samples included in a study. The newly proposed methodology, VALENCIA (VAGinal community state type Nearest Centroid clAssfier), overcomes this barrier by using an internal reference composition that was generated from 13,160 taxonomic profiles from 1,975 women in the United States [26]. This study additionally was able to characterize further subclasses to the original CSTs, especially the diverse group CST-IV where it is possible for non-*Lactobacillus* spp. to dominate the community such as *Streptococcus*, *Enterococcus*, *Bifidobacterium*, and *Staphylococcus*, some of which were not accounted for when Nugent scoring was designed to diagnose BV.

Non-optimal VMB states are associated with an altered vaginal microbiota including an increase in a diverse array of facultative and obligate anaerobes, frequently linked with cases of bacterial vaginosis (BV). BV is a condition that affects nearly one-third of reproductive-age women in the United States and common symptoms are an increase in vaginal pH, abnormal discharge, vaginal discomfort, and a fish-like odor which altogether can have a mild to severe impact on the quality of life [27–29]. BV is most commonly diagnosed using Amsel criteria, which are four parameters that capture symptoms of BV including (i) thin, white, yellow, homogenous discharge (ii) clue cells on wet mount microscopy (iii) vaginal fluid pH over 4.5

(iv) release of fishy odor when mixed with 10% potassium hydroxide solution (“whiff test”, Figure 1.1.1) [30]. Traditionally, three of the four criteria were required for diagnosis, but more recently this requirement has been relaxed to two of the four for diagnosis [31]. The gold standard methodology to diagnose BV is Nugent scoring, which is less commonly used because it requires a physician that is highly skilled at microscopy. The Nugent scoring system uses Gram staining of vaginal smears to examine the counts of *Lactobacillus*, *Gardnerella*, and curved Gram-variable rods resulting in a score of 0-10, where 0-3 is negative for BV, 4-6 is intermediate, and 7+ is positive for BV [32]. Although more complex, Nugent scoring is reported to have similar diagnosing power to Amsel criteria [33]. Recent shifts in diagnostics are focusing on capturing the composition of vaginal microbes using molecular methods such as 16S rRNA qPCR or sequencing. Basing a BV diagnosis based on sequencing that captures vaginal microbiome composition is referred to as molecular BV [34,35].

Understanding shifts between optimal and non-optimal VMB compositional states has been the focus of recent VMB research yet is limited due to the complex interactions between host physiology, behavior, and microbial ecology [36–41]. For example, longitudinal studies

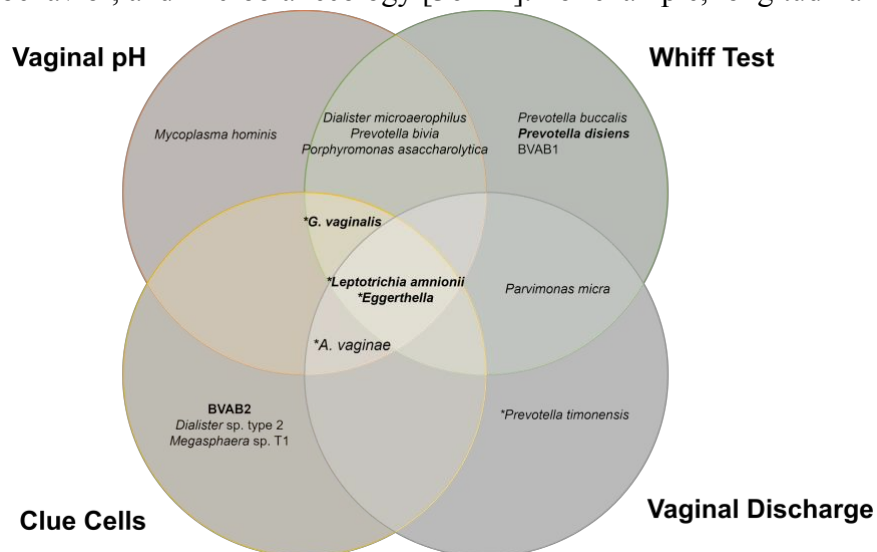


Figure 1.1.1 Amsel criteria and relationship with vaginal microbiota. Modified from Coleman and Gaydos, 2018.

have demonstrated that menses-related hormone changes are associated with fluctuations in

community composition and that the base community state type is associated with stability [22]. Additionally, hormonal birth control is associated with reduced susceptibility to BV compared to no contraceptives or copper intrauterine devices [39]. Pregnancy, which is also associated with hormonal shifts, has reported concomitant shifts in vaginal microbiome composition to be *Lactobacillus* spp. dominated, which is more pronounced in women of African descent [40]. Other studies have linked hygienic behaviors such as douching with shifts to non-optimal states [36]. In addition to these host factors, microbial inter-species interactions (through competition for vaginal microenvironment substrates) and antagonism (through the production of toxins by VMB) further complicate understanding of community composition and function and motivate the implementation of new analytical techniques [42–45].

1.2 The Ecosystem of the Vaginal Microbiome

The vagina hosts a diverse mucosal ecosystem. At the core of this ecosystem are vaginal epithelial cells, which form a stratified squamous non-keratinized epithelium covered by a mucosal layer with commensal bacteria bathed in cervicovaginal fluid [46]. The contents of the cervicovaginal fluid can change dramatically given the composition of the vaginal microbiome as well as the hormonal and inflammatory state of the vagina. For example, the menstrual phase has associated shifts in hormones, such as oestradiol and progesterone concentrations. During menstruation, there are lower levels of oestradiol and progesterone that are associated with lower levels of glycogen, IgA, and IgG [47]. In the proliferative phase, oestradiol increases alongside glycogen levels and then drops again post-ovulation in the secretory phase. Glycogen is believed to be one of the main carbon sources in the vagina, and higher levels of free glycogen are associated with *Lactobacillus* spp. dominated communities [48]. In addition to glycogen, mucus

produced in the cervix is hypothesized to also be a nutrient source full of proteins, lipids, and glycoproteins known as mucins [49].

The interplay between microbial species and their environment also impacts vaginal ecology [41]. For example, *L. crispatus*, *L. gasseri*, and *L. jensenii*-dominated communities are considered the most beneficial and stable from maintaining a low pH environment and producing antimicrobial compounds [50]. Antimicrobial compounds associated with maintaining *Lactobacillus* dominance include bacteriocins, surfactants, hydrogen peroxide, and lactic acid. In the 1990s, a popular belief was that hydrogen peroxide was the main driver of antimicrobial activity by *Lactobacillus* spp., which later met criticism because the molecular oxygen level *in vivo* is low (15 – 35 mmHg) and the cervicovaginal microenvironment is hypoxic [51]. The reducing capabilities of cervicovaginal fluid are reported to additionally inactivate hydrogen peroxide *in vivo* [52]. Thus, due to the oxidative state, lactic acid would be predominantly produced via the fermentation of polysaccharides [53]. Lactic acid is not only associated with lower vaginal pH, but also anti-inflammatory properties on cervicovaginal epithelial cells, and at physiological levels inhibited 17 BV-associated bacterial species in contrast to supra-physiological levels of hydrogen peroxide that only inhibited one of the evaluated BV-associated bacterial species [54]. Lower pH also is reported to aid the inhibitory effect of lactic acid and some bacteriocins are also more effective at low pH [55,56]. The polysaccharides needed to produce lactic acid are associated with glycogen and glycogen derivatives present in the vaginal microenvironment. Traditionally, it was believed that *L. crispatus* was dependent on amylases to break down glycogen in the vaginal microenvironment, but recent studies support that some *L. crispatus* strains can directly metabolize glycogen [57,58]. Metabolic variability is also likely tied to the variability observed in inhibiting BV-associated bacteria, as the production of lactic

acid is a core to the inhibition. For example, the ability of *Lactobacillus* spp. to inhibit BV-associated bacteria is reported to be strain dependent, with some strains able to have near total inhibition of BV-associated bacteria over the course of 4 hours while other strains had little to no effect [55].

In contrast, *L. iners*-dominated communities are more commonly associated with bacterial vaginosis than *L. crispatus*, *L. jensenii*, and *L. gasseri*. One explanation for the association of *L. iners* with BV is the observation that certain strains of *L. iners* can facilitate the adhesion and growth of a microbe commonly associated with bacterial vaginosis, *Gardnerella vaginalis* [59]. This observation is consistent with *in vitro* findings that support that *L. iners* does not produce the core health-associated compounds that the other three *Lactobacillus* spp. produce such as D-lactic acid and bacteriocins. Thus, due to the potential for *L. iners* to mediate the growth of BV-associated bacteria, recent efforts to develop selective *L. iners* inhibitors are of interest and include identification of *L. iners*-specific bacteriocins or capitalizing on unique metabolic requirements for *L. iners* growth, such as *L. iners* cysteine dependence [60,61]. *L. iners* also has a much smaller genome (~1.3 Mbp) than other *Lactobacillus* spp., which aligns with a parasitic and host-dependent lifestyle [62]. Additionally, *L. iners* exhibits a few characteristics that may promote the ability to adapt rapidly to changes in the vaginal microenvironment by unique mechanisms to obtain nutrients. For example, *L. iners* can produce a cholesterol-dependent cytolysin, inerolysin, which is active under acidic conditions and can lyse vaginal epithelial cells, increasing nutrients in the vaginal microenvironment [63,64]. Another unique characteristic is associated with PG synthesis and hydrolysis, which increases the absorption of nutrients compared to other *Lactobacillus* spp. [65]. Altogether, these adaptations

could help explain the ability of *L. iners* to coexist in both *Lactobacillus* spp. dominated communities and BV-associated bacteria dominated communities.

Lastly, non-optimal or BV-associated communities are linked with many facultative and strict anaerobes such as *Gardnerella*, *Atopobium*, *Prevotella*, *Peptostreptococcus*, *Mobiluncus*, *Sneathia*, *Leptotrichia*, and *Mycoplasma* [66–68]. Notably, an overgrowth of non-*Lactobacillus* spp. does not always result in symptomatic BV, which is more common in women of African or Hispanic heritage [21]. One of the most common species associated with BV is *G. vaginalis*, which has several strains with distinct characteristics (sialidase activity, antibiotic resistance, gene sequences) that are now defined into new species (*G. piotti*, *G. swidsinkii*, *G. leopoldii*) [69]. *Gardnerella* spp. produce a cholesterol-dependent cytolysin, vaginolysin, that can lyse vaginal epithelial cells, breaking down the mucosal barrier, increasing inflammation, and significantly altering the nutritional environment [63,70,71]. BV-associated bacteria are believed to mutually benefit species in the community through a variety of mechanisms, such as biofilm formation, cross-feeding, or acid tolerance mechanisms [72–75]. For example, *Mobiluncus* spp. generate biogenic amines that raise vaginal pH levels, which benefit species that do not produce biogenic amines like *G. vaginalis* [76]. Biogenic amines also are reported to impact the growth characteristics of *Lactobacillus* spp. such as lag time, growth rates, and lactic acid production [75]. Another example of cooperation is reported between four strains of *G. vaginalis* and six strains of *P. bivia*, where these two species exhibited cross-feeding between ammonia and amino acid metabolism and production [74]. Altogether, the diversity associated with BV-associated bacteria and the complex ecological interactions these species have with each other and *Lactobacillus* spp. contribute to challenges associated with understanding BV pathogenesis and additionally, treatment failure, discussed further next.

1.3 Therapies for Bacterial Vaginosis

First-line treatment regimens for BV include antibiotics with broad-spectrum anaerobic coverage, such as metronidazole (MNZ) and clindamycin. Dosing is typically over 5-7 days and includes both oral and intravaginal routes of administration such as a 7-day course of oral MNZ (500 mg, twice daily), a 7-day course of intravaginal clindamycin cream (2%, once daily), or a 5-day MNZ gel (0.75%, once daily) [77]. Treatment with these antibiotics is aimed at decreasing the overgrowth of the polymicrobial anaerobic bacteria associated with BV and facilitating the restoration of a *Lactobacillus* spp.-dominated microbiota. However, treatment outcomes remain suboptimal and exhibit variable responses ranging from no, delayed, or transient clearance of the polymicrobial anaerobic microbiota associated with BV [78]. Transient clearance, where initially women respond to antibiotic therapy and later experience another episode, is a hallmark of BV, occurring within 12 months for greater than 50% of women who undergo antibiotic therapy [77,79–81].

Immediately after antibiotic therapy, there is a reported 80% cure rate for BV [82,83]. For women who do not respond to therapy, there are a few potential mechanisms recognized such as inherent resistance of BV-associated bacteria or that biofilms may be limiting penetration of antibiotics to target microbes. *In vitro* studies support that some strains of *G. vaginalis* can be resistant to antibiotics, with a study on 50 strains of *G. vaginalis* reporting 68% were resistant to MNZ and 24% resistant to clindamycin [84]. Another common microbe present during episodes of BV, *Atopobium vaginae*, also has documented intrinsic resistance to MNZ [85,86]. Other studies report that antimicrobial susceptibility varies by culture type, with planktonic cultures more sensitive to antibiotics than biofilms. For MNZ, biofilm-forming isolates had a 10-fold higher MIC than planktonic isolates ($7.3 \pm 2.6 \mu\text{g/mL}$ vs. $72.4 \pm 18.3 \mu\text{g/mL}$; $p = 0.005$).

Clindamycin followed similar trends, where biofilm-forming *G. vaginalis* isolates had a MIC of 23.7 ± 9.49 $\mu\text{g/mL}$ compared to 0.099 ± 0.041 $\mu\text{g/mL}$ of planktonic isolates [87]. While clindamycin may seem like a better option to eradicate *G. vaginalis in vitro*, *Lactobacillus* spp. also are reported to be more sensitive to clindamycin, whereas MNZ typically has little to no effect on *Lactobacillus* spp. [88]. The resilience of BV-associated bacteria may be jointly associated with how *Lactobacillus* spp. interact with antibiotics aimed at decreasing BV-associated bacteria, as the impact of MNZ is hypothesized to be impacted by redox states within the vaginal microenvironment [89,90], with aerobic bacteria known to decrease levels of MNZ and efficacy for the treatment of *Trichomonas vaginalis* [91].

As suffering from repeat BV episodes is extremely common, developing new strategies to combat BV is of interest. One option for individuals experiencing repeat episodes of BV is a longer course of antibiotics, such as intravaginal metronidazole gel twice a week for 4-6 months. For recurrent BV, which is defined as having three or more episodes of BV within a year, maintenance therapy is recommended, which includes both long-term dosing of intravaginal MNZ gel and intravaginal boric acid. This regimen follows a course of antibiotics for 21-30 days, and boric acid a few times a week. Boric acid is believed to help disrupt the biofilm associated with BV and allow antibiotics to better access BV-associated bacteria; however, the mechanism of action is not well characterized [92]. Other biofilm-disrupting agents are in consideration for new therapies such as intravaginal boric acid enhanced with ethylenediaminetetraacetic acid (TOL-463), amphoteric tenside (WO3191), and pHyph (glucono-delta-lactone and sodium gluconate) [93–95]. TOL-463 completed a Phase 2 clinical trial in 2019 demonstrating safety and tolerance for BV. WO3191 is undergoing study for safety, tolerability, and efficacy and was based on *in vitro* results that supported that amphoteric tenside

could disrupt existing *G. vaginalis* biofilms [96]. In contrast, pHyph, which is hydrolyzed to gluconic acid in the vaginal microenvironment, has demonstrated in preclinical studies the ability to re-establish optimal pH, inhibit biofilm formation and remove established biofilms, as well as inhibit the growth of BV-associated bacteria [93,97]. Treatments aimed at lowering pH using compounds like lactic acid have had mixed results, and unlike boric acid, are not recommended for treating BV [98].

Live Biotherapeutic Products, more commonly referred to as probiotics, as well as vaginal microbiome transplantation (VMT) are proposed alternatives or combinational options to promote lasting treatment for BV [99,100]. Clinical trials have yielded promising, but mixed results for the use of these therapies for a variety of reasons including: the selection of strain(s) to be administered, administration method (oral or intravaginal, applicator formulations), whether the probiotic is administered in combination or sequentially with prebiotics or antibiotics, and a variation in time points during evaluation of intervention [80]. Until recently, a significant number of formulations included *Lactobacillus* spp. from the gut microbiome, which demonstrate markedly different phenotypic characteristics such as preferred carbon sources and microenvironment pH [57,101]. One of the most promising and well-designed studies uses a vaginal *Lactobacillus* spp., *L. crispatus* CTV-05 (LACTIN-V), which exhibited significantly decreased recurrence and increased *Lactobacillus* spp. colonization when administered intravaginally post-antibiotic treatment [102–104]. Several studies implement oral administration with the belief that either the impact on the gut microbiome will result in changes to the vaginal environment or that the probiotic strains will survive passage through the gastrointestinal tract and transfer to the vagina, which has exhibited limited success [105–107]. The few analyses assessing the importance of the route of administration suggest the intravaginal route may be

more effective as it allows for the strains to directly interact with the vaginal microbiome [108,109]. Lastly, many regimens include a pre-treatment with antibiotics aimed at increasing the likelihood that probiotic strains will colonize the microenvironment by reducing the species present that could impede probiotic growth.

Overall, developing new therapies for the vaginal microbiome presents unique challenges, as there are limited *in vitro* and animal models that satisfactorily recapitulate behaviors observed in the human vaginal microbiome [110]. Thus, the reliance on clinical samples presents unique challenges that arise from both host, microbiome, and temporal heterogeneity. The development of sophisticated experimental models, such as organ-on-a-chip systems, and *in silico* approaches will greatly benefit the study of new vaginal microbiome therapies [111].

1.4 Systems Biology and the VMB

Systems biology offers the ability to overcome some of the unique challenges presented by the VMB compared to other microbiome communities, especially its dynamic nature and lack of adequate experimental and clinical models (Table 1.4.1). For example, cross-sectional data, the most readily available data to study the microbiome, is best applied in scenarios where one time point is representative of an individual. This challenge is problematic for studying the VMB as it can shift between optimal and non-optimal compositional states over the course of a few days, which is a relatively rapid change compared to gut, skin, and oral microbiomes that are often stable in composition over the course of months to years [112,113]. Moreover, even healthy individuals can have a highly dynamic (unstable) VMB composition, specifically during menses when *Lactobacillus* spp. tend to decline [22,68,114]. Thus, the dynamic nature of the

VMB and BV means cross-sectional data should be used with caution presents a challenge not always associated with other, more stable microbiome sites [21,22,68,115].

Table 1.4.1 Comparison of microbiome characteristics

Site	Stability Associated with Health	Diversity & Health	Experimental Considerations	Human Sampling
Gut	Months to years, considered most stable [112]	Diversity is associated with health	Well-defined culture conditions and media; animal models share enough human physiological traits to be widely accepted tools	Non-invasive, stool samples, high bacterial load; many samples publicly available
Oral	Months to years, some reports of being more stable than skin[116,117]	Less diverse states are associated with health (subgingival)[117]	Less than half of species culturable using common anaerobic methods[118]; humanized murine models used	Relatively non-invasive, endodontic paper points or saliva, good bacterial load; trending to more data available
Skin	Months, up to 2 years[116,119]	High-diversity sites are less stable and diversity depends on skin site (foot, palm, etc.), overall healthy states are diverse [113]	80% of skin microbiota are culturable[120]; animal models exhibit more diversity[121]	Non-invasive, swabs and tape strips, primary source of samples for current studies good bacterial load; trending to more data available
Lung	Not well studied, considered to be more dynamic than the gut[122]	Limited knowledge of healthy microbiome, but is typically more diverse and distinct from diseased states	In vitro methods are not well defined; animal models are used but costly[123]	Invasive to collect (sputum, bronchial lavage or brushings) and has low bacterial load compared to gut an oral cavities[124], few studies in the healthy human lung
Vaginal	Days to weeks, considered least stable[21,115]	Diversity is associated with instability and unhealthy states	Key species are difficult to culture; animal models vary significantly from human physiology, preventing adoption of these models[125,126]	Relatively non-invasive, swabs or lavages, low bacterial load (slowed generation of metagenome sequencing data); hormonal cycles should be considered during sampling; good number of samples publicly available

Another major challenge is that both *in vitro* and *in vivo* animal studies have major discrepancies with the human VMB. *In vitro* studies are hindered because many species are fastidious or unculturable [127], and culture conditions can vary significantly across

media types and from the cervicovaginal microenvironment [128]. Likewise, there are no representative animal models of the VMB; even non-human primates lack core characteristics such as low pH and *Lactobacillus* spp. dominance [126,129]. Thus, studies of the VMB heavily rely on clinical measurements of microbial abundance that can be difficult to interpret due to confounding variables that arise from the host as well as inherent characteristics of 16S rRNA gene and metagenomic data, such as high dimensionality and compositionality. High dimensionality and compositional data can make integration of microbial abundance with functional data difficult, as these qualities require the implementation of feature selection methods, data transformations, and awareness of inherent correlation bias from compositional data that impact the use of a multitude of statistical methods [130,131]. This last challenge, while relevant to all microbiome sites, is particularly applicable to the VMB because of its lack of experimental models that allow for the interrogation of vaginal microbiota under controlled conditions. In other areas of medicine, the use of computational modeling to create *in silico* representations of patient factors has demonstrated promise. One example is the Digital Twin approach, which was first introduced in 2002 as a solution to manufacturing intelligence [132]. For precision medicine, the “Health Digital Twin” is proposed to be a virtual representation of ourselves that can capture personalized medical history using both data-driven and theory-driven knowledge which has been applied to disease cases in oncology [133–135], cardiology [136–139], infectious diseases [140,141], and neurology [142–144]. An extension of digital twin modeling is the use of virtual patients and virtual populations that then can be used to run *in silico* clinical trials [145]. These modeling techniques often use a mixture of quantitative system pharmacology (QSP) and statistical modeling to make predictions on drug efficacy and complete subpopulation analyses [145]. Thus, future advancements in characterizing VMB composition,

function, and host-microbiome interactions could be catalyzed by the development of human VMB *in silico* models.

Quantitative systems biology approaches, which encompasses statistical, mathematical, and computational techniques to study biological processes, have the potential to complement current experimental studies of the VMB by overcoming challenges associated with complexity, thus providing new insight into the key drivers of optimal and non-optimal VMB states. These approaches can effectively deconvolve large data sets, account for confounding host factors, test hypotheses prior to the use of animal models [146], and integrate data across time and physiological scales. In situations with large amounts of high-throughput data and little prior knowledge, data-driven (or statistical) models are especially useful for inferring microbial signatures associated with either health or disease states (, top). These methods are applicable when large amounts of data can be mined for further insight, and especially when there is limited pre-existing knowledge of relationships between system components [147]. For example, these approaches have been already applied when characterizing CSTs through hierarchical clustering and nearest centroid classifiers [21,26]. Other examples of data-driven approaches applied to the VMB include unsupervised techniques such as Principal Component Analysis (PCA), Principal Coordinate Analysis (PCoA) and hierarchical clustering and supervised techniques such as logistic regression, linear discriminant analysis (LDA) and partial least squares (PLS) methods. Sparse methods are often employed to minimize compositional effects, such as using Least Absolute Shrinkage and Selection Operator (LASSO) in combination with PLS methods or

correlational analyses [148]. LDA with effect size analysis (LDA/LEfSe) has been used to link species abundance with HPV and *Chlamydia* infections, as well as preterm prelabor rupture of fetal membranes, which emphasized the protective nature of *Lactobacillus* spp. [5,15,149].

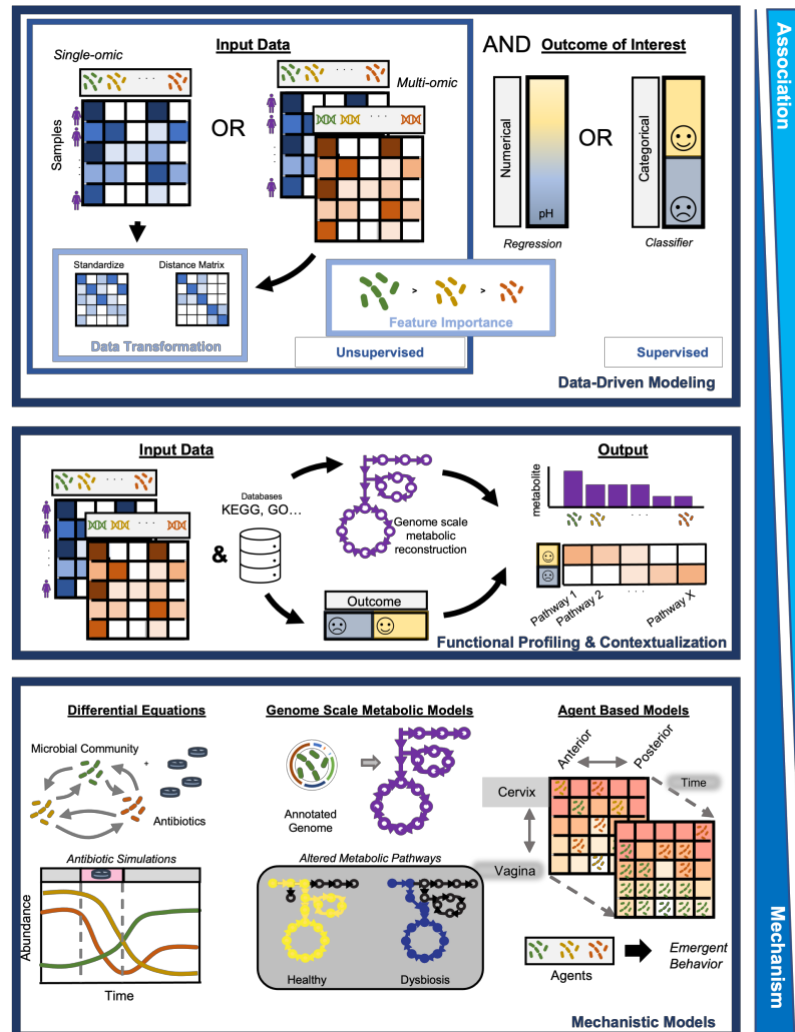


Figure 1.4.1 Overview of systems biology techniques applied to the vaginal microbiome.

The approaches go from the top, which provide statistical association to bottom which covers mechanistic methods. In the top section, input data such as 16S rRNA sequencing data or multi-omic data (such as 16S rRNA sequencing data and metabolomic data) can be used for unsupervised approaches, feature selection or data transformation techniques (medium blue box,). When an outcome is included in combination with the input data (medium blue box), supervised methods can be used to provide association with clinical outcomes or measurements using regression or classifiers and include the sub-methods in the light-blue boxes such as feature importance in respect to these outcomes. The middle section describes methods that use a combination of statistical methods and a priori knowledge from databases like KEGG, to connect microbial composition and –omics level data to mechanisms associated with different outcomes. The bottom section describes mechanistic methods based on a priori knowledge which can help build predictive models and test mechanistic hypotheses driving clinical outcomes.

In contrast, theory-based (or mechanistic) methods are best employed when *a priori* knowledge of the system is available or can be derived from biophysical, genetic, or other empirical observations [146,150]. Theory-based approaches have the added value of providing direct mechanistic insight into cause-effect relationships that drive biological function. These may include mass-action kinetic or population dynamics models (differential equation-based models), genome-scale metabolic models (GEMs), and agent-based models (ABM) [151–153] (, bottom) which each create predictive models with different strengths and weaknesses. These models are valuable because they can identify specific mechanisms that underpin community behavior or function that can then be targeted by therapeutics or to better understand drivers of therapeutic efficacy. However, theory-based methodologies have not been widely applied in the VMB, with only a few studies recently using GEMs [5,154]. The use of ordinary differential equation (ODE)-based models to predict drug efficacy has a longstanding history in understanding pharmacokinetics, drug metabolism, as well as any pharmacodynamic effects on bacterial populations [155–157]. Thus, models that can incorporate microbial-drug metabolism and therapeutic impact on microbial communities hold great promise to better understand VMB-associated therapeutics, particularly for BV, which has reported recurrence rates upwards of 50% [77,79]. ODE-based models have shown promise in understanding the gut microbiome which has emphasized the importance of capturing community inter-species interactions to understand compositional stability and resilience to perturbations [158–163]. For example, Coyte et al. 2015 used generalized Lotka-Volterra models to understand microbiome stability by exploring the impact of the frequency of competitive versus cooperative interspecies interactions, observing that cooperative communities are often unstable [158]. Stein et al. 2013 fit generalized Lotka-Volterra models directly to 16S rRNA sequencing data, and used stability analysis to understand

how antibiotic perturbations and *C. difficile* exposure could lead to dramatic shifts in gut microbiome composition [159]. Others used generalized Lotka-Volterra models to explore how community types form in the gut microbiome, demonstrating that heterogeneity in interspecies interactions or the presence of species that strongly interact with each other could promote

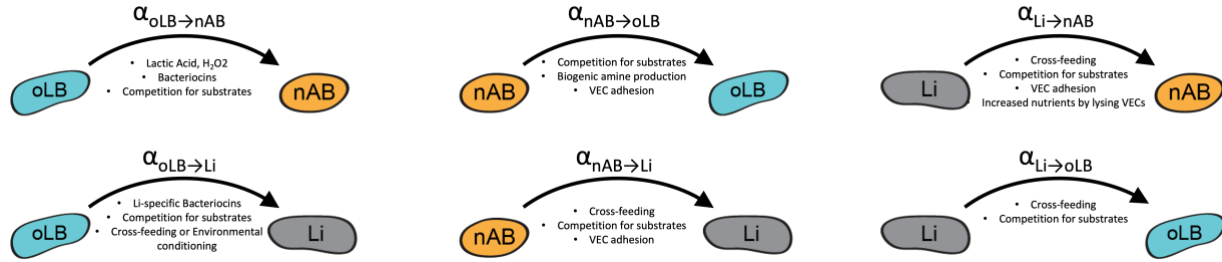


Figure 1.4.2. Vaginal microbiome ecological interactions translated to generalized Lotka-Volterra interspecies interaction terms.

distinct community compositional types [162]. The application of similar techniques using generalized Lotka-Volterra models could recapitulate known or uncertain interactions between vaginal microbiota (Figure 1.4.2). Altogether, the use of ODE-based models for the VMB could help identify mechanisms for BV treatment failure across both a drug-interaction and community inter-species interaction perspective, revealing new strategies to treat or prevent BV.

1.5 Structure of Thesis

The vaginal microbiome significantly lags behind gut microbiome research in terms of characterization and methodologies to develop new therapies. Here I present a dissertation that introduces a mechanistic ODE modeling framework for characterizing vaginal microbiota growth characteristics, which dictate community composition alterations that are associated with health and disease. By integrating principles of mathematical ecology with interventions such as antibiotics and prebiotics alongside host-driven factors like menses, these approaches will help guide better design for BV therapeutics and preventatives.

In the following aims, I developed models to interrogate different contributors to BV treatment failure and inherent community composition stability. Where possible, models were validated with *in vitro* and clinical data. This work aimed to quantify and characterize possible mechanisms of resistance and resilience to standard-of-care antibiotics aimed to treat BV and provide a high-level framework to assess the efficacy of alternative therapies. We addressed these challenges with the following aims:

Aim 1: Determine the relative importance of antibiotic uptake, sensitivity, and metabolism on antibiotic efficacy in multi-species models of BV. Antibiotics used to treat BV (such as metronidazole) influence multiple parallel parameters across VMB species. We will use an ODE model to determine the relative importance of each and understand how variability in these parameters may account for differences in antibiotic recurrence rates across women.

Aim 2: Determine how heterogeneity in microbial parameters drives differences in equilibrium behaviors observed clinically. VMB communities exhibit variable stability behavior across women, including stable optimal communities, stable non-optimal (BV) communities, and communities with bi-stable behavior between optimal and non-optimal states. To understand and identify microbial drivers of equilibrium behaviors, simulated VMB communities will be analyzed to determine which microbial parameters influence equilibrium state accessibility in response to common vaginal perturbations such as menses and antibiotic therapies.

Aim 3: Identify optimal probiotic design criteria to reorient vaginal communities to *Lactobacillus* spp. dominated states. Diverse post-treatment responses are observed from

probiotic and live biotherapeutic agent regimens ranging from no effect to increased endogenous *Lactobacillus* spp., to the dominance of the probiotic strain. To determine microbial characteristics that drive successful probiotic treatment, we will use ODE models to optimize probiotic strain characteristics across heterogeneous microbial communities.

Completion of these aims is presented in the following format. Aim 1 is addressed in **Chapter 2**, with published work that describes the impact of core vaginal microbiota on antibiotic sequestration and metabolism on antibiotic efficacy to reorient communities to *Lactobacillus* spp. dominance. Aim 2 is addressed in **Chapter 3**, which presents a published work that uses ordinary differential equation models to identify parameters that drive VMB equilibrium state using *in silico* population. This work captures clinical variability in microbial parameters to explain heterogeneity in individual responses to perturbations such as menses and antimicrobial therapy. **Chapter 4** presents a manuscript that describes work where *in silico* BV patient populations are used to screen probiotic candidates to determine optimal characteristics for re-orientation of communities to *Lactobacillus* spp. dominance.

Chapter 2 Quantitative Modeling Predicts Mechanistic Links between Pre-treatment Microbiome Composition and Metronidazole Efficacy in Bacterial Vaginosis

Christina Y. Lee^{1#}, Ryan K. Cheu^{2,3#}, Melissa M. Lemke¹, Andrew Gustin^{2,3}, Michael France⁴, Benjamin Hampel⁵, Andrea Thurman⁶, Gustavo F. Doncel⁶, Jacques Ravel⁴, Nichole R. Klatt^{2,3,7*}, Kell B. Arnold^{1*}

Nature Communications. 2020; 11: 6147.

2.1 Attributions

These authors contributed equally. * These authors jointly supervised this work.

¹Department of Biomedical Engineering, University of Michigan, Ann Arbor, MI, USA.

²University of Miami Department of Pediatrics, University of Miami, Miami, FL, USA.

³Department of Pharmaceutics, University of Washington, Seattle, WA, USA. ⁴Institute for Genome Sciences and Department of Microbiology and Immunology, University of Maryland School of Medicine, Baltimore, MD, 21201, USA. ⁵Division of Infectious Diseases and Hospital Epidemiology, University of Zurich, 8901, Zürich, Switzerland. ⁶Eastern Virginia Medical School, CONRAD, Norfolk, VA, United States of America. ⁷Department of Surgery, University of Minnesota, Minneapolis MN, USA.

2.2 Abstract

Bacterial vaginosis is a condition associated with adverse reproductive outcomes and characterized by a shift from a *Lactobacillus*-dominant vaginal microbiota to a polymicrobial

microbiota, consistently colonized by strains of *Gardnerella vaginalis*. Metronidazole is the first-line treatment; however, treatment failure and recurrence rates remain high. To understand complex interactions between *Gardnerella vaginalis* and *Lactobacillus* involved in efficacy, we developed an ordinary differential equation model that predicts bacterial growth as a function of metronidazole uptake, sensitivity, and metabolism. Here we report model findings that a critical factor in efficacy is *Lactobacillus* sequestration of metronidazole, and efficacy decreases when the relative abundance of *Lactobacillus* is higher pre-treatment. We validate results in *Gardnerella* and *Lactobacillus* co-cultures, and in two clinical cohorts, finding women with recurrence have significantly higher pre-treatment levels of *Lactobacillus* relative to bacterial vaginosis-associated bacteria. Overall results provide mechanistic insight into how personalized differences in microbial communities influence vaginal antibiotic efficacy.

2.3 Introduction

Bacterial vaginosis (BV) is a condition that affects 30-60% of women worldwide [29,164], with negative outcomes including increased susceptibility to sexually transmitted infections (STIs) and greater likelihood for adverse reproductive outcomes [6,10,11,17,165]. BV is characterized by a shift from *Lactobacillus* species (spp.)-dominated vaginal microbiota to a wide array of anaerobic bacteria including *Gardnerella vaginalis* (*Gv*) and *Atopobium vaginae* [66–68]. Treatment of symptomatic BV with metronidazole (MNZ) aims to restore *Lactobacillus*-dominated microbiota; however, recurrence rates remain high, occurring in 57-90% of women who receive adequate treatment [77,79–81]. Recurrence is associated with several host factors including previous episodes of BV, douching, and sexual activity, but no one factor emerges as a single driver of treatment failure [36,79,166–168]. Additionally, associations

between vaginal microbiota composition and BV recurrence have been reported but remain poorly understood, with several studies citing conflicting results [166,167,169].

Recent improvements in 16S rRNA sequencing have enhanced the ability to identify and more accurately quantify the composition of the vaginal microbiota in BV,[22,35] finding that the transition is frequently associated with an abundance of *Lactobacillus iners* (*Li*) [170,171]. Despite the association between *Li* and incidence of BV, identifying how *Li* dictates communities of optimal and non-optimal microbiota remains elusive, as the vaginal microbiota can change significantly over time and vary between women [172–174], especially in the presence of MNZ. The recommended treatment regimen for BV consists of oral or vaginal MNZ oriented towards selectively targeting anaerobic bacteria with little effect on *Lactobacillus* spp.,[175,176] but high variability in efficacy indicates that further study is required to understand the reestablishment of optimal vaginal microbiota ecosystems.

Recent research in the HIV microbicide field has highlighted the importance of vaginal microbiome composition in drug treatment efficacy. In a landmark study, variability in tenofovir (TFV) microbicide efficacy was accounted for by differences in the vaginal microbiome, specifically the presence of the non-target species *Gv*, which were shown to metabolize TFV [19]. Likewise for MNZ treatment of *Trichomonas vaginalis*, a proposed mechanism of treatment failure was decreased bioavailability of MNZ due to the absorbance of the antibiotic by other microorganisms in the vagina [91,177,178]. In the context of BV, it is difficult to discern the role of multiple possible interactions that have the potential to influence MNZ efficacy, including MNZ metabolism, resistance, and sequestration across multiple bacterial species that vary considerably among women. We propose that variability in MNZ efficacy may result from underlying differences in MNZ uptake and susceptibility in target and non-target species, and

therefore would be highly dependent on individual differences in pre-treatment vaginal microbiota composition.

In this work, we use an ordinary differential equation based (ODE) model and experimentally measure parameters (MNZ internalization by bacteria, metabolism, and bacterial antibiotic susceptibility) to predict *Li* and *Gv* growth dynamics with MNZ treatment. The model demonstrates that a critical factor in MNZ efficacy may be *Li* sequestration of MNZ and predicts that MNZ efficacy decreases in individuals with higher pre-treatment amounts of the non-target species, *Li*, relative to the target species, *Gv*. We validate this finding with *in vitro* co-cultures and extend our analysis to more representative models which illustrate that this behavior is also expected in microbial environments with additional species, interspecies interactions, and strain variability. Finally, by analyzing cervicovaginal samples from BV-infected women treated with MNZ in two distinct cohorts we demonstrate that our initial findings have clinical relevance in characterizing BV treatment outcomes [78,115]. Overall, our findings highlight the importance of leveraging quantitative models that evaluate interactions of target bacteria and non-target *Lactobacillus* spp. with MNZ in improving insight into personalized differences in BV recurrence and treatment failure.

2.4 Results

2.4.1 The model predicts Lactobacillus MNZ sequestration influences efficacy

To determine how MNZ treatment efficacy can be altered by bacterial-mediated interactions *in vitro*, we created an ODE model to predict growth of *Gv* and *Li* upon co-culture and treatment with MNZ (Figure 2.4.1). Parameters for each bacterial species were obtained by least squares fitting of *in vitro* kinetic data and dose-response curves for MNZ exposure with each species in monoculture (Figure 2.7.1), before the ODE model was used to predict co-

culture conditions with *Gv* and *Li* both interacting with extracellular MNZ. The model assumes that *Gv* and *Li* internalize or sequester MNZ at rates k_{int-Gv} and k_{int-Li} , respectively, and *Gv* can convert MNZ to the stable metabolite, acetamide and unknown metabolites at rate k_{met} . [179] The model additionally assumes logistic growth at rates $k_{grow-Gv}$ and $k_{grow-Li}$, with carrying capacities of K_{Gv} and K_{Li} and growth inhibition by MNZ toxicity at rates $k_{kill-Gv}$ and $k_{kill-Li}$ in a dose-dependent manner based on 50% effective concentrations of MNZ on *Gv* and *Li* ($EC50_{Gv}$, $EC50_{Li}$) [180,181]. Since MNZ is a pro-drug that is activated when internalized by anaerobic

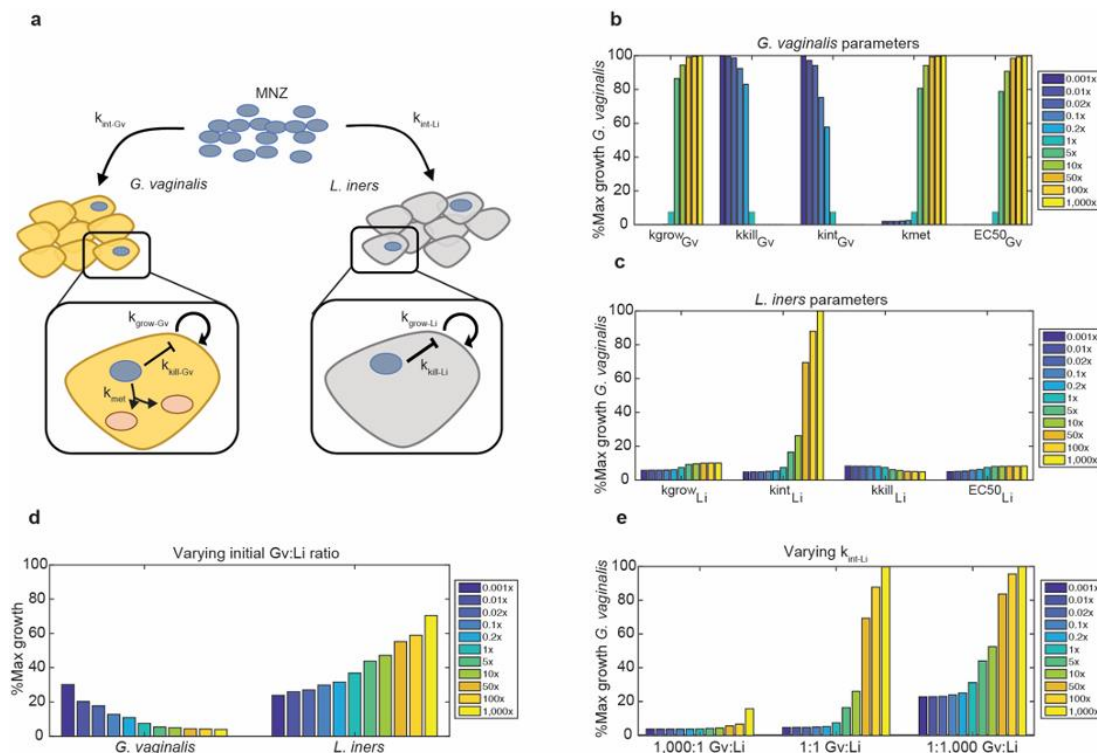


Figure 2.4.1 Model schematic for bacterial growth dynamics in BV with MNZ treatment.

(a) MNZ is internalized by both *G. vaginalis* (*Gv*) and *L. iners* (*Li*) at rates k_{int-Gv} and k_{int-Li} , cells are proliferating at $k_{grow-Gv}$ and $k_{grow-Li}$ and MNZ inhibits growth by $k_{kill-Gv}$ and $k_{kill-Li}$. For *G. vaginalis*, a potential mechanism of MNZ resistance is the bacterial-mediated interactions to the drug leading to the formation of metabolites (k_{met}). (b) Sensitivity of *Gv* growth with 500 $\mu\text{g/ml}$ MNZ when parameters directly related to *Gv* growth are varied 0.001x to 1,000x baseline values. Percent maximal growth refers to the final cell count compared to the carrying capacity of the culture, or the maximum cell density the unperturbed culture can reach at 48h based on initial cell density (c) Sensitivity of *Gv* growth with 500 $\mu\text{g/ml}$ MNZ when parameters related to *Li* survival are varied 0.001x to 1,000x baseline values. (d) Percent maximal growth of *Gv* (left) and *Li* (right) when the initial ratio of *Gv* to *Li* is varied with 500 $\mu\text{g/ml}$ MNZ treatment. e Percent maximal growth of *Gv* when MNZ internalization rate of *Li* is varied at three different population compositions with 500 $\mu\text{g/ml}$ MNZ treatment.

bacteria, the cytotoxicity of MNZ in the model is dependent on the intracellular concentration of

MNZ rather than extracellular MNZ concentration; however, we used the external MNZ concentration as the basis for EC50 of internalized MNZ, as experimentally determining the intracellular level of MNZ per cell was challenging and the main goal was to capture the relative sensitivity between *Gv* and *Li* [175–177,182].

To identify model parameters that were most critical for decreasing *Gv* growth, we performed a 1-dimensional (1D) sensitivity analysis by altering each parameter three orders of magnitude above and below baseline and evaluated *Gv* growth (Figure 2.4.1B-C). Growth was scaled relative to the predicted growth in an unperturbed co-culture based on the time point and initial population sizes evaluated and is referred to as percent maximum growth. The sensitivity analysis identified *Gv* growth as highly dependent on the MNZ internalization/sequestration rate into *Li* ($k_{\text{int-Li}}$). A 50-fold increase in this rate increased the growth of *Gv* from 7.42% to 69.5% its maximal growth upon 48h treatment with MNZ, where percent maximal growth describes the expected proportion of cell density with antibiotic treatment relative to cell density with the same initial culture conditions without antibiotic (Figure 2.4.1C). Likewise, changing the MNZ internalization rate into *Gv* ($k_{\text{int-Gv}}$) has similar effects on *Li*, where increasing this rate 50-fold resulted in 89.7% *Li*'s maximal growth (Figure 2.7.3). Overall, these results illustrate how MNZ efficacy in inhibiting *Gv* growth is influenced by the competition between each bacterium to internalize the drug.

From this result we hypothesized that the relative quantity of cells internalizing MNZ (ratio of *Gv* and *Li*) could significantly influence growth of both strains. We tested this hypothesis in our computational framework by predicting *Gv* survival after varying the starting ratio of *Gv* to *Li* (*Gv*:*Li* ratio) from 1,000x fold to 0.001x. Results indicated that altering the initial *Gv*:*Li* ratio influences the growth of both *Gv* and *Li*. Counterintuitively, *Gv* survival was

high when *Li* initially outnumbers *Gv* 1,000x and *Li* growth is optimal when *Gv* initially exceeds *Li* 1,000x (Figure 2.4.1D). Stated differently, the model suggested that more *Gv* present at MNZ treatment initiation resulted in a better treatment outcome. The importance of MNZ internalization rate into *Li* became more apparent as *Li* became the predominating species,

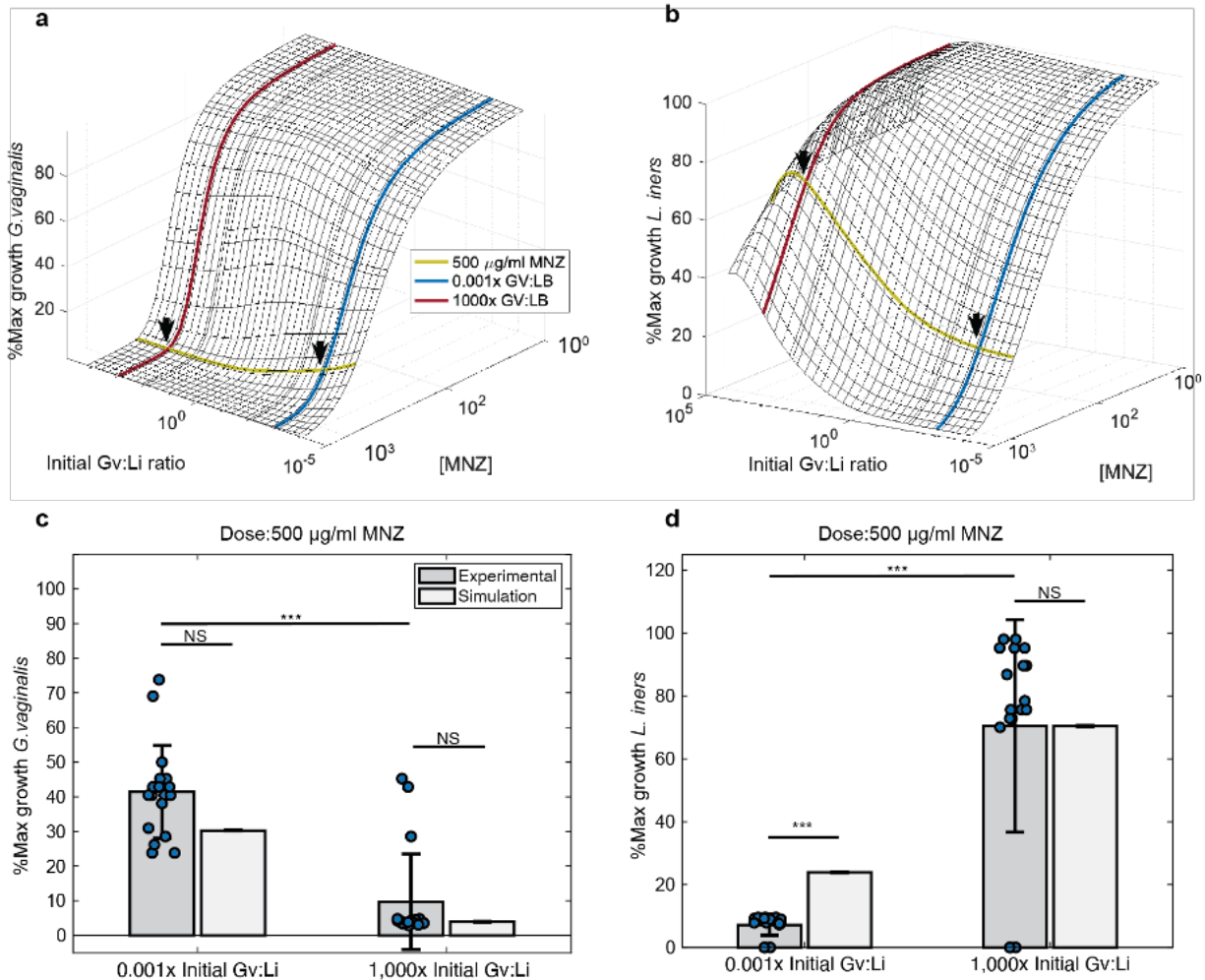


Figure 2.4.2 A higher initial Gv:Li ratio improves MNZ treatment efficacy.

(a) Surface plot to illustrate predicted percent maximal growth of *Gv* (z-axis) when concentration of MNZ (x-axis) and the ratio of *Gv*:*Li* (y-axis) are varied in simultaneously. Arrows indicate the concentration of MNZ and ratios of *Gv*:*Li* used for model validation. (b) Percent maximal growth of *Li* after simultaneous variation of MNZ dose and *Gv*:*Li* ratio. (c – d) Comparison of model simulations to experimental data for 500 µg/ml MNZ at 1,000x and 0.001x *Gv*:*Li*. *Gv* percent maximal growth 0.001x initial *Gv*:*Li* ratio and 1,000x initial *Gv*:*Li* ratio experimental vs simulation, and experimental vs experimental P-values were: P = 0.430, t = 0.809, df = 17; P = 4.67x10⁻⁸, t = 6.99, df = 34, respectively. *Li* percent maximal growth 0.001x initial *Gv*:*Li* ratio and 1,000x initial *Gv*:*Li* ratio experimental vs simulation, and experimental vs experimental P-values were P = 1.43x10⁻⁵, t = 6.00, df = 17; P = 0.726, t = 0.357, df = 17; P = 3.29x10⁻⁹, t = 7.91, df = 34, respectively. Data are presented as mean ± SD, n = 18 independent, biological replicates for each initial ratio, asterisks indicate significance as: * P < 0.05, ** P < 0.01, *** P < 0.001 without adjustment for multiple comparisons, unpaired two-sided t-test.

leading to increased growth of *Gv* (Figure 2.4.1E). This result additionally supports that *Li* competes with *Gv* to internalize or sequester extracellular MNZ, as when one bacterial strain is in excess, it likely depletes available extracellular MNZ and decreases the amount of drug internalized by the non-dominating bacterial strain.

We used our model to explore this ratio-dependent behavior over a range of relevant MNZ concentrations extending from 100 $\mu\text{g/ml}$ to 1,600 $\mu\text{g/ml}$, as estimates for vaginal accumulation range from 20 $\mu\text{g/ml}$ to greater than 1,000 $\mu\text{g/ml}$ (Figure 2.4.2A-B)[45,183]. Doses below 100 $\mu\text{g/ml}$ had no effect on *Gv* or *Li* growth and doses above 1,600 $\mu\text{g/ml}$ exhibited near complete cell killing for both bacterial strains (Figure 2.4.2A-B); these data are in agreement with experimentally determined effective concentrations of MNZ on *Gv* and *Li* cultured individually (Figure 2.7.2). However, for doses between 100 and 1,600 $\mu\text{g/ml}$ there were significant differences depending on the initial *Gv*:*Li* ratio, where MNZ was most efficacious in eliminating *Gv* when more *Gv* than *Li* was present.

2.4.2 Model validation in *Gv* and *Li* co-cultures

We validated these counterintuitive model predictions experimentally *in vitro* by varying the initial *Gv*:*Li* ratios in the presence of 500 $\mu\text{g/ml}$ MNZ and tracking growth for 48h (Figure 2.4.2C-D). Experimental measurements confirmed model predictions that MNZ efficacy for inhibiting *Gv* growth decreased when *Li* was initially dominant ($P = 4.67 \times 10^{-8}$), and were not significantly different than model predictions (0.001x *Gv*:*Li*, $P = 0.430$; 1,000x *Gv*:*Li* ratio, $P = 0.689$, Fig. 3c), with *Gv* exhibiting a predicted 30.3% and experimental $41.4\% \pm 13.3\%$ maximal growth after treatment when *Li* was initially dominant compared to a predicted 2.1% and experimental $9.4\% \pm 13.8\%$ maximal growth when *Gv* initially was dominant. *Li* growth in the

presence of 500 µg/ml MNZ was also dependent on the initial Gv:Li ratio, where MNZ inhibited *Li* growth the most when *Li* was initially dominant, $7.2\% \pm 3.9\%$ maximal growth compared to when *Gv* was initially dominant, $70.5\% \pm 33.8\%$ ($P = 3.29 \times 10^{-9}$, Fig. 2d). Notably, the model over-predicted the growth of the *Li* population when *Li* was initially dominant (0.001x Gv:Li), where the model prediction of 23.9% maximal growth was over 3-fold higher than experimentally observed, $7.19\% \pm 3.91\%$ growth (0.001x Gv:Li experiment vs simulation, $P = 1.43 \times 10^{-5}$), suggesting efficacy dependence on a high pre-treatment Gv:Li ratio may be even greater than that predicted by the model. Experimental and model predictions of *Li* growth were not significantly different when *Gv* was initially dominant (1,000x Gv:Li, $P = 0.726$). Likewise, model predictions of MNZ and MNZ metabolite concentrations were not significantly different from experimental results in cultures starting with a 0.001x Gv:Li ratio (extracellular MNZ: $p = 0.255$, intracellular MNZ: $p = 0.336$, acetamide: $p = 0.877$), but predictions for extracellular MNZ, intracellular MNZ, and acetamide concentrations in cultures with a 1,000x Gv:Li ratio did vary significantly from experimental data (Figure 2.7.4). The deviation of model predictions when *Gv* is initially dominant suggests that experimental investigation of detailed mechanisms of *Gv* interactions with MNZ is warranted (for example the potential ability of *Gv* to externally degrade MNZ). Despite some deviation of peripheral model predictions from experimental measurements, the Gv:Li ratio-dependent trends were reproduced by the model. The dependency on initial culture ratios of *Gv* to *Li* on growth suggests that non-target bacteria that sequester MNZ could significantly alter drug efficacy.

We observed some variation in the sensitivity (EC50) of *Li* to MNZ. Variability in minimum inhibitory concentrations (MIC) estimations have been reported, as changes in culture conditions including incubation length and the inoculum effect can influence the apparent

sensitivity of bacteria to antibiotic [181,184]. Additionally, the sensitivity of *Lactobacillus* sp. and *Gv* to MNZ and their MICs are reported to range from 500 µg/ml – 4,000 µg/ml and 0.75 µg/ml to greater than 256 µg/ml, respectively [88,185,186]. To ascertain whether our results would be influenced by variation in *Li* sensitivity to MNZ, we repeated the simulations over a range of EC50 values. To represent the reported resistance of *Lactobacillus* sp. *in vitro*, we increased the EC50 value of *Li* to be 10-fold higher than *Gv* (EC50_{Li} = 4,200 µg/ml). MNZ efficacy in inhibiting *Gv* growth was similarly decreased at low Gv:Li ratios (36.5% max growth at 0.001x Gv:Li) compared to high Gv:Li ratios (3.96% max growth at 1000x Gv:Li, *Figure 2.7.5*). *Li* had little to no susceptibility over the range of MNZ concentrations tested (*Figure 2.7.5*). Additionally, these EC50 values replicated trends in experimental data for growth kinetics. These results support that the initial Gv:Li ratio dependent trends in MNZ efficacy for inhibiting *Gv* growth are independent of *Li*'s sensitivity to MNZ.

2.4.3 Optimal MNZ doses are dependent on pre-treatment microbiome

We next used the model to determine specific combinations of MNZ concentrations and initial Gv:Li ratios that resulted in optimal final *Li* proportion after 48 MNZ exposure. The initial Gv:Li ratio was highly associated with the final Gv:Li ratio for doses of MNZ greater than 250 µg/ml (*Figure 2.4.3A*). Interestingly, cultures that were initially *Li* dominant (0.001x Gv:Li), were nearly insensitive to any dose of MNZ, resulting consistently with >50% *Gv* (*Figure 2.4.3A*). This result carries the surprising implication that women with *Li*-dominant vaginal microbiomes at treatment initiation are likely to undergo recurrence, regardless of MNZ dose. Of note, cultures that were originally *Gv* dominant (Gv:Li > 1) were the most likely to be *Li* dominated after 48h exposure to MNZ. Experimental data supported these trends, as the

simulation predictions were not significantly different for the final proportion of *Li* at 500 $\mu\text{g/ml}$ for 1,000x ($p = 0.680$, $t = 0.420$, $df = 17$). The model did over-estimate the final proportion of *Li*

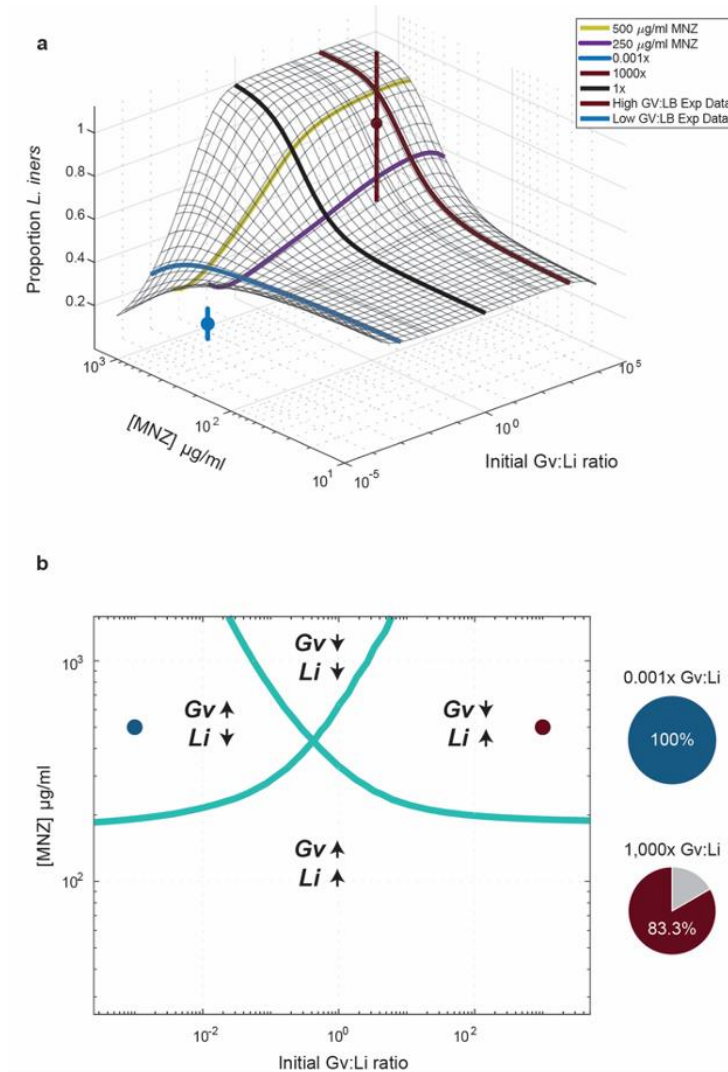


Figure 2.4.3 Initial Gv:Li ratios dictate final microbial populations.

(a) Surface plot illustrates model predictions for proportion of *Li* relative to *Gv* 48h at different starting Gv:Li ratios (x-axis) and at different doses of MNZ (y-axis). Experimental validation was performed in in vitro co-cultures of *Li* and *Gv* ($n = 18$ independent, biological replicates for each ratio) and is plotted on the surface, with mean \pm SD represented by nodes and vertical lines. (b) Phase diagram of microbial growth dynamics 48hrs after exposure to various MNZ doses, dots indicate experimental conditions evaluated. There are four possibilities: Both *Gv* and *Li* populations are increased after treatment, both *Gv* and *Li* populations are decreased, only the *Gv* population is increased and only the *Li* population is increased. Pie charts indicate the fraction of experimental samples that agree with the predicted trends (right).

at the 0.001x Gv:Li ratio (predicting a 44.1% proportion of *Li* compared to $14.2\% \pm 7.16\%$

obtained experimentally); however, this result suggests an even more significant reduction in *Li* proportion when *Gv* is initially dominant ($P = 0.008$, $t = 4.06$, $df = 17$).

A phase diagram of MNZ therapy outcomes at 48h was created to characterize both *Li* and *Gv* endpoint growth dynamics, which depict either an increase/expansion or decrease in population size relative to the initial population. The optimal growth dynamics would depict the expansion of only the *Li* population and the least optimal growth dynamics would be the expansion of only *Gv*. A decrease in both populations is additionally not optimal, as lower levels of beneficial microbiota are often associated with opportunistic infections or overgrowth of non-optimal species.[187][188] We observed that higher initial *Gv*:*Li* ratios in conjunction with MNZ concentrations over 250 $\mu\text{g}/\text{mL}$ were more likely to result in optimal final growth dynamics where the *Li* bacterial population was the only population expanding (*Figure 2.4.3B*). Likewise, it was possible for only the *Gv* population to grow and the *Li* population to decrease when the initial *Gv*:*Li* ratio was less than 1x. Interestingly, the diagram predicts that it is possible that both *Gv* and *Li* populations would decrease for intermediate ratios of *Gv*:*Li*, which expand to include a wider range of ratios as the dose of MNZ is increased. Overall, *in vitro* co-culture experimental data supported the model predictions for endpoint growth dynamics, with 15 of 18 samples agreeing with the dynamics predicted by the phase diagram for the 1,000x *Gv*:*Li*, 500 $\mu\text{g}/\text{ml}$ group and for all 18 samples agreeing with the predictions for the 0.001x *Gv*:*Li* ratio, 500 $\mu\text{g}/\text{ml}$ group (*Figure 2.4.3B*, right). This result reinforces the importance of pre-treatment *Gv*:*Li* ratio on post-treatment bacterial community composition.

2.4.4 Initial composition influences efficacy in more complex models

While our model results emphasize the importance of pre-treatment Gv:Li ratios in MNZ efficacy in co-cultures, BV in women is more complex, and involves interspecies interactions and strain variability across many different bacterial species. We created three additional model structures to evaluate the above results in more complex settings that include multiple species,

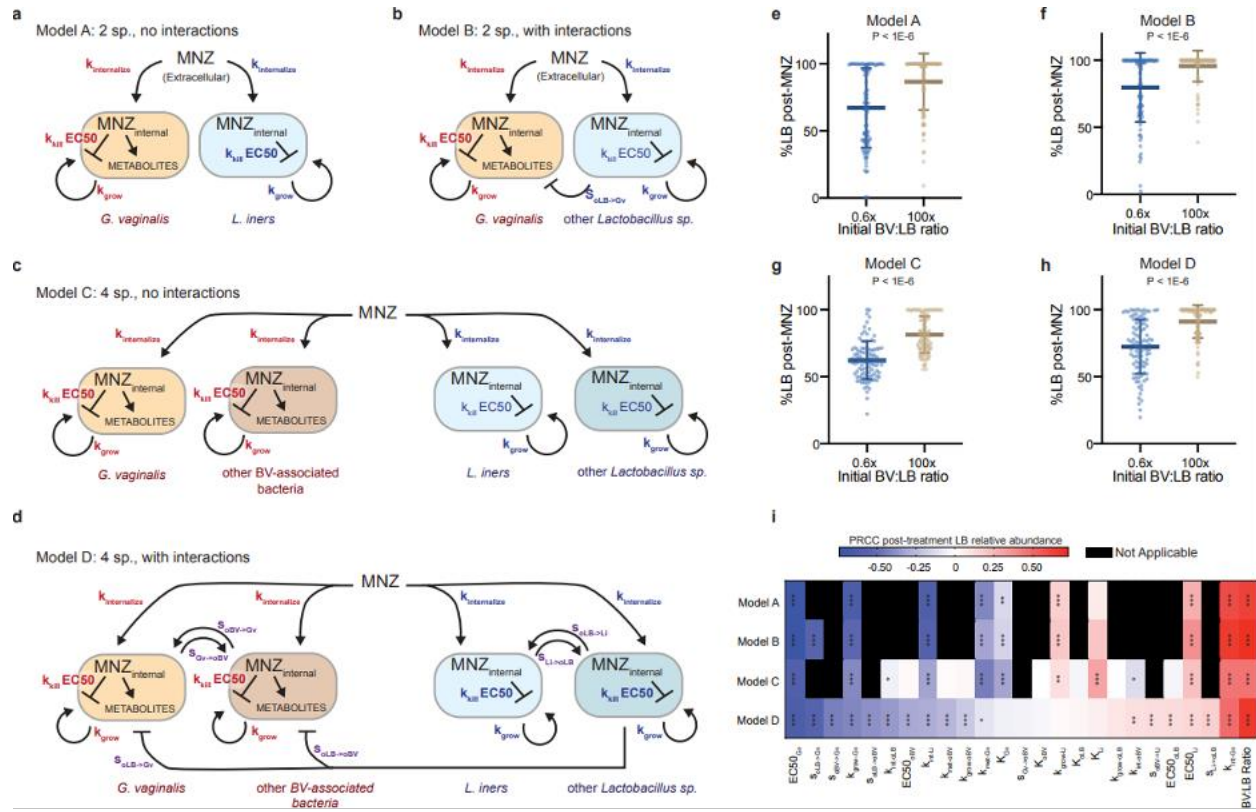


Figure 2.4.4 High pre-treatment BV:LB ratio is predicted to reduce MNZ efficacy in more complex microbial environments regardless of strain variability.

(a) Original model structure validated in Fig. 2.2. (b) Two species model with negative interaction between other *Lactobacillus* sp. (oLB) and Gv. (c) Four species model of Gv and Li with additional representative bacteria for BV-associated bacteria and *Lactobacillus* sp. (d) Four species model with inter-species interactions. Within BV-associated bacteria and *Lactobacillus* sp. interactions were simulated from mutualistic (both benefit) to commensal (one benefits, the other is neutral). Inhibitory (amensal) interactions are included between D-lactic acid producing bacteria, other *Lactobacillus* sp., with both BV-associated bacteria. (e – h) post-MNZ treatment (48h, 500 μ g/ml) *Lactobacillus* spp. relative abundances at 0.6x and 100x BV-associated bacteria to *Lactobacillus* spp (BV:LB) ratios for each model type (n = 100 independent simulations for each ratio, data are presented as mean \pm SD). Each point represents a parameter set randomly sampled from physiological ranges. Statistical analysis was completed using unpaired, two-sided t-tests: Model A (P = 7.20×10^{-7} , t ratio = 5.32, df = 198), Model B (P = 1.67×10^{-7} , t ratio = 5.649, df = 198), Model C (P = 8.05×10^{-18} , t ratio = 9.725, df = 198), and Model D (P = 1.70×10^{-13} , t ratio = 7.954, df = 198), which were corrected for multiple comparisons using the Benjamini and Hochberg method. (i) Significantly sensitive parameters were assessed by partial rank correlation for each model structure (a-d) in a global sensitivity and uncertainty analysis, multiple comparisons were adjusted for using Bonferroni correction (asterisks indicate significance as: * P < 0.05, ** P < 0.01, *** P < 0.001).

interspecies interactions, and strain variability (Figure 2.4.4). In Model B and Model D, we account for potential interspecies interactions, such as amensalism between *Lactobacillus* spp. and BV-associated bacteria and commensal or mutualistic behavior within BV-associated bacteria subpopulations and *Lactobacillus* spp. (Figure 2.4.4A,D) [53,55,56,74]. In Models C and D, we add additional representative species; a second BV-associated species and a second *Lactobacillus* sp. (Figure 2.4.4C,D). To address potential variability in associated parameters, we randomly selected parameter values from physiologically relevant ranges determined from previously published studies (Table 2.7.1 and Table 2.7.2). Notably, across all four model structures we found that higher initial relative amounts of BV-associated bacteria to *Lactobacillus* spp. had higher relative post-antibiotic levels of *Lactobacillus* spp. (BV:LB ratio, Figure 2.4.4E-F, Figure 2.7.6, $P < 1E-6$, $P < 1E-6$, $P < 1E-6$, $P < 1E-6$). This result held for a range of ratios (0.6x BV:LB and 100x BV:LB) chosen to reflect the observed relative abundance of *Lactobacillus* spp. in BV positive women (60% - 1.0%) [21]. Moreover, for each of these model structures, the global sensitivity analyses consistently selected the MNZ internalization/sequestration parameter (k_{int}) and the initial relative abundance of BV-associated bacteria to *Lactobacillus* sp. (BV:LB ratio) as significantly sensitive parameters in post-antibiotic treatment *Lactobacillus* spp. relative abundance. Variability in *Gv* sensitivity to MNZ (EC50) and growth rate were also selected as critical parameters in dictating response to MNZ treatment, which of interest as there is significant variability across *Gv* subclasses in terms of resistance to MNZ, and metabolism [189]. Furthermore, when models were modified such that *Lactobacillus* spp. could not internalize/sequester MNZ, the ratio-dependent effect was abrogated, and was additionally independent of the sensitivity of *Lactobacillus* spp. to MNZ (Figure 2.7.7).

Altogether, this provides additional quantitative evidence that *Lactobacillus* spp. sequestration of MNZ may contribute to BV recurrence in more complex microbial environments.

2.4.5 Pre-treatment composition is associated with clinical outcome

We next evaluated whether the influence of initial BV:LB ratio on MNZ efficacy is observed clinically. We compared the pre-treatment ratio of BV-associated bacteria to *Lactobacillus* spp. (BV:LB ratio) in vaginal samples collected from women who underwent MNZ treatment for BV and were cured or experienced recurrence, in two clinical studies; the UMB-HMP study [115] (n = 11) and CONRAD BV study [78] (n = 33). We chose to evaluate each study separately to minimize effects of differences in sample collection and in methods of microbial species measurements. In the UMB-HMP cohort, 11 women were observed over the course of 10 weeks and provided cervicovaginal lavage (CVLs) samples each day for quantification of relative microbial abundances by sequencing of the V3 and V4 regions of 16S rRNA. Patients underwent treatment for BV that consisted of one week of 500-mg oral MNZ, taken twice daily. Of the 11 women, 8 met inclusion criteria and were classified as recurrent or cured dependent on Nugent scoring, where recurrent patients were described as women who responded to treatment but exhibited a second episode of BV during the 10-week period (*Table 2.7.4*). Results resonated with model predictions where individuals who experienced recurrence had higher amounts of *Lactobacillus* spp. relative to BV-associated bacteria (lower BV:LB ratios, $P = 0.0366$) and tended to have higher abundances of *Lactobacillus* spp., particularly *Li*, but abundance of individual species were not statistically significant after adjustment for multiple comparisons ($P = 0.201$, *Figure 2.4.5A*, *Figure 2.7.8A*). Additionally, *Gv* relative abundance was not significantly different between groups ($P = 0.984$, *Figure 2.7.8B*). Furthermore, when we analyzed the specific species in the original two-species model, we also

observed similar results where cured women had significantly higher ratios of *Gv* to *Li* ($p = 0.0497$, Figure 2.4.5B). It is important to note that since the Gv:Li ratio comparison was a selective analysis, we did not correct for multiple comparisons based on individual species in the

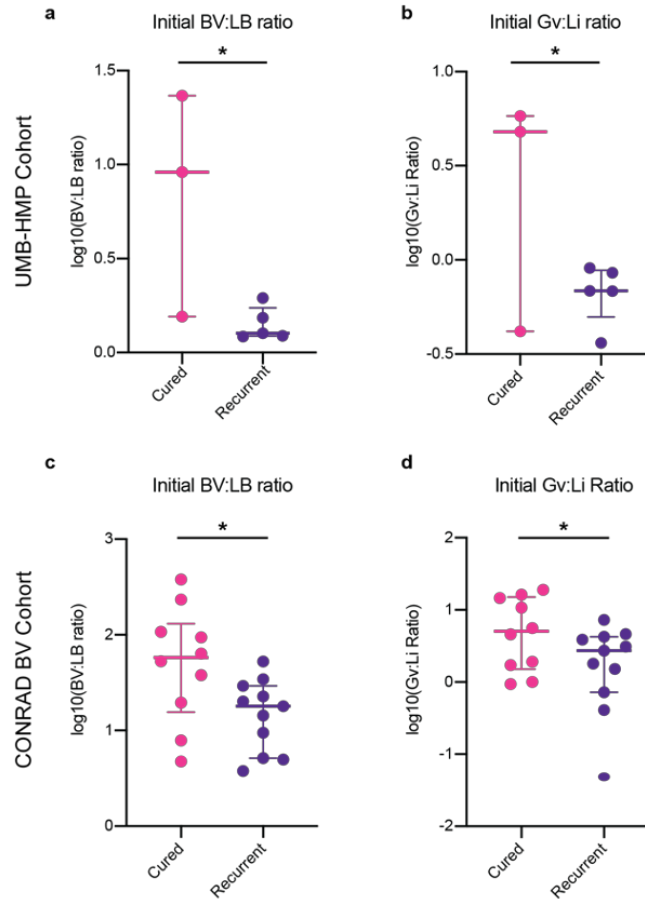


Figure 2.4.5 Increased initial BV:LB ratios associated with successful treatment of BV.

(a – b) Clinical results for the UMB-HMP cohort (n = 3 individuals for the cured group, n = 5 individuals for the recurrent group) describing the (a) log base 10 transform of initial BV-associated bacteria relative abundance to *Lactobacillus* spp. relative abundance, $P = 0.0366$, $t = 2.678$, $df = 6$. (b) initial Gv:Li ratio, $P = 0.0497$, $t = 2.451$, $df = 6$. (c – d) Clinical results for the CONRAD BV cohort (n = 10 individuals for the cured group, n = 11 individuals for the recurrent group) describing (c) log base 10 transform of initial BV-associated bacteria relative abundance to *Lactobacillus* spp. relative abundance, $P = 0.0242$, $t = 2.449$, $df = 19$. (d) initial Gv:Li ratio, $P = 0.0338$, $t = 2.287$, $df = 19$. Data are presented as median, 25th and 75th quartiles, statistical analysis was completed with unpaired, two-sided t-tests that were not adjusted for multiple comparisons. original data set (over ~190 species measured). These results support both the *in vitro*

experimental data and model results that predicted a lower efficacy of MNZ treatment when a lower ratio of *Gv* to *Li* was present pre-treatment.

We also evaluated model findings in a second clinical cohort, the CONRAD BV study, which consisted of 33 women whose vaginal microbiome was sampled at enrollment in the study, one week after MNZ treatment and one month after MNZ treatment. Relative abundances were determined by sequencing of the V4 region of the 16S rRNA. Women were excluded from this subset analysis if they failed to finish antibiotic regimen, contracted a secondary vaginal infection, did not respond, or had delayed response of treatment. Of the 33 women, 21 met inclusion criteria and were evaluated by molecular-BV criteria (dominance of *Lactobacillus* spp.) at one week and one month, with women exhibiting a vaginal microbiota composition of less than 50% *Lactobacillus* sp. classified as BV positive. The group analyzed consisted of women who were cured (n=10) and or were determined to have recurrent BV (n=11; *Lactobacillus* was dominant at one week, but molecular-BV returned after one month, Table 2.7.5). Like the previous study, we found that women who experienced recurrence had higher levels of *Lactobacillus* spp. relative to BV-associated bacteria (lower BV:LB ratio, $P = 0.0242$, Figure 2.4.5C). Comparison of CLR-transformed relative abundance did not result in statistically significant differences for *Li* or *Gv*, but tended to support the trend of recurrent women having higher *Li* and lower *Gv* (Figure 2.7.8C, D; $P = 0.521$, $P = 0.694$). Similarly, analysis of the *Gv*:*Li* ratio supported higher pre-treatment *Gv* relative to *Li* was associated with better treatment outcomes (Figure 2.4.5D; $p = 0.0338$). Though preliminary and limited by low sample numbers, these results support the model predictions and suggest that successful BV treatment could be driven by competition for MNZ, where non-target bacterial populations, *Lactobacillus* spp., like *Li* sequester MNZ away from target bacterial populations like *Gv*, *A. vaginae*, *Sneathia*, etc., ultimately decreasing MNZ efficacy.

2.5 Discussion

Here we show a personalized tolerance mechanism that may contribute to BV recurrence and treatment failure. Our model illustrates how non-target bacteria, such as *Li* or other *Lactobacillus* spp., may sequester antibiotic and lower the amount of MNZ available to target bacteria like *Gv*. This model result implies that MNZ efficacy may be dependent on highly variable pre-treatment relative abundances of *Lactobacillus* spp. such as *Li* to BV-associated bacteria populations (BV:LB ratios) and raises the question of whether patients with higher levels of *Lactobacillus* spp. are more susceptible to recurrent BV than those with higher degrees of dysbiosis. Importantly, results from the model, *in vitro* experiments, and clinical data all point to a higher pre-treatment BV-associated bacteria population relative to *Lactobacillus* spp. as a driver of MNZ efficacy in inhibiting *Gv* growth and facilitating post-treatment *Lactobacillus*-dominance. This study complements ongoing work in the search for drivers of BV treatment efficacy, in which experimental studies are often limited to delineating the role of individual bacteria, and it is challenging to assess the importance of numerous clinical and microbial variables that are associated with treatment outcome [166].

The potential for non-antibiotic-target bacterial populations to act as a sink for MNZ and alter efficacy is similar to a concept that has been previously explored in bacterial ecology, termed the inoculum effect (IE), which describes an increase in antibiotic MICs due to increased bacterial load and decreased per cell antibiotic concentration [190]. While the IE and the ability of bacterial species to influence MNZ bioavailability has been previously reported, to our knowledge its role in BV recurrence has not yet been considered. Furthermore, the ODE model used here was essential for determining the critical importance of MNZ sequestration by *Lactobacillus* spp. across multiple interactions that have the potential to influence efficacy and

recurrence, including metabolism, proliferation, and susceptibility to MNZ of both target and non-target species. The model was also necessary for translating the importance of this parameter to microbial communities with varying compositions and with different MNZ dosing regimens. Though the proposed MNZ sequestration mechanisms were not experimentally validated in this study, the model predictions for associated relationships between pre-treatment microbial composition and BV recurrence were recapitulated in both co-cultures and in cervicovaginal samples providing an additional mechanism for recurrence that has not previously been considered.

Recent studies evaluating pre-treatment vaginal microbiota composition on MNZ efficacy have reported inconsistent results, likely due to differences in patient exclusion criteria, timepoint of treatment outcome assessment, drug regimen, and methods to collect and quantify the vaginal microbiota. One study that employed a similar drug regimen (oral MNZ) and sample collection methods to the clinical cohorts evaluated here supported our results, finding higher pre-treatment loads of antibiotic-target species, *Gv* and *A. vaginae*, associated with BV treatment efficacy [169]. Other studies that used different sample collection methods and antibiotic regimens did not explicitly evaluate the pre-treatment ratio of BV-associated bacteria to *Lactobacillus* spp.; generally suggested there was an association between total *Lactobacillus* relative abundance and successful treatment [166,191,192]. Notably, some of these studies focused on analyzing treatment outcome immediately after antibiotic therapy was completed, and in some cases treatment failure was due to no response to therapy. We propose that recurrence and failure to respond to therapy likely arise from different factors, where recurrence is due to a collective bacterial population's resilience to antibiotic therapy and failure to respond is due to inherent resistance of BV-associated bacteria. Studies that have associated higher *Gv* loads with

treatment failure correspond with the latter and could be due to the formation of biofilms or other resistance mechanisms [192]. As our model predicts immediate post-therapy *Lactobacillus* spp. relative abundance, no response to treatment would be equivalent to predicting no change or low *Lactobacillus* spp. relative abundance at 48h. An additional limitation of our model is that it does not appear to be applicable to cases of MNZ treatment failure in women who initially had very low levels of *Lactobacillus* sp. (<1%), which our model would predict should promote MNZ efficacy [78]. However, we propose that treatment failure in this case may be a result of the Allee effect [193,194], which can be caused by a variety of mechanisms that lead to decreased fitness at low population densities, suggesting these women have *Lactobacillus* abundances that are too low to recolonize the vagina and may be associated with more precisely modeling inter-species interactions. Moreover, since *Li* is the only *Lactobacillus* sp. observed to date to significantly sequester MNZ, it will be important to characterize how other vaginal bacterial species interact with MNZ to further explore the role of non-target bacterial species on MNZ efficacy. Altogether, conflicting results in clinical studies of pre-treatment vaginal microbiota composition support the need for the development of quantitative platforms to evaluate the interplay between multiple microbial species, clinical variables, and dosing regimens that contribute to personalized differences in treatment failure.

Models presented here are only simple reconstructions of the minimal possible interactions between bacterial species and an antibiotic that have been established as key species by the existing literature [68,166,167], with a time-scale that was limited by *in vitro* co-culture conditions. While the model provided useful insight into how non-target bacterial species may influence BV recurrence after MNZ treatment, predicting regrowth of *Lactobacillus* spp., and the full quantitative mechanisms underlying responses to treatment are likely more nuanced. More

complex model frameworks did suggest key results would hold true in microbial communities with additional microbial species, interspecies interactions, and strain variability, though we were not able to validate this experimentally. Interspecies interactions in our models were incorporated with generalized Lotka-Volterra equations which simplifies relationships to a single term, but represent a good starting point for recapitulating ecosystem-level complexities [159,195–198]. Specific metabolic interactions that dictate survival and elimination of bacterial species in the vagina could be included with greater mechanistic detail in the future. In instances where parameters are unknown or difficult to measure experimentally, this work demonstrates the value of a global computational sensitivity analysis for understanding the relative importance of strain-level differences in antibiotic uptake, metabolism, or sensitivity. Predictive simulations can be run across multiple possible parameter ranges to determine the effects of variation prior to costly experimental measurements. This tool will be valuable in isolating the role of individual parameters in making a bacterial population or community more tolerant to antibiotic therapy. In this study we demonstrated that ODE models can provide insights into antibiotic-microbe interactions pertinent to understanding BV treatment efficacy. Our work highlights that it is possible for BV treatment to fail, even if target bacteria are not resistant to MNZ as vaginal bacterial populations as a whole can be resilient to antibiotic, resulting in recurrent BV. While our clinical analysis is limited in sample size and therefore should be considered preliminary, future extensions of this work could be used to inform clinical decision-making regarding personalized therapy options. More generally, we envision that the use of quantitative models such as this will provide a framework for integrating knowledge of interactions between multiple bacterial species and drug treatments in mucosal tissues to give insight into the diverse responses observed in infectious disease and other syndromes of the female reproductive tract.

2.6 Methods

2.6.1 Bacterial Strains and Culture Conditions

Lactobacillus iners ATCC 55195 and *Gardnerella vaginalis* ATCC 14018 (group C) were obtained from the American Type Culture Collection (ATCC) and maintained on Human Bilayer Tween Agar (BD) plates and New York City III (NYCIII) medium according to the manufacturer's instructions. Agar plates and liquid cultures were incubated at 37°C with anaerobic gas mixture, 80% N₂, 10% CO₂, and 10% H₂. Frozen stocks of strains were stored at -80°C in 40% (v/v) glycerol.

2.6.2 Metronidazole Quantification by Tandem Mass Spectrometry

MNZ concentrations were determined by validated LC-MS/MS assays. Sample aliquots were centrifuged at 3000xG and divided between supernatant and cell pellet. Extracellular MNZ was extracted from supernatant via protein precipitation using acetonitrile. For intra-cellular concentration measurements, cell pellets were lysed using sonication and re-suspended in 100µL of sterile water. Samples were subjected to positive electrospray ionization (ESI) and detected via multiple reaction monitoring (MRM) using a LC-MS/MS system (Agilent Technologies 6460 QQQ/MassHunter). Calibration standards were prepared with an inter- and intra-day precision and accuracy of ≤5% with an r² value of 0.9988±0.0009. Quantification was performed using MRM of the transitions of m/z 172.2→128.2 and 176.2 → 128.2 for MNZ and MNZ-d4 respectively. Each transition was monitored with a 100-ms dwell time. Stock solutions of MNZ and MNZ-d4 were prepared at 1mg/mL in acetonitrile-water and stored at -20°C. Mobile phase A is 0.1% acetic acid in H₂O and mobile phase B is 0.1% acetic acid in ACN, and chromatographic separation was achieved using a gradient elution with a Chromolith

Performance RP-C18 column maintained at 25°C from 0-4.6 minutes, B% 0-100, with 0.5µL/min flow. During pre-study validation, calibration curves were defined in multiple runs on the basis of triplicate assays of spiked media samples as well as QC samples. This method was validated for its sensitivity, selectivity, accuracy, precision, matrix effects, recovery, and stability. Replicates of reference samples were included every 6 samples and evenly distributed throughout the MS analysis to monitor consistency and performance and to utilize for downstream normalization.

2.6.3 Bacterial Quantification

Bacterial quantification determined via turbidimetry was completed by measuring the optical density at each time point, 100 µL of sample inoculum was read at O.D. 600nm using a SpectraMax Plus 384 UV spectrophotometer. Time points were recorded within 5 minutes of sampling and stored at 4°C.

Bacterial quantification using plate counting was done by doing a 10-fold dilution using sterile water and aliquoting 100 µL spread evenly onto BD agar plates. Cultures were incubated at 37°C. Plating was done in triplicates and were counted manually. Prior optimization ensured the dilution would result in no more than 300 colonies making quantification as accurate as possible.

For co-culture validation experiments, 100uL of sample was aliquoted on Rogosa agar and *Gardnerella* selective agar. Experiments were conducted to verify absence of *Lactobacillus* growth on *Gardnerella* selective media and absence of *G. vaginalis* growth on Rogosa agar, to confirm that colony formation specific to respective taxa. Cultures were incubated at 37°C, with a total of 36 biological replicates for the 1,000x and 0.001 Gv:Li ratio cultures (n = 18 cultures

for each ratio). Plating was done in triplicates and were counted manually. Prior optimization ensured the dilution would result in no more than 300 colonies making quantification as accurate as possible.

2.6.4 Bacteria-MNZ experiments

For the MNZ experiments, 50 μ L MNZ was added at appropriate concentrations to 5mL of NYCII media. Samples equilibrated at 37°C for 1 hour prior to the addition of 50 μ L of bacterial inoculum (2×10^6). 150 μ L aliquot was taken for time point readings for MNZ and bacterial quantification (as described above). Samples were incubated at 37°C under constant mixing and only removed for time point measurements.

For the co-culture experiments, Gv:Li ratios were added at appropriate experimental conditions in a likewise manner. For each varying ratio sample within each experiment, a side-by-side duplicate was performed without MNZ as a negative control. The negative control was assessed only for bacterial quantification to ensure that no growth condition or external stimuli promoted the growth of one over another. Negative control experiments demonstrated bacterial proliferation that modelled growth curves of each individual bacterium cultured alone thus confirming any changes in growth seen in our bacteria-MNZ experiments were the result of the addition of MNZ.

2.6.5 ODE Models

The model equations were constructed assuming both *Li* and *Gv* internalize MNZ at rates $k_{\text{int-Li}}$ and $k_{\text{int-Gv}}$, MNZ toxicity to *Li* and *Gv* occurred at rates dependent on the maximum rates $k_{\text{kill-Li}}$ and $k_{\text{kill-Gv}}$ and the concentration of internalized MNZ where growth inhibition increased as internalized MNZ exceeded a threshold as described by 50% effective concentrations, $EC_{50_{Li}}$

and $EC50_{Gv}$. The growth of *Li* and *Gv* was assumed to be logistic in behavior at rates $k_{grow-Li}$ and $k_{grow-Gv}$ with distinct carrying capacities for each bacterium, K_{Li} and K_{Gv} . The parameters for $k_{grow-Li}$, $k_{grow-Gv}$, K_{Li} and K_{Gv} were determined by nonlinear least squares fitting of the logistic function to growth curves for *Li* and *Gv* grown in separate cultures (*Figure 2.7.2*) [199]. The $k_{kill-Li}$, $k_{kill-Gv}$, $EC50_{Li}$ and $EC50_{Gv}$ were determined by fitting the Hill equation to kill curves for *Li* and *Gv* cultured in isolation (*Figure 2.7.2*). Internalization rates, k_{int-Li} and k_{int-Gv} and metabolism rates, k_{acet} and k_{met} were determined from fitting the ODE model to time course mass spectrometry data for external MNZ, internal MNZ and acetamide and cell densities (Optical density) using a multi-start local optimization strategy (*Multistart*) with the local solver *lsqcurvefit*.

2.6.6 Model Simulations and Validation.

Unless otherwise noted, all simulations were completed at MNZ concentration of 500 $\mu\text{g/ml}$ over the course of 48h. Growth outputs were normalized to the maximal growth density (K_{Li} and K_{Gv}) for comparison across simulations and to experimental data. External MNZ, internal MNZ and acetamide concentrations were relative to the total volume of cellular pellet. Sensitivity analyses were completed by perturbing a single model parameter while keeping the rest of the parameters constant over $1,000\times$ - $0.001\times$ the original value. Surfaces were generated over three orders of magnitude for MNZ concentration (10 – 1,500 $\mu\text{g/ml}$) and eight orders of magnitude for ratio of *Gv:Li* (1.6×10^{-4} – 1.6×10^4) at 1225 combinations of MNZ concentration and *Gv:Li* ratio. Model validation was completed by comparing the experimental co-culture data to model predictions using unpaired t-tests.

2.6.7 Generalized Models and Global Sensitivity Analysis

To incorporate intraspecies and interspecies variation we developed three additional model structures and ran simulations with randomized parameter sets to determine if the influence of initial Gv:Li ratio, or the more generalized BV:LB ratio, on endpoint *Lactobacillus* spp. composition is consistently observed across these model structures.

For capturing intraspecies variation, we used Latin Hypercube Sampling of parameter ranges for each parameter to create 100 parameter sets. We derived these parameter ranges from the literature and a summary of these ranges can be found in *Table 2.7.2* and *Table 2.7.3*. These same parameter ranges and sampling method were used for the global sensitivity and uncertainty analysis, which analyzed the partial rank correlation coefficient with 2,000 randomly generated parameter sets with endpoint (48h, 500 µg/ml MNZ) *Lactobacillus* spp. relative abundance (Marino et al., 2008) [200]. For capturing interspecies variation, and microbe-microbe interactions like cross-feeding, we developed a four species model that includes two representative BV-associated bacteria, and two *Lactobacillus* species, *L. iners* and a second species representing *L. crispatus*, *L. jensenii*, or *L. gasseri*.

Internalization/Uptake Rates (k_{int}): To our knowledge, this is the first publication that demonstrates that *G. vaginalis* and *L. iners* uptake or sequester MNZ. Previous literature describing uptake of MNZ in other bacterial species, including both obligate and facultative anaerobes has been published by Ralph and Denise Clarke (1978) [178], Tally et al (1978) [175] and Narikawa (1986) [201]. These publications demonstrate that even bacteria that are resistant to MNZ can still uptake MNZ, and at similar rates. Despite the fact that facultative anaerobes are believed to be largely insensitive to MNZ, Narikawa specifically demonstrates that nitroreductase activity is associated with the ability to uptake MNZ, and that pyruvate: ferredoxin activity is associated with sensitivity to MNZ as an explanation for why the

facultative anaerobes *Escherichia coli*, *K. pneumoniae*, *M. morganii* and *S. faecalis* exhibited high MICs, but reduced supernatant MNZ. We calculated the rates of MNZ uptake for five species, one obligate anaerobe, *B. fragilis*, and four facultative anaerobes (*E. coli*, *S. aureus*, *P. morganii* and *S. faecalis*) by digitizing the kinetic data for cell counts and extracellular MNZ concentrations in Ralph and Denise Clarke (1978) [178] and fitting second order reaction kinetics by ordinary least squares regression. The rates ranged from 2×10^{-17} to $0.15 \text{ cell density}^{-1} \text{ h}^{-1}$. To determine the likelihood that these parameters could be a basis for *Lactobacillus* spp. uptake of MNZ, we assessed the similarity between *E. coli*'s oxygen independent NADPH-nitroreductase, *nsfA*, with nitroreductase protein sequences of *G. vaginalis* (34.7%), *L. crispatus* (31.0%), *L. iners* (29.4%), *L. jensenii* (19.4%) and *L. gasseri* (18.52%). Additionally, Guillen et al (2009) [202] reported that *L. plantarum* had selective nitroreductase activity, that shared 32-43% sequence similarity with several *Lactobacillus* species, and in comparison had similarity with *G. vaginalis* (24.0%), *L. crispatus* (38.5%), *L. iners* (25.5%), *L. jensenii* (52.8%) and *L. gasseri* (30.0%). Sequence similarity was assessed by NCBI's protein BLAST [203]. As obligate anaerobes were observed to uptake MNZ at higher rates, we assumed that the other BV-associated bacteria, which could be an obligate anaerobe could potentially have higher capacity to internalize MNZ.

Growth Rates (k_{grow}) and Carrying Capacities (K): To account for potential variability in growth rates, we surveyed previously published to determine ranges in growth. For *Lactobacillus* species, we calculated growth rates by digitizing growth curves from Chetwin et al (2019) [101] and analyzed growth rates reported in Juárez-Tomás (2003) [204], Anukam and Reid (2008) [187]. *G. vaginalis* and other bacterial strains growth curves were less abundant in the literature, but we did calculate growth rates from Atassi et al., 2019 [56] and Anukam and Ried (2008)

[187]. Generally, *G. vaginalis* and other BV-associated bacteria seemed to have slower growth rates than *Lactobacillus* species, and in the same culture conditions, this was observed in Anukam and Reid (2008) [187]. For carrying capacity we assumed that there were similar carrying capacities for all species, except the BV-associated bacteria based on data from Castro et al. (2020) [73], that reported *A. vaginae* at lower levels than *G. vaginalis* at steady state [73].

Sensitivity to MNZ (EC50 and k_{kill}): MNZ is highly variable, and typically obligate anaerobes are considered the most sensitive to MNZ. The strain of *G. vaginalis* used in the basis of this model is relatively resistant to MNZ, with growth barely inhibited at 256 $\mu\text{g/ml}$ (9% inhibition compared to 0 $\mu\text{g/ml}$ control, *Figure 2.7.2*). For *A. vaginae*, the MIC can range 2 $\mu\text{g/ml}$ – 256 $\mu\text{g/ml}$ and *G. vaginalis* can range from 0.75 $\mu\text{g/ml}$ to > 500 $\mu\text{g/ml}$ [88,186]. Generally, it is assumed that *Lactobacillus* spp. are insensitive to MNZ; however, this also appears to be highly strain and species dependent with some *Lactobacillus* isolates in similar ranges of sensitivity as *G. vaginalis* [185,187]. The rate at which MNZ inhibits growth is more difficult to find, as the experiments to determine this rate are more laborious than the standard kill curve to calculate EC50 so we assumed all kill rates to be equal across all species.

Metabolism of MNZ: To our knowledge, this is the first manuscript to describe the metabolism of MNZ by vaginal microbiota. We solely based the parameter value on the rate observed for the *G. vaginalis* strain from the model. Additionally, we assumed that only BV-associated bacteria metabolize MNZ based on the observation that only BV-associated bacteria metabolize HIV microbicide drugs [19].

Inter-species Interaction Terms: Gause (1934) [205] first noted the calculation for interaction terms for a generalized Lotka-Volterra model describing competitive exclusion (Equations (1) and (2)). In our model, we generalized the interaction terms further to be able to

capture many different interactions, specifically amensal behavior where *Lactobacillus* spp. can inhibit BV-associated bacterial growth with no effect of BV-associated bacteria on *Lactobacillus* species growth (-/0) as well as mutualistic (both species benefit from the other +/+) and commensal behaviors (one species benefits 0/+) between BV-associated bacteria or within the *Lactobacillus* population. The amensal behavior between *Lactobacillus* species has been documented experimentally in co-culture (Jackman et al., 2019)[206] and we calculated the interaction term for many different species and strains of *Lactobacillus* on *G. vaginalis* and *Prevotella bivia* from Atassi et al. (2006) [55]. It is largely believed that D-lactic acid produced by many *Lactobacillus* species inhibits the growth of BV-associated bacteria; however, *L. iners* does not produce this isomer of lactic acid and is the reasoning behind not including an interaction term between *L. iners* and the BV-associated bacteria [53,62]. It is believed that commensal behavior exists between *G. vaginalis* and *P. bivia* in the form of cross-feeding, so we allowed the model to simulate this behavior [74]. Additionally, *G. vaginalis* is associated with promoting the growth of other BV-associated bacteria like *A. vaginae* [73]. Calculations were completed assuming the reported mono and co-cultures were at steady state to derive Equation (3) and (4). Equations (3) and (4) relate to the parameters in Table 2.7.3 by Equations (5) and (6), which generalizes the reported interaction strength from the literature to be able to be adjusted for varying carrying capacities simulated in the model that do not equal the carrying capacities from the literature.

$$\frac{dN}{dt} = r_N N \left[1 - \frac{N + s_{P \rightarrow N} P}{K_N} \right] \quad (1)$$

$$\frac{dP}{dt} = r_P P \left[1 - \frac{P + s_{N \rightarrow P} N}{K_P} \right] \quad (2)$$

$$s_{P \rightarrow N} = \left[\frac{K_N - N}{P} \right] \quad (3)$$

$$s_{N \rightarrow P} = \left[\frac{K_P - P}{N} \right] \quad (4)$$

$$S_{P \rightarrow N} = \left[\frac{K_N - f_{P \rightarrow N} K_N}{f_{N \rightarrow P} K_P} \right] \quad (5)$$

$$S_{N \rightarrow P} = \left[\frac{K_P - f_{N \rightarrow P} K_P}{f_{P \rightarrow N} K_N} \right] \quad (6)$$

2.6.8 Software

Parameterization, ODE modeling, sensitivity analyses, and PLSDA were completed using Matlab® 2018b (Matlab, Natick, MA). Statistical analyses were performed using PRISM 8, exact p-values less than 1E-6 were calculated in Matlab.

2.6.9 Clinical data and study population

The UMB-HMP cohort: The study results and associated clinical data were previously published (Ravel et al., 2013) [115] and all data provided was de-identified to this study. The UMB-HMP study was not an interventional study, but an observational prospective study, where treatment information was recorded during a clinical exam at week 5 and week 10 for 135 nonpregnant women of reproductive age. Within this study, MNZ treatment was provided as standard of care, as recommended by the CDC (Metronidazole 500 mg orally twice a day for 7 days) [207]. The original study protocol was approved by the Institutional Review Board of the University of Alabama at Birmingham and the University of Maryland School of Medicine. Written informed consent was appropriately obtained from all participants, who also provided consent for storage and use in future research studies related to women's health.

Women self-collected cervicovaginal swabs for 10 weeks. Vaginal microbiota data was generated by sequencing the V3-V4 regions of the 16S rRNA gene and is available at in dbGAP BioProject PRJNA208535. In this study, the vaginal microbiota composition data from 11 women who experienced BV and were treated with MNZ during the UMB-HMP study were analyzed. Any participants who failed to complete the MNZ regimen, who did not have BV

according to Nugent scoring at the time of MNZ treatment, or who did not have follow-up data available were excluded from the analysis. The initial relative abundances were averaged across the week before starting MNZ treatment. Patients were classified to have recurrent BV if they exhibited a second episode of BV based on Nugent scoring (7-10) during remaining of the 10-week observation period.

The CONRAD BV cohort: The study results and associated clinical data were previously published (Thurman et al., 2015) [78] and all data provided was de-identified to this study. The original clinical study protocol was approved by the Chesapeake Institutional Review Board (IRB) (Pro #00006122) with a waiver of oversight from the Eastern Virginia Medical School (EVMS) and registered in ClinicalTrials.gov (#NCT01347632). A total of 69 women were screened from symptomatic discharge and 35 women were enrolled in the study. Vaginal microbiota data was generated by sequencing the V4 region of the 16s rRNA gene, providing taxonomic resolution at the genera level.

Thirty-three women completed all three visits. BV was evaluated by vaginal microbiota compositional data (molecular-BV) [208]. After biological samples were obtained at visit 1 (V1), women with BV were prescribed twice daily, 500-mg MNZ for 7 days. Participants returned for visit 2 (V2) 7-10 days after completing the course of MNZ therapy and visit 3 (V3) 28-32 days after completing treatment. At all three visits samples were obtained to evaluate vaginal semen (ABAcard, West Hills, Ca), vaginal pH, gram stain for Nugent score and semiquantitative vaginal flora culture. CVLs were collected, followed by vaginal swabs and three full-thickness biopsies.

2.6.10 Analysis of Clinical Outcomes.

In the Human Microbiome Project cohort, patients were defined as cured or recurrent based on whether after initial MNZ treatment the patient suffered an additional episode of BV (Nugent 7-10) during the 10-week course of data collection. For analysis, initial flora relative abundances were averaged across the 7 days prior to the reported treatment start date. To analyze the relative ratio between BV-associated bacteria and *Lactobacillus* spp., we combined the relative abundances for the top twenty BV-associated bacteria and all *Lactobacillus* spp. The genera BV-associated bacteria included were: *Gardnerella*, *Atopobium*, *Megasphaera*, BVAB1-3, *Streptococcus*, *Prevotella*, *Leptotrichia*, *Anaerococcus*, *Peptoniphilus*, *Eggerthella*, *Veillonella*, *Sneathia*, *Mobiluncus*, *Corynebacterium*, *Ureaplasma*, *Eubacterium*, *Porphyromonas*, *Dialister*, *Peptostreptococcus*, *Bacteroides*, *Fusobacterium*, *Actinomyces*, *Bifidobacterium*. Before statistical analysis, the BV:LB ratio was log-transformed, and the relative abundances of *L. iners*, *G. vaginalis* were center-log ratio (CLR) transformed, with pseudocounts added to taxonomic units with relative abundances equal to zero. Statistical analysis of the BV:LB ratio and Gv:Li ratio was completed using two-sided unpaired Student's t-tests and analysis of the CLR-transformed single species abundances were completed using two-sided unpaired Student's t-tests and were corrected using the FDR method of Benjamini and Hochberg (PRISM 8).

For the CONRAD BV cohort, treatment outcome was defined based on *Lactobacillus* dominance evaluated at enrollment, 7 days after treatment and 28-32 days after treatment. Patients that exhibited *Lactobacillus* dominance at both 1 week and 1 month after treatment were considered cured, and patients that exhibited *Lactobacillus* dominance only at week 1 and not at 1 month were considered recurrent. The statistical analysis followed the same methodology as the HMP Cohort.

2.7 Appendix

2.7.1 Supplementary Figures

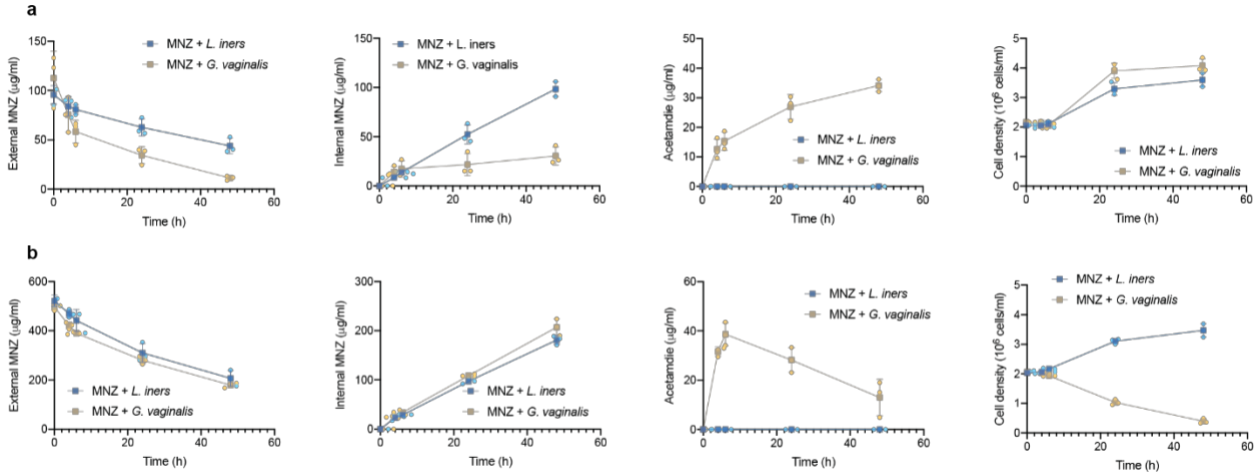


Figure 2.7.1 Kinetic data for parameterization of MNZ interactions with *L. iners* and *G. vaginalis*.

Kinetic data was collected at two doses of MNZ (a) low dose (100 µg/ml) and (b) high dose (500 µg/ml) for cultures with Gv and Li treated with MNZ Data are presented as mean ± SD, n = 3 biological replicates for each treatment group. Source data are provided as a Source Data file.

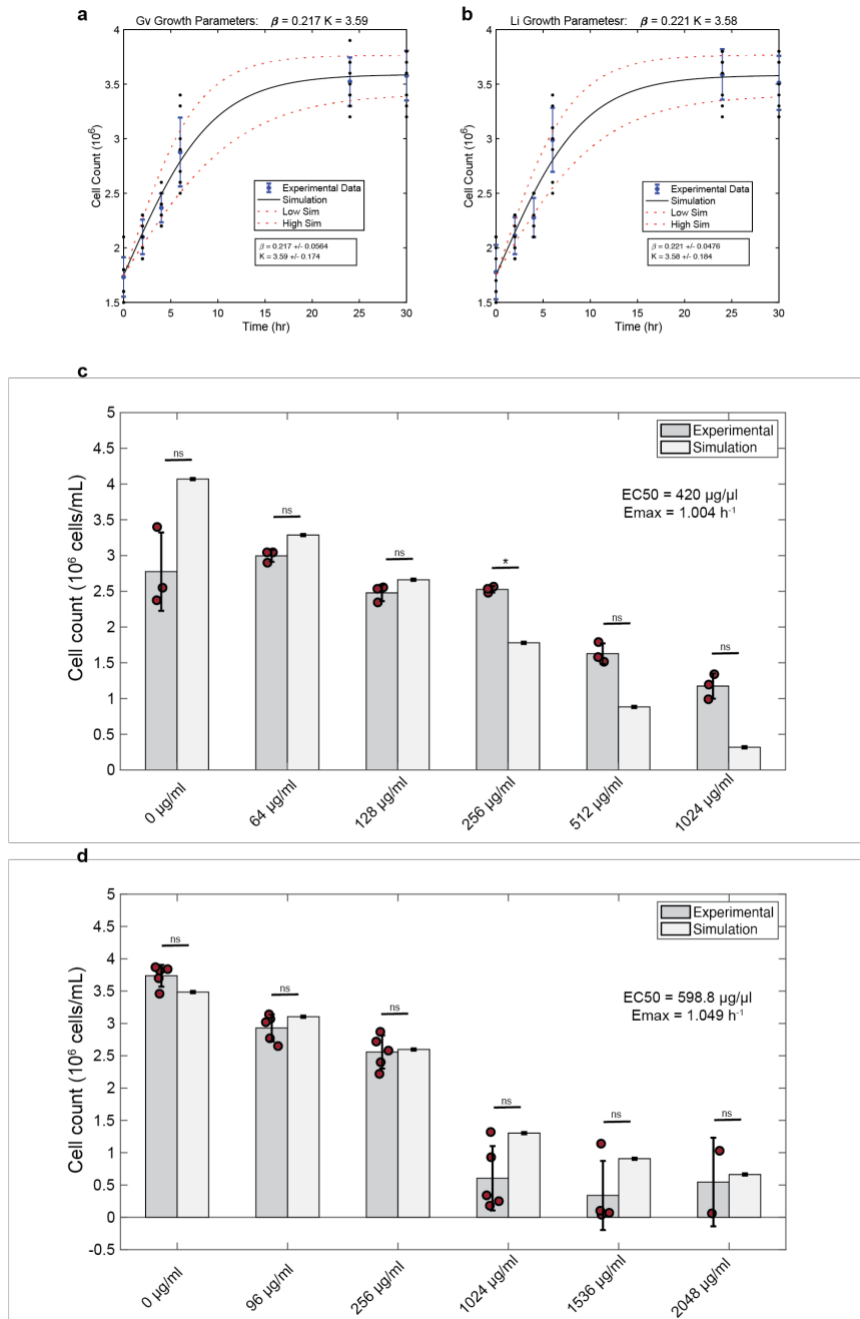


Figure 2.7.2 Model parameterization of growth dynamics with and without MNZ.

a-b growth curves fit to a logistic equation using least-squares regression, growth rates and carrying capacity was determined from this data ($n = 9$ independent, biological replicates for each species). Red dashed lines represent the confidence interval, values represent mean \pm SD. **c-d** Kill curves used to determine the maximal kill rate and EC50 of MNZ for Gv ($n = 3$ independent, biological replicates for each dose, statistical analysis was completed using multiple unpaired two-tailed t-tests corrected using the Benjamini and Hochberg method: $P = 0.212$, t ratio = 2.05, $df = 2$; $P = 0.152$, t ratio = 2.90, $df = 2$; $P = 0.415$, t ratio = 1.02, $df = 2$; $P = 0.030$, t ratio = 14.2, $df = 2$; $P = 0.104$, t ratio = 4.58, $df = 2$; $P = 0.104$, t ratio = 4.21, $df = 2$) and Li ($n = 5$ independent, biological replicates for each dose, statistical analysis was completed using multiple unpaired two-tailed t-tests corrected using the Benjamini and Hochberg method: $P = 0.736$, t ratio = 1.37, $df = 4$; $P = 0.736$, t ratio = 0.758, $df = 4$; $P = 0.912$, t ratio = 0.135, $df =$

4; $P = 0.736$, t ratio = 1.282, $df = 4$; $P = 0.736$, t ratio = 0.950, $df = 3$; $P = 0.912$, t ratio = 0.1388, $df = 1$). Data in **c-d** are presented as mean \pm SD, P-value * $P < 0.05$. Source data are provided as a Source Data file.

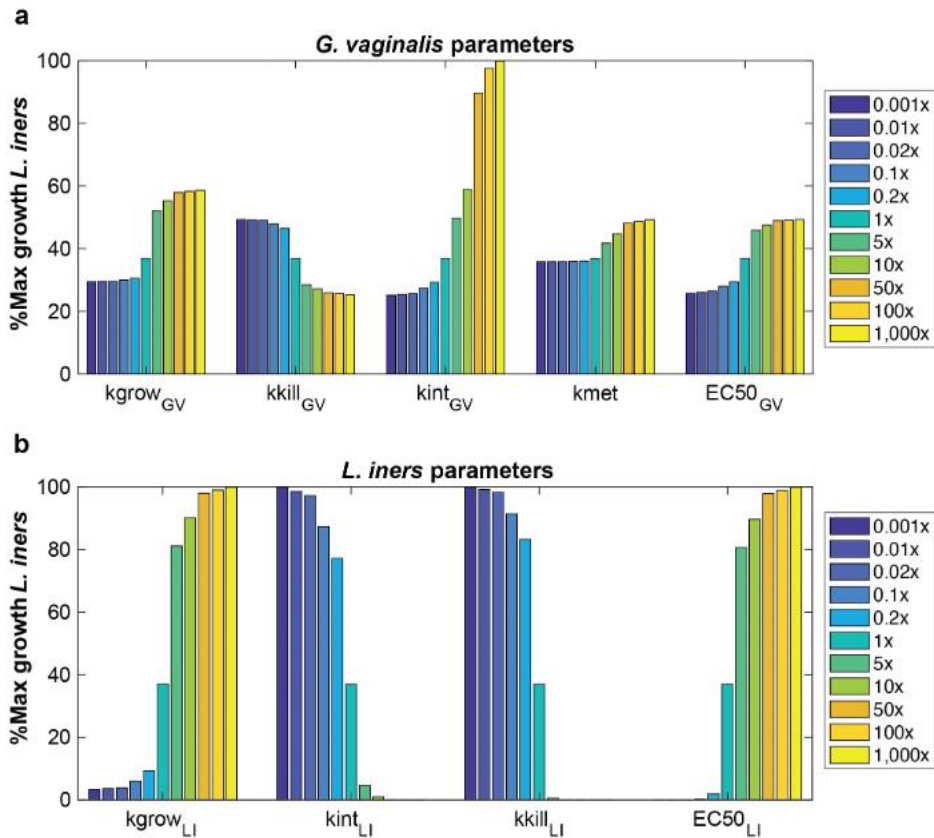


Figure 2.7.3 *L. iners* 1D sensitivity analysis.

a Sensitivity of Li growth with 500 $\mu\text{g/ml}$ MNZ when parameters directly related to Li growth and survival are varied 0.001x to 1,000x fold baseline values. Percent maximal growth refers to the final cell count compared to the carrying capacity of the culture, the maximum cell density the culture can reach. **b** Sensitivity of Li growth with 500 $\mu\text{g/ml}$ MNZ when parameters related to Li survival are varied 0.001x to 1,000x fold baseline values.

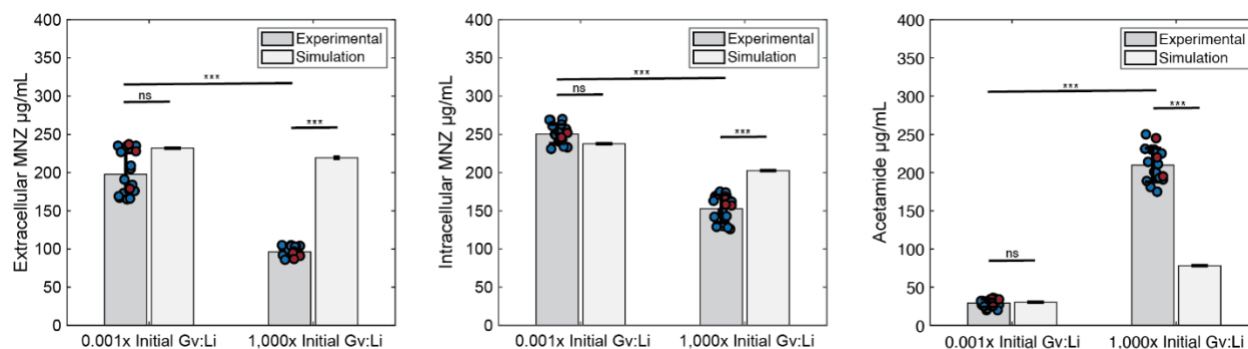


Figure 2.7.4 Comparison of model predictions with observed levels of MNZ and metabolites.

Validation for the model for extracellular MNZ, intracellular MNZ and acetamide. Intracellular MNZ is the sum of MNZ concentration in Li and Gv in the model. Statistical analyses were completed with unpaired two-sided t-tests. Extracellular MNZ 0.001x initial Gv:Li ratio and 1000x initial Gv:Li ratio experimental vs simulation, and experimental vs experimental P-values were: $P = 0.2551$, $t = 1.178$, $df = 17$; $P = 2.17 \times 10^{-12}$, $t = 17.70$, $df = 17$; $P = 2.33 \times 10^{-16}$, $t = 14.77$, $df = 34$, respectively. Intracellular MNZ: $P = 0.3356$, $t = 0.991$, $df = 17$; $P = 0.0149$, $t = 2.71$, $df = 17$; $P = 1.12 \times 10^{-19}$, $t = 18.99$, $df = 34$. Acetamide: $P = 0.8766$, $t = 0.1576$, $df = 17$; $P = 2.24 \times 10^{-5}$, $t = 5.811$, $df = 17$; $P = 9.68 \times 10^{-28}$, $t = 33.77$, $df = 34$. P-values: * $P < 0.05$, ** $P < 0.01$, *** $P < 0.001$. Data are presented as mean \pm SD with $n = 18$ biological replicates for each ratio. Source data are provided as a Source Data file.

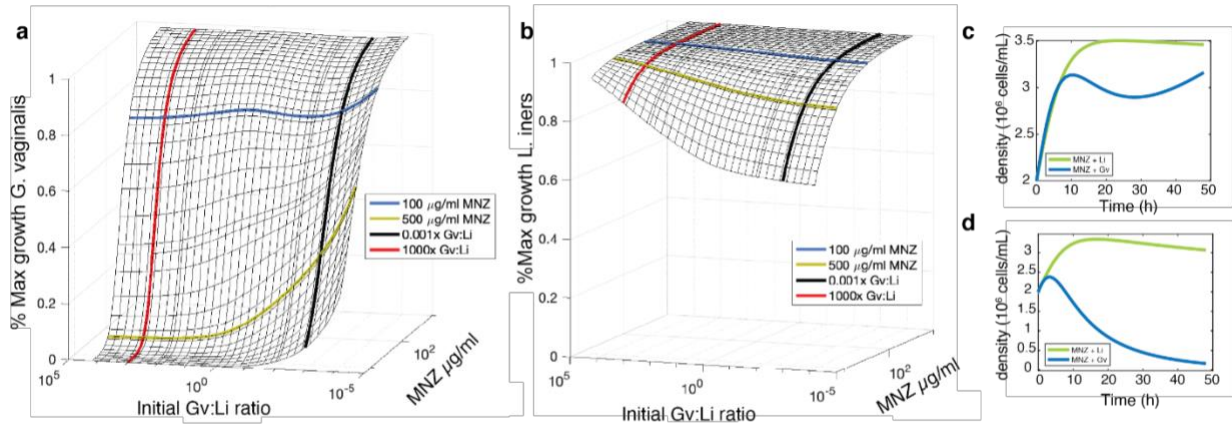


Figure 2.7.5 *L. iners* susceptibility to MNZ does not influence Gv:Li ratio dependent MNZ efficacy.

a – b Surface plot to illustrate predicted percent maximal growth of Gv and Li (z-axis) when concentration of MNZ (x-axis) and the initial ratio of Gv:Li (y-axis) are varied in simultaneously. **c – d** Model predicted growth dynamics for monoculture response to MNZ at 100 µg/ml and 500 µg/ml, respectively.

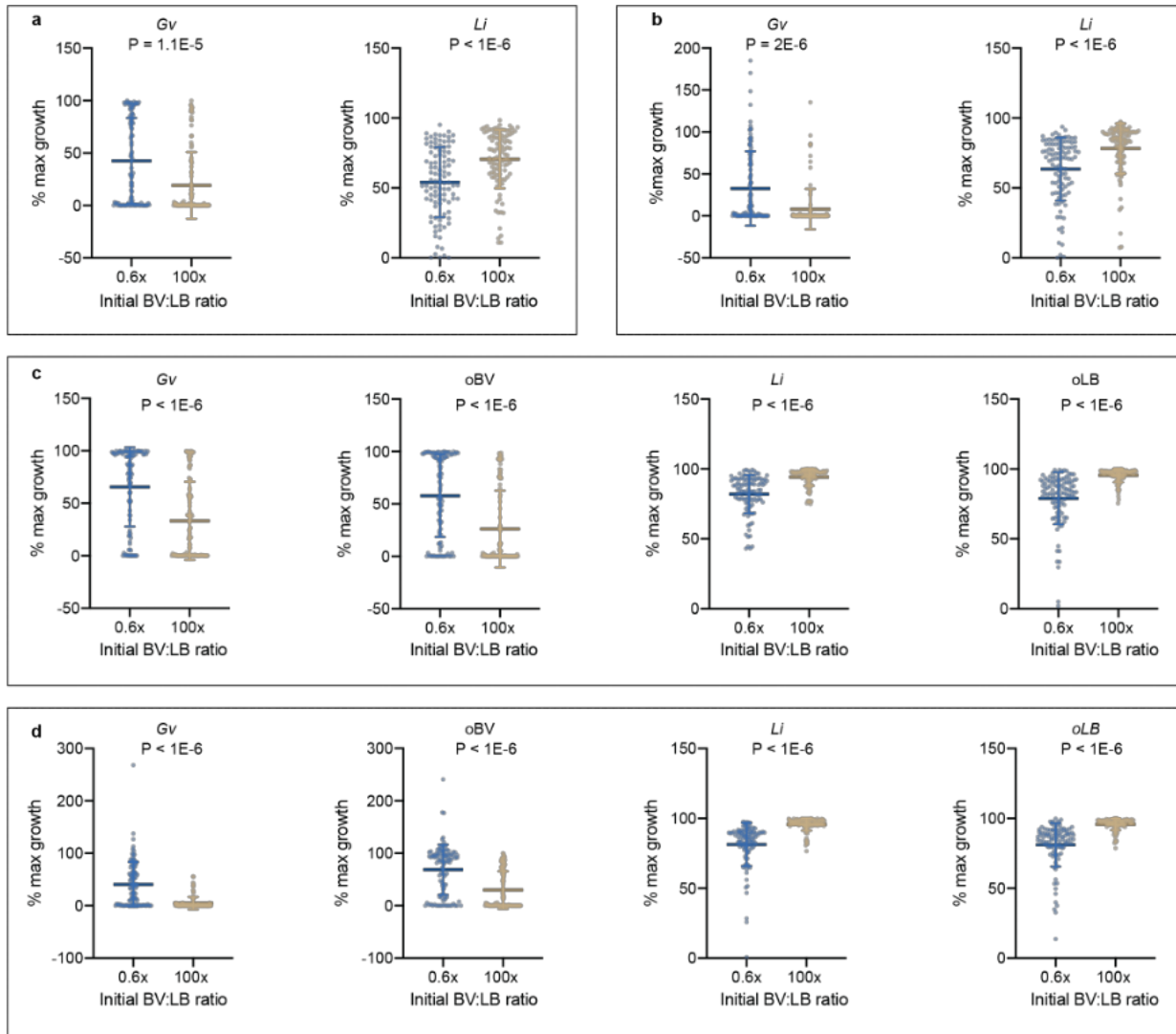


Figure 2.7.6 : BV:LB ratios influence endpoint BV-associated bacteria and *Lactobacillus spp.* abundances even with strain variation.

a Model A: two species, no interactions percent of maximal growth for Gv ($P = 1.08 \times 10^{-5}$, t ratio = 4.52, $df = 198$) and Li ($P = 1.40 \times 10^{-6}$, t ratio = 5.06, $df = 198$). **b** Model B: two species with interactions percent of maximal growth for Gv ($P = 2.21 \times 10^{-6}$, t ratio = 4.877, $df = 198$) and Li ($P = 1.17 \times 10^{-6}$, t ratio = 5.10, $df = 198$). **c** Model C: four species, no interactions percent of maximal growth for Gv ($P = 6.89 \times 10^{-9}$, t ratio = 6.10, $df = 198$), other BV-associated bacteria (oBV, $P = 1.62 \times 10^{-8}$, t ratio = 5.89, $df = 198$), Li ($P = 9.08 \times 10^{-14}$, t ratio = 8.10, $df = 198$), and other *Lactobacillus sp.* (oLB, $P = 6.50 \times 10^{-15}$, t ratio = 8.59, $df = 198$). **d** Model D: four species, with interactions percent of maximal growth for Gv ($P = 1.03 \times 10^{-13}$, t ratio = 8.08, $df = 198$), other BV-associated bacteria (oBV, $P = 7.88 \times 10^{-10}$, t ratio = 6.46, $df = 198$), Li ($P = 9.73 \times 10^{-16}$, t ratio = 8.89, $df = 198$), and other *Lactobacillus sp.* (oLB). Data are presented as mean \pm SD, multiple unpaired two-tailed t -test p -values were adjusted using Benjamini and Hochberg correction, $n = 100$ independent simulations for each ratio.

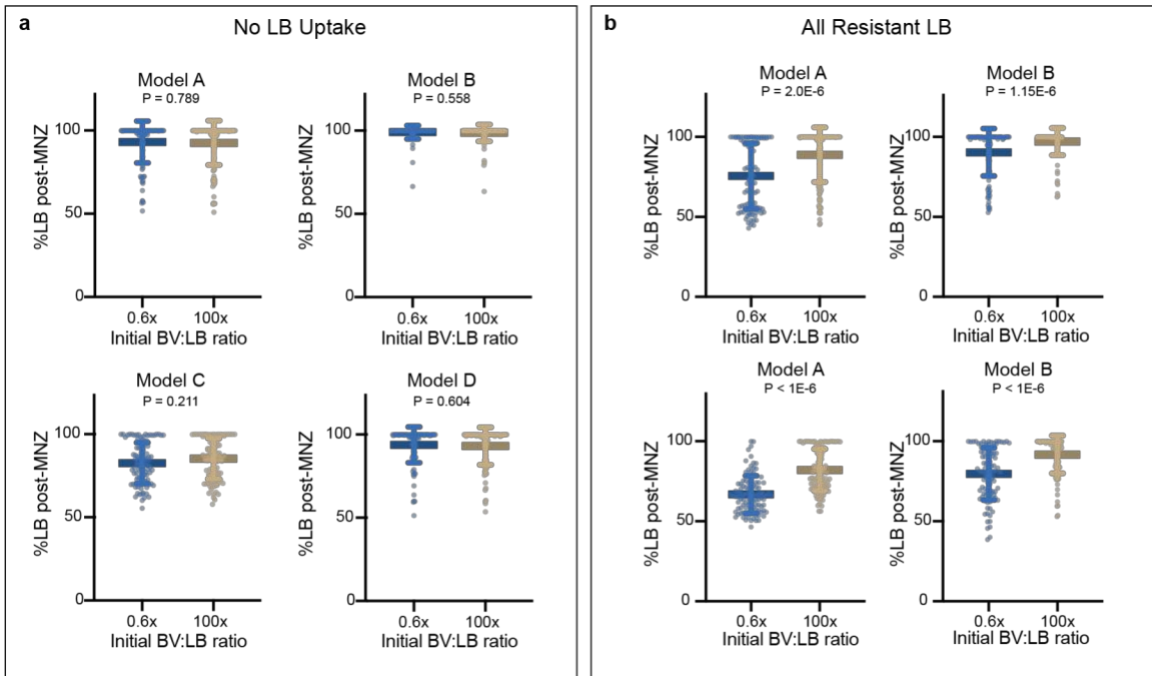


Figure 2.7.7 Uptake or Sequestration of *Lactobacillus* spp. with MNZ drives initial BV:LB ratio influence of MNZ efficacy.

a Post-treatment proportion of *Lactobacillus* sp. for Models A – D at 48h with 500 $\mu\text{g/ml}$ MNZ with the rate of internalization of all *Lactobacillus* spp. (LB) set to zero. P-values for Model A-D respectively: $P = 0.789$, t ratio = 0.268, $df = 198$; $P = 0.558$, t ratio = 0.587, $df = 198$; $P = 0.211$, t ratio = 1.54, $df = 198$; $P = 0.604$, t ratio = 0.519, $df = 198$. **b** Post-treatment proportion of *Lactobacillus* sp. for Models A – D at 48h with 500 $\mu\text{g/ml}$ MNZ with the EC50 set to 10,000 $\mu\text{g/ml}$ for all *Lactobacillus* spp. (LB). P-values for Model A-D respectively: $P = 2.04 \times 10^{-6}$, t ratio = 4.98, $df = 198$; $P = 1.15 \times 10^{-4}$, t ratio = 3.94, $df = 198$; $P = 3.68 \times 10^{-15}$, t ratio = 8.68, $df = 198$; $P = 2.35 \times 10^{-8}$, t ratio = 6.00, $df = 198$. Data are presented as mean \pm SD, multiple unpaired two-sided t-test p-values were adjusted using Benjamini and Hochberg correction, $n = 100$ independent simulations for each ratio. Source data are provided as a Source Data file.

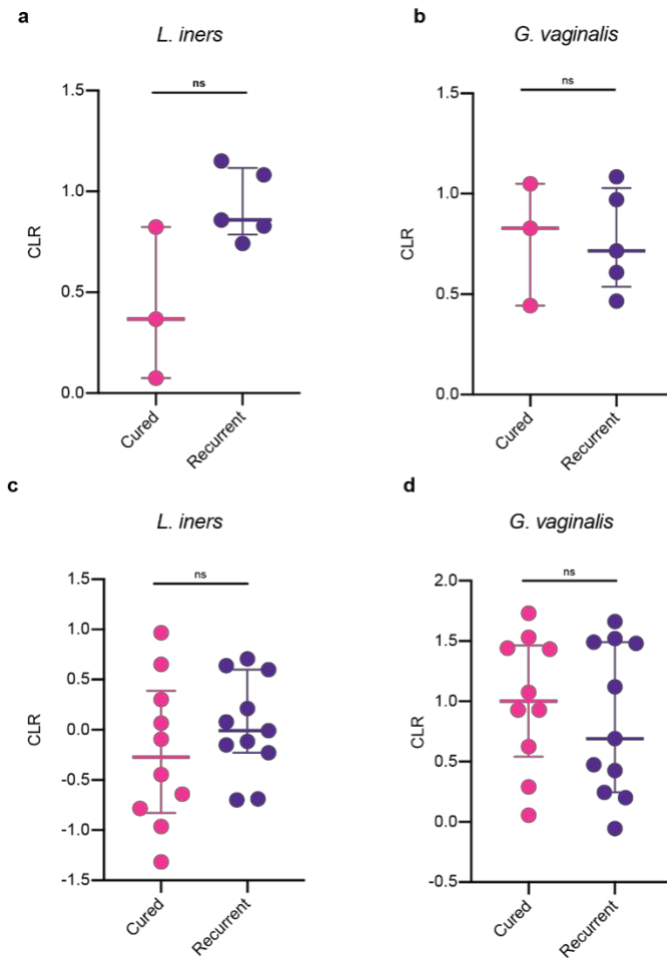


Figure 2.7.8 Initial relative abundance data for *L. iners* and *G. vaginalis* for clinical outcomes.

a - b UMB-HMP cohort (n = 3 individuals for cured group, n = 5 individuals for recurrent group) for CLR-transformed relative abundances of *L. iners* ($P = 0.201$, $t = 2.69$, $df = 6$) and *G. vaginalis* ($P = 0.984$, $t = 0.0204$, $df = 6$). **c - d** CONRAD BV cohort (n = 10 individuals for cured group, n = 11 individuals for recurrent group) CLR-transformed relative abundances for *L. iners* ($P = 0.521$, $t = 0.963$, $df = 19$) and *G. vaginalis* ($P = 0.694$, $t = 0.624$, $df = 19$). Data are presented as median (centre), 25th and 75th percentiles. Statistical analysis was completed with multiple two-sided unpaired t-tests, with p-values adjusted for multiple comparisons using the Benjamini and Hochberg method. Source data are provided as a Source Data file.

2.7.2 Supplementary Tables

Table 2.7.1 Parameters for two species model.

[1] Determined from Figure 2.7.1

Parameter Name	Description	Value	Units	Ref
$k_{\text{int-GV}}$	internalization rate of MNZ into GV	0.0139	cell density ⁻¹ hr ⁻¹	[1]
$k_{\text{grow-GV}}$	maximal growth rate of GV	0.2269	hr ⁻¹	[2]
K_{GV}	carrying a capacity for GV	4.2	cell density (10 ⁶ mL ⁻¹)	[2]
$k_{\text{kill-GV}}$	kill rate of MNZ on GV	1.004	hr ⁻¹	[3]
$EC50_{\text{GV}}$	concentration of MNZ to kill 50% of GV	420	μg mL ⁻¹	[3]
k_{met}	rate of MNZ conversion to unknown metabolites	0.0174	cell density ⁻¹ hr ⁻¹	[1]
$k_{\text{int-LI}}$	internalization rate of MNZ into LI	0.0042	cell density ⁻¹ hr ⁻¹	[1]
$k_{\text{grow-LI}}$	maximal growth rate of LI	0.2309	hr ⁻¹	[2]
K_{LI}	carrying a capacity for LI	3.569	cell density (10 ⁶ mL ⁻¹)	[2]
$k_{\text{kill-LI}}$	kill rate of MNZ on LI	1.049	hr ⁻¹	[3]
$EC50_{\text{LI}}$	concentration of MNZ to kill 50% of LI	598.87	μg mL ⁻¹	[3]

[2] Determined from **Figure 2.7.2a, b**

[3] Determined from **Figure 2.7.2c, d**

Table 2.7.2 Parameter ranges used to simulate intra-species variability.

	Units	<i>G. vaginalis</i>	Other BV-associated	<i>L. iners</i>	Other <i>Lactobacillus</i>
1) k_{int}	cell density ⁻¹ hr ⁻¹	0.015 – 0.15	0.0 – 0.20	0.0015 – 0.15	0.0 – 0.10
2) k_{grow}	hr ⁻¹	0.20 – 0.60	0.20 – 0.40	0.20 – 0.80	0.20 – 1.00
3) K	cell density (10 ⁶ mL ⁻¹)	3.0 – 4.5	2.0 – 4.5	3.0 – 5.0	3.0 – 5.0
4) EC50	µg mL ⁻¹	50 - 500	50 - 500	400 – 4,000	400 – 4,000
5) k_{kill}	hr ⁻¹	1	1	1	1
6) k_{met}	cell density ⁻¹ hr ⁻¹	0.005 – 0.05	0.005 – 0.05	0	0

Table 2.7.3 Inter-species interaction terms.

These terms describe the fold change in bacterial population that occurred from monoculture compared co-culture, a number greater than 1 indicates an increase in growth and less than 1 indicates an inhibition of growth.

Target	Source ($f_{s \rightarrow t}$)				
	Gv	oBV	Li	oLB	
Gv	1.0 – 2.5	1.0 – 1.3	1.0 – 1.0	1x10 ⁻⁶ – 1.0	
oBV	1.0 – 1.0	1.0 – 1.0	1.0 – 1.0	1x10 ⁻⁶ – 1.0	
Li	1.0 – 1.0	1.0 – 1.0		1.0 – 1.3	
oLB	1.0 – 1.0	1.0 – 1.0	1.0 – 1.3		

Table 2.7.4 UMB-HMP cohort data.

Patient ID	log10 (BV:LB ratio)	BV:LB ratio	Total BV relative abundance	Total LB relative abundance	log10 (Gv:Li ratio)	Gv:Li ratio	<i>Li</i> relative abundance	<i>Gv</i> relative abundance
UAB128	0.291	1.954	0.620	0.317	-0.164	0.685	0.492	0.337
UAB003	0.185	1.532	0.574	0.374	-0.044	0.903	0.372	0.336
UAB005	0.090	1.230	0.517	0.420	-0.068	0.855	0.318	0.272
UAB035	0.086	1.219	0.502	0.411	-0.165	0.684	0.348	0.238
UAB053	0.104	1.269	0.535	0.422	-0.440	0.363	0.52	0.189
UAB127	0.961	9.143	0.799	0.087	0.683	4.817	0.093	0.448
UAB130	1.367	23.295	0.916	0.039	0.764	5.809	0.047	0.273
UAB135	0.192	1.555	0.548	0.352	-0.381	0.416	0.394	0.164

Grey shading denotes patients that exhibited recurrent BV.

Table 2.7.5 CONRAD BV cohort data.

Patient ID	log10 (BV:LB ratio)	BV:LB ratio	Total BV relative abundance	Total LB relative abundance	log10 (Gv:Li Ratio)	Gv:Li ratio	Gv relative abundance	Li relative abundance
24_v1	0.976	9.453	0.713	0.075	0.667	4.640	0.348	0.075
25_v1	1.357	22.747	0.386	0.017	0.247	1.765	0.03	0.017
26_v1	0.577	3.776	0.609	0.161	-1.304	0.050	0.008	0.161
27_v1	1.537	34.442	0.136	0.004	0.628	4.250	0.017	0.004
28_v1	1.303	20.071	0.837	0.042	0.176	1.500	0.063	0.042
29_v1	1.722	52.692	0.290	0.006	0.544	3.500	0.021	0.006
30_v1	1.156	14.307	0.293	0.020	-0.125	0.750	0.015	0.02
31_v1	1.254	17.934	0.723	0.040	0.495	3.125	0.125	0.04
33_v1	1.465	29.206	0.581	0.020	0.860	7.250	0.145	0.02
34_v1	0.697	4.975	0.660	0.133	-0.391	0.406	0.054	0.133
35_v1	0.712	5.155	0.656	0.127	0.437	2.738	0.345	0.126
14_v1	1.579	37.958	0.824	0.022	0.740	5.500	0.121	0.022
15_v1	1.803	63.541	0.438	0.007	0.660	4.571	0.032	0.007
16_v1	2.369	233.627	0.823	0.004	1.224	16.750	0.067	0.004
17_v1	1.973	93.879	0.798	0.009	1.139	13.778	0.124	0.009
18_v1	0.896	7.868	0.747	0.095	0.282	1.916	0.182	0.095
19_v1	1.290	19.506	0.342	0.018	-0.051	0.889	0.016	0.018
20_v1	1.723	52.821	0.783	0.015	0.000	1.000	0.015	0.015
21_v1	2.032	107.535	0.223	0.002	1.230	17.000	0.034	0.002
22_v1	0.675	4.734	0.633	0.134	0.236	1.723	0.224	0.13
23_v1	2.578	378.471	0.440	0.001	1.114	13.000	0.013	0.001

Grey shading denotes patients that exhibited recurrent BV.

2.7.3 Supplementary Equations

$$\frac{d[Li]}{dt} = [G_{Li} - D_{Li}] \cdot [Li] \quad (3)$$

$$\frac{d[Gv]}{dt} = [G_{Gv} - D_{Gv}] \cdot [Gv] \quad (4)$$

$$\frac{d[MNZ_{ext}]}{dt} = -k_{int_{Li}} \cdot [MNZ_{ext}] \cdot [Li] - k_{int_{Gv}} \cdot [MNZ_{ext}] \cdot [Gv] \quad (5)$$

$$\frac{d[MNZ_{int_{Li}}]}{dt} = k_{int_{Li}} \cdot [MNZ_{ext}] \cdot [Li] - D_{Li} \cdot [Li] \cdot [MNZ_{int_{Li}}] \quad (6)$$

$$\frac{d[MNZ_{int_{Gv}}]}{dt} = k_{int_{Gv}} \cdot [MNZ_{ext}] \cdot [Gv] - k_{met} \cdot [MNZ_{int_{Gv}}] \cdot [Gv] - D_{Gv} \cdot [Gv] \cdot [MNZ_{int_{Gv}}] \quad (7)$$

$$\frac{d[Met]}{dt} = k_{met} \cdot [MNZ_{int_{Gv}}] \cdot [Gv] \quad (8)$$

$$D = k_{kill} \left(\frac{[MNZ_{int}]}{EC50 + [MNZ_{int}]} \right) \quad (9)$$

$$G = k_{grow} \left(1 - \frac{[cell\ density]}{K} \right) \quad (10)$$

$$MNZ_{int/cell} = \frac{[MNZ_{int}]}{[cell\ density] \cdot V_{culture}} V_{cell} \quad (11)$$

Equation (1) represents the growth dynamics of the *Li* population, Equation (2) the *Gv* population, Equation (3) the extracellular MNZ concentration, Equation (4) the bulk intracellular MNZ concentration for *Li*, Equation (5) the bulk intracellular MNZ concentration for *Gv*, Equation (6) the concentration of metabolites produced by *Gv*. In Equation (7), “D” represents the death rate of the population and is dependent on the respective intracellular MNZ concentrations, EC50s and maximum kill rates. In Equation (8), “G” represents the logistic growth of the respective populations dependent on the maximum growth rate and carrying capacities. In Equation (9), “MNZ_{int/cell}” represents the mass of MNZ internalized in each cell and is dependent on the bulk concentration of MNZ, per cell (cell density * culture volume) and cell volume.

Chapter 3 Evaluation of Vaginal Microbiome Equilibrium States Identifies Microbial Parameters Linked to Resilience after Menses and Antibiotic Therapy

Christina Y. Lee¹, Jenna Diegel¹, Michael France², Jacques Ravel², Kelly B. Arnold^{1*}

PLOS Computational Biology. 2023; 19:8

3.1 Attributions

¹Department of Biomedical Engineering, University of Michigan, Ann Arbor, MI, United States of America

²Institute for Genome Sciences and Department of Microbiology and Immunology, University of Maryland School of Medicine, Baltimore, MD, 21201, United States of America

*Lead contact: Kelly Arnold (kbarnold@umich.edu)

3.2 Abstract

The vaginal microbiome (VMB) is a dynamic and complex ecological community closely tied to reproductive health. Understanding community stability is critical for preventing shifts to communities associated with adverse reproductive outcomes (including bacterial vaginosis, BV). Understanding drivers of stability is challenging as women with similar composition can exhibit either sustained or temporary transitions in response to perturbations such as antibiotic therapy or menses. Here, we use a computational model to determine whether differences in microbial growth and interaction parameters could alter equilibrium state accessibility and account for variability in stability across women. Using a global uncertainty and sensitivity analysis that

captures parameter sets sampled from a physiologically relevant range, model simulations suggested that 79% of communities were predicted to be mono-stable and 21% were predicted to be multi-stable, which was not significantly different from observations in clinical measurements (81% and 19%, respectively). The model identified key microbial parameters that governed equilibrium state accessibility, pinpointing the non-intuitive importance of non-optimal anaerobic bacteria on the growth of *Lactobacillus* spp., which is largely understudied. Finally, simulations were performed to illustrate how this quantitative framework can be used to gain insight into the development of new combinatorial therapies involving altered prebiotic and antibiotic dosing strategies. Altogether, dynamical models could guide development of more precise therapeutic strategies to manage BV.

3.3 Introduction

The vaginal microbiome is a complex system that plays a fundamental role in women's health, influencing fertility [209,1], susceptibility to infectious disease [15,210], and drug efficacy [18–20]. An optimal vaginal microbiome is characterized by low microbial diversity and an abundance of *Lactobacillus* species (spp.), which can shift to a non-optimal state associated with a diverse array of anaerobic bacterial spp., commonly *Gardnerella vaginalis*, *Atopobium vaginae* and *Prevotella* spp. [21]. Previously published clinical observations suggest that the VMB gravitates to five main compositions known as community state types (CSTs): three that are dominated by *Lactobacillus* (LB) species and associated with optimal health (*L. crispatus*, CST -I; *L. gasseri*, CST -II; *L. jensenii*, CST -V); one dominated by *L. iners* and associated with an increased transition rate to non-optimal states (CST -III); and a high bacterial diversity state, lacking *Lactobacillus* spp., commonly associated with BV (CST -IV) [21]. Understanding the equilibrium states and associated stability is challenging and limited by a lack

of longitudinal studies in humans with frequent (daily) sampling; however, the limited longitudinal studies support a biological system that has set equilibrium points where perturbations impacting the cervicovaginal environment such as menses, sexual or hygienic behaviors and antibiotics, can either transiently influence the system or result in dramatic, sustained shifts in composition that are hallmarks of mono-stable versus multi-stable systems.

Assessing the propensity for a community to have multiple equilibrium states has been studied in macro-ecology to determine factors driving dramatic composition (regime) shifts after short term environmental changes with hopes these factors could be used to regulate ecosystem composition and function [211,212]. Whether the vaginal microbial community has a single equilibrium state (mono-stable) or multiple equilibrium states (multi-stable) could have important implications in understanding community responses to menses or antibiotic therapies. For example, several studies report changes in the VMB composition during menses, typically characterized by temporary high diversity states lacking *Lactobacillus* spp. However, not all women are affected to the same degree, with some women exhibiting little to no fluctuations which would be indicative of a mono-stable system and others undergoing dramatic, sustained switches in composition indicative of multiple possible equilibrium states [22,114,115]. Similarly, understanding non-optimal mono-stable systems could help explain the high rate of BV recurrence after standard of care antibiotic, metronidazole or clindamycin, as mono-stable systems would be resilient to the temporary regimen of antibiotics and would require other specific and lasting alterations to prevent recurrent BV episodes [165].

Factors that dictate whether the VMB exists in a mono-stable or multi-stable equilibrium state are likely a mix of host and microbial factors that impact growth characteristics and interactions between species. Both host characteristics and microbial characteristics are highly

variable, with individuals of comparable VMB compositions exhibiting variable phenotypes due to complex inter-species interactions working in concert or antagonistically to regulate community composition and function [115]. For example, a common assumption is that certain *Lactobacillus* spp. (including *L. crispatus*, *L. jensenii* and *L. gasseri*) inhibit the growth of BV-associated bacteria by producing compounds like D-lactic acid, L-lactic acid (except *L. jensenii*), and bacteriocins [53,73,74]. Despite this assumption, reports suggest that these species have variable inhibitory strengths and even strains of the same *Lactobacillus* spp. can have vastly differing capabilities at decreasing the abundance of BV-associated bacteria [55]. One *Lactobacillus* sp., *L. iners*, does not produce D-lactic acid and is more commonly associated with BV [213]. *L. iners* can produce a cytolysin similar to *G. vaginalis*, suggesting this *L. iners* may play a different role in vaginal ecology than those aforementioned. Additionally, of the core *Lactobacillus* spp., *L. iners* is most associated with vaginal dysbiosis [115,214]. Communities associated with BV have high species diversity as well as have the ability to engage in cooperative behavior via cross-feeding or biofilm formation that could influence system stability and susceptibility to antibiotics [215,216]. Like the *Lactobacillus* spp., there is also a high degree of intra-species variability, especially for one of the most commonly observed bacteria with BV, *G. vaginalis*, where some species and strains are more associated with recurrent BV and suboptimal treatment outcomes [55,71,189,217]. The combination of intra-species variability with inter-species ecological interactions complicates assembly of microbial communities and convolutes understanding of BV pathogenesis as well as responsiveness to antibiotic treatment. Considering all these contributing factors, the ability to quantitatively assess how combinations of these variables contribute to community stability or multi-stability could be essential in understanding VMB composition shifts after menses or antibiotic therapy.

The application of quantitative mathematical models to unravel complexities of inter-species interactions and host-microbiota interactions demonstrate promise for understanding complex microbial dynamics. Generalized Lotka-Volterra models (gLVM), which represent inter-species interactions with a coefficient that describes pairwise, additive, abundance (density) dependent interaction strengths, have been used to model the gut microbiome [159,218] and in theoretical microbial ecology [158,162]. However, obtaining parameters for these models requires dense longitudinal sampling, absolute abundance data, and population level consistency of species present, which are features that are lacking for *in vivo* studies of the VMB due to inadequate animal models [110], difficulty in clinical sample collection, and unique characteristics of VMB composition, where communities can be nearly completely dominated by a single species [21,22,26,115]. Even when all these conditions are met, the fitting of these models to noisy temporal data can lead to variable results dependent on data pre-processing steps or from assumptions that arise across different model fitting algorithms [219]. As a result, these methods have not yet been used to reveal mechanistic insight into the VMB, which would be especially valuable for understanding which microbial parameters govern mathematical equilibrium states related to VMB CSTs.

Here we use a simplified gLVM of VMB community state types (CSTs) consistently observed across women to understand how variability in microbial parameters may govern equilibrium state accessibility and differences in resilience after antibiotic therapy or menses. We address challenges related to parameter availability by capturing physiologically relevant variability using a global sensitivity and uncertainty analysis [200] and compare results to clinical subpopulations based on observed equilibrium behaviors in a longitudinal clinical study of women. By matching clinically observed equilibrium behavior subpopulations to parameter

spaces that share that same behavior, we can interrogate which parameters differentiate these subpopulations and make predictions on how each subpopulation responds to perturbations and overcome challenges associated with inconsistent parameter estimations that arise from fitting gLVs directly to *in vivo* data. Our goal was to pinpoint key species interaction and growth terms that determine mono- vs. multi-stability, which could be used to focus future research regarding specific interspecies interactions that can re-orient a system to an ideal stability type, which could encompass metabolic targets (such as substrates that promote or inhibit the growth of select species or production of lactic acid [47,48,61]) or selective bacteriocins [60]. We also demonstrate how this framework could be used to identify new dosing regimens and combinatorial therapies to improve BV treatment outcomes across heterogenous populations and given individual's equilibrium state accessibility.

3.4 Results

3.4.1 The model reveals the potential for the VMB to exist in mono-stable or multi-stable states depending on microbial parameters that vary across individuals

A computational model that linked microbial growth and interaction characteristics to community composition and stability was created using a generalized Lotka-Volterra ODE Model (gLV) that represent simplified, core groups of VMB CSTs. The simplified CSTs included the “optimal” *Lactobacillus* spp. (oLB dominated, combined CST -I, -II, -V), the transitory *Lactobacillus* sp., *L. iners* (Li dominated, CST -III), and the high bacterial diversity group associated with non-optimal anaerobic bacteria (nAB) and BV (nAB dominated, CST -IV; Figure 3.4.1A). This model had seven nonzero steady states with the potential for multiple of the seven states to be stable for a given set of microbial parameters (multi-stability, Supplementary

Text). The model steady states describe the inherent stability of the microbial community to exist

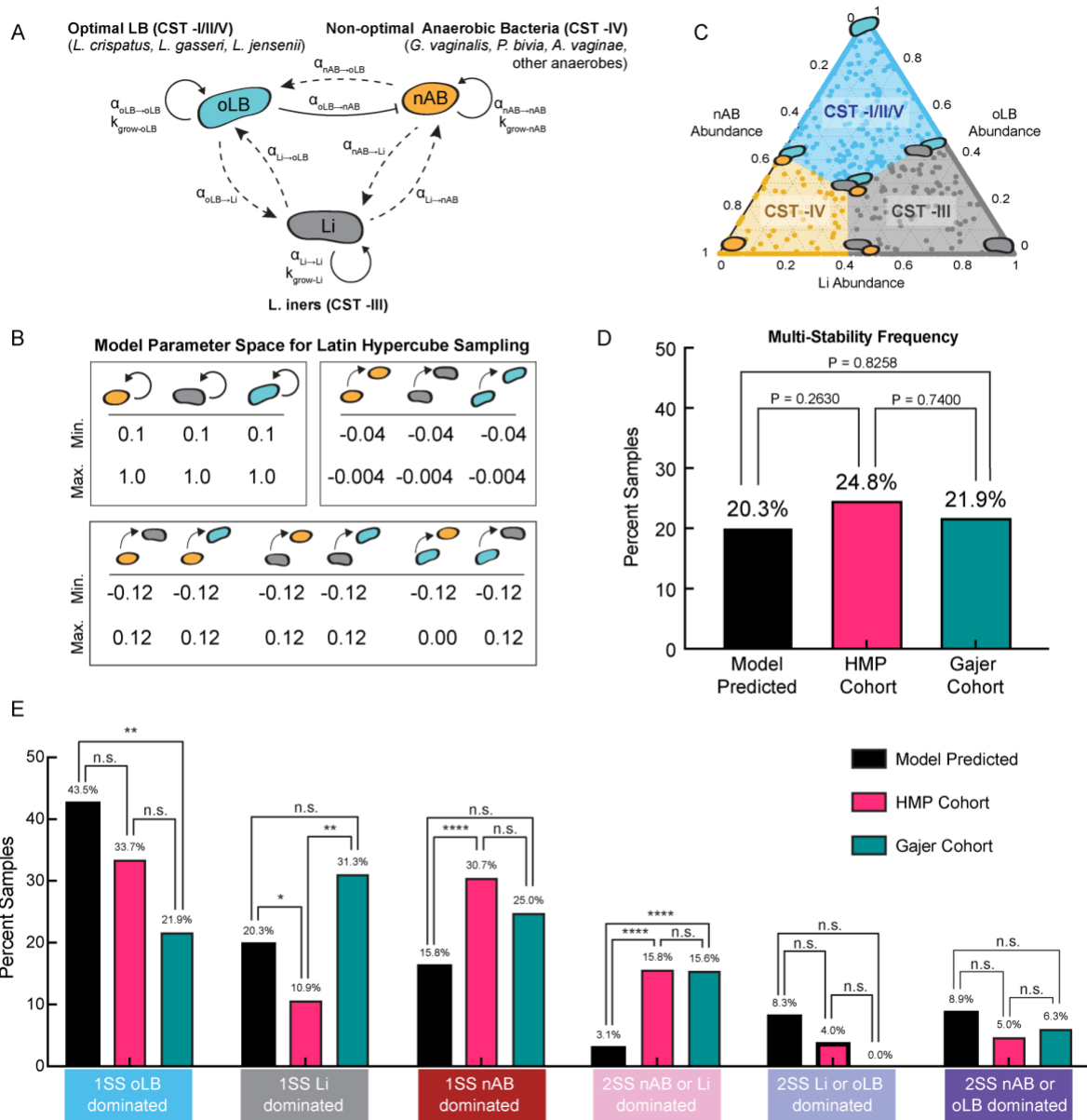


Figure 3.4.1 Mathematical model of vaginal community state types.

(A) Model schematic of a generalized Lotka-Volterra Model for three community groups: optimal *Lactobacillus* spp. (oLB), *L. iners* (Li), and non-optimal anaerobic bacteria (nAB). Model equations capture growth rates, carrying capacity and interaction terms. (B) Mapping of the predicted steady-state compositions to clinically defined CSTs using a nearest centroid model based on VALENCIA centroids. (C) Parameter ranges used to define uniform distributions for a global uncertainty and sensitive analysis using Latin Hypercube Sampling (LHS). (D) Model predicted frequencies of equilibrium behaviors which include 1SS oLB dominated (CST -I/II/V), 1SS Li dominated, (CST -III), 1SS nAB dominated (CST -IV), 2SS nAB dominated/oLB dominated, 2SS Li dominated/oLB dominated, and 2SS nAB dominated/Li dominated. (E) Analysis of overall frequency of mono-stable (gold) and

multi-stable (blue) states from the model predicted to the clinical observation. Statistical comparisons were made using χ^2 -tests.

at a given community composition without the impact of external perturbations like antibiotic, menses, sexual behavior, hygienic behavior, or contraceptives, which can be simulated as perturbations to the model system. To characterize the relationship between microbial growth characteristics and ecological interactions on the internal stability of VMB community composition a physiological parameter space was generated using Latin Hypercube Sampling (LHS) of uniform distributions created from experimental and empirical observations for each microbial parameter (*Table 3.7.1; Figure 3.7.1*; group associated with non-optimal anaerobic bacteria (nAB) and BV (nAB dominated, CST -IV; *Figure 3.4.1B*). Then, local stability analysis was performed to analytically determine the steady states for each parameter set (simulated sample) generated from the LHS (N = 5,000; Supplementary Text). Model predictions for community steady states were converted to CSTs (oLB dominated CST -I/II/V, nAB dominated CST -IV, and Li dominated CST -III) using a nearest centroid classifier on the analytically predicted equilibrium composition similar to previously used methodologies to classify CSTs clinically (*Table 3.7.2, [26]*). This classification method link predicted *in silico* equilibrium behavior subtypes to clinically observed subpopulations at the CST level (*Figure 3.7.2*). Overall model results demonstrated six, physiologically relevant equilibrium behavior subtypes that were either mono-stable (1SS, one stable state) or multi-stable (>2SS, two or more stable states; *Figure 3.7.1D-E*).

The most common equilibrium behavior subpopulations corresponded to three mono-stable systems: (1) the optimal *L. crispatus* species dominant mono-stable equilibrium subtype (1SS oLB dominated CST -I/II/V; 43.5% of simulated samples), (2) the *L. iners* species dominant equilibrium subtype (1SS Li dominated CST -III ; 20.3% of simulated samples), and

(3) the nAB species dominated (BV-associated) equilibrium subpopulation (1SS nAB dominated CST -IV; 15.8% of simulated samples; *Figure 3.7.1E*). To compare model predictions to clinical equilibrium behavior frequencies, clinical equilibrium behavior subtypes were determined from two longitudinal cohorts, the Human Microbiome Project Cohort (HMP Cohort, N = 101 patients) [115] and the Gajer et al. 2012 cohort (Gajer cohort, N = 32 patients [22]; *Figure 3.7.1E*). Equilibrium behavior subtypes were calculated from each time series by calculating a CST transition matrix (*Figure 3.7.2*). For example, patients whose transition matrix was primarily associated with within-state transitions (i.e. CST -I/II/V to CST -I/II/V) were classified as mono-stable (1SS oLB dominated; *Figure 3.7.2A*), whereas patients whose transition matrix had two cases of high within state transitions rates (for example, 65% were CST -IV to CST -IV and 31% were CST -I/II/V to CST -I/II/V) were classified as multi-stable (2SS nAB dominated/oLB dominated; *Figure 3.7.2B*). There was no significant difference in the frequency of predicted multi-stable vaginal communities compared to the clinical data (predicted 20.3% vs. 24.8% in the HMP cohort and 21.9% in the Gajer cohort; $P = 0.2630$ and 0.8258 , respectively; *Figure 3.7.1D*). At the equilibrium behavior level, frequencies differed both between the model and clinical observations and between the two clinical cohorts (*Figure 3.7.1E*). The model tended to underestimate nAB dominated equilibrium behaviors in favor of oLB dominated equilibrium behaviors, with the 2SS nAB dominated/Li dominated subtype having the most consistent discrepancy when compared to the two clinical cohorts (*Figure 3.7.1E*). The underestimation of subtypes that exhibit nAB dominated compositions is likely due to constraining the interaction of oLB on nAB to be negative (inhibitory), favoring oLB dominated equilibrium subtypes. Calibration of the parameter distributions to be more representative of the population could increase the predictive power of the model when external perturbations are

simulated. Overall, this analysis supports that the vaginal microbiome can exist as either a mono-stable or a multi-stable system, and the predominant state can be replicated by the specific growth and microbial interaction parameters that vary across women.

3.4.2 Mono-stability is driven by specific interspecies interaction terms

To understand intrinsic factors that drive stability toward one equilibrium composition (mono-stable) versus factors that facilitate more than one possible equilibrium composition for a given community (multi-stable) communities, simulated samples generated from the global sensitivity analysis of known equilibrium behavior subtypes were compared using multiple Mann-Whitney rank sum tests with FDR-adjusted p-values (*Figure 3.4.2*). This analysis characterizes the inherent stability of the microbial community, which helps define whether the community will undergo compositional shifts given an external perturbation such as sexual and hygienic behaviors, menses, or antibiotic therapies (*Table 3.7.3*). The comparison of mono-stable optimal subtypes (1SS Li dominated and 1SS oLB dominated) to multi-stable optimal/non-optimal subpopulations (2SS Li dominated/nAB dominated and 2SS oLB dominated/nAB dominated) revealed that the interaction of nAB with Li and oLB ($\alpha_{nAB \rightarrow Li}$, $\alpha_{nAB \rightarrow oLB}$) was significantly associated with mono-stable subtypes (*Figure 3.4.2A,B*). This result indicates the effect nAB have on *Lactobacillus* spp. could dictate inherent community stability from external perturbations. This observation is notable, as there are few studies that describe the impact nAB on *Lactobacillus* spp. (oLB or Li). The comparison of the stable non-optimal subpopulations (1SS nAB dominated) to multi-stable subpopulations (2SS nAB dominated/Li dominated and 2SS nAB dominated/oLB dominated) supported the importance of the associated *Lactobacillus* spp. in driving mono-stability, where weaker interactions between oLB or Li with nAB were

associated with the 1SS nAB dominated group ($\alpha_{Li \rightarrow nAB}, \alpha_{oLB \rightarrow nAB}$; *Figure 3.4.2C,D*).

Additionally, the interactions between *Lactobacillus* spp. were associated with the 1SS nAB dominated group, with more positive interactions between *Lactobacillus* spp. associated with the 1SS nAB dominated communities ($\alpha_{Li \rightarrow oLB}, \alpha_{oLB \rightarrow Li}$; *Figure 3.4.2C,D*). Mediation of pairwise *Lactobacillus* spp. interactions is a potential non-intuitive target for altering microbial

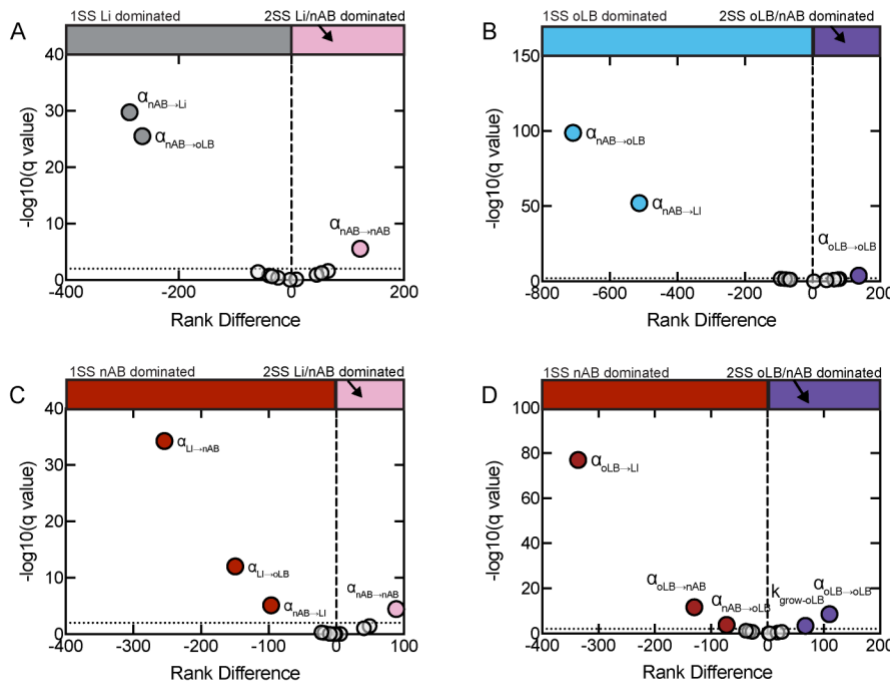


Figure 3.4.2 Assessment of parameters that drive multi-stable vs mono-stable states.

Volcano plots from multiple Mann-Whitney rank sum tests with FDR-adjusted p-values. Colored points indicate parameters that were significantly different between comparison groups. (A) 1SS Li dominated (gray) vs 2SS Li dominated/nAB dominated (pink) (B) 1SS oLB dominated (blue) vs 2SS oLB dominated/nAB dominated (purple) (C) 1SS nAB dominated (red) vs 2SS nAB dominated/Li dominated (pink) (D) 1SS nAB dominated (red) vs 2SS nAB dominated /oLB dominated (purple).

community equilibrium behavior, as interactions between species like *L. iners* and *L. crispatus*, *L. jensenii* or *L. gasseri* remain poorly characterized. Altogether these results indicate that drivers of mono- vs multi-stability are specific to equilibrium subpopulations and indicate that inter-species interactions are drivers of mono-stable versus multi-stable states.

3.4.3 Equilibrium subpopulations may explain variability in temporary vs. sustained CST switches observed from menses

The vaginal microbiota is subject to external and internal factors that dictate whether the community will undergo changes in composition over time. One common perturbation is menses, where studies report changes in VMB composition during menses, typically a temporary change from low diversity, *Lactobacillus* spp. dominance, to high diversity states associated with BV. Notably, reports indicate variability in the degree of impact of menses on composition, ranging from no noticeable impact on VMB composition to individuals undergoing dramatic and sustained shifts after menses [22,114,115]. To explore the impact of menses on initially optimal microbial communities, equilibrium behavior subtypes that could exhibit oLB or Li dominance were evaluated (1SS oLB dominated, 1SS Li dominated, 2SS oLB dominated/nAB dominated, 2SS Li dominated/oLB dominated). To be able to assess model predictions to clinical data at a population level, an *in silico* HMP cohort was created by resampling the base parameter space and matching the equilibrium behavior distribution exhibited by the HMP cohort (*Figure 3.7.3*). The parameters were also scaled to be on the time scale observed for growth rates and interaction terms observed in a murine gut microbiome model [159]. Menses was simulated based on the connection between elevated levels of certain biogenic amines during menstruation and their associated connection with transitions to BV positive states [75]. These biogenic amines were reported to alter *Lactobacillus* spp. characteristics *in vitro* including decreased growth rates of *Lactobacillus* spp. ($k_{\text{grow-Li}}$, $k_{\text{grow-oLB}}$) and decreased production of lactic acid (less inhibitory $\alpha_{\text{Li} \rightarrow \text{nAB}}$ and $\alpha_{\text{oLB} \rightarrow \text{nAB}}$).

First, a two-dimensional sensitivity (bifurcation) analysis was used to assess how menses-related parameter changes could shift steady-state accessibility across the four *Lactobacillus* dominated equilibrium behavior subtypes. The global bifurcation analysis of the 1SS oLB dominated and the 2SS oLB dominated/nAB dominated equilibrium behavior subpopulations demonstrated that the mono-stable groups were resilient to changes in menses-affected

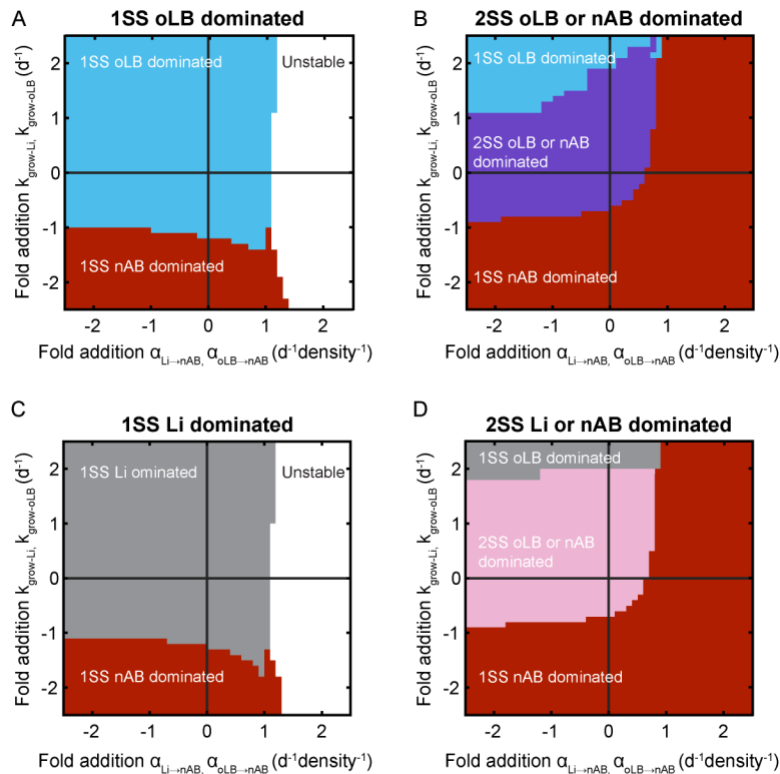


Figure 3.4.3 Bifurcation analysis to explore menses-associated parameter alterations.

Bifurcations were completed on each simulated sample for a given equilibrium behavior. Bifurcation plots represent the predicted equilibrium behavior subtype over a range of parameter changes. The most frequently observed equilibrium behavior across all simulated samples for a given parameter combination is plotted. Parameter changes are represented as a fold addition from the original parameter value. For example, the origin (0,0) indicates the baseline values for each sample and (-1,0.5) would indicate a 100% decrease in $\alpha_{oLB \rightarrow nAB}$ and $\alpha_{Li \rightarrow nAB}$ and a 50% increase in $k_{grow-Li}$ and $k_{grow-oLB}$. Menses-associated changes are in the lower right quadrant (decrease in the growth of oLB and Li, less negative interactions between oLB and Li on nAB). (A) 1SS oLB dominated (N = 388) (B) 2SS oLB dominated/nAB dominated (N = 58) (C) 1SS Li dominated (N = 123) (D) 2SS Li dominated/nAB dominated (N = 186) equilibrium subtypes.

parameters, requiring growth rates of oLB to be inhibited to point where these populations would be actively dying (negative; Figure 3.4.3A). In contrast, the multi-stable simulated samples

required less significant inhibition of oLB/Li growth and could be switched to a 1SS nAB dominated equilibrium behavior with only increases in the interaction of oLB and Li. on nAB ($\alpha_{Li \rightarrow nAB}$ and $\alpha_{oLB \rightarrow nAB}$; *Figure 3.4.3B*). These trends were mirrored in the global bifurcation of the 1SS Li dominated and the 2SS Li dominated/nAB dominated subtypes where the mono-stable groups were more resilient to changes in equilibrium behavior, and the multi-stable systems were more sensitive to switching to the 1SS nAB dominated equilibrium behavior (*Figure 3.4.3C,D*). These results demonstrate that multi-stable communities are more likely to switch to nAB dominated equilibrium subtypes for the same alteration of parameters than mono-stable communities.

Since the bifurcation analyses assume sustained alterations in parameters, it does not necessarily demonstrate mechanisms for dynamic and dramatic changes that can occur due to temporary. external alterations on microbial communities such as menses. Thus, a simulated seven-day menses was completed at four different menses ranging from a 50% decrease in $k_{grow-Li}$ and $k_{grow-oLB}$ and 50% increase in $\alpha_{Li \rightarrow nAB}$, $\alpha_{oLB \rightarrow nAB}$ to a 200% decrease in $k_{grow-Li}$ and $k_{grow-oLB}$ and 100% increase in $\alpha_{Li \rightarrow nAB}$, $\alpha_{oLB \rightarrow nAB}$ (*Figure 3.7.4*, *Figure 3.7.5*). Four magnitudes were evaluated because of uncertainty on how strongly vaginal microbiota. Of the simulated magnitudes, the perturbation that was most similar to the HMP clinical cohort was the 200% decrease in $k_{grow-Li}$ and $k_{grow-oLB}$ and 100% increase in $\alpha_{Li \rightarrow nAB}$, $\alpha_{oLB \rightarrow nAB}$ which was further evaluated by patients that were oLB dominated or Li dominated pre-menses (*Figure 3.4.4*).

For samples with equilibrium behaviors that are oLB dominant (1SS oLB dominated and 2SS oLB dominated/nAB dominated) the average sample exhibited a transient decrease in oLB abundance during menses (*Figure 3.4.4A*, left). Of the oLB dominated equilibrium behavior samples, 33.0% exhibited nAB dominance on the last day of menses (day 0, resilient group) and

8.1% of simulated samples exhibiting sustained nAB dominance at 1 month (day 30, *Figure 3.4.4A, middle*). Lastly, a subset of samples did not undergo a shift to nAB dominance as evaluated on the last day of menses (resilient group, *Figure 3.4.4A, right*).

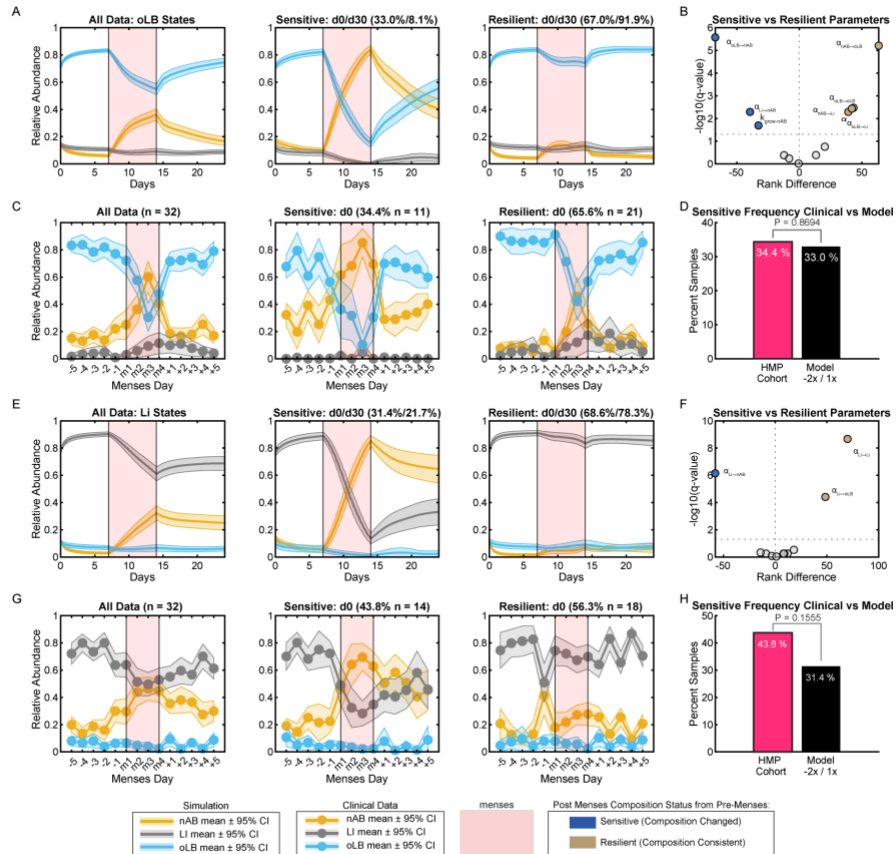


Figure 3.4.4 Menses-associated compositional fluctuations in silico and in clinical samples.

The analysis was stratified dependent on the *Lactobacillus* spp. that was dominant pre-menses (A-D) are associated with oLB dominated equilibrium behavior (1SS oLB dominated and 2SS oLB dominated/nAB dominated) and (E-H) are associated with Li dominated equilibrium behavior (1SS Li dominated and 2SS Li dominated/nAB dominated subtypes). (A) Mean and \pm 95% confidence interval of model predicted composition before, during (red), and after menses for nAB, Li, and oLB relative abundance. Data are plotted in aggregate (all data) and stratified by composition on the last day of menses. Samples that were nAB became dominant by the last day of menses were considered sensitive (middle) and those that remained *Lactobacillus* spp. dominant were considered resilient (right). (B) Mean and \pm 95% confidence interval of nAB, Li, and oLB relative abundance for the HMP cohort data five days before menses, four representative time points during menses, and five days after menses. Data are plotted by aggregate and response types as described in panel A. (C) Volcano plot comparing parameter differences between the sensitive (blue) and resilient (gold) response types from the model simulation. (D) Comparison of clinical versus model predictions for the frequency of menses-sensitive samples. (E-H) Corresponding analysis for the Li dominated states (E) Model simulations in aggregate and stratified by response type (F) Clinical observations in aggregate and stratified by response type. (G) Volcano plot of parameters that differ between response types. (H)

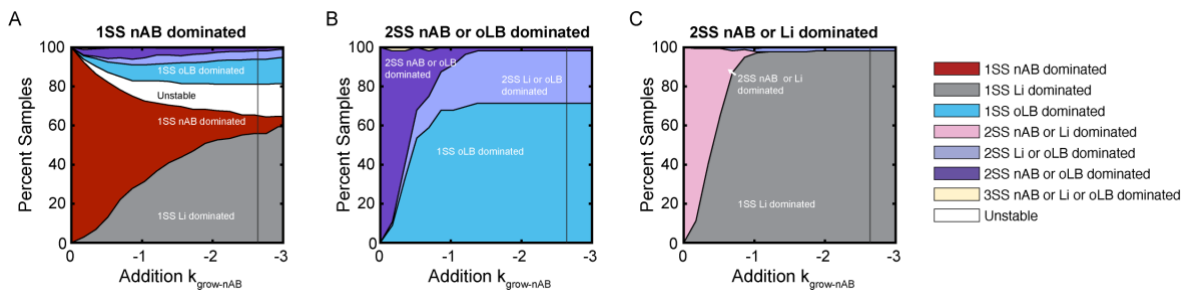
Comparison of clinical versus model predictions for the frequency of menses-sensitive samples. Statistical comparisons of frequency were made using χ^2 -tests. The magnitude of menses perturbation in this figure was $-200\% k_{\text{grow-oLB}}/k_{\text{grow-Li}}$ and $+100\% \alpha_{\text{oLB} \rightarrow \text{nAB}}/\alpha_{\text{oLi} \rightarrow \text{nAB}}$.

To identify microbial characteristics driving the differences in response to, multiple Mann-Whitney Rank Sum tests were completed to compare parameters associated with sensitive versus resilient menses response groups (*Figure 3.4.4B*). Drivers of sensitivity were the growth rate of the nAB species ($k_{\text{grow-nAB}}$) and the strength of oLB and Li inhibition of the nAB species ($\alpha_{\text{oLB} \rightarrow \text{nAB}}$ $\alpha_{\text{Li} \rightarrow \text{nAB}}$). In contrast, the interaction of the nAB species on oLB ($\alpha_{\text{nAB} \rightarrow \text{oLB}}$) was associated with resilience and stability. This parameter is an understudied interaction in vaginal communities as most research focuses on the inhibitory properties of oLB on nAB species when assessing probiotics and vaginal ecology [55]. Menses data from the HMP cohort was categorized by equilibrium behavior subtype and visualized in a comparable manner to the simulations, demonstrating similar trends in composition fluctuations due to menses (*Figure 3.4.4C*). Evaluation of the frequency of communities switched to nAB dominance after menses was comparable between the model predicted and clinically observed frequency (*Figure 3.4.4D*, 33.0% versus 34.4%, $P=0.8694$). This analysis was repeated for the Li-dominated equilibrium states (1SS Li dominated and 2SS Li dominated/ nAB dominated). Like the oLB states, on average Li abundance underwent transient composition shifts over time (*Figure 3.4.4E*, left). Of the simulated samples, 31.4% underwent a switch to nAB dominance as evaluated on the last day of menses (day 0, sensitive group, *Figure 3.4.4E*, middle) and 21.7% underwent sustained switches to nAB dominance (day 30). The remaining 68.6% of samples did not undergo a switch to nAB dominance at the last day of menses (resilient group, *Figure 3.4.4E*, right). Comparison of parameter value differences by volcano plot implicated the importance of Li on nAB ($\alpha_{\text{Li} \rightarrow \text{nAB}}$) and Li on oLB ($\alpha_{\text{Li} \rightarrow \text{oLB}}$) with the response groups, highlighting the need to better understand the

relationship of Li with facilitating or inhibiting vaginal microbiota associated with health and BV states (Figure 3.4.4F). Clinical data for the Li states was visualized by the overall average abundances (Figure 3.4.4G, left), the subset of sensitive samples (middle) and the subset of resilient samples (right). Evaluation of the frequency of communities switched to nAB dominance after menses was comparable between the model predicted and clinically observed frequency (Figure 3.4.4H, 31.4% versus 43.8%, $P = 0.1555$). Overall, this assessment supports the use of this modeling framework to predict response types to menses and to links microbial parameters that could be potential targets to promote stability of optimal composition.

3.4.4 BV clearance responses after antimicrobial therapy are associated with equilibrium behavior subtype

Antimicrobial therapies to treat bacterial vaginosis exhibit high rates of treatment failure, particularly recurrence [79]. To explore factors that can contribute to treatment failure, a bifurcation analysis and simulated course of antibiotics were completed for equilibrium behavior subtypes that can exhibit nAB dominance (1SS nAB dominated, 2SS nAB dominated/oLB dominated, 2SS nAB dominated/Li dominated). Like the menses analysis, the *in silico* HMP



population was used to replicate expected frequencies of each equilibrium behavior subtype. The

Figure 3.4.5 Bifurcation analysis to explore the impact of antibiotics on nAB dominated communities.

One-dimensional bifurcation analysis altering $k_{\text{grow-nAB}}$ to decrease to negative (death rates) to model antibiotic therapy. Colors indicate the equilibrium behavior subtype, and the y-axis is the percent of samples at each given value of $k_{\text{grow-nAB}}$ perturbation for (A) 1SS nAB dominated subtypes (B) 2SS nAB dominated/oLB dominated subtypes (C) 2SS nAB dominated/oLB dominated subtypes.

bifurcation analysis, which explore sustained alterations in the inhibition magnitude of nAB growth ($k_{\text{grow-nAB}}$) demonstrated that the 1SS nAB dominated communities required stronger inhibition to reach *Lactobacillus* spp. dominated equilibrium behavior subtypes (Figure 3.4.5A), whereas the 2SS nAB dominated/oLB dominated and 2SS nAB dominated/Li dominated communities switched to 1SS oLB dominated or 1SS Li dominated communities in greater than 50% of samples by the lowest decay rate reported in Mayer et al. 2015 (0.95 d^{-1} ; Table 3.7.4; Figure 3.4.5B,C).

Another challenge to understanding treatment failure arises from the temporal differences in BV clearance patterns. Individuals can exhibit no clearance of nAB during therapy (BV

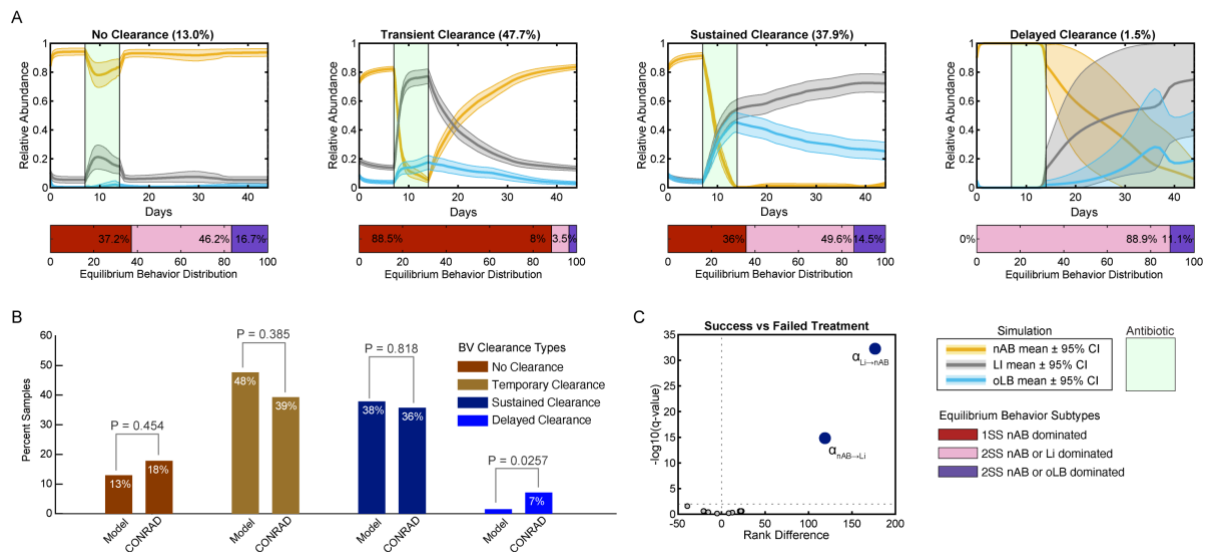


Figure 3.4.6 Predicted and clinically observed antibiotic response types.

(A) Model predicted antibiotic response types. Each plot depicts the mean and $\pm 95\%$ confidence interval for the relative abundance of nAB, Li, and oLB before antibiotic therapy, during antibiotic therapy (green), and the following month after therapy. The four plots represent trends observed in each response type (left to right): No response (no shift to oLB or Li dominance), temporary response (recurrence, initial oLB/Li dominance by last day of treatment, but returns to nAB dominance by 1 month), sustained response (cured, oLB/Li dominance at last day of treatment and 1 month later), and delayed response (nAB dominance at last day of treatment, oLB/Li dominance by 1 month). Below each plot is a breakdown of the percentage of equilibrium behaviors associated with each response type. (B) Comparison of model frequencies to the CONRAD BV cohort described in Gustin et al. 2022 ($N = 28$, χ^2 -tests). (C) Volcano plot exploring the parameter differences of model predicted treatment success group (sustained and delayed response) versus the treatment failure group (no response and recurrent response) samples using multiple Wilcoxon rank sum tests with FDR-adjusted p-values.

positive at therapy cessation and one month later), temporary clearance (BV negative at therapy

cessation, BV positive at 1 month), delayed clearance (BV positive at therapy cessation, BV negative at 1 month), or sustained clearance (BV negative at therapy succession and 1 month post [220]). To understand the complexities that microbial characteristics can contribute to these variable response types, a 7-day course of antibiotic was simulated by changing the growth rate of nAB ($k_{\text{grow-nAB}}$) to a decay rate. The decay rate was determined from clinical measurements of BV-associated bacteria abundance after a 5-day course of metronidazole gel (*Table 3.7.4*, [221]). Simulations were assessed across three equilibrium behavior subtypes associated with BV, the mono-stable subpopulation (1SS nAB dominated), and two types of multi-stable subpopulations (2SS nAB dominated/Li dominated and 2SS nAB dominated/oLB dominated) at frequencies defined by the HMP cohort. Simulation results recapitulated all four clearance types reported for bacterial vaginosis, with 13.0% of samples exhibited no shift to oLB/Li dominance (no clearance), 47.7% of samples exhibiting a temporary shift to oLB/Li dominance (BV recurrence, temporary clearance), 37.9% exhibiting a sustained shift to oLB/Li dominance through 1 month post therapy (cured, sustained clearance), and 1.5% exhibiting no composition shift by the end of treatment, but oLB/Li dominance 1 month post (delayed clearance, *Figure 3.4.6A*). These results agreed well with a cohort of 28 women reported by Gustin et al. 2022 (BV CONRAD cohort), which reported 18% no clearance, 39% temporary clearance, 36% sustained clearance, and 7% delayed clearance ($P = 0.454$, $P = 0.385$, $P = 0.818$, $P = 0.0257$, respectively with model predictions; *Figure 3.4.6B*). Using the model to gain insight into microbial parameters that may drive differences in therapy success, model parameters in simulated samples that underwent successful treatment vs failed treatment by 1 month were evaluated with multiple Wilcoxon Rank Sum tests and visualized on a volcano plot (*Figure 3.4.6C*). The main drivers that differentiated response types were the pairwise interactions between nAB and Li ($\alpha_{\text{Li} \rightarrow \text{nAB}}$,

$\alpha_{nAB \rightarrow Li}$), supporting the importance for better characterizing the relationship between Li and different species or strains of nAB. Notably, certain response types were associated with equilibrium behavior subtypes, particularly the transient BV clearance group suggesting recurrent BV may be driven by inherent microbial community stability to perturbations (*Figure 3.4.6A*).

3.4.5 Combinatorial therapies and modified treatment duration demonstrate alternative strategies to treat BV

To demonstrate how this framework could benefit the development of new BV therapies, we assessed how the combination of an antibiotic and prebiotic would impact treatment efficacy and the relationship between dose and treatment duration. For the combination prebiotic (increase in

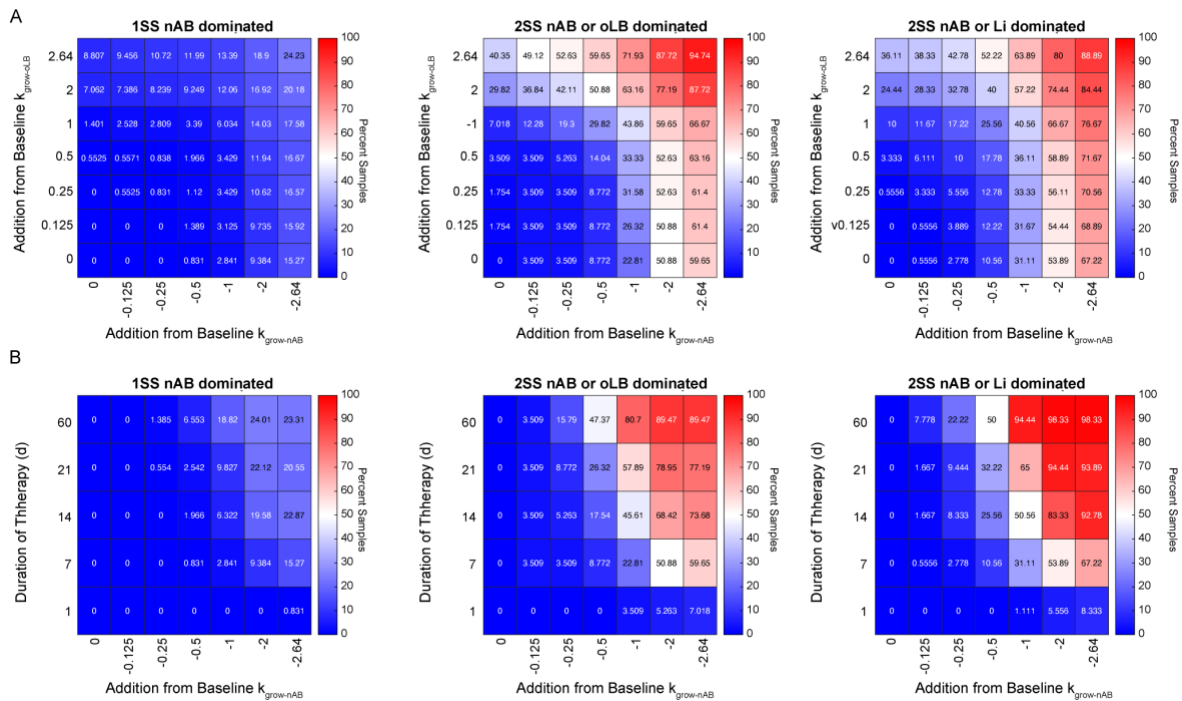


Figure 3.4.7 Simulated antibiotic regimens.

(A) Combination antibiotic ($k_{\text{grow-nAB}}$) and prebiotic ($k_{\text{grow-oLB}}$) across mono- and multi-stable subtypes. The percentage of parameter sets that underwent successful treatment 30 days after the regimen is displayed in the heatmap. (B) Alterations of antibiotic dose ($k_{\text{grow-nAB}}$) and duration. The percentage of parameter sets that underwent successful treatment 30 days after the regimen is displayed in the heatmap.

$k_{\text{grow-oLB}}$) and antibiotic (decrease in $k_{\text{grow-nAB}}$), forty-nine combinations of doses were tested ranging from no change to a 2.64 d^{-1} increase or decrease was simulated (*Figure 3.4.7A*). As observed previously, the 1SS nAB dominated subtype had the lowest rates of successful treatment (decreased nAB relative abundance to less than 50% at day 30 post treatment; maximally 24.2%) compared to the multi-stable subpopulations, which generally had higher success rates across all combinations of therapies (maximally 94.7% and 88.9% for the 2SS nAB dominated/oLB dominated and 2SS nAB dominated/Li dominated, respectively). Antibiotic impact on nAB growth rates was more important than prebiotic impact on oLB growth rates. Additionally, the maximum dose of only antibiotic had significantly higher success rates across the 1SS nAB dominated, 2SS nAB dominated/oLB dominated and 2SS nAB dominated/Li dominated subtypes compared to the maximum dose of only prebiotic ($P = 0.0091$, $P = 1.175 \times 10^{-5}$, $P = 3.50 \times 10^{-9}$). Similar trends were observed across the equilibrium subpopulations for the dose-duration analyses where the 1SS nAB dominated had lower success rates (maximally 23.3%) compared to the 2SS nAB dominated/oLB dominated and the 2SS nAB dominated/Li dominated (maximally 89.5% and 98.3%, *Figure 3.4.7B*). Long-term antibiotic therapies (60 days) had similar efficacy in clearing BV at one month as the maximum dose combination of prebiotic and antibiotic across the three groups (1SS nAB dominated group: 23.3% vs 24.2%, $P = 0.6389$; 2SS nAB dominated/oLB dominated: 89.5% vs 94.7%, $P = 0.0813$; and 2SS nAB dominated/Li dominated: 98.3% vs 88.9%, $P = 0.0511$). Overall, these results demonstrate that the model can be used to assess trade-offs between dose, duration, and the addition of new therapeutic strategies such as prebiotics.

3.5 Discussion

Here we show how linking ODE model equilibrium behavior with clinical VMB equilibrium behavior can give important insights into clinical VMB stability and dynamics in terms of microbial growth characteristics and interactions between species that are variable across women. This methodology overcomes challenges associated with the application of gLVMS to *in vivo* data, by using a top-down approach of matching parameter sets to observed equilibrium behaviors, rather than depending on direct parameter estimation from noisy, longitudinal data. From this methodology, the model predicted similar frequencies of mono- and multi-stable subpopulations as observed in a clinical cohort, which highlighted how clinically women exist in three main states: (1) Mono-stable optimal (1SS oLB dominated, 1SS Li dominated subpopulations); (2) Mono-stable non-optimal (1SS nAB dominated subpopulation) and (3) Multi-stable (many combinations). The multi-stable subpopulations, which comprised about a fifth of women, were observed across different combinations of CSTs, and were mainly associated with the 2SS Li dominated/nAB dominated subpopulation. We further demonstrated how mono-stable vs multi-stable subpopulations could help explain variable responses to menses and suboptimal treatment outcomes for BV. Moreover, the model helped identify microbial factors that dictated differences between subpopulations which could provide potential targets for new strategies to manage recurrent BV, pointing to the importance of nAB and *L. iners* interactions with oLB (*L. crispatus*, *L. jensenii*, *L. gasseri*). Overall, the results suggest modeling the VMB as an ecosystem with set equilibrium behaviors based on bacterial growth characteristics and interactions can improve understanding of VMB dynamics and help identify target microbial characteristics to assess at a mechanistic level (such as by characterizing metabolic drivers behind these terms) to treat or prevent BV.

Our work highlighted how ecological interactions could explain variable responses to menses and mainly pointed to the strength of *Lactobacillus* spp. inhibition of non-optimal anaerobic bacteria (nAB), suggesting supplementation of that interaction with treatments such as lactic acid supplements could promote stability in healthy individuals [98]. Notably, the model predicted that most women would undergo little to no shifts due to menses with even multi-stable simulated individuals switching in less than a quarter of scenarios. This result could be due to limitations in knowledge on how and to what degree menses impacts microbial parameters (growth characteristics or interaction terms). In comparison to the antibiotic simulations, the simulated impact of the menses parameters was small in absolute change, maintaining net positive growth rates for the *Lactobacillus* spp. and decreased interaction strengths by 50%, whereas the antibiotic simulations led to net negative growth rates for the nAB likely contributing to increased importance of multi-stability for antibiotic regimens [221].

A major motivation of this study was to determine if it is possible for the VMB to exist in mono-stable or multi-stable equilibrium states was to provide insight into responses to antibiotic therapy. The model and clinical observations support that many women exist in a mono-stable nAB dominated state, which suggests that most women with BV will have difficulty successfully resolving the condition after a 5-7 day regimen of antibiotics, even if the BV-associated bacteria (nAB) are sensitive to the antibiotic. This prediction was comparable to two clinical cohorts were assessed and aligns with the high rates of recurrence reported in the literature which range from 15-52% at 4 weeks or more after therapy [82]. In some women with a history of recurrent BV, alternative dosing regimens are recommended such as 750 mg metronidazole twice weekly for 3 months, but typically the benefits observed during treatment do not continue if the dosing is stopped [222]. Other regimens and new formulations have also been tested and have shown to

prolong time to BV recurrence, but no one method appears to be completely effective [223–225]. Overall, the implication of the VMB as a primarily mono-stable system suggests that long-term treatments (antibiotics, probiotics, prebiotics, intravaginal gels with active agents that inhibit BV-associated bacterial growth) would be more effective for those with recurrent BV, as these systems require permanent alterations that impact microbial parameters such as growth rates or interaction terms to re-orient the system to a new state. Candidate parameters implicated by our model included inhibition of the growth of the nAB ($k_{\text{grow-nAB}}$), and an understudied characteristic, the inhibition strength of nAB on oLB community members ($\alpha_{\text{nAB} \rightarrow \text{oLB}}$). The former would relate to traditional inhibition of BV-associated bacteria growth rates with long-term antibiotic treatments or other therapies inhibiting BV-associated bacteria growth (such as lactic acid containing products and boric acid) and the latter points to potential alternative strategies to re-condition the cervicovaginal microenvironment by decreasing the ability of nAB to outcompete oLB spp., which is likely mediated by metabolic phenotypes that are still poorly understood [47,48,57,226]. Additionally, the response of multi-stable subpopulations to antibiotic therapy indicated the importance of *L. iners*, both in its interaction with the oLB and nAB, suggesting competition between *L. iners* and oLB as well as cooperation with nAB could promote treatment failure. This duality is interesting, as reports indicate the *L. iners* phenotype can vary dependent on environmental and community contexts and may be a fulcrum point that leads to dramatic shifts in community composition [227]. *L. iners* is also of interest as a target during BV treatment, with recent publications suggesting elimination of *L. iners* promotes stable transition to more optimal *Lactobacillus* spp. dominance [60,61].

Lastly, the model was used to explore alternative regimens for BV therapy, including combinatorial therapies and alterations to antibiotic dose and duration. These simulations

highlight how the model may be applied to identify treatments that are most efficacious across a population with unknown stability status or to identify personalized regimens given a known stability status. A known stability status could be determined from a patient's history, which could be as simple as known recurrent episodes of BV (1SS nAB dominated subpopulation) to more nuanced identification of stability behavior which is becoming more accessible with companies tailored to personalized VMB characterization like Juno Bio and Evvy. Future developments of the model can also begin to characterize efficacy of probiotic therapies and the how the timing of probiotic therapy relative to the antibiotic regimen can impact predicted treatment efficacy[80]. Notably, from the context of our results and ecological theory, it will be important to characterize not only how the probiotic interacts with target, BV-associate bacteria (nAB), but also how a woman's existing vaginal microbiota interacts with the probiotic, as communities can commonly exclude newly introduced species (competitive exclusion) [228,229]. While the latter is likely intractable clinically as women can vary significantly in terms of composition, species, and strains, it could be simulated to identify key characteristics that make a probiotic most likely to succeed across a multitude of different VMBs.

While developing a personalized predictive model of VMB dynamics may be challenging, the generation of representative models that recapitulate clinically observed equilibrium subpopulations could provide insights for strategies to mitigate BV. By defining appropriate physiological ranges that capture interpersonal and intrapersonal variability, these models could be used to help develop therapies that are either effective in specific subpopulations (mono-stable vs multi-stable) or are effective more universally across heterogenous populations. Future studies are warranted to better define parameters that dictate the growth and interactions between microbial species in the vagina, as well as how host-

microbiome interactions may contribute to system dynamics (i.e., role of host-provided nutrients such as mucus). Cervicovaginal fluid composition, which is impacted by host-hormone and immune responses, likely dictates substrates required for microbial growth and ability to cross-feed or produce compounds that regulate the growth of other microbial species [47,230]. Additionally, interactions between BV-associated bacteria (nAB) or *L. iners* with vaginal epithelial cells could impact microbiome dynamics, as both produce cytolysins that lyse VECs increasing available nutrients, such as glycogen, which is preferentially metabolized by select vaginal species [48,57,63,70]. Models with increased resolution into these interactions through microbial metabolism of preferred carbon sources could help identify mechanisms of microbial shifts at the molecular level and help define new strategies to regulate the VMB.

3.6 Methods

3.6.1 Model Construction

A generalized Lotka-Volterra model (gLVM) with three equations was used as the ordinary differential equation-based model. gLVM include the growth rate of each species, the self-interaction term (contributes to carrying capacity) and inter-species interaction terms. Growth rates were always assumed to be positive when the system is not under any perturbation like menses of antibiotic therapy, self-interaction terms are assumed to always be negative and the inter-species interaction terms can be either positive or negative. For the three species model (oLB, Li or nAB), there are seven possible non-zero steady states. These seven states were related to clinical data using a nearest centroid classifier of the predicted relative abundances. The centroids were determined from VALENCIA (*Table 3.7.2*) [26]. All model simulations were completed in MATLAB 2020b and are published at: <https://doi.org/10.5281/zenodo.7843698>.

$$\begin{aligned}\frac{d[nAB]}{dt} &= k_{grow-nAB}[nAB] + \alpha_{nAB \rightarrow nAB}[nAB][nAB] + \alpha_{Li \rightarrow nAB}[nAB][Li] \\ &\quad + \alpha_{oLB \rightarrow nAB}[nAB][oLB] \\ \frac{d[Li]}{dt} &= k_{grow-Li}[Li] + \alpha_{Li \rightarrow Li}[Li][Li] + \alpha_{nAB \rightarrow Li}[Li][nAB] + \alpha_{oLB \rightarrow Li}[Li][oLB] \\ \frac{d[oLB]}{dt} &= k_{grow-oLB}[oLB] + \alpha_{oLB \rightarrow oLB}[oLB][oLB] + \alpha_{nAB \rightarrow oLB}[oLB][nAB] \\ &\quad + \alpha_{Li \rightarrow oLB}[oLB][Li]\end{aligned}$$

3.6.2 Parameter Selection

Parameter values were selected based on experimental and empirical observations (S1 Table). Since many of these parameters are unknown or expected to be variable, parameter value ranges were used throughout the manuscript. Often these parameter ranges were either based on calculations from digitized data as reported in Lee *et al.* (2020) or on assumptions of directionality (positive or negative interaction) from calculations or empirical observation. As the relative magnitude of inter-species interaction term relative to self-interaction term provides a normalized metric of interaction strength, maximum and minimum inter-species interaction terms were matched with experimental observations. By selecting a minimal self-interaction term of $-0.04 \text{ time}^{-1} \text{ density}^{-1}$ and a maximal inter-species interaction term of $\pm 0.12 \text{ time}^{-1} \text{ density}^{-1}$, a maximal ratio of $\pm 30x$ inter-/self-interactions was observed which was matched to maximal inter-/self-interactions strengths estimated from *in vitro* observations of various *Lactobacillus* strains co-cultured with *G. vaginalis* or *Prevotella bivia* providing a maximal absolute ratio of $40x$ (Figure 3.7.1). *In vivo* estimated gLV parameters were on the same order of magnitude of maximal inter/self-interaction ratio of $11x$. *In vitro* and *in vivo* time scales are reported to be

different, so *in vitro* parameter values are in terms of hours and *in vivo* parameters are in terms of days where relative differences between parameters are maintained [159].

3.6.3 Base *in silico* Population

Sensitivity analyses were completed on a global scale and in a two-dimensional global bifurcation analysis. For the global sensitivity analysis, Latin Hypercube Sampling (LHS) was used to generate parameter sets that have biological feasibility. Briefly, LHS is a stratified sampling method that evenly samples across defined parameter distributions. The parameter distributions used in this publication were defined from uniform distributions with minimum and maximum values reported in *Table 3.7.1*. Growth rates and inter-species interaction terms we set to range 10-fold based on calculate values from *in vitro* studies and ranged from $0.1 - 1.00 \text{ time}^{-1}$ and the inter-species interaction terms ranged from -0.004 to $-0.04 \text{ density}^{-1}\text{time}^{-1}$ (See S1 Table). Interspecies interaction terms ranged from $-0.12 - 0.12 \text{ density}^{-1}\text{time}^{-1}$, except in the case of oLB on nAB, as many reports suggest this interaction is only negative ($-0.12 - 0 \text{ density}^{-1}\text{time}^{-1}$). Then, each of the parameter sets ($N = 5,000$) was analytically assessed for steady state stability using local stability analysis, which determines which of the seven non-zero states are stable (Supplementary Text).

3.6.4 Bifurcation Analyses

For the two-dimensional bifurcation analysis, a base parameter set with known steady-state behavior was selected and two groups of parameters (growth rates versus inter-species interaction terms) were varied from that starting point over the combination of 50x50 parameter combinations. For each of the 2,500 parameter combinations the stability of the steady states was evaluated using local stability analyses. This process was repeated for all LHS parameter sets

that had the same equilibrium behavior. For example, for all LHS sets that were 1SS oLB dominated 2,500 parameter combinations were calculated for each and the most frequently observed equilibrium behavior at each point was plotted.

3.6.5 Perturbation Analyses

Perturbation analyses were completed to simulate menses and antibiotic therapy using the *in silico* HMP cohort with certain equilibrium behaviors. For the menses analyses, the 1SS oLB dominated, 2SS oLB dominated/nAB dominated, 1SS Li dominated, 2SS Li dominated/nAB dominated were assessed with a perturbation that decreased the growth rates for Li and oLB ($k_{\text{grow-Li}}$ and $k_{\text{grow-oLB}}$) as well as the interaction terms for oLB/Li on nAB ($\alpha_{\text{oLB} \rightarrow \text{nAB}}$ and $\alpha_{\text{Li} \rightarrow \text{nAB}}$) over four set menses indices where “p” indicates the original parameter value (control/no change: $k_{\text{grow-Li}}$ and $k_{\text{grow-oLB}} = p + 0.0 \times p$, $\alpha_{\text{oLB} \rightarrow \text{nAB}}$ and $\alpha_{\text{Li} \rightarrow \text{nAB}} = p + 0.0 \times p$; light: $k_{\text{grow-Li}}$ and $k_{\text{grow-oLB}} = p - 0.5 \times p$, $\alpha_{\text{oLB} \rightarrow \text{nAB}}$ and $\alpha_{\text{Li} \rightarrow \text{nAB}} = p + 0.5 \times p$; moderate: $k_{\text{grow-Li}}$ and $k_{\text{grow-oLB}} = p - 1.0 \times p$, $\alpha_{\text{oLB} \rightarrow \text{nAB}}$ and $\alpha_{\text{Li} \rightarrow \text{nAB}} = p + 1.0 \times p$; and strong: $k_{\text{grow-Li}}$ and $k_{\text{grow-oLB}} = p - 2.0 \times p$, $\alpha_{\text{oLB} \rightarrow \text{nAB}}$ and $\alpha_{\text{Li} \rightarrow \text{nAB}} = p + 1.0 \times p$). The average trajectory $\pm 95\%$ confidence interval of all the parameter sets exhibiting sensitivity or resilience to the menses perturbation were plotted and the number of simulated samples that had switched to a BV state (nAB composition greater than 50%) at day 0 and 30 after menses completed was reported. Menses sensitive individuals were defined as shifting to nAB dominance evaluated on the last day of the simulated menses. Parameters differentiated sensitive versus resilient groups were compared using multiple Mann-Whitney Rank Sum tests with FDR-adjusted p-values. Frequencies of menses sensitive individuals were compared with the strongest menses index to the clinical data using χ^2 -tests.

For the antibiotic simulations, the simulated samples analyzed were in the 1SS nAB dominated, 2SS nAB dominated/Li dominated and the 2SS nAB dominated/oLB dominated

subpopulations, with the perturbation modeled off a decrease in nAB growth rate ($k_{\text{grow-nAB}}$ minus 2.64 d^{-1}) calculated from digitized data in reporting shifts in BV associated bacteria (nAB) following antibiotic treatment clinically (*Table 3.7.4*) [221]. The average trajectory $\pm 95\%$ confidence interval of all the parameter sets exhibiting sensitivity or resilience to the antibiotic perturbation were plotted and the number of simulated samples that had switched to a *Lactobacillus* spp. dominated state (nAB composition less than 50%) at day 0 and 30 after the antibiotic regimen was completed was reported. The frequency of four BV clearance profiles was analyzed and compared to reported frequencies in the CONRAD BV cohort based on the day 0 and day 30 post-antibiotic composition. Parameters differentiated sensitive versus resilient groups were compared using multiple Mann-Whitney Rank Sum tests with FDR-adjusted p-values.

3.6.6 Clinical Datasets

The University of Maryland Baltimore, Human Microbiome Project (UMB-HMP) cohort data was previously published (Ravel et al., 2013 [115]) and all data provided was de-identified to this study. The original study was an observational prospective study, where treatment information was recorded daily by the participants and during a clinical exam at week 5 and week 10 for 135 nonpregnant women of reproductive age. Self-identified ethnicities of the 101 patients that met inclusion criteria (greater than 10 samples) were Black/African descent (60%), White/Caucasian (34%), Hispanic/Latina (5.0%), multi-racial (1%). Within this study, metronidazole treatment was provided as standard of care, as recommended by the CDC (Metronidazole 500 mg orally twice a day for 7 days) [82,207]. The original study protocol was approved by the Institutional Review Board of the University of Alabama at Birmingham and the University of Maryland School of Medicine. Written informed consent was appropriately

obtained from all participants, who also provided consent for storage and use in future research studies related to women's health. Patients self-collected cervicovaginal swabs for 10 weeks. Vaginal microbiota data was generated by sequencing the V3-V4 regions of the 16S rRNA gene and is available in dbGAP under BioProject PRJNA208535. Menses time series data were analyzed by extracting composition data for the five days prior and five days post menses, for all occurrences of menstrual bleeding longer than 3 days.

The Gajer cohort was previously published and data were downloaded from the supplementary files [22]. Briefly, the study collected longitudinal samples, twice weekly for 16 weeks in healthy reproductive-age women (n = 32) and quantified bacterial diversity using pyrosequencing of V1-V2 regions of 16S rRNA genes. Ethnicities of the 32 women included individuals that self-identified as White (41%), Black (50%), Hispanic (6%), or other (3%).

The CONRAD BV study has previously been described [78,220]. Patients with Nugent score of 4 or higher were screened across three visits, pre-treatment (visit 1), 7-10 days post-treatment (visit 2), and 28-32 days post-treatment (visit 3). Self-reported ethnicities in the original study included Hispanic White (3%), Hispanic Black (3%), Non-Hispanic Black (79%), Non-Hispanic White (6%), and mixed race (9%). Response types were characterized by patterns observed across the three visits, namely whether individuals improved to a *Lactobacillus* spp. dominated CST. Of the 28 patients, 25% failed to clear BV (no clearance), 35.7% exhibited transient clearance, 7.1% exhibited clearance at the final visit (delayed clearance), and 32.1% exhibited sustained clearance. These frequencies were compared with model predicted BV clearance profiles using Chi-square tests.

The UMB-HMP and Gajer cohort data were assessed for multi-stability by analyzing patients who had greater than 10 sampled time points (HMP, N = 101; Gajer, N = 32). Each time

point was converted to a CST type using the nearest centroid classifier described above (required conversion of relative abundance data to oLB, Li and nAB dominated groups). Using the classified CSTs at each time point, a matrix of state transitions was generated, which describes the frequency fluctuations in CST states, with individuals who are stable staying in “within” state CSTs. Transition matrices were then used to identify mono-stable vs multi-stable individuals using a nearest centroid classifier, where centroids were based at 100% within state transitions (mono-stable) and 50%/50% of pairwise CSTs (bi-stable).

3.6.7 Code and Data Availability

The code and data used to generate the model simulations are published (<https://doi.org/10.5281/zenodo.7843698>).

3.7 Appendix

3.7.1 Supplementary Figures

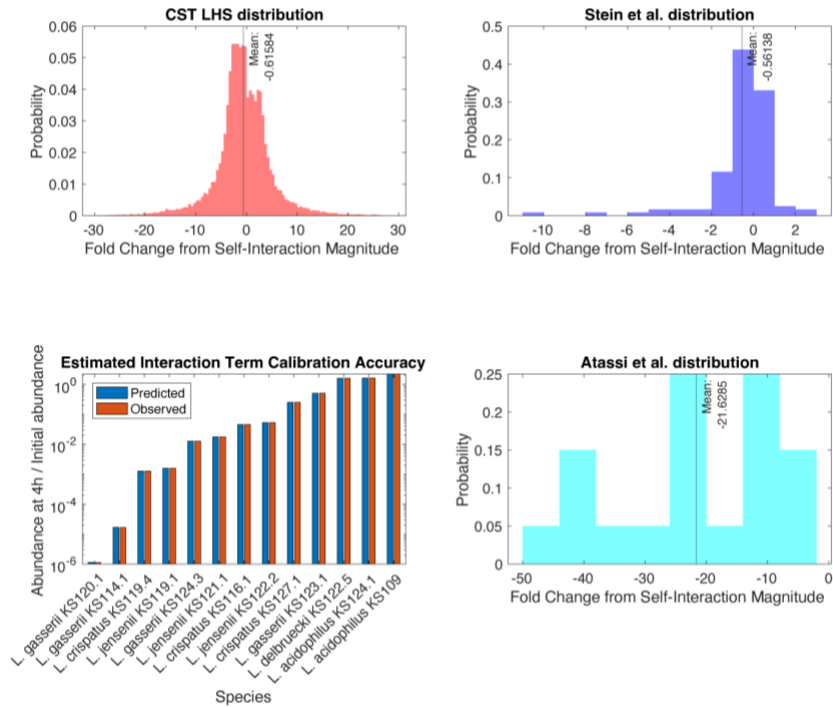


Figure 3.7.1 Analysis of Inter-species/Self-interaction Parameter Ranges.

The maximum magnitude of parameter ranges was set based on relative estimation of inter-species interaction terms to intra-species interaction terms, reaching $\pm 30x$ using the selected parameter ranges in S1 Table (top left histogram). These ranges are on the same order of magnitude as gLV parameters estimated from in vivo gut microbiome experiments (Stein et al., 2013/[159]; top right histogram). Interaction terms calculated from Atassi et al. 2006/[55] in vitro co-cultures observed high estimated ratios of inter/self-interaction terms, of up to 46x.

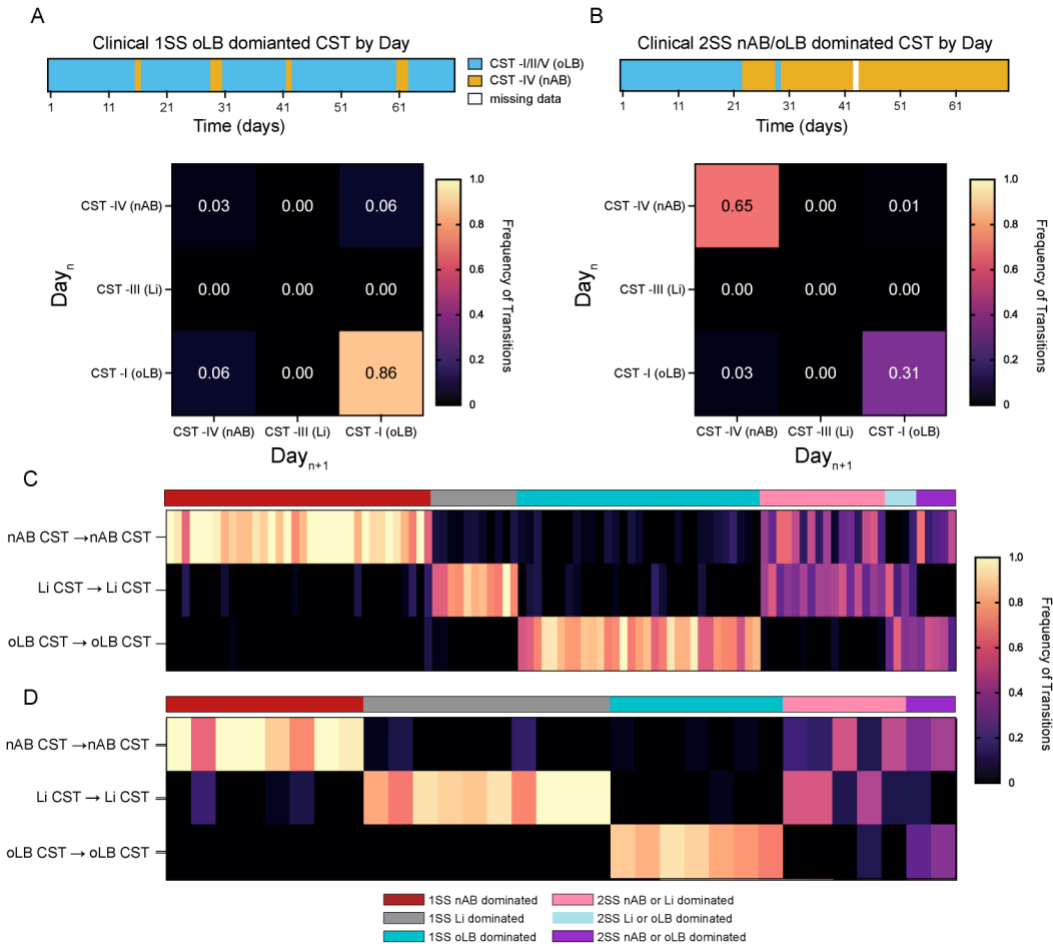


Figure 3.7.2 Determination of Clinical Equilibrium Behavior Subtypes.

(A-B) Example time series CST classifications from two patients in the HMP cohort and their respective state transition frequencies. State transition matrices display the frequency of switches across a time step, where combinations across the diagonal indicate the current time step and the next time step were in the same compositional state. (A) Example of a 1SS oLB dominated equilibrium behavior. (B) Example of 2SS nAB or oLB dominated equilibrium behavior. (C-D) Classification of each patient to an equilibrium behavior based on the frequency at which the patient remained within a transition state over each time step for (C) the HMP cohort (N = 101) and (D) the Gajer et al. cohort (N = 32).

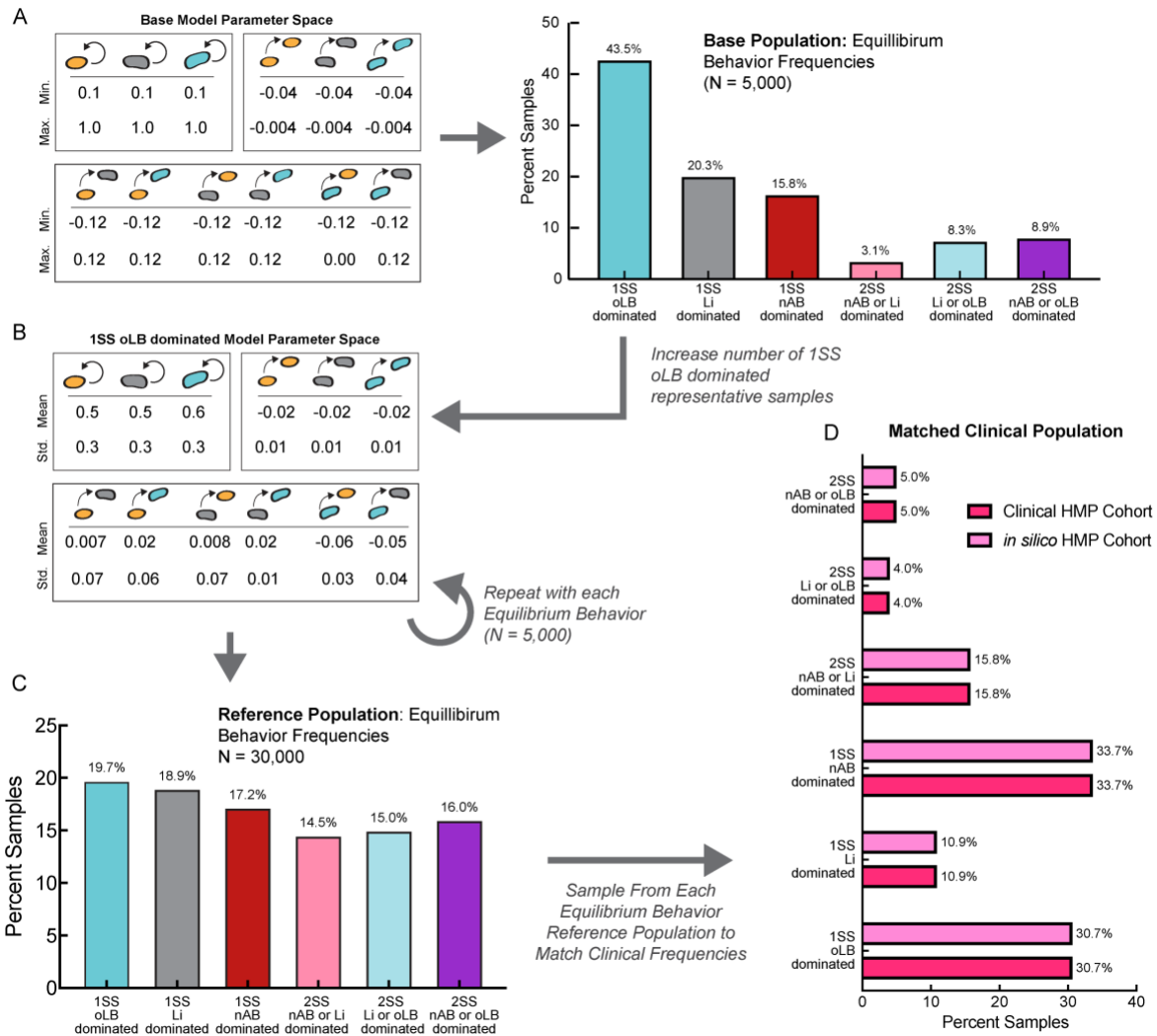


Figure 3.7.3 Generating matched *in silico* populations to clinical data.

(A) Workflow to create base population parameter sets from empirical observations for parameter ranges. (B) Creation of a reference population for each equilibrium behavior subtype. For example, the parameter sets generated in the base population that had 1SS oLB dominated equilibrium behavior were used to create a new probability distribution for each parameter to sample with Latin Hypercube Sampling. For each equilibrium behavior, 5000 parameter sets were selected from the equilibrium behavior specific probability distribution to create a reference population for each equilibrium type shown in panel (C). Lastly, parameter sets were randomly sampled at frequencies defined by clinical observations to create an *in silico* cohort tailored to a specific clinical cohort shown in (D).

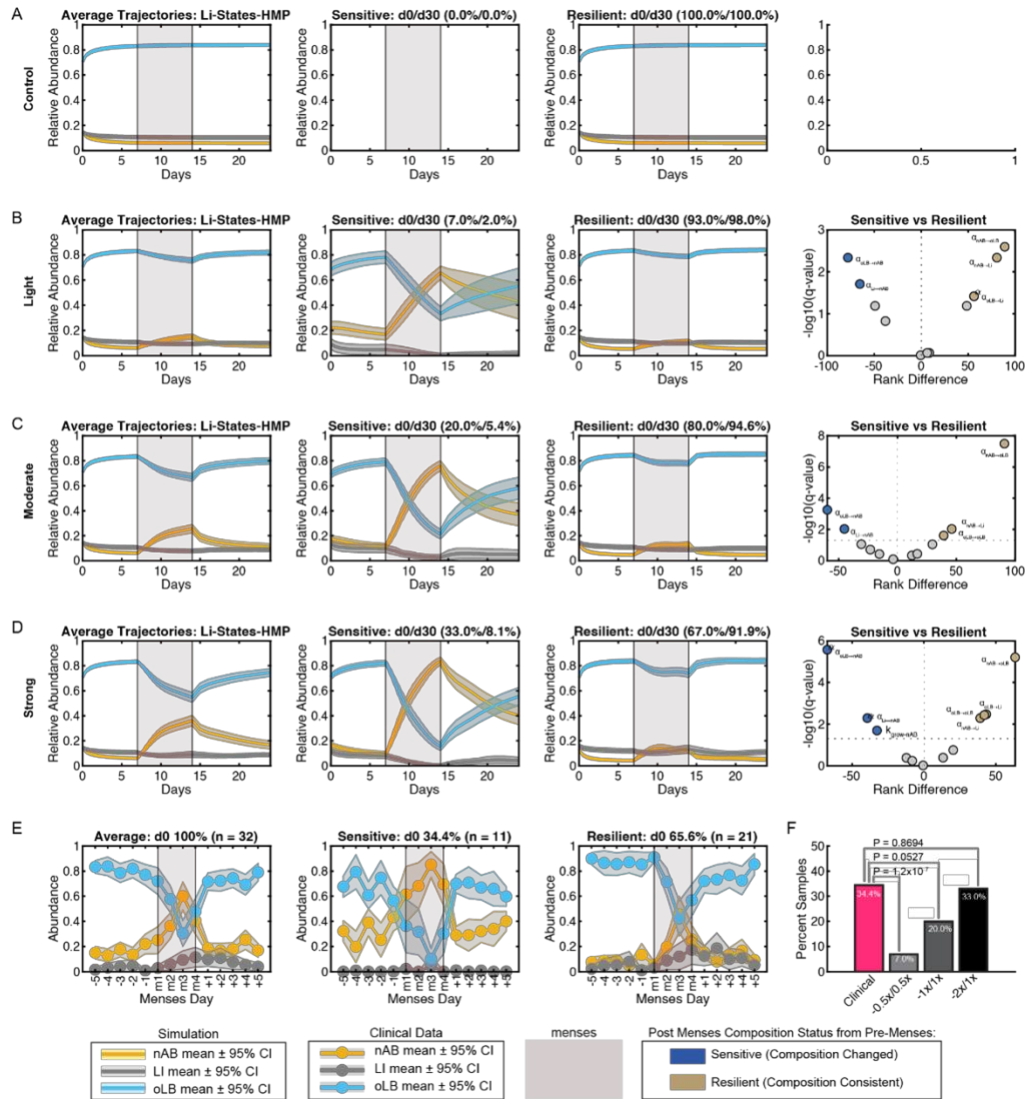


Figure 3.7.4 Menses simulations at varying degrees of simulated strength for oLB dominated states.

In (A-D) plots indicate the average of all simulated samples (left), the average for a subset of samples that undergo a composition shift (middle), and the average for a subset that does not undergo a composition shift (right) and a volcano plot representing parameters that significantly differed in the sensitive and resilient samples. (A) The impact of no parameter change on samples used in the menses analysis (control). (B) The impact of a $-0.5x$ fold addition to $k_{\text{grow-Li}}$ and $k_{\text{grow-oLB}}$ with a $+0.5x$ folder addition to $\alpha_{\text{Li} \rightarrow \text{nAB}}$ and $\alpha_{\text{oLB} \rightarrow \text{nAB}}$ (light perturbation). (C) The impact of a $-1x$ fold addition to $k_{\text{grow-Li}}$ and $k_{\text{grow-oLB}}$ with a $+1x$ folder addition to $\alpha_{\text{Li} \rightarrow \text{nAB}}$ and $\alpha_{\text{oLB} \rightarrow \text{nAB}}$ (moderate perturbation). (D) The impact of a $-2x$ fold addition to $k_{\text{grow-Li}}$ and $k_{\text{grow-oLB}}$ with a $+1x$ folder addition to $\alpha_{\text{Li} \rightarrow \text{nAB}}$ and $\alpha_{\text{oLB} \rightarrow \text{nAB}}$ (strong perturbation). (E) Clinical observations for all samples (left), sensitive samples (middle) and resilient samples (right). (F) Statistical comparison of clinically observed sensitive sample frequency with model predicted frequencies at varying degrees of menses strength described in panels B-D. Statistical comparisons were made using χ^2 -tests.

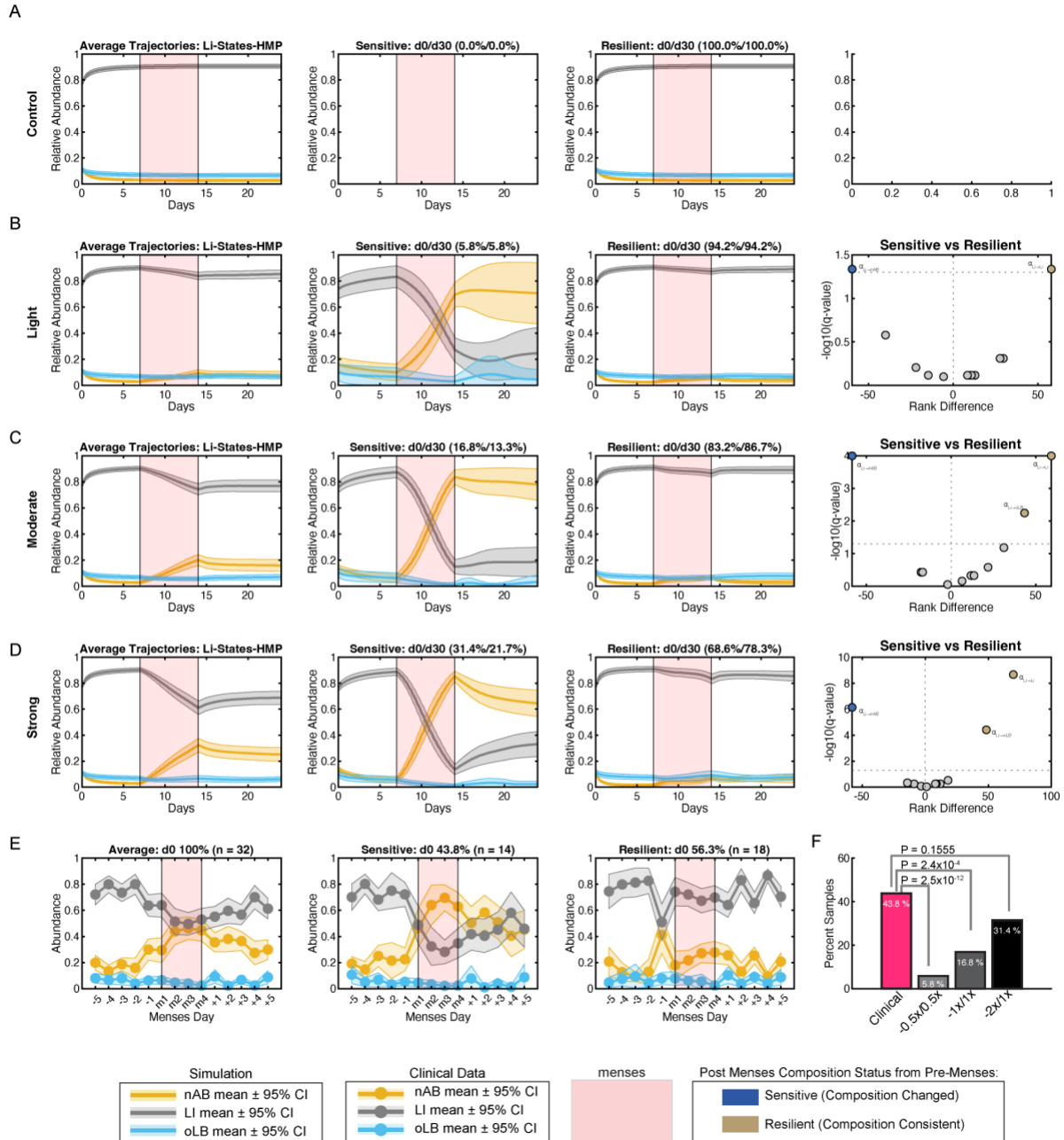


Figure 3.7.5 Menses simulations at varying degrees of simulated strength for Li dominated states.

In (A-D) plots indicate the average of all simulated samples (left), the average for a subset of samples that undergo a composition shift (middle), and the average for a subset that does not undergo a composition shift (right) and a volcano plot representing parameters that significantly differed in the sensitive and resilient samples. (A) The impact of no parameter changes on samples used in the menses analysis (control). (B) The impact of a $-0.5x$ fold addition to $k_{\text{grow-Li}}$ and $k_{\text{grow-oLB}}$ with a $+0.5x$ folder addition to $\alpha_{\text{Li} \rightarrow \text{nAB}}$ and $\alpha_{\text{oLB} \rightarrow \text{nAB}}$ (light perturbation). (C) The impact of a $-1x$ fold addition to $k_{\text{grow-Li}}$ and $k_{\text{grow-oLB}}$ with a $+1x$ folder addition to $\alpha_{\text{Li} \rightarrow \text{nAB}}$ and $\alpha_{\text{oLB} \rightarrow \text{nAB}}$ (moderate perturbation). (D) The impact of a $-2x$ fold addition to $k_{\text{grow-Li}}$ and $k_{\text{grow-oLB}}$ with a $+1x$ folder addition to $\alpha_{\text{Li} \rightarrow \text{nAB}}$ and $\alpha_{\text{oLB} \rightarrow \text{nAB}}$ (strong perturbation). (E) Clinical observations for all samples (left), sensitive samples (middle) and resilient samples (right). (F) Statistical comparison of clinically observed sensitive sample frequency with model predicted

frequencies at varying degrees of menses strength described in panels B-D. Statistical comparisons were made using χ^2 -tests.

3.7.2 Supplementary Tables

Table 3.7.1 Description of LHS parameter ranges.

Note the determination of inter-species interaction terms was based on empirical observation and hypothesis on interaction term strength and directionality. More information is in *Figure 3.7.1*.

Parameter	Value	Explanation	References
$k_{\text{grow-nAB}}$ (hr^{-1})	0.1 to 1.00	Growth rate calculated in previous publication from growth curves (Lee et al., 2020)[20] and assessed from digitized growth curves from literature such as Atassi et al., 2019[55] and Anukam and Reid (2008)[187].	[20,56,187]
$k_{\text{grow-Li}}$ (hr^{-1})	0.1 to 1.00	Growth rate calculated in previous publication from growth curves (Lee et al., 2020)[20] and from doubling times (Borgogna et al., 2021)[75].	[20,75]
$k_{\text{grow-oLB}}$ (hr^{-1})	0.1 to 1.00	Growth rate calculated in previous publication from growth curves (Lee et al., 2020) and from digitized data in Chetwin et al., 2019[101] and Juarez-Tomas (2003) [204] as well as Borgogna et al (2021)[75].	[20,75,101,230]
$\alpha_{\text{nAB} \rightarrow \text{nAB}}, \alpha_{\text{Li} \rightarrow \text{Li}}, \alpha_{\text{oLB} \rightarrow \text{oLB}}$ ($\text{hr}^{-1}\text{cell density}^{-1}$)	-0.004 to -0.04	Assumed similar carrying capacities are possible across species and a 10-fold variability. This value and the growth rate value facilitate up to 100-fold variation in carry capacity and clinically relative abundance can upwards of range 1000-fold.	[21,22,115]
$\alpha_{\text{nAB} \rightarrow \text{Li}}, \alpha_{\text{nAB} \rightarrow \text{oLB}}, \alpha_{\text{Li} \rightarrow \text{nAB}}, \alpha_{\text{Li} \rightarrow \text{oLB}}, \alpha_{\text{oLB} \rightarrow \text{Li}}$ ($\text{hr}^{-1}\text{cell density}^{-1}$)	-0.12 to 0.12	Assumed directionally of these parameters to be positive or negative dependent on the literature. Magnitude of the values was determined from the largest ratio of interaction term to self-interact term observed experimentally (S1 Fig). The fold-ratio is on the same order of magnitude as clinically estimated gLV terms (Stein et al. 2013).	[59,159,206]
$\alpha_{\text{oLB} \rightarrow \text{nAB}}$ ($\text{hr}^{-1}\text{cell density}^{-1}$)	-0.12 to 0.00	Assume directionality based on experimental observations that oLB spp. commonly inhibit non-optimal spp. (nAB), such as in Atassi et al. (2006).	[55,206]

Table 3.7.2 Model CST centroids.

	Relative Abundance		
	nAB	Li	oLB
[nAB dominated] CST-IV	0.912	0.0592	0.0289
[Li dominated] CST-III	0.146	0.759	0.0946
[oLB dominated] CST -I/II/V	0.153	0.0952	0.752

Table 3.7.3 Examples of how external factors can be simulated in the modeling framework.

External Factor	Methodology	Parameters Impacted
BV Therapy (Metronidazole or Clindamycin)	1. Identified metronidazole impact on nAB is <i>in vivo</i> , from reported estimates on nAB population decay rates across multiple species with absolute abundance measurements [221]	1. Population growth rate of nAB becomes negative (death rate), metronidazole is bactericidal
Menses	1. Identified how menses impact vaginal microbial species (impact of increased biogenic amines associated with CST -IV and menses)	1. Biogenic amines are associated with decreased growth rates <i>L. crispatus</i> , <i>L. gasseri</i> , <i>L. jensenii</i> , and <i>L. iners</i> as well as decreased D/L-lactic acid production [75]
Sexual Behavior / Partner Microbiome	1. Model transfer of microbial species by “spiking in” microbial species into pre-existing <i>in silico</i> patient 2. Model the impact of increased pH associated with sexual activity (semen, lubricant, etc.)	1. Alter abundance of model species at the frequency of sexual activity 2. Increased pH could alter growth rates (increase growth rate of nAB [96,231]) and decrease the impact of lactic acid/bacteriocins on nAB [55,56,232]
Hygienic Behavior	1. Model loss or “wash out” of microbial species present in the pre-existing <i>in silico</i> patient 2. Model the impact of increased pH due to douching	1. Alter abundance of model species at the frequency of douching 2. Increased pH could alter growth rates (increase growth rate of nAB [96,231]) and decrease the impact of lactic acid/bacteriocins on nAB [55,56,232]
Antifungal Therapy	1. Would need to identify the impact of antifungals on microbial growth rates (reports are limited and some indicate that azithromycin, clotrimazole, or fluconazole have no substantial impact on <i>Lactobacillus</i> spp. [233,234])	1. Model change in microbial parameters (currently no <i>in vitro</i> data to support which parameters are impacted)
Contraceptives	1. Identify impact of contraceptive on the vaginal microenvironment (e.g., glycogen and mucus levels) 2. Model competitive advantages gained by <i>Lactobacillus</i> spp.	Increased glycogen is associated with acidification of the vaginal that would promote stronger inhibition of nAB [47,48]

Table 3.7.4 Digitized decay rates of BV associated bacteria treated with intravaginal metronidazole.

Calculated Decay Rate (d ⁻¹)					
<i>G. vaginalis</i>	BVAB2	BVAB1	<i>Sneathia/Lepto</i>	<i>Megasphaera</i>	<i>A. vaginae</i>
3.82	4.61	3.50	5.04	4.08	5.44
3.12	2.15	2.26	4.18	4.08	4.81
2.45	2.15	2.26	3.19	3.88	4.81

2.12	2.15	2.08	2.87	2.76	3.80
1.84	1.88		2.41	2.03	3.48
1.72	1.69		2.13	2.03	3.23
1.40	1.66		2.07	2.03	2.38
1.33			1.82	1.74	1.88
1.33			1.73		1.88
0.95			1.44		1.54

3.7.3 Supplementary Text

Steady-States:

1. $(0, 0, 0)$
2. $\left(\frac{\alpha_{Li \rightarrow nAB} \mu_{Li} - \alpha_{Li \rightarrow Li} \mu_{nAB}}{\alpha_{nAB \rightarrow nAB} \alpha_{Li \rightarrow Li} - \alpha_{nAB \rightarrow Li} \alpha_{Li \rightarrow nAB}}, - \frac{\alpha_{nAB \rightarrow nAB} \mu_{Li} - \alpha_{nAB \rightarrow Li} \mu_{nAB}}{\alpha_{nAB \rightarrow nAB} \alpha_{Li \rightarrow Li} - \alpha_{nAB \rightarrow Li} \alpha_{Li \rightarrow nAB}}, 0 \right)$
3. $\left(\frac{\alpha_{oLB \rightarrow nAB} \mu_{oLB} - \alpha_{oLB \rightarrow oLB} \mu_{nAB}}{\alpha_{nAB \rightarrow nAB} \alpha_{oLB \rightarrow oLB} - \alpha_{nAB \rightarrow oLB} \alpha_{oLB \rightarrow nAB}}, 0, \frac{\alpha_{nAB \rightarrow nAB} \mu_{oLB} - \alpha_{nAB \rightarrow oLB} \mu_{nAB}}{\alpha_{nAB \rightarrow nAB} \alpha_{oLB \rightarrow oLB} - \alpha_{nAB \rightarrow oLB} \alpha_{oLB \rightarrow nAB}} \right)$
4. $\left(0, \frac{\alpha_{oLB \rightarrow Li} \mu_{oLB} - \alpha_{oLB \rightarrow oLB} \mu_{Li}}{\alpha_{oLB \rightarrow oLB} \alpha_{Li \rightarrow Li} - \alpha_{oLB \rightarrow Li} \alpha_{Li \rightarrow oLB}}, - \frac{\alpha_{Li \rightarrow Li} \mu_{oLB} - \alpha_{Li \rightarrow oLB} \mu_{Li}}{\alpha_{oLB \rightarrow oLB} \alpha_{Li \rightarrow Li} - \alpha_{oLB \rightarrow Li} \alpha_{Li \rightarrow oLB}}, 0 \right)$
5. $\left(- \frac{\mu_{nAB}}{\alpha_{nAB \rightarrow nAB}}, 0, 0 \right)$
6. $\left(0, - \frac{\mu_{Li}}{\alpha_{Li \rightarrow Li}}, 0 \right)$
7. $\left(0, 0, - \frac{\mu_{oLB}}{\alpha_{oLB \rightarrow oLB}} \right)$
8. $\left(- \frac{\alpha_{Li \rightarrow nAB} \alpha_{oLB \rightarrow Li} \mu_{oLB} - \alpha_{nAB \rightarrow Li} \alpha_{oLB \rightarrow oLB} \mu_{oLi} + \alpha_{Li \rightarrow Li} \alpha_{oLB \rightarrow oLB} \mu_{nAB} + \alpha_{Li \rightarrow oLB} \alpha_{oLB \rightarrow Li} \mu_{Li} - \alpha_{Li \rightarrow oLB} \alpha_{oLB \rightarrow Li} \mu_{nAB}}{\alpha_{nAB \rightarrow nAB} \alpha_{Li \rightarrow Li} \alpha_{oLB \rightarrow oLB} - \alpha_{nAB \rightarrow nAB} \alpha_{Li \rightarrow oLB} \alpha_{oLB \rightarrow Li} - \alpha_{nAB \rightarrow Li} \alpha_{Li \rightarrow nAB} \alpha_{oLB \rightarrow Li} + \alpha_{nAB \rightarrow oLB} \alpha_{Li \rightarrow nAB} \alpha_{oLB \rightarrow Li} + \alpha_{nAB \rightarrow oLB} \alpha_{Li \rightarrow Li} \alpha_{oLB \rightarrow nAB}}, \right.$
 $\left. - \frac{\alpha_{Li \rightarrow nAB} \alpha_{oLB \rightarrow Li} \mu_{oLB} - \alpha_{Li \rightarrow nAB} \alpha_{oLB \rightarrow oLB} \mu_{Li} + \alpha_{Li \rightarrow Li} \alpha_{oLB \rightarrow nAB} \mu_{oLB} + \alpha_{Li \rightarrow Li} \alpha_{oLB \rightarrow oLB} \mu_{nAB} - \alpha_{Li \rightarrow oLB} \alpha_{oLB \rightarrow Li} \mu_{nAB}}{\alpha_{nAB \rightarrow nAB} \alpha_{Li \rightarrow Li} \alpha_{oLB \rightarrow oLB} - \alpha_{nAB \rightarrow nAB} \alpha_{Li \rightarrow oLB} \alpha_{oLB \rightarrow Li} - \alpha_{nAB \rightarrow Li} \alpha_{Li \rightarrow nAB} \alpha_{oLB \rightarrow Li} + \alpha_{nAB \rightarrow oLB} \alpha_{Li \rightarrow nAB} \alpha_{oLB \rightarrow Li} + \alpha_{nAB \rightarrow oLB} \alpha_{Li \rightarrow Li} \alpha_{oLB \rightarrow nAB}}, \right.$
 $\left. \frac{\alpha_{NO \rightarrow NO} \alpha_{oLB \rightarrow Li} \mu_{oLB} - \alpha_{NO \rightarrow NO} \alpha_{oLB \rightarrow oLB} \mu_{Li} + \alpha_{NO \rightarrow Li} \alpha_{oLB \rightarrow oLB} \mu_{NO} + \alpha_{NO \rightarrow oLB} \alpha_{oLB \rightarrow NO} \mu_{Li} - \alpha_{NO \rightarrow oLB} \alpha_{oLB \rightarrow Li} \mu_{NO}}{\alpha_{nAB \rightarrow nAB} \alpha_{Li \rightarrow Li} \alpha_{oLB \rightarrow oLB} - \alpha_{nAB \rightarrow nAB} \alpha_{Li \rightarrow oLB} \alpha_{oLB \rightarrow Li} - \alpha_{nAB \rightarrow Li} \alpha_{Li \rightarrow nAB} \alpha_{oLB \rightarrow Li} + \alpha_{nAB \rightarrow oLB} \alpha_{Li \rightarrow nAB} \alpha_{oLB \rightarrow Li} + \alpha_{nAB \rightarrow oLB} \alpha_{Li \rightarrow Li} \alpha_{oLB \rightarrow nAB}} \right)$

Example Stability Conditions:

The 100% nAB state, the eigen values of the Jacobian must be less than zero. Therefore, given the below eigen values the effect of the existing species (nAB) on the eliminated species (Li and oLB) must be negative.

$$\lambda_1 = \mu_{Li} + \alpha_{nAB \rightarrow Li}[nAB]$$

$$\lambda_2 = \mu_{oLB} + \alpha_{nAB \rightarrow oLB}[nAB]$$

$$\lambda_3 = \mu_{NO} + 2\alpha_{nAB \rightarrow nAB}[nAB]$$

The mixed nAB and Li state eigen values are more complicated and suggest the growth rate of the excluded species contributes to stability of this state, as well as at least one of the co-existing communities (nAB or Li) must inhibit the excluded species (oLB). The second eigen value also indicates the interactions between the co-existing species contribute to the stability of this state.

$$\lambda_1 = \mu_{oLB} + \alpha_{nAB \rightarrow oLB}[nAB] + \alpha_{Li \rightarrow oLB}[Li]$$

$$\lambda_{2/3} = \frac{\alpha_{nAB \rightarrow nAB}[nAB] + \alpha_{Li \rightarrow Li}[Li]}{2} \pm \frac{\sqrt{\alpha_{nAB \rightarrow nAB}^2[nAB]^2 - 2\alpha_{nAB \rightarrow nAB}\alpha_{Li \rightarrow Li}[nAB][Li] + \alpha_{Li \rightarrow Li}^2[Li]^2 + 4\alpha_{nAB \rightarrow Li}\alpha_{Li \rightarrow nABnAB}[nAB][Li]}}{2}$$

Chapter 4 An *in silico* Framework for Rational Design of Vaginal Probiotic Therapy

Christina Y. Lee¹, Sina Bonakdar¹, Kelly B. Arnold¹

4.1 Attributions

¹Department of Biomedical Engineering, University of Michigan, Ann Arbor, MI, United States of America

*Lead contact: Kelly Arnold (kbarnold@umich.edu)

In submission

4.2 Abstract

Bacterial vaginosis is a common condition characterized by a shift in vaginal microbiome composition, linked to negative reproductive outcomes and increased susceptibility to sexually transmitted infections. Despite the commonality of BV, standard of care antibiotics provide limited control of recurrent BV episodes. Development of new therapies is limited by the lack of controlled models of the vaginal microbiome needed to evaluate new treatments and regimens. Here, we develop an *in silico* framework to evaluate selection criterion for probiotic strains, test adjunctive therapy with antibiotics, and alternative dosing strategies. This framework highlighted the importance of resident microbial species on the efficacy of probiotic strains, identifying specific interaction parameters between resident non-optimal anaerobic bacteria (nAB) and *Lactobacillus* spp., and candidate probiotic strains that should be a selection criterion. Model predictions were able to replicate results from a recent phase 2b clinical trial for the live

biotherapeutic product, Lactin-V, demonstrating the relevance of our novel *in silico* platform. Results from the model support that the probiotic strain in Lactin-V requires adjunctive antibiotic therapy to be effective, and that increasing dosing frequency of probiotic could have a moderate impact on BV recurrence at 12 and 24 weeks. Altogether, this framework could provide evidence for rational selection of probiotic strains and help optimize dosing frequency or adjunctive therapies.

4.3 Introduction

The vaginal microbiome (VMB) is critical to female reproductive health, with the composition of the VMB associated with benefits such as decreased risk for sexually transmitted infections [14,15,17,235,236], pelvic inflammatory disease [1,10,11], and pre-term birth [4,5,237]. The most health-associated compositions are associated with *Lactobacillus* spp. dominance, particularly by *L. crispatus*, *L. gasseri*, and *L. jensenii* which are observed to be dominant species across three community state types (CSTs, CST -I, CST -II, CST -V). A fourth *Lactobacillus* sp., *L. iners*, is less associated with health, lacks the ability to produce compounds most associated with the inhibition of pathogens (H₂O₂, D-lactic acid), and is commonly associated with shifts to a non-optimal composition characterized by an overgrowth of facultative and obligate anaerobes known as bacterial vaginosis (BV). BV is a common condition, affecting approximately 30% of reproductive-age women resulting in abnormal vaginal discharge and odor, discomfort, and higher risk for the adverse reproductive outcomes. Despite the commonality of BV, treatment outcomes with standard antibiotic regimens (nitroimidazoles or clindamycin) remain suboptimal, with short-term cure rates around 80% [83] and long-term (6-12 months) cure rates at less than 50% [79]. Thus, alternative methods for long-term resolution of BV are needed.

Several alternative strategies for treating recurrent and repeated episodes of BV have been evaluated based on empirical observations, which include extended first-line antimicrobial regimens, combinatorial first-line regimens, therapies targeted at biofilm removal (boric acid, TOL-463), pH lowering agents (lactic acid), and probiotics. Women with persistent or recurrent BV prescribed twice weekly doses of metronidazole for three months had reduced recurrences during therapy, but once discontinued had repeat episodes of BV [225,238]. There is limited data on the use of boric acid in conjunction with long-term suppressive antimicrobial regimens, with one study supporting higher cure rates at 12, 16 and 28 weeks, but by week 36 was less than 50% [223]. pH lowering agents like lactic acid have also been studied, but have not shown ability to significantly impact VMB composition and are not recommended by any guidelines [98]. Many randomized control trials have tried to support the use of probiotics for the treatment of BV, with mixed results [103,104,239–242]. One recent trial of *L. crispatus* CVT-05 (Lactin-V) showed promise for reducing the recurrence of BV at 12 weeks when compared to placebo, but is not yet cleared by the FDA or commercially available [104]. The study and use of probiotics for the treatment of BV has been limited by inconsistent probiotic characteristics (vaginal vs intestinal species, vaginal strains), routes of administration (oral vs vaginal), and dosing strategies (frequency and duration) [99]. Methodical selection of probiotic characteristics and dosing regimens could greatly improve efforts to develop a probiotic or live biotherapeutic products that can resolve recurrent BV.

Here, we develop a model that can systematically test probiotic characteristics and dosing strategies against a variety of *in silico* BV communities. The model reveals that resident community members can have a significant impact on probiotic efficacy, particularly highlighting that any antagonistic interaction of non-optimal anaerobic bacteria (nAB) on the

probiotic strain can drastically decrease probiotic success at re-orienting communities to a *Lactobacillus* spp. dominated state. Additionally, we observe that the relationship between resident *Lactobacillus* spp. with probiotic can impact whether the post-treatment communities will be dominated by optimal *Lactobacillus* (oLB), *L. iners*, or the probiotic species. Lastly, the modeling framework was evaluated in the context of regimen reported for Lactin-V in a phase 2b clinical trial demonstrating the model can replicate clinical observations. Overall, these results highlight the importance of characterizing probiotic strains in co-culture with endogenous VMB and suggest personalized differences in microbial characteristics can help explain variability efficacy observed clinically.

4.4 Results

4.4.1 Simulated probiotic strains result in variable response types across a virtual population

To simulate BV communities, a three-community state type (CST) ODE model was used to represent core VMB compositional types: optimal *Lactobacillus* (*L. crispatus*, *L. jensenii*, or *L. gasseri*) dominated (oLB; CST -I/II/V), *L. iners* (Li; CST -III), and non-optimal anaerobic bacteria (nAB, associated with BV; CST -IV). The model captures the growth characteristics and interspecies interaction terms between each community group as well as how the community and the probiotic interact using generalized Lotka-Volterra equations (*Figure 4.4.1A*). To test probiotic regimens, a base virtual population was created using Latin Hypercube Sampling of

defined parameter distributions (30,000 parameter sets; *Table 4.7.1, Figure 4.7.1*). From the base virtual population of Latin Hypercube Sampling generated parameter sets, 2,000 virtual patients were selected to replicate a distribution of BV-relevant CST equilibrium behaviors observed clinically [243]. BV-relevant CST equilibrium behaviors were defined as virtual patients that were analytically predicted to be nAB dominant at steady-state. For proof of concept, a simple, 7-day regimen of probiotic was simulated on each virtual patient, and the impact on community composition was evaluated at several time points from therapy cessation (therapy cessation, 1 month, 3 months, 6 months, 12 months; *Figure 4.4.1B*). The impact of the probiotic on

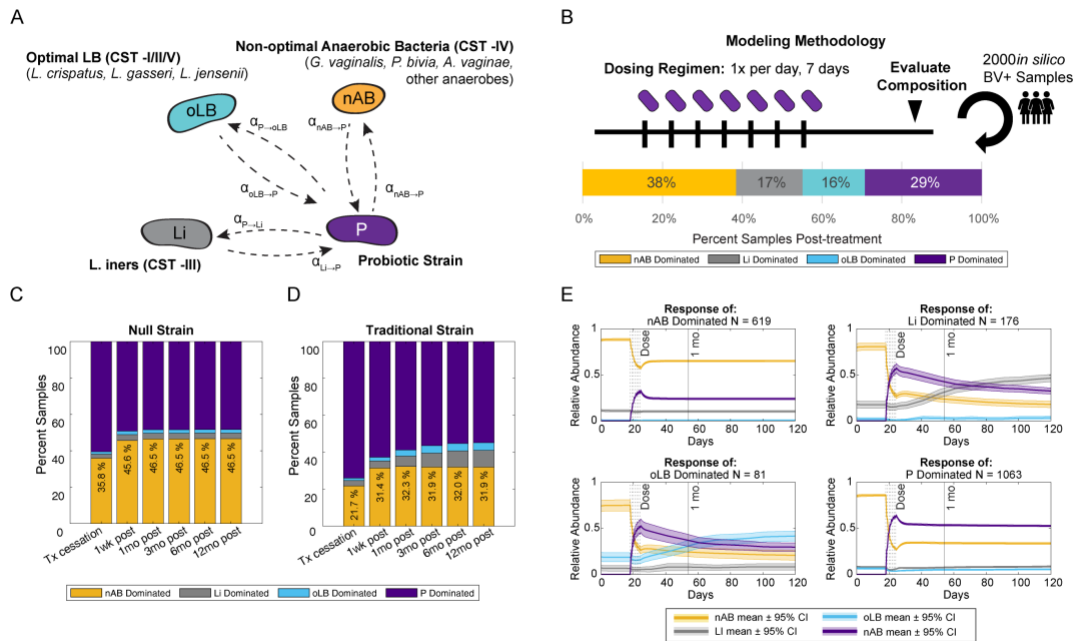


Figure 4.4.1 Overview of probiotic strain modeling.

(A) Schematic of parameters associated with probiotic – resident community interactions. (B) Base probiotic dosing regimen modeling. Unless otherwise specified, probiotic dosing occurs once daily for seven days across 2000 virtual BV+ patient samples. At several time points the dominating species is assessed, which can result in a mix of nAB-, Li-, oLB-, or Probiotic-dominant communities for the same strain of probiotic. (C) Results for a “null” strain probiotic that has a moderate growth rate (0.5 d^{-1}) and negligent interspecies interactions, the stacked bar graph represents the frequency of communities in one of four states: nAB dominant, Li Dominant, oLB Dominant, or Probiotic dominant at time points therapy cessation, 1 wk, 2wk, 1 mo, 3mo, 6mo and 12mo post. (D) Example of a conceptually traditional probiotic strain (null parameters with $P \rightarrow nAB = -0.010 \text{ density}^{-1} \text{d}^{-1}$). (E) Example time series relative abundance responses of the *in silico* BV+ patients. Each plot is the average \pm 99% confidence interval of the relative abundance for each species of *in silico* BV+ patients that exhibited a set response type of nAB dominant (top left), Li dominant (top right), oLB dominant (bottom left), and P dominant (bottom right).

community composition was defined by CST classification at a set evaluation time point. These classifications included nAB dominant (probiotic failure rate) as well as dominance by *Lactobacillus* spp. (probiotic efficacy rate): Li-dominant, oLB-dominant, or Probiotic (P)-dominant.

Current characterization or interactions between probiotic bacteria strains and bacteria present in the vagina primarily focus on the impact of the probiotic on nAB associated with BV. There is limited data on how probiotic strains impact endogenous *Lactobacillus* spp. or how endogenous community members impact probiotic strains. For simplicity, a null probiotic strain and a traditional probiotic strain were developed to explore the possible response types. The null probiotic strain was modeled as having negligible interspecies interactions ($\alpha_{nAB \rightarrow P}$, $\alpha_{nAB \rightarrow Li}$, $\alpha_{nAB \rightarrow oLB}$, $\alpha_{P \rightarrow nAB}$, $\alpha_{P \rightarrow Li}$, $\alpha_{P \rightarrow oLB} = 0.0$ density⁻¹d⁻¹) a moderate growth rate ($k_{grow-P} = 0.5$ d⁻¹), and a moderate self-interaction term ($\alpha_{P \rightarrow P} = -0.022$ density⁻¹d⁻¹). Resulting model predictions indicated that the null probiotic strain was predicted to have primarily P-dominated or nAB-dominated response types at each evaluation point, with a maximal failure rate of 46.5% at 12 months (*Figure 4.4.1C*). A second strain, designed with traditional or standard considerations of ensuring the probiotic strain could inhibit nAB growth was simulated using the null probiotic strain parameters and $\alpha_{P \rightarrow nAB}$ set to -0.01 density⁻¹d⁻¹ (*Figure 4.4.1D*). The traditional strain had a lower rate of treatment failure, with nAB dominant communities comprising 32% of virtual patients for times greater than 1-month post-treatment cessation. To demonstrate how community composition changes during and after the probiotic therapy, abundance-time profiles were plotted for each response type (*Figure 4.4.1E*). For nAB-dominated and P-dominated response groups, nAB relative abundance was lowest on the last day of therapy and then re-equilibrated to a higher abundance. For responses where endogenous *Lactobacillus* spp. were the

most abundant post-treatment (Li- or oLB-dominant response types), nAB populations continued to decline over time alongside the probiotic population. Altogether these results demonstrate the utility of testing a probiotic strain and regimen across a heterogenous simulated population, as even the same probiotic strain can induce variable responses across patients.

4.4.2 Sensitivity analyses reveal alternative probiotic characteristics that can improve probiotic strain efficacy

To determine which parameters are most associated with improving probiotic efficacy (frequency of Li-, oLB-, P-dominant states post-treatment), local sensitivity analyses were completed for all parameters describing probiotic strain characteristics (*Figure 4.4.2*). Notably, the two most sensitive parameters were between nAB and probiotic ($\alpha_{nAB \rightarrow P}$ and $\alpha_{P \rightarrow nAB}$). The importance of probiotic inhibition of nAB ($\alpha_{nAB \rightarrow P}$) is unsurprising, given the selection of probiotics that produce inhibitory compounds (D/L-lactic acid, hydrogen peroxide, or bacteriocins) for nAB is a standard practice [55,56,128,244,245]. In contrast, the high degree of sensitivity for nAB on probiotic ($\alpha_{nAB \rightarrow P}$) is less intuitive and not well characterized *in vitro* or *in vivo*. The pairwise interactions of endogenous *Lactobacillus* (Li and oLB) with the probiotic did not have as strong of an effect on predicted probiotic efficacy ($\alpha_{nAB \rightarrow Li}$, $\alpha_{nAB \rightarrow oLB}$, $\alpha_{P \rightarrow Li}$,

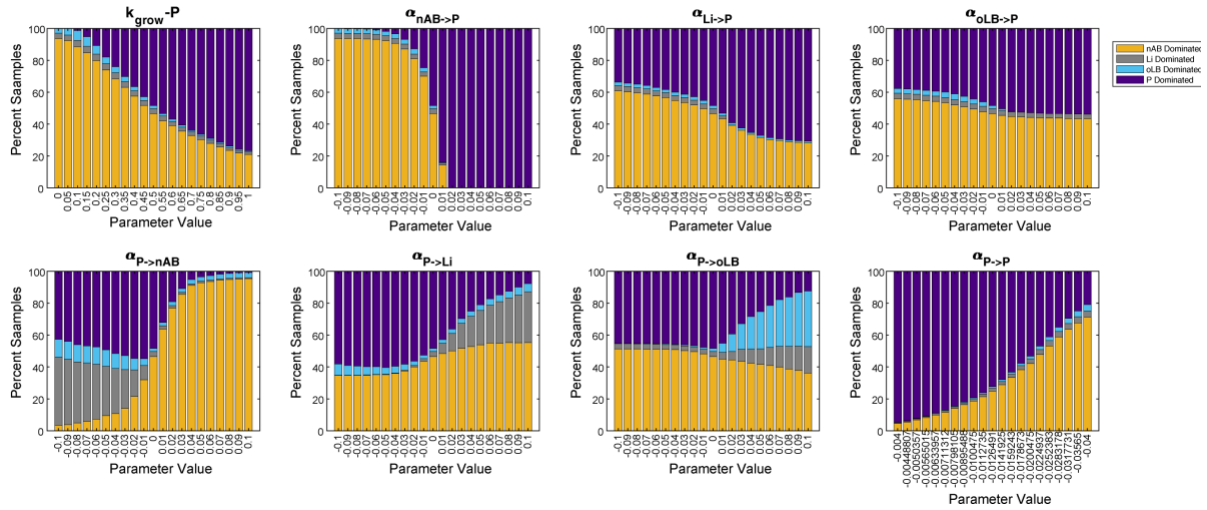


Figure 4.4.2 Local sensitivity analysis of probiotic characteristics.

One-at-a-time parameter perturbation analysis for probiotic characteristics. The proportion of the 2,000 *in silico* BV+ communities that exhibited each response type is plotted on the y-axis. The x-axis represents the parameter value change from the defined “null” probiotic strain.

$\alpha_{P \rightarrow oLB}$), but could alter which type of *Lactobacillus* spp. dominated state the community assembled to post-treatment ($\alpha_{P \rightarrow Li}$, $\alpha_{P \rightarrow oLB}$). The ability to dictate which *Lactobacillus* spp. community dominates post-treatment could be useful, as recent studies have started to design therapies to inhibit *L. iners* populations as a methodology to prevent BV recurrence [60,61].

To analyze the impact of combinatorial changes in probiotic characteristics, a four-parameter sensitivity analysis was used. The four-parameter sensitivity analysis covered the two parameters most sensitive for probiotic efficacy ($\alpha_{nAB \rightarrow P}$ and $\alpha_{P \rightarrow nAB}$) and for specificity to boost oLB or Li-dominated response types ($\alpha_{P \rightarrow Li}$, $\alpha_{P \rightarrow oLB}$; Figure 4.7.2). Each parameter was simulated as a -0.01, 0.00, or +0.01 density⁻¹d⁻¹ value, for all possible combinations (81 parameter combinations total). Overall, the probiotics with the lowest failure rate (nAB-dominant frequency) exhibited a positive value for $\alpha_{nAB \rightarrow P}$. The next important driver was $\alpha_{P \rightarrow nAB}$. Statistical analysis of select strains versus the null probiotic strain was used to emphasize the best 1-parameter, 2-parameter, and 3-parameter probiotic designs (Figure 4.4.3A). All selected strains were significantly from the null strain. The traditional strain had a

significantly higher rate of treatment failure than the 1-parameter alteration of $\alpha_{nAB \rightarrow P}$ (31.9% vs 14.4%; $P < 1 \times 10^{-6}$), highlighting the importance of considering the effect of endogenous nAB populations on probiotic efficacy. Combining the two best single-parameter perturbations decreased the treatment failure rate to 4.8%, promoting probiotic growth rates alongside the 2-parameter change decreased the failure rate to 1.9% ($P = 6.141 \times 10^{-7}$).

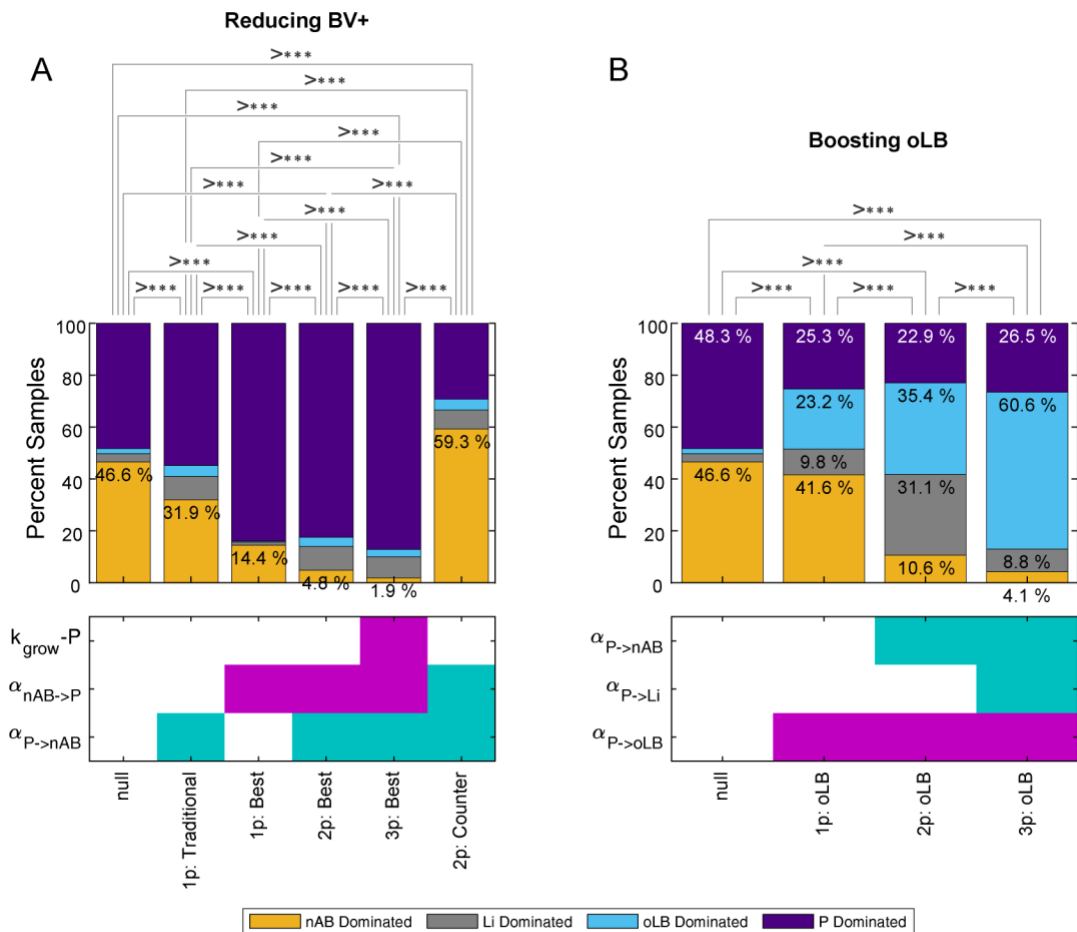


Figure 4.4.3 Selection of optimal probiotics.

(A) Probiotics that improve probiotic efficacy by reducing nAB-dominant response types. (B) Probiotics that boost endogenous oLB populations to increase oLB-dominant response types. Plots indicate the percentage of the 2,000 in silico BV+ positive samples for a given response type. The heatmap below the plots indicates the parameter change and the value of the change: no change (white), +0.01 (pink), -0.01 (green). Statistical comparisons were made with chi-square tests, asterisks indicate statistical significance.

When $\alpha_{nAB \rightarrow P}$ is negative, it can counteract the effect of a probiotic selected for inhibition of nAB (negative $\alpha_{P \rightarrow nAB}$) and perform worse than a probiotic with no interspecies interactions (null strain, 59.3% vs 46.5%; $P = 1.221 \times 10^{-15}$). Altering the impact of probiotic on nAB, Li, and oLB were observed to impact the selection of Li- and oLB-dominant response types in the 1-parameter sensitivity analysis. Selection of parameter modifications to boost oLB-dominant response types was assessed, increasing the oLB-dominant response type from 2.0%, to 23.2% with a 1-parameter modification ($+0.05 \alpha_{P \rightarrow oLB}$), 35.4% with a 2-parameter modification ($+0.05 \alpha_{P \rightarrow oLB}$ & $-0.05 \alpha_{P \rightarrow nAB}$), and 60.6% with a 3-parameter modification ($+0.05 \alpha_{P \rightarrow oLB}$, $-0.05 \alpha_{P \rightarrow Li}$, & $-0.05 \alpha_{P \rightarrow nAB}$; *Figure 4.4.3B*). These results suggest that understanding the interaction between nAB and probiotic, as well as the impact probiotic has on endogenous *Lactobacillus* spp. can help tailor desired compositional changes with probiotics.

4.4.3 Combinatorial regimens can lower BV recurrence rates

Commonly, a course of probiotics is given after treatment with standard antimicrobial therapy [99] (*Table 4.7.3*). To evaluate the impact of different treatment regimens, the model was used to simulate pre-treatment with antibiotics followed by a short-term probiotic regimen, versus a short-term probiotic only regimen, and antibiotic only regimens (*Figure 4.4.4A*). The antibiotic therapy simulated was a 7-day course of oral MTZ and the probiotic regimen was a short-term (7-day), daily regimen using the traditional strain (null strain with $\alpha_{P \rightarrow nAB} = -0.01 \text{ density}^{-1} \text{d}^{-1}$). Treatment outcomes were evaluated at the end of treatment, 1 month, 3 months, and 6 months post-treatment cessation (*Figure 4.4.4A*). The antibiotic regimen without probiotic performed the worst at all time points except immediately after treatment cessation, where the antibiotic regimen had a 15% failure rate versus the 21.6% failure rate for the probiotic only regimen ($P < 1 \times 10^{-6}$). At all evaluation time points, the combination pre-treatment antibiotic

followed by probiotic was most efficacious. At the later time points, the difference between combination antibiotic with probiotic versus probiotic only regimen decreased with the failure rate within 4% of each other. The failure rate for antibiotic at 3 month and 6 months was nearly double that of the regimens including probiotic, supporting the use of probiotic to reduce repeat episodes of BV.

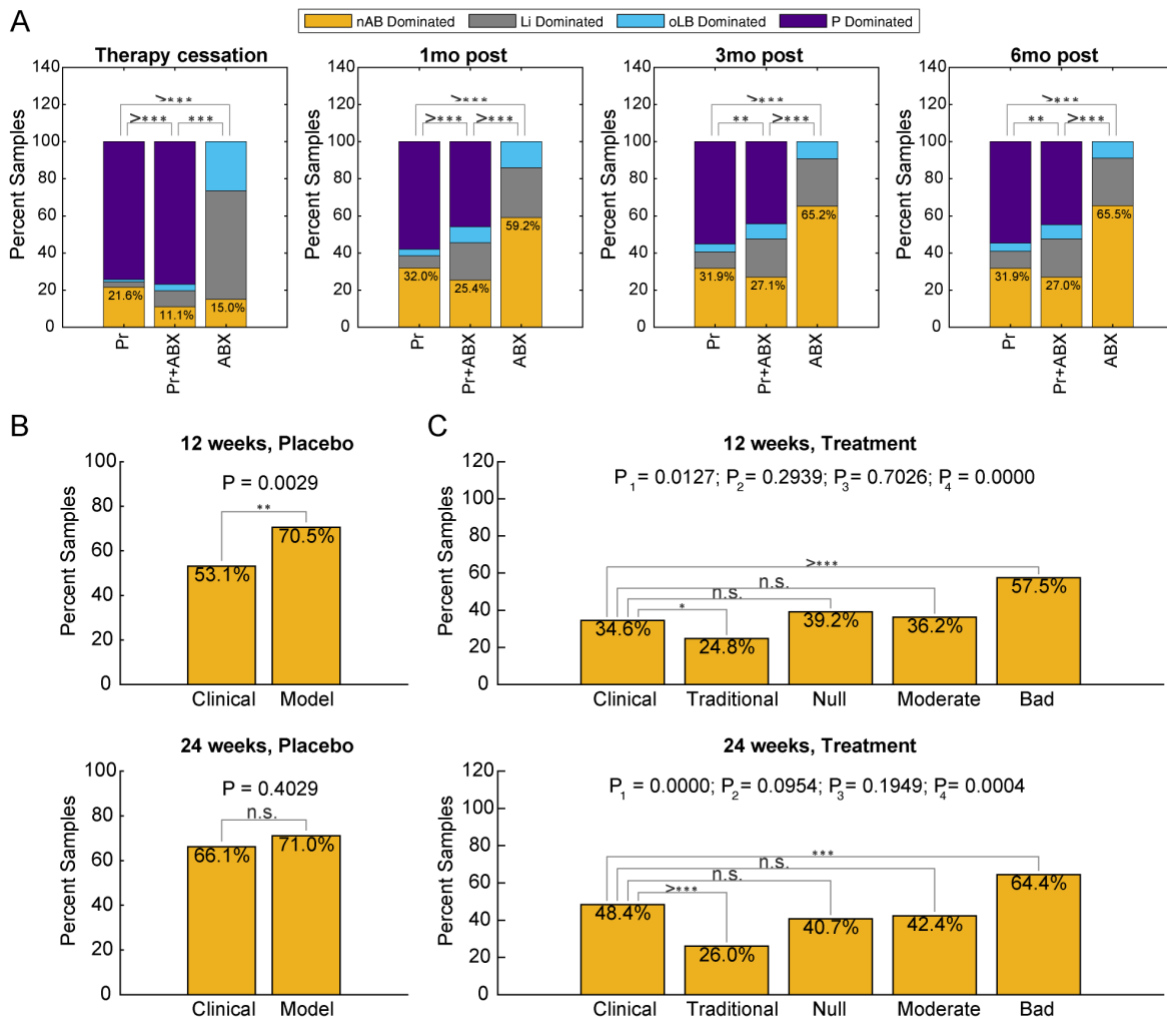


Figure 4.4.4 Adjunct antimicrobial therapy versus probiotic or antibiotic therapies in isolation.

(A) Assessment of the impact of adjunct antimicrobial therapy (ABX + Pr) versus probiotic only (Pr) or antibiotic only (ABX) BV treatment regimens across four time points (therapy cessation, 1 month post, 3 months post and 6 months post). The percent of the 2,000 in silico BV+ subjects that exhibit each response type are reported. (B-C) Comparison of model predictions with Lactin-V trial results at 12 and 24 weeks for (B) placebo (C) treatment arm. For the treatment arm, 4 strains were simulated by the model encompassing a traditionally designed probiotic, null probiotic, moderately/conservatively designed probiotic, and bad/negative control probiotic.

Probiotic regimens can vary significantly, with some strategies using short-term (daily) regimens, intermittent regimens (weekly), or long-term regimens (treatment over several months). A promising probiotic and associated regimen (Lactin-V) recently underwent phase 2 clinical trials demonstrating significant reduction in BV recurrence and utilized a combination of the aforementioned dosing strategies [104]. The phase 2b trial administered a 5-day regimen of intravaginal MTZ, followed by vaginally administered Lactin-V or placebo. Dosing of Lactin-V/placebo occurred over 11 weeks, where week 1 was dosed once daily for 4 days, and weeks 2 – 11 were dosed twice weekly. To demonstrate the model can recapitulate complex dosing strategies and replicate clinical observations, the Lactin-V regimen was simulated across 2,000 virtual patients and the predicted recurrence rates at 12 weeks and 24 weeks were compared to clinically reported frequencies. The placebo (Lactin-V regimen with no probiotic strain added) results agreed well between clinical observation and model results (66.1% versus 71.0%; $P = 0.4029$), but deviated at the 12 week mark (53.1% versus 70.5%; $P = 0.002$; *Figure 4.4.4B*). Since the strength of antibiotic is a parameter that exhibits significant variability (5-fold differences in decay rates; *Table 4.7.2*), a stronger dose was simulated which demonstrated comparable results at both the 12 and 24 week mark for the placebo arm (*Figure 4.7.3*). The simulation of the Lactin-V treatment arm included for possible probiotic strains: the traditional probiotic strain (positive control), the null probiotic strain, a strain with moderate competition with endogenous vaginal microbiota, and a strain where nAB is antagonistic with the probiotic (negative control). The traditional probiotic strain had significantly lower rates of treatment failure at both 12 weeks and 24 weeks compared to the clinical observations ($P = 0.0127$, $P < 1 \times 10^{-6}$, respectively). In contrast, the null and moderate strains had comparable predicted BV treatment failure rates at both time points. At 12 weeks, the clinically reported frequency was

34.6% versus the null strain (39.2%; $P = 0.294$) and moderate strain (36.2%; $P = 0.703$). At 24 weeks, the clinically reported frequency was 48.4% versus the null strain (40.7%; $P = 0.0954$) and moderate strain (42.4%; $P = 0.1949$). A negative control was evaluated to demonstrate that probiotics could perform worse than the null strain, which exhibited a 57.5% and 64.4% recurrence rate at 12 weeks and 24 weeks. Altogether, these results suggest the Lactin-V probiotic strain has a relatively neutral interaction with endogenous *Lactobacillus* spp. and the probiotic has a stronger impact on nAB ($\alpha_{P \rightarrow nAB}$) than nAB has on the probiotic ($\alpha_{nAB \rightarrow P}$). Selection of probiotic strains with less competition with endogenous *Lactobacillus* spp. may help promote treatment efficacy.

4.4.4 Adjunctive antimicrobial therapy improves probiotic strain efficacy for underperforming strains

To systematically assess the importance of probiotic strain characteristics with respect to promoting *Lactobacillus* spp. dominated communities post-treatment, 500 *in silico* strains were evaluated. The 500 *in silico* strains were generated by Latin Hypercube Sampling of probability distributions similar to the reference virtual population. Each of the 500 strains was then evaluated on the 2,000 subject virtual patient population for both the short-term probiotic regimen (no pre-treatment antibiotic) and the Lactin-V regimen. Each strain was assigned to a designated response profile based on the strain's performance across the 2,000 subjects. A Partial Least Squares Discriminant Analysis was used to evaluate the relationship between model parameters and response profiles (*Figure 4.4.5*). For the short-term therapy without antibiotic pre-treatment, the most important parameters driving a *Lactobacillus* spp. dominated response were separated along latent variable 1 (LV1) with $\alpha_{nAB \rightarrow P}$ having the strongest association (*Figure 4.4.5A*). Separation across LV2 captured differences between *Lactobacillus* spp., with

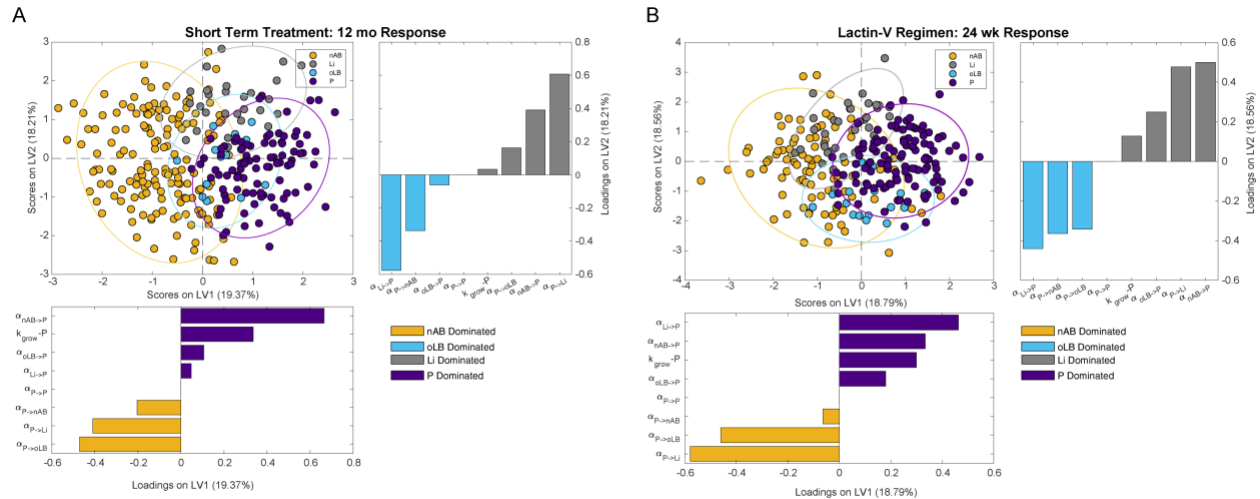


Figure 4.4.5 Drivers of population level composition alterations for a short-term regimen and Lactin-V regimen.

Partial least squares discriminant analysis (PLS-DA) models were constructed using strain characteristics to predict a population-level profile type (consistently nAB, Li, oLB, or P-dominated across the 2,000 subject virtual population) after (A) short-term regimen of probiotic and (B) Lactin-V regimen of probiotic.

Li-dominated responses most associated with Li inhibiting probiotic (more negative $\alpha_{Li \rightarrow P}$) and probiotic promoting the growth of Li (more positive $\alpha_{P \rightarrow Li}$). In contrast, the Lactin-V regimen (antibiotic pre-treatment followed by 11-week probiotic regimen) was more sensitive to the interaction of endogenous *Lactobacillus* spp., namely Li ($\alpha_{Li \rightarrow P}$, Figure 4.4.5B). Between the two regimens, there were several probiotic strains that were predicted to promote probiotic dominance across greater than 99% of the virtual patients.

Characteristics of strains that were best at promoting a certain response over the 2,000 virtual patient population were similar between the regimens (Figure 4.7.4, Figure 4.7.5). Strains most associated with treatment failure (nAB dominant response profiles) typically had strong negative interactions of nAB on P ($\alpha_{nAB \rightarrow P}$). Strains that most frequently exhibited boosted endogenous *Lactobacillus* spp. were associated with probiotic having a positive impact on Li ($\alpha_{P \rightarrow Li}$) for Li response types and oLB ($\alpha_{P \rightarrow oLB}$) for oLB response types. Lastly, high probiotic abundance was associated with the probiotic inhibiting all resident vaginal microbiota ($\alpha_{P \rightarrow nAB}$,

$\alpha_{P \rightarrow Li}$, $\alpha_{P \rightarrow oLB}$) and with the resident microbiota tending to have positive interactions ($\alpha_{nAB \rightarrow P}$, $\alpha_{Li \rightarrow P}$, $\alpha_{oLB \rightarrow P}$).

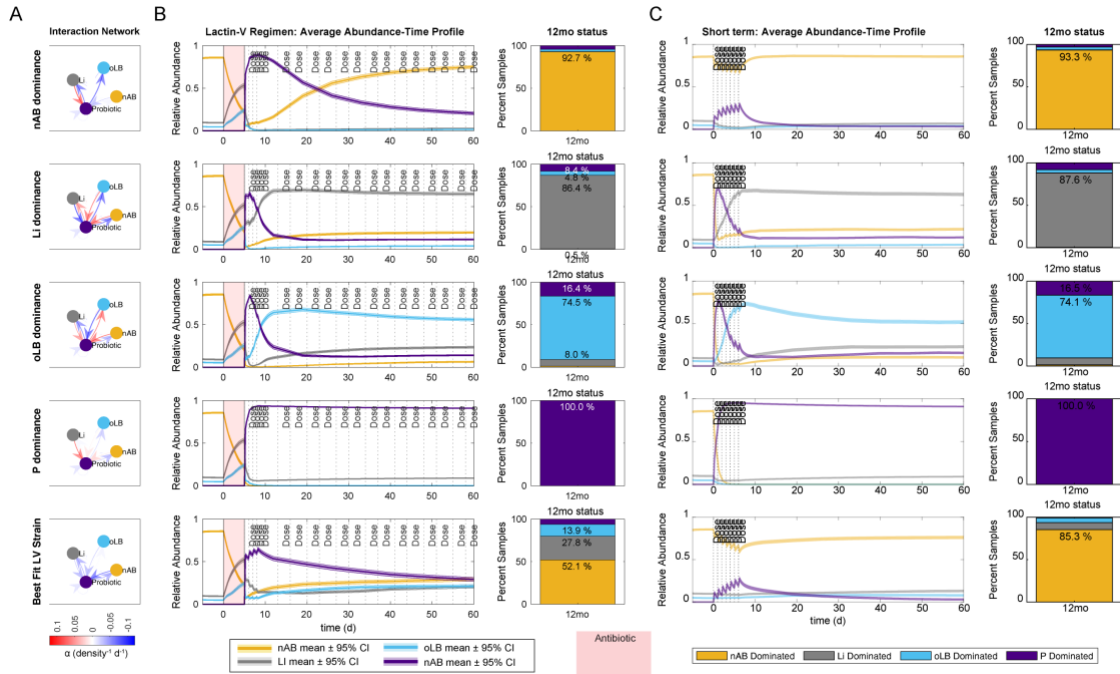


Figure 4.4.6 Comparison of Lactin-V regimen with the short-term probiotic only regimen.

(A) Interspecies interaction parameter values of top probiotic strains for the Lactin-V regimen. (B) Abundance-time profile of community groups for each probiotic strain and predicted 12mo frequency of response types. (C) Short-term regimen abundance-time profile and predicted 12mo frequency of response types for strains defined in (A). Red indicates time of antibiotic dosing.

To evaluate the impact of regimen on probiotic efficacy, 5 strains were evaluated with the Lactin-V regimen and the short-term probiotic regimen (Figure 4.4.6). The 5 strains selected were strains that promoted one of the four response types across the highest percent of the virtual population. For example, the strain for nAB response types elicited nAB dominance in 91% of the virtual patients, the strain for Li elicited Li dominance in 86% of virtual patients, the oLB strain elicited oLB dominance in 73% of the virtual patients, and the probiotic strain elicited a probiotic dominant response in 100% of the patients. The fifth strain was a strain that most closely replicated the Lactin-V phase 2b clinical trial results for BV recurrence at 12 and 24

weeks. Overall, the selected strains had similar long-term effects on compositions for the Lactin-V regimen and the short-term regimen (Figure 4.4.6B,D). This result was also observed when the top strains selected from the short-term regimen were tested with the Lactin-V regimen (Figure 4.7.6). Effects differed for the representative strain for the Lactin-V formulation, where without the pre-treatment of antibiotic, the addition of the probiotic had little to no impact on re-orienting the vaginal microbiome composition. This result suggests that pre-treatment with antibiotics is critical for probiotics that cannot stably engraft into the existing vaginal community.

4.4.5 Lactin-V efficacy is moderately dependent on probiotic dosing frequency

Lastly, the Lactin-V probiotic dosing regimen was analyzed across 5 representative strains. The dosing regimen during weeks 2 – 10 were altered to be, bi-weekly (1 dose every

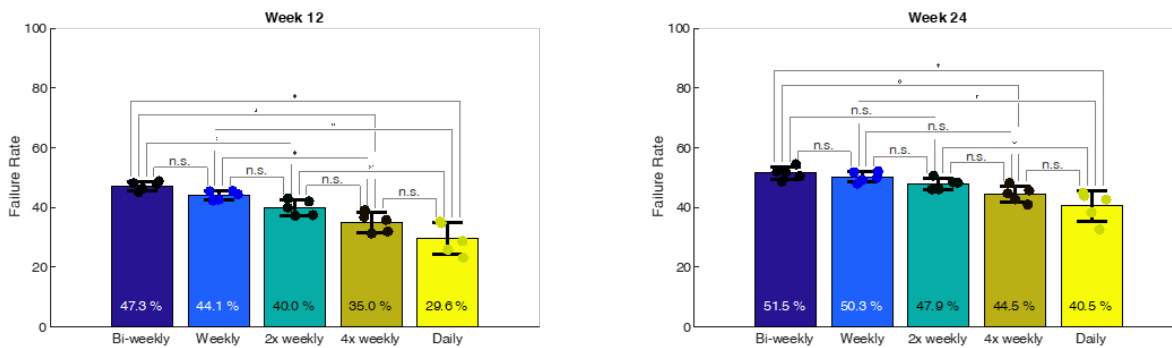


Figure 4.4.7 Impact of alternative dosing frequency on predicted BV recurrence rates.

The Lactin-V regimen has a 10-week period of intermittent dosing (2x weekly). Alternative dosing strategies for the 10-week period tested were bi-weekly, weekly, 4x weekly and daily. Treatment failure rate (recurrence rate) was evaluated at week 12 and 24. Dots indicate the recurrence rates of the 5 representative strains that recapitulated observed Lactin-V recurrence rates. Bars are the mean \pm standard deviation. Multiple Mann-Whitney rank sum tests were used to compare groups and were adjusted using Benjamini & Hochberg procedure.

other week), once weekly, twice weekly, four times weekly, and daily. There was a gradual decrease in treatment failure rate with increasing dose frequency (Figure 4.4.7). Differences were more prominent at week 12, where the original Lactin-V regimen (twice weekly) had a statistically significant failure rate (40.0%) than the bi-weekly (47.3%) and daily (29.6%) dosing

frequencies ($P = 0.0165$ and $P = 0.0165$, respectively; Figure 4.4.7A). At 24 weeks, results were more similar regardless of the dosing regimen and only the daily regimen differed from the less frequent dosing strategies (Figure 4.4.7B). Altogether these results demonstrate that dosing regimen for Lactin-V can have moderate impacts on BV recurrence rates in the short-term, and dosing regimen becomes less impactful in the long-term.

4.5 Discussion

To examine characteristics of probiotic strains that can aid in re-orienting the vaginal microbiome from a nAB-dominated, BV-associated state, to a *Lactobacillus* spp. dominated state, we developed an *in silico* framework. This framework used generalized Lotka-Volterra ODEs to represent growth characteristics and interspecies interactions of three core community compositional types of the VMB. Probiotic strain characteristics were systematically evaluated across a virtual patient population, allowing for the investigation of probiotic parameters and probiotic regimens that elicit desired compositional changes that include Li-dominant, oLB-dominant, or probiotic-dominant communities.

Local and global sensitivity analyses implicated the importance of resident community members on probiotic efficacy. This result is not unsurprising, as it aligns with the ecological principle of community invasibility, which is driven by how the resident community members interact with the invading species (probiotic strain) [246,247]. Regimens without a course of antibiotics prior to probiotic were particularly sensitive to the impact of nAB on the probiotic strain ($\alpha_{nAB \rightarrow P}$). This parameter is interesting as few studies report the impact of nAB on *Lactobacillus* spp. or probiotic strains. One study that reports the pairwise impact of *G. vaginalis* with *L. jensenii* observed a 50% decrease in *L. jensenii* cell density from mono-culture to co-culture [206]. Another study reported that certain *G. vaginalis* strains could selectively inhibit

the *L. crispatus* to adherence to epithelial cells over *L. iners* [59]. nAB associated with BV may also inhibit the growth of *Lactobacillus* spp. through the production of biogenic amines, which were shown to increase *Lactobacillus* spp. lag-time, decrease growth rates, and decrease the production of D/L-lactic acid [75]. These results suggest that critical selection criteria for probiotic strains used to treat BV include the ability for the strain to outcompete a variety of nAB for adhesion to epithelial cells, disrupt biofilms, as well as be tolerant to biogenic amines.

For probiotic regimens that include pre-treatment with antimicrobials like metronidazole or clindamycin, the impact of nAB on the probiotic strain becomes less important and the impact of endogenous *Lactobacillus* spp. is more prominent ($\alpha_{Li \rightarrow P}$, $\alpha_{oLB \rightarrow P}$). Notably, colonization with endogenous *Lactobacillus* spp. is reported to decrease probiotic (*L. crispatus* CTV-05) in healthy individuals [228], supporting the importance in considering probiotic strain interactions with *Lactobacillus* spp. Despite the importance of interactions between resident *Lactobacillus* spp. and the probiotic strain, little is known about the pairwise relationship. A publication analyzing 17 *L. crispatus* strains, two *L. gasseri* strains, two *L. jensenii* strains and a *L. iners* strain using spot agar tests demonstrated that all human strains of *L. crispatus* could slightly inhibit *L. iners* growth [42]. Not all strains of *L. gasseri* and *L. jensenii* inhibited *L. iners*. Co-culture data demonstrated that some *Lactobacillus* strains had a 4-6 log reduction in cells with certain *L. crispatus* strains [42]. Thus, screening of the relationship between probiotic strains and endogenous *Lactobacillus* spp. could help improve probiotic design.

Boosting endogenous levels of optimal species like *L. crispatus*, *L. gasseri*, or *L. jensenii* (oLB) could be preferential to stably incorporating a probiotic strain, particularly if the strain is not native or known to have the same functional capacity in the vaginal microbiome as endogenous *Lactobacillus* spp. This framework indicated for endogenous oLB to become

dominant after treatment that probiotic strains must have a facilitative interaction with oLB (positive $\alpha_{P \rightarrow oLB}$), inhibitory interaction with Li (negative $\alpha_{P \rightarrow Li}$), and oLB must have a weak or inhibitory (negative $\alpha_{oLB \rightarrow P}$) interaction with the probiotic strain. A potential oLB-promoting probiotic strain could be strains that exhibit selective inhibition of *L. iners* such as the human intestinal *Lactobacillus* spp. strain (*L. paragasseri* K7) and less potent vaginal strain (*L. gasseri* 105-1) [60]. Combinatorial therapy that is selective against *L. iners*, could possibly supplement a probiotic strain that is not inherently selective against *L. iners*. Recent studies indicated that *L. iners* cysteine dependence could be a potential target to reduce competition between *L. iners* and oLB [61]. Overall, this result further supports the idea that increased characterization between probiotic strains and endogenous *Lactobacillus* spp. could greatly benefit probiotic design.

This framework replicated the results of the phase 2b clinical trial for Lactin-V and indicated that *L. crispatus* CTV-05 likely exhibits weak competitive interactions with resident community members. Of *in silico* strains that could replicate the Lactin-V trial results at 12 and 24 weeks, most were predicted to not stably integrate into the community. Additionally, the efficacy of these strains was highly dependent on pre-treatment antibiotic, supporting the need for adjunctive use of antibiotics with Lactin-V. In published randomized control trials, dosing frequency is variable and often not clearly justified (Table 4.7.3). To evaluate the impact of dose frequency for Lactin-V, dosing was simulated bi-weekly, once weekly, twice weekly (Lactin-V), four times weekly, and daily and the frequency of BV recurrence was evaluated at 12 and 24 weeks. Dosing frequency had a moderate impact on probiotic efficacy evaluated at 12 weeks, but less of an impact at 24 weeks, which is 3 months after subjects finished therapy. The importance of dosing frequency is likely strain dependent, with strains that are unable to engraft into the

community most dependent on frequent dosing. This framework could help guide, optimize, and provide rationale for future probiotic regimen designs.

A major limitation of this model is that it does not account for variability in host behavior. Factors such as hormonal fluctuations due to menstrual cycles, birth control, or pregnancy can impact the stability and composition of the vaginal microbiome over time [22,115,68,248,249]. Additionally, sexual and hygienic behavior would also be predicted to impact composition by introducing or removing species present and changes in vaginal pH [36,228,250]. Additionally, this methodology is a reductionist approach at recapitulating the vaginal microbiome and capturing species interactions. Species interactions are likely dependent on competition for limited substrates as well as cross-feeding, which in future iterations can be incorporated into the model using methodologies like Monod equations [44,197,251]. Future iterations of the model can begin to incorporate these levels of detail and be personalized to subject behavior and metabolic microenvironment.

Overall, this work provides a new framework to characterize and predict how probiotic strain characteristics contribute to compositional changes during and after treatment cessation. An *in silico* framework to test probiotic strains is particularly important for the vaginal microbiome, as standard *in vitro* and *in vivo* models fail to replicate the base characteristics of the vaginal microenvironment such as co-existence of appropriate vaginal microbiota or low vaginal pH [111,129]. Moreover, current therapeutic regimens to modulate vaginal microbiome composition have high rates of treatment failure, emphasizing the need to develop better tools to evaluate alternative therapies [29]. This framework could be particularly informative in combination with newly developed vagina-on-a-chip technologies to effectively screen new probiotic strains [111]. Together, the use of *in silico* models and new developments in

experimental technologies will inform rational selection of probiotic strains and intelligent design of dosing regimens with or without adjunct antimicrobial use.

4.6 Methods

4.6.1 Model Construction

We used a generalized Lotka-Volterra model (gLVM) [252,253] with four equations was used as the ordinary differential equation-based model. gLVMs include the growth rate of each species, the self-interaction term (contributes to carrying capacity) and inter-species interaction terms. Growth rates were always assumed to be positive when the system is not under any perturbation like menses of antibiotic therapy, self-interaction terms are assumed to always be negative and the inter-species interaction terms can be either positive or negative. For the three species model (oLB, Li or nAB), there are seven possible non-zero steady states. These seven states were related to clinical data using a nearest centroid classifier of the predicted relative abundances. The centroids were determined from VALENCIA as described in Lee *et al.* 2023 [26,243]. For the addition of the probiotic into the model, a fourth microbial population was created resulting in the following equations. All model simulations were completed in MATLAB 2020b and are published at: https://github.com/chyylee/CST_Probiotic

$$\begin{aligned} \frac{d[nAB]}{dt} &= k_{grow-nAB}[nAB] + \alpha_{nAB \rightarrow nAB}[nAB][nAB] + \alpha_{Li \rightarrow nAB}[nAB][Li] \\ &\quad + \alpha_{oLB \rightarrow nAB}[nAB][oLB] + \alpha_{P \rightarrow nAB}[nAB][P] \\ \frac{d[Li]}{dt} &= k_{grow-Li}[Li] + \alpha_{Li \rightarrow Li}[Li][Li] + \alpha_{nAB \rightarrow Li}[Li][nAB] + \alpha_{oLB \rightarrow Li}[Li][oLB] \\ &\quad + \alpha_{P \rightarrow Li}[Li][P] \end{aligned}$$

$$\frac{d[oLB]}{dt} = k_{grow-oLB}[oLB] + \alpha_{oLB \rightarrow oLB}[oLB][oLB] + \alpha_{nAB \rightarrow oLB}[oLB][nAB] \\ + \alpha_{Li \rightarrow oLB}[oLB][Li] + \alpha_{P \rightarrow oLB}[oLB][P]$$

$$\frac{d[P]}{dt} = k_{grow-P}[P] + \alpha_{P \rightarrow P}[P][P] + \alpha_{nAB \rightarrow P}[P][nAB] + \alpha_{Li \rightarrow P}[P][Li] + \alpha_{oLB \rightarrow P}[P][oLB]$$

4.6.2 Virtual Population Development

To test the impact of a probiotic strain at the population level, a virtual patient population was generated using Latin Hypercube Sampling of physiologically defined parameter ranges as described in Lee *et al.* 2023 ([243], Table 4.7.1). The virtual patient population was selected to match the CST equilibrium behavior distribution pattern of the Human Microbiome Project Cohort (HMP) described in Lee *et al.* 2023. Briefly, the CST equilibrium behavior describes the stability in CST classification over time, where subjects that consistently exhibit the same CST are considered mono-stable (1SS) and those that switch between different CSTs are considered multi-stable (2SS). Probiotic strains were tested on virtual patients that could obtain a nAB-dominant (BV positive) state at equilibrium which includes the 1SS nAB dominant (60%), 2SS nAB dominant / Li dominant (31%), and 2SS nAB dominant / Li dominant CST (9%) equilibrium behaviors. The HMP cohort had a similar frequency of self-identified White/Caucasian subjects relative to persons of color as the Lactin-V cohort (32% versus 35%, respectively).

4.6.3 BV Treatment Regimens

The probiotic dose was calibrated to the relative abundance distribution observed in Dausset *et al.* [239], 1 day after an initial dose was given and kept constant throughout the manuscript. Two main probiotic regimens were evaluated: a short-term probiotic therapy without

antibiotic pre-treatment and a long-term probiotic therapy with antibiotic treatment modeled after the regimen for a phase 2b study of Lactin-V [104]. The short-term therapy included a 7-day, once daily dosing of probiotic strains. The Lactin-V regimen included a 5-day antibiotic regimen followed by 4-days of daily dosed probiotics and then 10-weeks of twice weekly probiotic doses. Evaluation of the impact of probiotic was evaluated at multiple time points. The 5-day antibiotic regimen was simulated as a negative impact on nAB growth rate at magnitudes calculated from Mayer et al. [221]. For the short-term probiotic, impact on composition was evaluated at treatment cessation, 1 week, 1 month, 3 months, 6 months, and 12 months. For the Lactin-V regimen, impact on composition was evaluated at 12 weeks (1 week after therapy cessation) and 24 weeks (3 months after therapy cessation). Impact of composition was assessed by classifying the CST after treatment using a nearest centroid classifier. Possible classes were nAB-dominant (BV+), Li-dominant, oLB-dominant, or P-dominant. The regimens were simulated across 2,000 patients, and the frequency of each response type was reported per strain tested.

4.6.4 Local Sensitivity Analysis

Local sensitivity analyses were centered at the parameters for a null probiotic strain and evaluated at 12 months post treatment cessation. The null probiotic strain was defined as a probiotic strain that had a moderate growth rate (0.5 d^{-1}) and negligible interspecies interactions ($\alpha_{\text{nAB} \rightarrow \text{P}}, \alpha_{\text{nAB} \rightarrow \text{Li}}, \alpha_{\text{nAB} \rightarrow \text{oLB}}, \alpha_{\text{P} \rightarrow \text{nAB}}, \alpha_{\text{P} \rightarrow \text{Li}}, \alpha_{\text{P} \rightarrow \text{oLB}} = 0.0 \text{ density}^{-1} \text{d}^{-1}$) and a moderate self-interaction term ($\alpha_{\text{P} \rightarrow \text{P}} = -0.022 \text{ density}^{-1} \text{d}^{-1}$). For the 1 dimensional (1D) perturbation analysis, each probiotic strain parameter was altered one-at-a-time over a set parameter range. The range was -0.10 to $0.10 \text{ density}^{-1} \text{d}^{-1}$ for the interspecies interaction terms, 0 to 1.0 d^{-1} for the growth rate, and -0.004 to $-0.04 \text{ density}^{-1} \text{d}^{-1}$ for the self-interaction term. For the four-parameter perturbation analysis, up to four parameters were modified at a time. Two parameters that were

most sensitive to altering probiotic efficacy (changes in rate of nAB-dominant states) and two parameters most sensitive to altering frequency of Li/oLB-dominated states were selected. Parameters could undergo a positive change (+0.01 density⁻¹d⁻¹), no change (0.00 density⁻¹d⁻¹), or negative (-0.01 density⁻¹d⁻¹) alteration for each parameter, in combination (3 values⁴ parameters = 81 combinations).

4.6.5 Systematic Probiotic Strain Selection

A global uncertainty analysis was used to systematically evaluate probiotic strain characteristics that could consistently promote nAB-dominant, Li-dominant, oLB-dominant, P-dominant communities across the 2,000 subject virtual population as described in Lee *et al.* 2023 [243]. Latin Hypercube Sampling was used to generate 500 *in silico* candidate probiotic strains. Parameter values were sampled from uniform distributions defined with the same ranges used to create the virtual population, excluding $\alpha_{P \rightarrow nAB}$, which was constrained to be negative. Each of the 500 candidate strains was tested in the framework for the short-term regimen and the Lactin-V regimen. Each strain was then classified by the response type that occurred in the highest frequency across the virtual population. For example, if a strain was 10% nAB-dominant, 20% Li-dominant, 60% oLB-dominant, and 10% P-dominant the strain would be classified as an oLB-promoting strain. The association between probiotic strain characteristics and the response classification was assessed using Partial Least Squares Discriminant Analysis (PLS-DA). The top 5 strains that promoted nAB, Li, oLB, and P-dominant states for each regimen were visualized and compared against the other regimen. To understand the Lactin-V regimen, the top 5 *in silico* strains that had similar BV recurrence rates at 12 and 24 weeks were identified by the sum of absolute distance from the predicted and observed rates.

4.6.6 Statistical Analyses

All statistical analyses were completed in MATLAB. Chi-square tests were used to compare frequencies of response types between groups. Wilcoxon rank sum tests were used to compare numerical data. Where noted, P-values were adjusted using Benjamini & Hochberg procedure. The PLS-DA model was created using the PLS Toolbox in MATLAB 2017b using 10-fold cross-validation. Briefly, PLS models are a supervised approach that assigns a loading to each feature (probiotic strain characteristics) and identifies a linear combination of loadings that best separates the response variable (nAB-, Li-, oLB-, P-promoting classification). The linear combination of loadings is referred to as a latent variable (LV) and indicates the magnitude of association between a feature and the response group.

4.6.7 Code and Data Availability

All code and data used in this study are available at: https://github.com/chyylee/CST_Probiotic

4.7 Appendix

4.7.1 Supplementary Tables

Table 4.7.1 Explanation of LHS parameter ranges.

Note the determination of inter-species interaction terms was based on empirical observation and hypothesis on interaction term strength and directionality. More information is in supplementary note 1. Values were scaled to in vivo rates based on Stein et al. [159]

Parameter (<i>in vitro/in vivo</i>)	Value	Explanation	References
$k_{\text{grow-nAB}}$ (hr^{-1})/(d^{-1})	0.1 to 1.00	Growth rate calculated in previous publication from growth curves (Lee et al., 2020)[20] and assessed from digitized growth curves from literature such as Atassi et al., 2019[55] and Anukam and Reid (2008)[187].	[20,56,187]

$k_{\text{grow-Li}} (\text{hr}^{-1})/(\text{d}^{-1})$	0.1 to 1.00	Growth rate calculated in previous publication from growth curves (Lee et al., 2020)[20] and from doubling times (Borgogna et al., 2021)[75].	[20,75]
$k_{\text{grow-oLB}} (\text{hr}^{-1})/(\text{d}^{-1})$	0.1 to 1.00	Growth rate calculated in previous publication from growth curves (Lee et al., 2020) and from digitized data in Chetwin et al., 2019[101] and Juarez-Tomas (2003) [204] as well as Borgogna et al (2021) [75].	[20,75,101,230]
$\alpha_{\text{nAB} \rightarrow \text{nAB}}, \alpha_{\text{Li} \rightarrow \text{Li}},$ $\alpha_{\text{oLB} \rightarrow \text{oLB}}$ ($\text{hr}^{-1}\text{cell density}^{-1}$)/ ($\text{d}^{-1}\text{cell density}^{-1}$)	-0.004 to -0.04	Assumed similar carrying capacities are possible across species and a 10-fold variability. This value and the growth rate value facilitate up to 100-fold variation in carry capacity and clinically relative abundance can upwards of range 1000-fold.	[21,22,115]
$\alpha_{\text{nAB} \rightarrow \text{Li}}, \alpha_{\text{nAB} \rightarrow \text{oLB}},$ $\alpha_{\text{Li} \rightarrow \text{nAB}}, \alpha_{\text{Li} \rightarrow \text{oLB}},$ $\alpha_{\text{oLB} \rightarrow \text{Li}}$ ($\text{hr}^{-1}\text{cell density}^{-1}$)/ ($\text{d}^{-1}\text{cell density}^{-1}$)	-0.12 to 0.12	Assumed directionally of these parameters to be positive or negative dependent on the literature. Magnitude of the values was determined from the largest ratio of interaction term to self-interact term observed experimentally (S1 Fig). The fold-ratio is on the same order of magnitude as clinically estimated gLV terms (Stein et al. 2013).	[59,159,206]
$\alpha_{\text{oLB} \rightarrow \text{nAB}}$ ($\text{hr}^{-1}\text{cell density}^{-1}$)/ ($\text{d}^{-1}\text{cell density}^{-1}$)	-0.12 to 0.00	Assume directionality based on experimental observations that oLB spp. commonly inhibit non-optimal spp. (nAB), such as in Atassi et al. (2006).	[55,206]

Table 4.7.2 Calculated antibiotic impact on BV-associated bacteria (nAB).

Calculated Decay Rate (d^{-1})					
<i>G. vaginalis</i>	BVAB2	BVAB1	<i>Sneathia/Lepto</i>	<i>Megasphaera</i>	<i>A. vaginae</i>
3.82	4.61	3.50	5.04	4.08	5.44
3.12	2.15	2.26	4.18	4.08	4.81
2.45	2.15	2.26	3.19	3.88	4.81
2.12	2.15	2.08	2.87	2.76	3.80
1.84	1.88		2.41	2.03	3.48

1.72	1.69		2.13	2.03	3.23
1.40	1.66		2.07	2.03	2.38
1.33			1.82	1.74	1.88
1.33			1.73		1.88
0.95			1.44		1.54

Table 4.7.3 Clinical probiotic regimens.

Probiotic Duration	Reference	Antibiotic	Route	Probiotic Regimen	Strain	Results	Metric	End Point
Acute	Petricevic et al. 2008	Yes	Vaginal	7 days	L. casei var. rhamnosus (Lcr35)	Significant	Nugent	5 weeks
Acute	Hemmerling 2010	Yes	Vaginal	5 days, 1/wk for 2 weeks	L. crispatus CTV-05	Significant	Recurrence rate	28 days
Acute	Happel 2020	Yes	Both	oral or vaginal spray (15 days, 5 days oral followed by 10 days oral + vaginal spray)	L. acidophilus, L. rhamnosus GG, B. bifidum and B. longum	Mixed results		
Acute	Ehrstrom 2010	Yes	Vaginal	5 days	L. gasseri LN40, L. fermentum LN99, L. casei subsp. rhamnosus LN113 and P.	Not significant	Cure rate	

					acidilactici LN23			
Acute	Mastro-marino 2009	No	Vaginal	7 days	Florisia (<i>L. brevis</i> CD2 + <i>L. salivarius</i> subsp. Salicinius FV2 + <i>L. plantarum</i> FV9)	Significant	Cure rate, Recurrence rate	
Acute	Bradshaw 2012	Yes	Vaginal	12 days	Gynoflor (<i>L. acidophilus</i> KS400 + 0.03 MG ESTRIOL)	Mixed results	Cure rate	30 days
Acute	Hemalatha 2012	No	Vaginal	8 days	Florisia (<i>L. brevis</i> CD2 + <i>L. salivarius</i> subsp. Salicinius FV2 + <i>L. plantarum</i> FV9)	Not significant		
Acute	Ling 2013	Yes	Vaginal	7 days	<i>L. delbrueckii</i> subsp. <i>Lactis</i> <i>DM8909</i>	Significant	Recurrence rate	5 days
Acute	Bisanz 2014	Yes	Vaginal	3 days	<i>L. rhamnosus</i> GR-1, <i>L. reuteri</i> RC-14	Not significant		

Acute	Verdenelli 2016	Yes	Vaginal	7 days	SYNBIO gin (<i>L. rhamnosus</i> IMC 501 + <i>L.</i> <i>paracasei</i> IMC 502)	Significant	Nugent	21 days
Acute	Rapisarda 2018	No	Vaginal	14 days	<i>L. acidophilus</i> LA 14	Significant	Cure rate	28 days
Intermittent	Marcone et al. 2008	Yes	Vaginal	2 months (1/wk)	<i>L. rhamnosus</i>	Significant		
Intermittent	Marcone et al. 2010	Yes	Vaginal	6 months (1/wk)	<i>L. rhamnosus</i>	Significant		12 mo
Intermittent	Heczko 2015	Yes	Oral	10 days/mont h	<i>L. fermentum</i> 57A, <i>L.</i> <i>plantarum</i> 57B, <i>L.</i> <i>gasseri</i> 57C	Significant	Time to recurrence	
Intermittent	Hummelen 2010	Yes	Oral	2x/wk, ~6 months	<i>L. rhamnosus</i> GR-1, <i>L.</i> <i>reuteri</i> RC-14	Not significant	Nugent	
Intermittent	Larsson 2008	Yes	Vaginal	10days/cy cle, 3 cycles	EcoVag (<i>L.</i> <i>gasseri</i> , <i>L.</i> <i>rhamnosus</i>)	Significant		
Intermittent	Eriksson 2005	Yes	Vaginal	2 cycles	<i>L. fermentum</i> , <i>L. casei</i> , <i>L. rhamnosus</i> , and <i>L.</i> <i>gasseri</i>	Not significant	Nugent	
Intermittent	van de Wijger 2020	Yes	Vaginal	Intermitte nt	EF+ (<i>Bifidobacteri</i> <i>um</i> <i>bifidum</i> W28, <i>Lactobacillus</i> <i>acidophilus</i> W70, <i>L.</i>	Significant	Reduce BV bacteria	

					helveticus W74, L. brevis W63, L. plantarum W21, L.			
Intermittent	van de Wijgert 2020	Yes	Vaginal	Intermittent	Gynophilus LP (Lcr regenerans, L. rhamnosus 35)	Significant	Reduce BV bacteria	
Long-term	Bohbo et al. 2018	Yes	Vaginal	56 days	<i>Physioflor</i> (L. crispatus IP 174178)	Significant	Time to recurrence	
long-term	Martinez 2009	Yes	Oral	28 days	L. rhamnosus GR-1, L. reuteri RC-14	Significant	Cure rate	
long-term	Sudha 2012	Yes, non- traditional	Oral	90 days	B. coagulans Unique IS-2	Significant	Symptoms	
long-term	Anukam 2006	Yes	Oral	30 days	L. rhamnosus GR-1, L. reuteri RC-14	Significant	Cure rate, Recurrence rate	30 days
long-term, intermittent	Cohen 2020	Yes	Vaginal	4 days, 2/wk for 10 weeks	L. crispatus CTV-05	Significant	Recurrence rate	12 wk, 24 wk
long-term, intermittent	Marcotte 2019	Yes, non- traditional	Vaginal	30days, 1x/wk 190days	L. rhamnosus DSM 14870, L. gasseri DSM 14869	Not significant	Cure rate, Recurrence rate	

4.7.2 Supplementary Figures

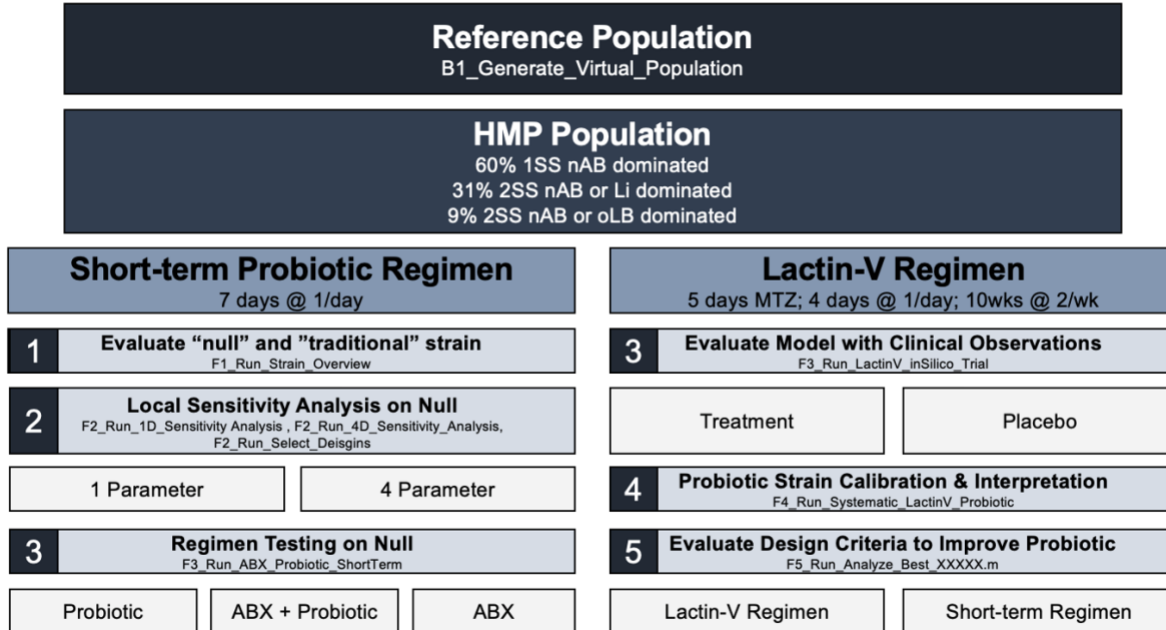


Figure 4.7.1 Overview of analysis methodology.

A virtual population was generated based on the Human Microbiome Project cohort. The analysis included two regimen types, a short-term probiotic regimen with no antibiotic pre-treatment and the regimen described in a phase 2b Lactin-V clinical trial (Cohen et al. 2020).

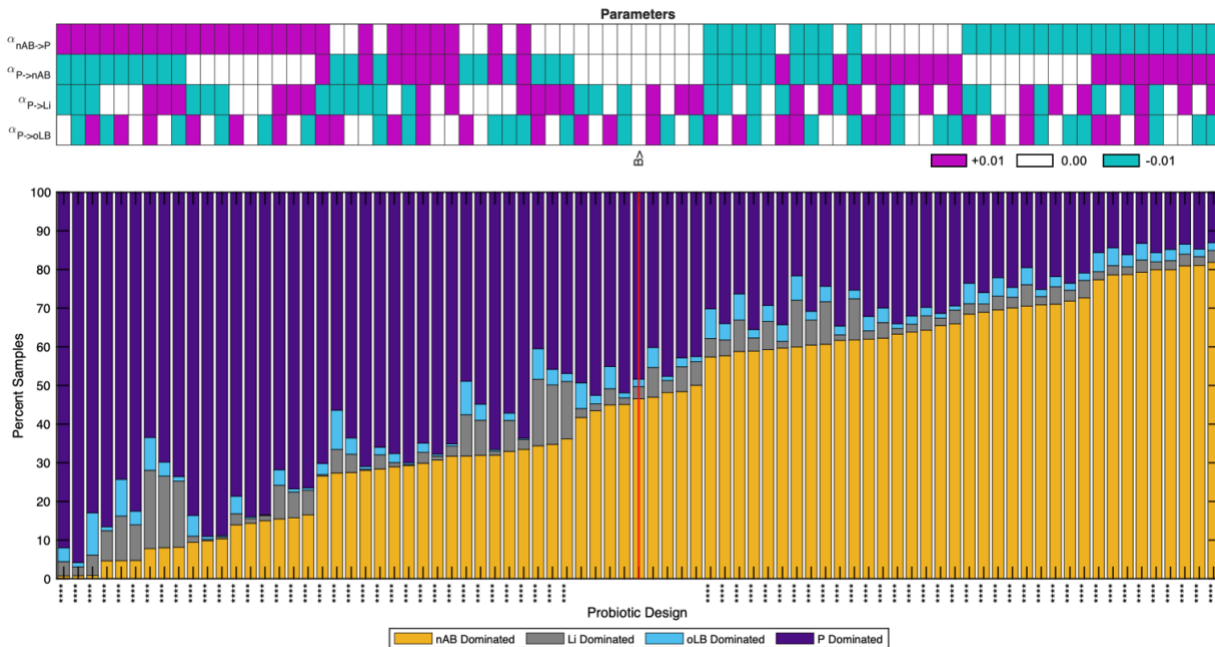


Figure 4.7.2 Four parameter local sensitivity analysis.

The top sensitive parameters for BV clearance and top parameters for modulating endogenous *Lactobacillus* spp. levels were modified systematically from -0.01, 0.00, +0.01 density⁻¹d⁻¹ from the null probiotic strain parameter values giving rise to 81 possible parameter combinations (top heatmap). The percent of the 2,000 in silico BV+ subjects that elicited a certain response type were visualized (nAB-dominant, Li-dominant, oLB-dominant, or P-dominant). Data is plotted from most efficacious (left) to least (right). The null probiotic strain is indicated by “B>” and the red line. Asterisks indicate a significant change in efficacy relative to the null probiotic strain.

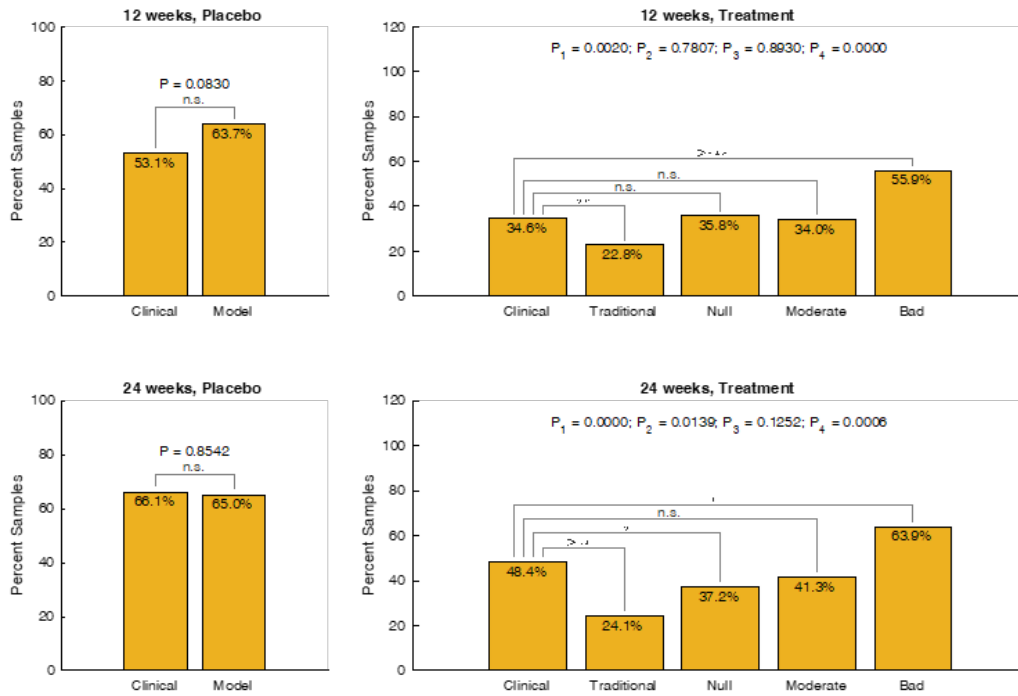


Figure 4.7.3 *Lactin-V* phase 2b clinical trial versus model simulations with increased antibiotic effect.

Comparison of model predictions with *Lactin-V* trial results at 12 and 24 weeks for the placebo and the treatment arm. For the treatment arm, 4 strains were simulated by the model encompassing a traditionally designed probiotic, null probiotic, moderately/conservatively designed probiotic, and bad/negative control probiotic. The impact of antibiotic was simulated at a magnitude that was equivalent to the most sensitive *G. vaginalis* strain in Mayer et al. 2015.

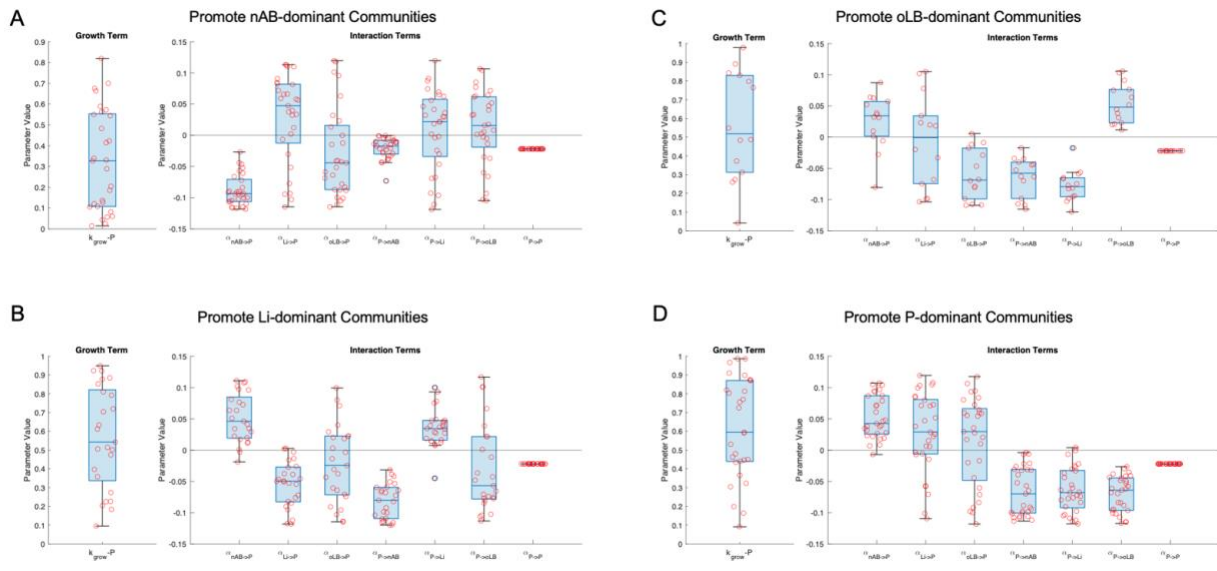


Figure 4.7.4 Parameter values for strains that could elicit consistent population-level compositional changes for a short-term regimen.

Strains in the 90th percentile or higher for imparting a certain compositional effect across the virtual population are visualized. (A) Consistently promote nAB-dominant communities (B) Li-dominant communities (C) oLB-dominant communities (D) P-dominant communities.

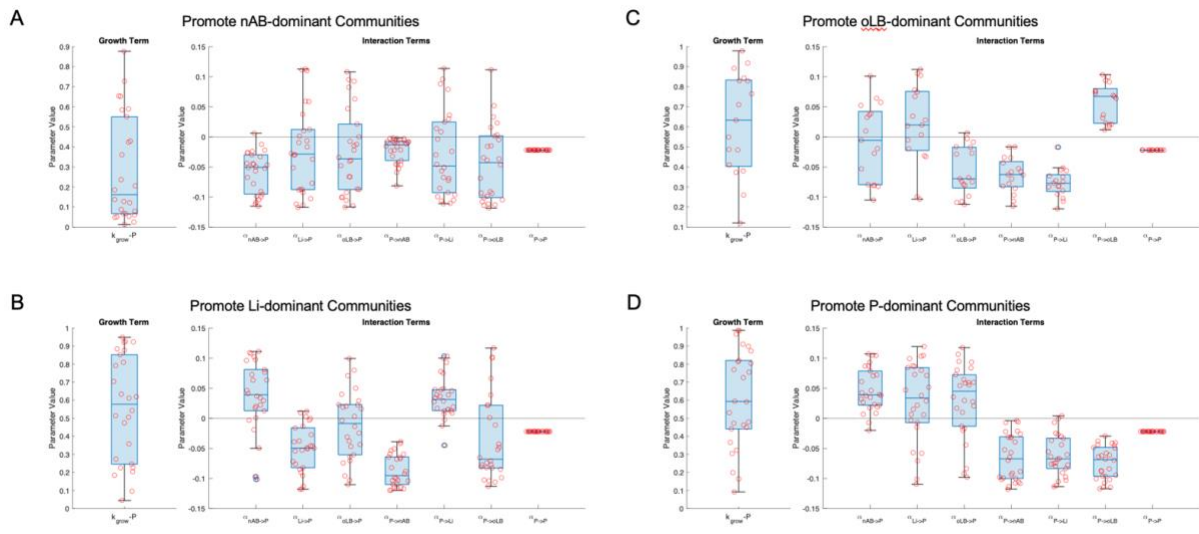


Figure 4.7.5 Parameter values for strains that could elicit consistent population-level compositional changes with the Lactin-V regimen.

Strains in the 90th percentile or higher for imparting a certain compositional effect across the virtual population are visualized. (A) Consistently promote nAB-dominant communities (B) Li-dominant communities (C) oLB-dominant communities (D) P-dominant communities.

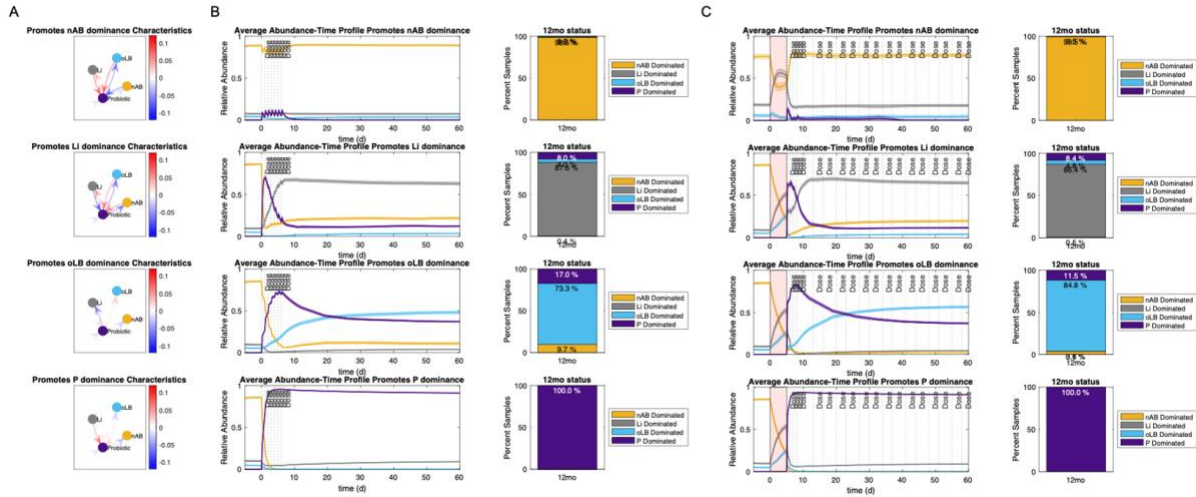


Figure 4.7.6 Comparison short-term probiotic only regimen top strains with Lactin-V regimen.

(A) Interspecies interaction parameter values of top probiotic strains for the short-term probiotic only regimen. (B) Abundance-time profile of community groups for each probiotic strain and predicted 12mo frequency of response types. (C) Lactin-V regimen abundance-time profile and predicted 12mo frequency of response types for strains defined in (A). Red indicates time of antibiotic dosing.

Chapter 5 Discussion and Conclusion

5.1 Concluding Remarks

The vaginal microbiome is centrally important to female reproductive health, yet treatments to re-establish optimal composition exhibit high recurrence rates [29]. In this thesis, I present new frameworks for mechanistic analysis of factors that drive community composition that can also be used to test new therapies on *in silico* populations. In my first aim, we address how analysis of both target species for BV therapy and non-target, optimal species, can impact BV clearance demonstrating the importance of pre-treatment composition on treatment outcomes which were validated *in vitro* and clinically. In my second aim, we characterized and developed a framework to simulate patterns in community composition (CSTs) over time that could replicate menses and antimicrobial associated composition shifts observed clinically. In my third aim, we examined the impact of probiotic strains across virtual patient populations to identify strain characteristics most predictive of BV clearance. Within this aim we also replicated the findings of a recent phase 2b clinical trial, demonstrating the applicability of the model *in vivo*. Altogether, the work in this dissertation has demonstrated the utility of using ordinary differential equations-based models to understand shifts in vaginal microbiome composition and lays the groundwork for the use of *in silico* models to make decisions on new therapies or optimize dosing regimens.

5.1.1 Model Predicts Importance of Pre-treatment Composition on Treatment Efficacy

For the first time, a multi-species *in vitro* model was used to determine antibiotic efficacy in the context of BV [20]. The model accounted for the metabolism and degradation of the standard of care antibiotic, metronidazole, by BV-associated bacteria, *G. vaginalis*, as well as the unexpected uptake of metronidazole by *L. iners*. This two-species model represented a BV-associated state (*G. vaginalis*) and a more optimal state (*L. iners*). Using this model, the importance of pre-treatment relative abundance of *G. vaginalis* to *L. iners* was identified, where higher levels of *L. iners* resulted in decreased efficacy in reducing the *G. vaginalis* population. This result, which would suggest less severe cases of dysbiosis would be less likely to respond to treatment, was accredited to the *L. iners* population reducing the amount of metronidazole in the extracellular environment and validated *in vitro*. Models with additional species, interspecies interactions, and simulated heterogeneity, were created to assess if this finding would generalize across microbial communities. Consistently, results pointed toward the importance of higher pre-treatment ratios of BV-associated bacteria to *Lactobacillus* spp. to decrease the efficacy of metronidazole. This result was then validated in two clinical cohorts, that supported higher pre-treatment ratios of BV-associated bacteria relative to *Lactobacillus* spp. were associated with higher rates of BV recurrence 1 month after metronidazole therapy.

Pre-treatment bacterial abundances have been linked to varying outcomes of antimicrobial therapy in other settings. The impact of bacterial load on antimicrobial efficacy is known as the inoculum effect and is commonly reported for beta-lactam antibiotics when treating beta-lactamase-producing bacteria [190]. We propose a similar effect is contributing to BV recurrence, where higher levels of non-target species are reducing the concentration of metronidazole that can act on target species to treat BV. In line with bacterial populations impacting metronidazole efficacy, inactivation of metronidazole is reported for aerobic

organisms, and associated with decreased metronidazole efficacy to treat *Trichomonas vaginalis* [91]. Thus, the finding that *Lactobacillus* spp. can also sequester MNZ and reduce effective concentrations aimed to reduce BV-associated bacteria would mirror reported drivers for decreased *T. vaginalis* treatment efficacy.

In contrast, studies that aimed to use pre-treatment abundances of BV-associated bacteria and *Lactobacillus* spp. to predict BV treatment outcomes have had mixed results. One study aligned with our findings, reporting that treatment failure was not associated with higher levels of BV-associated bacteria, *G. vaginalis* and *A. vaginae*, [169]. Other reports have observed difficulty in linking microbial pre-treatment abundances to treatment outcomes [254–257]. These observations are likely due to a variety of confounding factors such as antibiotic route of administration, history of BV, time during menstrual cycle, and sexual or hygienic behaviors. Inconsistency in how BV treatment failure is defined likely contributes from differences in observations, as mechanisms that drive tolerance to metronidazole therapy versus recurrence likely differ as some BV-associated strains are reported to be resistant to metronidazole [217]. For example, Armstrong et al. 2023 stratified their data as responders and non-responders based on Nugent score 1 month post-treatment, whereas our study focused specifically on patients that initially responded to therapy, but were BV positive 1 month post-treatment [257]. Turner et al. 2021 defined their cohort into three groups, refractory, recurrent, and remission where refractory patients were BV positive by Amsel criteria at their second visit and recurrent if negative at the second visit, and positive at a later date. Again, the main findings were linked with the refractory group, where higher levels of BV-associated bacteria (Gsp07) were reported pre-treatment [256]. Another study reported higher relative abundances of *L. iners* pre-treatment with treatment success also evaluated refractory BV rather than recurrent BV and used intravaginal

metronidazole rather than oral metronidazole [255]. Lastly, the impact of non-target species on metronidazole is likely one of many contributors to suboptimal treatment outcomes, as aspects such as biofilm penetration, genetic or phenotypic resistance mechanisms from BV-associated bacteria are also linked with antibiotic efficacy [69,87,189].

While our modeling technique was useful at quantifying the relative importance of factors that contribute to metronidazole efficacy, it lacks several components that could make the model more translational to clinical data. First, the model was parameterized to a limited number of bacterial species and strains. This limitation was partially abrogated using sensitivity analyses, but further characterization of interactions of specific species and strains would be helpful for understanding the interactions between vaginal microbiota and antibiotic as well as between species. Second, the model assumes a well-mixed environment, which is likely not the case *in vivo* as biofilms are hypothesized to be key contributors to BV pathogenesis and treatment failure [258]. The incorporation of a biofilm compartment could help better understand synergistic interactions within BV communities and characterize the protective properties of biofilms against antibiotic penetration [72,92,95,96,259,260]. Lastly, the current model does not capture host factors that may dictate the vaginal microenvironment, such as the concentration of antibiotic that is present in the *in vivo* microenvironment, immune milieu, nutrients, or pH levels. As the relationship between vaginal microbiota and the vaginal microenvironment improves, these factors can be incorporated into a model that is more representative of *in vivo* conditions.

5.1.2 Compositional States of VMB Demonstrate Mono- and Multi-Stability

In this work, we were able to link equilibrium composition states observed in human clinical data to predicted steady states using an ordinary differential equations-based model. By making this link, information about microbial characteristics was inferred from the relationship

of growth rates, self-interaction terms, and interspecies interaction terms which govern predicted equilibrium behavior. A global uncertainty analysis was used to recapitulate a physiological parameter space, predicting that around 20% of the population would exhibit alternative compositional states (multi-stability) which was validated by two clinical cohorts [22,115]. By building a virtual patient population based on the frequency at which each equilibrium composition subtype was observed in the Human Microbiome Project cohort, we were able to compare model predictions against clinical observations of compositional changes due to menses and antimicrobial therapy. The strongest simulated menses was predicted to not have a statistically significant difference in the frequency of subjects predicted to switch to nAB-dominated states. For antimicrobial therapy, BV clearance profiles based on two evaluation points were used and compared to the CONRAD BV study [220]. Overall, the predicted frequency of each clearance type was comparable to the clinically observed frequencies and suggested that mono-stability was a major driver of recurrent BV. Lastly, we demonstrated that the model could be used to simulate new therapy types, such as combination prebiotics and antibiotics, as well as alternative dosing regimens. Overall, the use of a mechanistic model that can predict compositional changes in the vaginal microbiome will be useful for the rational design of new strategies to treat and prevent BV.

This work is an extension to classical studies of ecosystems, where communities have been reported to exhibit stability in their species-level populations over time as well as undergo dramatic shifts to an alternative composition of community members [261]. These shifts in composition are hypothesized to be associated with alternative stable states in the system, or multi-stability. Macro-scale examples of these events have been observed in coral reefs [262], standing water vegetation [263], savanna vegetation [211], and lakes [212]. Evidence of multi-

stability also exists for microbial communities [44,160,229,264,265]. For example, a study of the gut microbiome identified evidence of alternative compositional states by analyzing a thousand western adults for bimodal distributions of gut microbiota in a cross-sectional study, followed by an analysis of compositional stability in a longitudinal study [160]. Another study of the gut microbiome and osmotic perturbations from laxatives additionally supported alternative compositional states [266]. The potential of alternative compositional states is important, particularly in the vaginal microbiome where there are compositional states associated with health and disease. Empirical evidence supports that some individuals can be either stable in an optimal state or stable in a non-optimal compositional state [22,115]. The latter is important in the context of BV therapy, as it suggests that a temporary regimen of antibiotics would not be able to re-establish *Lactobacillus* spp. dominance if only one stable state is accessible (mono-stable). This connection to ecological stability could potentially explain why recurrence rates to standard of care antibiotic regimens are so high, and why individuals with recurrent BV respond to therapy while the regimen persists, but ultimately return to pre-treatment compositions upon therapy cessation [29].

Lastly, this work introduces the idea of using *in silico* or virtual cohorts to assess vaginal microbiome therapeutics. Virtual cohort modeling of the vaginal microbiome provides a powerful tool, as the study of the vaginal microbiome is limited by the lack of relevant animal and *in vitro* models and allows for characterization uncertainty that arises in clinical samples (both host and microbial-related) on treatment success [267]. Virtual cohorts and populations historically have been used in quantitative systems pharmacology models to explore possible ranges in outcomes and can help predict dose feasibility [268,269]. The ultimate result is a prediction for the likelihood of attaining a set treatment success metric, which occurs from

sampling parameter values defined by probability distributions that recapitulate population-level variability [270]. By using this approach with the vaginal microbiome, new regimens and therapeutic targets can more easily be assessed.

5.1.3 Probiotic Strain Efficacy is Driven by Resident Community Characteristics

In our work, we used a virtual patient population with equilibrium composition frequencies observed in the Human Microbiome Cohort and focused on communities that were able to reach a BV state (nAB-dominated) [115]. Two probiotic regimens were assessed, one that was a short-term 7-day regimen of probiotic with no pre-treatment period with antibiotic and the other modeled a regimen reported in a phase 2b clinical trial for Lactin-V [104]. Response types were quantified by the classified community state type after probiotic treatment and were observed to be nAB-dominant (treatment failure), Li-dominant, oLB-dominant, or probiotic dominant. Outcomes were then expressed a percentage of the virtual patient population that exhibited each response type. To unilaterally assess drivers of probiotic strain efficacy, we created a control or “null” probiotic that had a moderate growth rate and no interspecies interactions. Local sensitivity analyses were then used to identify drivers, revealing the importance of resident nAB populations on probiotic strain efficacy. We were additionally able to show that probiotic interactions with Li and oLB could be designed to selectively boost a specific *Lactobacillus* spp. response type. The model was then used to assess the Lactin-V regimen, resulting in comparable predictions of the placebo arm at 24 weeks and the treatment arm at 12 and 24 weeks. We systematically screened probiotic strains to identify characteristics that were associated with probiotic efficacy in the two regimen types. Notably, the probiotic strains were more sensitive to the impact of resident *Lactobacillus* spp. with pre-treatment antibiotic. Additionally, strains that exhibited similar predicted BV recurrence rates as Lactin-V

were observed to be dependent on pre-treatment antibiotic therapy to have a significant effect on vaginal microbiome composition. Overall, these results demonstrate that this framework could be used to help guide the selection of probiotic strain characteristics and evaluate dosing frequency and duration for probiotic therapies.

The limitations of this modeling framework are similar to those previously described, as the model does not capture any host characteristics or the impact of biofilms. Additionally, while our model predicted similar outcomes as reported for the phase IIb Lactin-V study, there is a high degree of uncertainty in key microbial growth and interspecies interaction strengths of the Lactin-V strain. Further characterization of the probiotic strain with common resident community members such as *Lactobacillus* spp. (*L. crispatus*, *L. gasseri*, *L. jensenii*, *L. iners*) and BV-associated bacteria (*G. vaginalis*, *A. vaginae*, *P. bivia*) are needed for higher confidence in model predictions to ensure appropriate parameter distributions are selected for the *in silico* populations [271].

A computational framework to screen probiotics will be a useful tool to help develop alternative therapies that can combat recurrent episodes of BV. The development of probiotics has been popular but remains relatively unregulated [99]. Traditionally, strains have been selected based on their ability to inhibit urogenital pathogens and adhere to epithelial cells; however, strain selection criteria vary significantly and are dependent on the route of administration. For example, probiotics given orally need to be able to survive the gastrointestinal tract and thus exhibit acid, bile salt, and lysozyme tolerance [272]. Then, probiotics must engraft into the community or survive long enough to promote a state that increases the abundance of endogenous *Lactobacillus* spp. [273]. Screening for probiotic strains does not often include co-cultures with strains expected to be present in resident communities,

especially endogenous *Lactobacillus* spp. which may directly compete for the same niche [228]. Our work suggests that an additional criterion for probiotic strain selection may be competition with common *Lactobacillus* spp., particularly *L. iners* which is most associated with BV. Screening of probiotics on the impact of *ex vivo* cultures with human vaginal microbiota could also help identify strains that have the highest probability of survival when introduced to pre-existing communities.

5.2 Future Work

The use of modeling frameworks to understand the vaginal microbiome can provide powerful insights into the vaginal microbiome that are difficult to assess with current techniques, particularly because the VMB is highly dynamic and there is a lack of adequate *in vitro* and preclinical models [129]. However, to curate increasingly realistic models of the VMB some additional experimental data is needed. For example, knowledge of how key vaginal microbiota grow under the same conditions is needed to better recapitulate *in vivo* conditions. Furthermore, metabolism likely drives how microbial consortia assemble, dictating the need for measuring key substrates that are growth-limiting or cross-fed between species [196,229,274]. By assessing the metabolic interactions, we will be able to start answering questions surrounding how changes in vaginal microenvironment (e.g., glycogen [47,48,275], amylases [58,276,277], biogenic amines [75,278], sialidases, mucins, and organic acids [279]) relate to changes in community composition, which can be incorporated into future iterations of model mechanistic resolution. Secondly, our models have been limited to focusing specifically on vaginal microbiota, while the interactions with host cells such as vaginal epithelial and stromal cells likely dictate the composition of the vaginal microenvironment [64,70,111,280]. The addition of vaginal epithelial cells will also allow for interrogation beyond compositional shifts associated with BV to

characterizing epithelial barrier damage that is hypothesized to drive negative reproductive outcomes. Moreover, we would also be able to explore a key outstanding question of the VMB, of what are the functional differences between asymptomatic and symptomatic BV, which are associated with similar shifts to non-optimal composition, but vastly different impacts on host health [21,71,281]. Lastly, biofilm formation is hypothesized to be a major driver of treatment recurrence in the vaginal microenvironment but is not captured in our modeling framework [87,92,165,225,258–260,282–285]. Model development that can capture key components of biofilms that promote the existence of BV-associated microbiota and tolerance to antibiotics will be critical to testing new therapies and answering questions surrounding the importance of disrupting biofilms on treatment outcomes for BV.

5.2.1 Validation in Controlled Systems

One of the major challenges in developing *in silico* models for the VMB is that there is limited experimental data to calibrate and validate the models. *In vitro* studies rarely have more than two species in co-culture, and when the two species are in co-culture it becomes difficult to quantify each population. Moreover, it is difficult to co-culture non-optimal vaginal microbiota like *G. vaginalis* with both *L. iners* and *L. crispatus* as each species has unique growth requirements. As a result, skilled experimentalists are required to generate this data and access to such data is limited. *In vivo* studies also present challenges as data are noisy and have many external factors impacting the system that makes relating a model directly, such as through standard calibration processes, intractable as the estimated parameter values have a high degree of uncertainty.

Ideal experimental data would include pairwise co-culture of representative vaginal microbiota similar to Venturelli et al [286]. Venturelli et al proposed a data-driven pipeline to

elucidate ecological forces in synthetic gut microbiome communities [286]. The first step in their pipeline was to evaluate temporal behaviors in monoculture and pairwise co-cultures for major phyla of the gut microbiome (12-member synthetic community) using a serial dilution methodology. Community member relative abundance was quantified by 16S rRNA gene sequencing and biomass was measured by OD600. Model calibration was completed on the pairwise co-culture data and validation was completed using multi-species assemblages. Another study that analyzed urinary tract infection assemblages used conditioned media experiments to determine interspecies interaction strengths, which constrained their Lotka-Volterra model parameters [161]. For analysis of communities relevant to the vaginal microbiome, pairwise co-cultures between different *G. vaginalis* strains, *L. crispatus* strains, and *L. iners* strains should be, at minimum, analyzed. It is important that multiple strains of each be evaluated as growth requirements and interspecies interactions are reported to vary *in vitro* [42,55,57,59,69,276,287]. For example, a *G. vaginalis* strain (5-1) that was isolated from a woman without BV and a woman with BV (strain 101) had variable interactions with *L. iners*, where the pathogenic strain exhibited enhanced cell adhesion when in co-culture with *L. iners* [59]. Additionally, *L. crispatus* strains have exhibited variable production of lactic-acid and ability to metabolize glycogen [57,226,276].

Recently, a new microfluidic culture model was developed for the human vaginal mucosa [111]. This organ-on-a-chip model was able to host consortia of optimal *L. crispatus* and non-optimal *G. vaginalis* containing consortia. The model also included primary vaginal epithelium and underlying stroma fibroblasts, which together work to replicate the vaginal microenvironment. Model design for a vagina-on-a-chip could be based on a chemostat or continuous-flow culture model. Basic chemostat equations are well-established for tracking

microbial biomass and the amount of nutrient in a vessel [288]. In the simplest framework, only a flow rate will need to be added to the system of ordinary differential equations. Bacteria populations can then be described as a reproduction term minus an outflow term. For example, the vagina-on-a-chip, the reported flow rate was 40 μ l/h and measured effluent abundances of bacterial species that would be necessary to understand the system dilution rate [111]. Often chemostat models relate bacterial growth to nutrient concentration, which includes the impact of cell growth on depleting nutrients, depletion due to outflow, and replenishment due to stock solution. Monod equations are often used to relate nutrient concentration to the growth rate of microbial species. Development of this relationship would require the identification of rate-limiting substrates for the microbial species of interest.

5.2.2 Resolution of Interspecies Interactions

The generalized Lotka-Volterra model is a reductionist approach to capturing ecological interactions between microbial species [158]. One important distinction from classical use of pairwise interaction modeling from macro-scale ecology (e.g., hare-lynx) is that microbial interactions can be contact-independent [197,289]. The difficulty with contact-independent mediators is that these metabolites or substrates may not be directly proportional to the bacterial abundance. One study analyzed the difference between reducing the interaction term to one parameter versus modeling the intermediary substrates [197]. This work highlighted that pairwise Lotka-Volterra models can fail under certain circumstances where interactions are chemically-mediated and could be sensitive to the relative fitness of the species and the initial conditions in each model. Notably, the authors discuss that the level of abstraction (mechanism) for models is dependent on the amount of information available on the interactions within a

community. Currently, the information on pairwise, chemically-mediated, interactions is limited, but is an area of growth within the field (Figure 5.2.1).

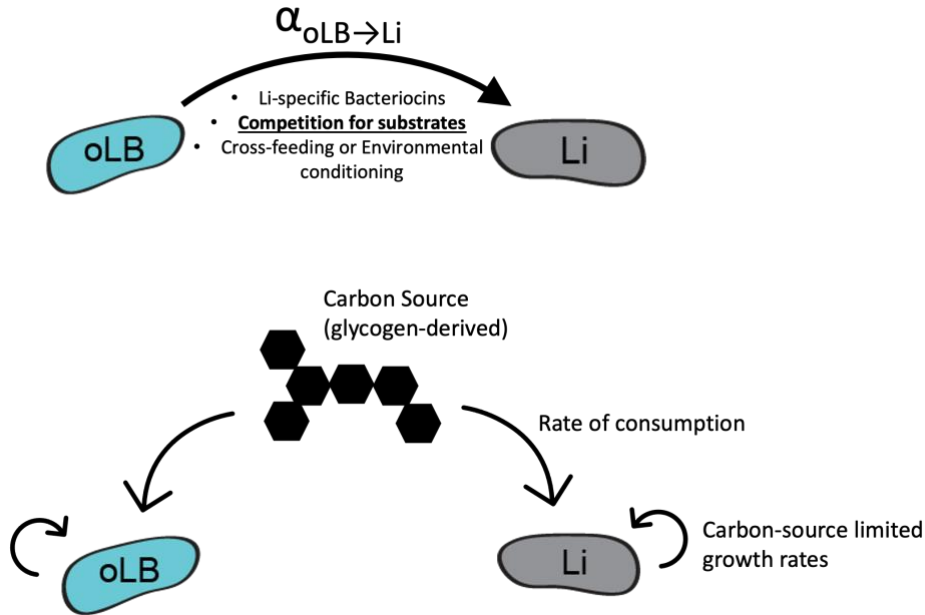


Figure 5.2.1 Comparison of *gLV* interspecies interaction term versus modeling with a chemically-mediated interaction for the competition for a growth limiting carbon source.

To improve modeling of vaginal communities, pairwise co-culture or spent media experiments could help resolve the magnitude and directionality of interspecies interactions as well as the chemical mediators. For gut microbiota, one experimental and computational framework unraveled the interactions between six members of a defined murine microbiota *in vitro* [196]. This group used pair-wise co-cultures to understand growth interactions between species and then incorporated mono- versus co-culture supernatant metabolomics into a Constant Yield Expectation (ConYE) framework. From the mono- and co-culture growth data, the group was able to identify the interaction type between species as amensal (0/- or -/0), competitive (-/-), parasitic (+/- or -/+), commensal (0/+ or 0/+), mutual (+/+), or neutral. ConYE identifies metabolites that have consumption or production behavior changed in co-culture, where significant differences from the null hypothesis indicates that at least one strain altered its

metabolism. ConYE was then used to identify cross-fed metabolites that could explain a growth benefit between two species by analyzing patterns in metabolites relative to ConYE predictions. Candidate substrates that did not reject the null hypothesis by ConYE were tyramine, valine, and choline and candidate substrates that did reject the null hypothesis were isoleucine, alanine, proline, and formate. However, from the mono- vs co-culture data it was difficult to resolve what drove differences in biomass production. Another strategy to assess the impact of metabolites on biomass is the use of genome-scale metabolic reconstructions (GENREs). GENREs mathematically reconstruct all metabolic reactions of an organism and can be related to biomass production [152]. Using flux based analysis, *in silico* predictions on the dependence of biomass production on the presence or absence of a metabolite can be tested [290]. Using this analysis on the candidate metabolites from ConYE, Medlock et al. determined that valine was most essential for *Clostridium* ASF356 growth, whereas alanine, proline, choline, and formate were not predicted to impact growth rates [196]. The observation that individual metabolites in excess did not confer a growth benefit led to the assessment of interactions between metabolites, leading to the validation of combinations of proline (Strickland reaction electron acceptors) and electron donors (such as alanine) in promoting growth *in vitro*.

GENREs can be used to assess pairwise interactions between species [291–293]. Pairwise interaction analysis involves determining the metabolic exchange between two GENREs using a joint matrix. In the gut microbiome, this work was employed as a part of the characterization of 773 human gut bacteria (AGORA, assembly of gut organisms through reconstruction and analysis) [291]. These models have been used to demonstrate the importance of environmental conditions, such as the impact of diet, on interspecies interactions. For example, one report tested 13 different diet types and analyzed the change in growth rate for *Eubacterium halli* and

Bifidobacterium adolescentis, reporting amensalism, neutralism, commensalism, and parasitism dependent on the diet type [292]. Such an analysis could be useful for understanding the vaginal microbiome, as host associated behavior and hormone shifts are linked to changes in the vaginal microenvironment that may dynamically shift the way the vaginal community interacts. Notably, a second release of AGORA (AGORA2) was published in 2023 that covers 7,302 strains and several microbe-drug interactions [294]. Additionally, AGORA2 includes 83 vaginal strains including *Atopobium vaginae*, *Bifidobacterium*, *Dialister*, *G. vaginalis*, several *L. crispatus*, *L. jensenii*, *L. iners*, and *L. gasseri* strains, *Mobiluncus*, and *Prevotella* spp.

Methodologies to use genome-scale metabolic models in dynamic and multi-species settings exist [295]. These methodologies extend dynamic flux balance analysis (dFBA), which relate the growth rate of the microbial species and the consumption/production rate to every metabolite in the model environment. These rate parameters are then coupled to ordinary differential equations that predict species abundance and metabolite concentrations [296]. One such study demonstrated multi-stability and hysteresis in a two species model relevant to small intestinal bacterial overgrowth [296]. This work was particularly interested in the role of oxygen flux in promoting shifts between aerobe-anaerobe compositions, identifying two metabolic pathways that lead to two distinct steady states under the same environmental conditions. A hybrid generalized Lotka-Volterra and joint GENRE FBAs has also been proposed [297]. Unlike traditional model fitting for generalized Lotka-Volterra models which requires dense, longitudinal sampling, this methodology only requires a single compositional sample. Using this framework, Brunner and Chia demonstrated that this methodology could predict engraftment of a probiotic, which they validated with previously published invasion experiments [298–300]. Similar work in the vaginal microbiome to understand shifts between optimal and non-optimal

compositions could help pinpoint metabolic drivers of conditions like bacterial vaginosis and explain why some individuals undergo compositional shifts and others do not [22,115]. Within the past few years the first GENREs for vaginal microbiota have been reported, which will make these analyses more obtainable [5,154,301].

A main drawback of GENREs is the intensive curation needed to validate core metabolic processes. An alternative approach to capturing metabolic interactions is to use Monod growth equations or a MacArthur consumer resource model [251,289,302]. Monod equations quantify the growth of a microbe on a growth limiting substrate. If two species compete for the same substrate, the interaction can be captured through the consumption and requirement for that substrate for the species to grow rather than the generalized Lotka-Volterra interspecies interaction term [44]. Examples could be glycogen, glucose, or other glycogen metabolites. Until recently, *L. crispatus* strains were not believed to be able to directly metabolize glycogen [57]. Other reports suggest that BV-associated bacteria such as *G. vaginalis* may degrade glycogen more efficiently than *Lactobacillus* spp., providing an opportunity for their growth [303]. To be able to parameterize vaginal microbiota Monod-kinetic models, experimental data relating the growth rate of each microbe needs to be characterized at several different concentrations of the carbon source. For example, to fit a *G. vaginalis* Monod-kinetics model, growth curves of *G. vaginalis* collecting biomass measurements over 24-48h would need to be conducted at 0.125, 0.25, 0.5, 1, 2, 4 g/L glucose. Metabolites that benefit the growth of another species could be modeled in an additive manner and characterized similarly to the proposed *G. vaginalis* experiment. An example could be characterizing the dependence of *G. vaginalis* growth on ammonia, given the reports that ammonia produced by *P. bivia* promotes *G. vaginalis* growth [74]. Cross-feeding, or the potential for microbial species to facilitate the growth of other

species, has been explored using the MacArthur consumer-resource model. A landmark application of quantitative consumer-resource models analyzed community assembly in soil microbiomes [198]. The MacArthur consumer-resource model contained a single carbon source (glucose) and non-specific cross-feeding interactions using a stoichiometric matrix describing the ratio of consumed resources to secreted resources. This methodology allowed the group to explore the stabilization effect cross-feeding has on a community that is competing for the same carbon source. The use of MacArthur consumer-resource models have also been applied to human microbiomes [163,304].

5.2.3 Incorporation of Vaginal Epithelium

A major limitation in our current modeling framework is the inability to precisely integrate the impact of the host on microbial communities and vice versa. The vagina-on-a-chip will facilitate the collection of experimental data required to build and validate computational models of microbe-epithelial interactions, including adhesion or lysis of vaginal epithelial cell barriers, as well as how vaginal microbiota impact immune responses [101,280,305]. Moreover, this experimental framework could provide insights into the interplay of host hormones with vaginal microbiota, as the vagina-on-a-chip model was shown to be responsive to hormones, mimicking accumulation and thickening of vaginal epithelium at increased estrogen levels that will allow for the interrogation of the impact of contraceptives and menstrual cycles. Altogether, the vagina-on-a-chip technology will provide a valuable tool to build improved *in silico* models of the VMB through the characterization of interactions between vaginal epithelium and vaginal microbes. To model vaginal epithelial cells, an additional cell population will need to be incorporated into the model. This addition will require identifying possible growth rates and carrying capacities for the vaginal epithelial cell populations, which will can be determined from

growth curves like those reported in Iguchi et al. 1983 [306]. Next, the interaction between BV-associated bacteria and vaginal epithelial cells could be incorporated by modeling the impact of vaginolysin (which is produced by BV-associated bacteria) on vaginal epithelial cell lysis. This lysis could be modeled using a death rate and half-maximal killing model like those used to model antibiotic killing. Parameters can be estimated from previous publications that demonstrate the relationship between vaginolysin concentration and epithelial cell lysis [70]. Similarly, the impact of *L. iners* inerolysin could be modeled [64]. The function of both cytolytins is pH dependent with inerolysin more active at acidic pH and vaginolysin more active at neutral pH and less active at acidic pH. Thus, incorporation of the pH in the model will be critical for predicting the impact of community member composition on vaginal epithelial cells [307]. Expression of vaginolysin is also tied to phenotype, where mono-species biofilms of *Gardnerella* were associated with less production of vaginolysin [308,258]. However, multi-species biofilms were reported to have higher expression vaginolysin, driving additional complexity that could be captured by incorporating biofilm-specific populations into the model. Lastly, *L. crispatus* was observed to decrease vaginolysin expression and could be modeled as a negative feedback loop within the system [309].

To model pH, either the rate of acidification or the production rate of lactic acid by *Lactobacillus* spp. would need to be simulated [54]. For the former, some publications have reported the rate of acidification for a variety of *Lactobacillus* spp. [310]. Absolute measurements of lactic acid production are most commonly reported [55,75,213,232,311–313], but some publications have reported time curves of lactic acid production required to calculate the production rate [314]. The concentration of lactic acid and its impact on BV-associated bacteria cell killing can be parameterized from previously published kill curves [54]. Acid

tolerance mechanisms from BV-associated bacteria may also be of interest, with the predominating mechanism believed to be through the production of biogenic amines [278,75]. Modeling the impact of pH and lactic acid concentration using ODE models has been reported, and requires the addition of equations relating the impact of pH on the bulk growth rate of the desired species [315].

Lastly, modeling the competition for substrates will be vital to predicting community composition. The primary carbon source in the vagina on a chip could be controlled or assumed to be glycogen from the vaginal epithelial cells [47,275]. For example, the model could capture nuances in the ability of certain microbiota to metabolize glycogen prior to its degradation into simpler metabolites like glucose or maltose [58,316]. Recently, publications on the kinetics of carbon source metabolism were reported for key vagina microbiota, *L. crispatus*, *L. iners*, and *G. vaginalis* for glycogen, amylose and pullulan [58]. The kinetic parameters characterized include k_{cat} , K_m and the specificity constant needed to model the consumption of these substrates in an ODE-based framework using Michaelis Menten kinetics. The enzymes associated with glycogen metabolism are also pH-dependent, which supports another mechanism that could promote *L. crispatus* dominance at low pH [58]. Thus, the mechanistic exploration of competition for glycogen and environmental conditions (pH) could provide new insights for drivers of compositional shifts or stability.

Altogether, the incorporation of both microbial composition and key functional outputs such as pH and damage to vaginal epithelial cells will make understanding the nuances of BV more obtainable. One major outstanding question is why some healthy women exhibit compositions that are similar to those who are BV-positive [21]. This framework could help interrogate what functional factors could be different, such as the impact of the community on

vaginal epithelium. Additionally, it could help settle questions between asymptomatic and symptomatic BV, such as whether these conditions are unique health states or different stages of BV [317]. For example, typically adverse effects of BV are associated with increased epithelium shedding with a recent report suggesting that asymptomatic BV had decreased shedding even compared to healthy controls [317]. When assessing cell maturity, it was revealed that asymptomatic patients may be in a phase post-symptomatic BV as cells were less mature than healthy samples. Our framework could be used to test this hypothesis, by tracking longitudinal changes in vaginal epithelium and microbial composition which then can be validated using the vagina-on-a-chip technology. Altogether, the vagina-on-a-chip technology will facilitate the controlled study of vaginal consortia needed to develop mechanistic *in silico* models that can pinpoint drivers of BV pathogenesis and treatment failure.

5.2.4 Incorporation of Biofilms

An important characteristic of BV is the polymicrobial biofilm that adheres to the vaginal epithelium. Biofilms are reported to decrease sensitivity to antibiotics as well as compounds produced by *Lactobacillus* spp. typically associated with inhibited BV-associated bacteria [259,260]. Thus, new therapies and regimens to treat BV are being designed to disrupt these biofilms such as through the use of boric acid [223], enhanced derivatives of boric acid (TOL-463) [94], and amphoteric tensides (WO3191) [95]. To be able to simulate and capture the importance of biofilm disruption in BV treatment outcomes, additional components will need to be incorporated into our modeling framework. A minimal model for biofilm formation would require delineation between planktonically growing species and biofilm-growing species. This framework could be similar to semimechanistic PK/PD models used to predict antibiotic efficacy [157,318]. These models capture phenotypic switching between two populations of cells:

normally growing cells and persister cells that typically have reduced growth rates and decreased susceptibility to antibiotics. In relation to biofilm modeling, each species would have two states to transition between a planktonic state with increased sensitivity to antibiotics and a biofilm state that is less sensitive to antibiotic and antimicrobial agents generated by other species in the vaginal microbiome. Modeling of the impact of disrupting agents would be simulated as changing the rate at which cells switch between these two phenotypes. More complex models of biofilms have been extensively studied, but likely not necessary for our framework [319]. These models include capturing heterogeneity in fluid flow associated with the physical properties of the biofilm and require partial differential equations. Since decreased antibiotic penetration can be captured as a decreased sensitivity (higher EC50), there is not a current need to capture the system at a resolution that models advection-diffusion in biofilms.

Bibliography

1. Haggerty CL, Totten PA, Tang G, Astete SG, Ferris MJ, Norori J, et al. Identification of novel microbes associated with pelvic inflammatory disease and infertility. *Sex Transm Infect.* 2016;92: 441–446. doi:10.1136/sextrans-2015-052285
2. Kong Y, Liu Z, Shang Q, Gao Y, Li X, Zheng C, et al. The Disordered Vaginal Microbiota Is a Potential Indicator for a Higher Failure of in vitro Fertilization. *Front Med (Lausanne).* 2020;7. doi:10.3389/fmed.2020.00217
3. Moreno I, Codoñer FM, Vilella F, Valbuena D, Martinez-Blanch JF, Jimenez-Almazán J, et al. Evidence that the endometrial microbiota has an effect on implantation success or failure. *American Journal of Obstetrics and Gynecology.* 2016;215: 684–703. doi:10.1016/j.ajog.2016.09.075
4. de Freitas AS, Dobbler PCT, Mai V, Procianoy RS, Silveira RC, Corso AL, et al. Defining microbial biomarkers for risk of preterm labor. *Braz J Microbiol.* 2020;51: 151–159. doi:10.1007/s42770-019-00118-x
5. Fettweis JM, Serrano MG, Brooks JP, Edwards DJ, Girerd PH, Parikh HI, et al. The vaginal microbiome and preterm birth. *Nature Medicine.* 2019;25: 1012–1021. doi:10.1038/s41591-019-0450-2
6. Hillier SL, Nugent RP, Eschenbach DA, Krohn MA, Gibbs RS, Martin DH, et al. Association between bacterial vaginosis and preterm delivery of a low-birth-weight infant. The Vaginal Infections and Prematurity Study Group. *N Engl J Med.* 1995;333: 1737–1742. doi:10.1056/NEJM199512283332604
7. Rasmussen MA, Thorsen J, Dominguez-Bello MG, Blaser MJ, Mortensen MS, Bregner AD, et al. Ecological succession in the vaginal microbiota during pregnancy and birth. *The ISME Journal.* 2020;14: 2325–2335. doi:10.1038/s41396-020-0686-3
8. Feehily C, Crosby D, Walsh CJ, Lawton EM, Higgins S, McAuliffe FM, et al. Shotgun sequencing of the vaginal microbiome reveals both a species and functional potential signature of preterm birth. *npj Biofilms and Microbiomes.* 2020;6: 1–9. doi:10.1038/s41522-020-00162-8
9. McMillan A, Rulisa S, Sumarah M, Macklaim JM, Renaud J, Bisanz JE, et al. A multi-platform metabolomics approach identifies highly specific biomarkers of bacterial diversity in the vagina of pregnant and non-pregnant women. *Scientific Reports.* 2015;5: 14174. doi:10.1038/srep14174

10. Haggerty CL, Hillier SL, Bass DC, Ness RB. Bacterial Vaginosis and Anaerobic Bacteria Are Associated with Endometritis. *Clin Infect Dis*. 2004;39: 990–995. doi:10.1086/423963
11. Ness RB, Kip KE, Hillier SL, Soper DE, Stamm CA, Sweet RL, et al. A cluster analysis of bacterial vaginosis-associated microflora and pelvic inflammatory disease. *Am J Epidemiol*. 2005;162: 585–590. doi:10.1093/aje/kwi243
12. Brown SE, Schwartz JA, Robinson CK, O’Hanlon DE, Bradford LL, He X, et al. The Vaginal Microbiota and Behavioral Factors Associated With Genital *Candida albicans* Detection in Reproductive-Age Women. *Sex Transm Dis*. 2019;46: 753–758. doi:10.1097/OLQ.0000000000001066
13. Ceccarani C, Foschi C, Parolin C, D’Antuono A, Gaspari V, Consolandi C, et al. Diversity of vaginal microbiome and metabolome during genital infections. *Scientific Reports*. 2019;9: 14095. doi:10.1038/s41598-019-50410-x
14. Edwards VL, Smith SB, McComb EJ, Tamarelle J, Ma B, Humphrys MS, et al. The Cervicovaginal Microbiota-Host Interaction Modulates *Chlamydia trachomatis* Infection. *mBio*. 2019;10. doi:10.1128/mBio.01548-19
15. Houdt R van, Ma B, Bruisten SM, Speksnijder AGCL, Ravel J, Vries HJC de. *Lactobacillus iners*-dominated vaginal microbiota is associated with increased susceptibility to *Chlamydia trachomatis* infection in Dutch women: a case–control study. *Sex Transm Infect*. 2018;94: 117–123. doi:10.1136/sextrans-2017-053133
16. Lewis AL, Gilbert NM. Roles of the vagina and the vaginal microbiota in urinary tract infection: evidence from clinical correlations and experimental models. *GMS Infect Dis*. 2020;8: Doc02. doi:10.3205/id000046
17. Taha TE, Hoover DR, Dallabetta GA, Kumwenda NI, Mtimavalye LA, Yang LP, et al. Bacterial vaginosis and disturbances of vaginal flora: association with increased acquisition of HIV. *AIDS*. 1998;12: 1699–1706. doi:10.1097/00002030-199813000-00019
18. Cheu RK, Gustin AT, Lee C, Schifanella L, Miller CJ, Ha A, et al. Impact of vaginal microbiome communities on HIV antiretroviral-based pre-exposure prophylaxis (PrEP) drug metabolism. *PLOS Pathogens*. 2020;16: e1009024. doi:10.1371/journal.ppat.1009024
19. Klatt NR, Cheu R, Birse K, Zevin AS, Perner M, Noël-Romas L, et al. Vaginal bacteria modify HIV tenofovir microbicide efficacy in African women. *Science*. 2017;356: 938–945. doi:10.1126/science.aai9383
20. Lee CY, Cheu RK, Lemke MM, Gustin AT, France MT, Hampel B, et al. Quantitative modeling predicts mechanistic links between pre-treatment microbiome composition and metronidazole efficacy in bacterial vaginosis. *Nature Communications*. 2020;11: 6147. doi:10.1038/s41467-020-19880-w

21. Ravel J, Gajer P, Abdo Z, Schneider GM, Koenig SSK, McCulle SL, et al. Vaginal microbiome of reproductive-age women. *PNAS*. 2011;108: 4680–4687. doi:10.1073/pnas.1002611107
22. Gajer P, Brotman RM, Bai G, Sakamoto J, Schütte UME, Zhong X, et al. Temporal Dynamics of the Human Vaginal Microbiota. *Sci Transl Med*. 2012;4: 132ra52. doi:10.1126/scitranslmed.3003605
23. Zhou X, Brown CJ, Abdo Z, Davis CC, Hansmann MA, Joyce P, et al. Differences in the composition of vaginal microbial communities found in healthy Caucasian and black women. *ISME J*. 2007;1: 121–133. doi:10.1038/ismej.2007.12
24. Zhou X, Hansmann MA, Davis CC, Suzuki H, Brown CJ, Schutte U, et al. The Vaginal Bacterial Communities of Japanese Women Resemble Those of Women in Other Racial Groups. *FEMS Immunol Med Microbiol*. 2010;58: 169–181. doi:10.1111/j.1574-695X.2009.00618.x
25. Abdo Z, Schütte UME, Bent SJ, Williams CJ, Forney LJ, Joyce P. Statistical methods for characterizing diversity of microbial communities by analysis of terminal restriction fragment length polymorphisms of 16S rRNA genes. *Environmental Microbiology*. 2006;8: 929–938. doi:10.1111/j.1462-2920.2005.00959.x
26. France MT, Ma B, Gajer P, Brown S, Humphrys MS, Holm JB, et al. VALENCIA: a nearest centroid classification method for vaginal microbial communities based on composition. *Microbiome*. 2020;8: 166. doi:10.1186/s40168-020-00934-6
27. Payne SC, Cromer PR, Stanek MK, Palmer AA. Evidence of African-American women’s frustrations with chronic recurrent bacterial vaginosis. *Journal of the American Academy of Nurse Practitioners*. 2010;22: 101–108. doi:10.1111/j.1745-7599.2009.00474.x
28. Bilardi JE, Walker S, Temple-Smith M, McNair R, Mooney-Somers J, Bellhouse C, et al. The Burden of Bacterial Vaginosis: Women’s Experience of the Physical, Emotional, Sexual and Social Impact of Living with Recurrent Bacterial Vaginosis. *PLOS ONE*. 2013;8: e74378. doi:10.1371/journal.pone.0074378
29. Koumans E, Sternberg M, Bruce C, McQuillan G, Kendrick J, Sutton M, et al. The Prevalence of Bacterial Vaginosis in the United States, 2001–2004; Associations With Symptoms, Sexual Behaviors, and Reproductive Health. *Sexually Transmitted Diseases*. 2007;34: 864–869. doi:10.1097/OLQ.0b013e318074e565
30. Amsel R, Totten PA, Spiegel CA, Chen KCS, Eschenbach D, Holmes KK. Nonspecific vaginitis: Diagnostic criteria and microbial and epidemiologic associations. *The American Journal of Medicine*. 1983;74: 14–22. doi:10.1016/0002-9343(83)91112-9
31. Colonna C, Steelman M. Amsel Criteria. *StatPearls*. Treasure Island (FL): StatPearls Publishing; 2022. Available: <http://www.ncbi.nlm.nih.gov/books/NBK542319/>

32. Nugent RP, Krohn MA, Hillier SL. Reliability of diagnosing bacterial vaginosis is improved by a standardized method of gram stain interpretation. *Journal of Clinical Microbiology*. 1991;29: 297–301.
33. Mohammadzadeh F, Dolatian M, Jorjani M, Majd HA. Diagnostic Value of Amsel's Clinical Criteria for Diagnosis of Bacterial Vaginosis. *Glob J Health Sci*. 2015;7: 8–14. doi:10.5539/gjhs.v7n3p8
34. Brotman RM, Ravel J. Ready or Not: The Molecular Diagnosis of Bacterial Vaginosis. *Clin Infect Dis*. 2008;47: 44–46. doi:10.1086/588662
35. Coleman JS, Gaydos CA. Molecular Diagnosis of Bacterial Vaginosis: an Update. *Journal of Clinical Microbiology*. 2018;56. doi:10.1128/JCM.00342-18
36. Brotman RM, Klebanoff MA, Nansel TR, Andrews WW, Schwebke JR, Zhang J, et al. A Longitudinal Study of Vaginal Douching and Bacterial Vaginosis—A Marginal Structural Modeling Analysis. *Am J Epidemiol*. 2008;168: 188–196. doi:10.1093/aje/kwn103
37. Bautista CT, Wurapa E, Sateren WB, Morris S, Hollingsworth B, Sanchez JL. Bacterial vaginosis: a synthesis of the literature on etiology, prevalence, risk factors, and relationship with chlamydia and gonorrhoea infections. *Military Medical Research*. 2016;3: 4. doi:10.1186/s40779-016-0074-5
38. Ness RB, Hillier SL, Richter HE, Soper DE, Stamm C, McGregor J, et al. Douching in relation to bacterial vaginosis, lactobacilli, and facultative bacteria in the vagina. *Obstet Gynecol*. 2002;100: 765. doi:10.1016/s0029-7844(02)02184-1
39. Vodstreil LA, Hocking JS, Law M, Walker S, Tabrizi SN, Fairley CK, et al. Hormonal Contraception Is Associated with a Reduced Risk of Bacterial Vaginosis: A Systematic Review and Meta-Analysis. *PLoS One*. 2013;8: e73055. doi:10.1371/journal.pone.0073055
40. Serrano MG, Parikh HI, Brooks JP, Edwards DJ, Arodz TJ, Edupuganti L, et al. Racioethnic diversity in the dynamics of the vaginal microbiome during pregnancy. *Nature Medicine*. 2019;25: 1001–1011. doi:10.1038/s41591-019-0465-8
41. Hickey RJ, Zhou X, Pierson JD, Ravel J, Forney LJ. Understanding vaginal microbiome complexity from an ecological perspective. *Translational Research*. 2012;160: 267–282. doi:10.1016/j.trsl.2012.02.008
42. Argentini C, Fontana F, Alessandri G, Lugli GA, Mancabelli L, Ossiprandi MC, et al. Evaluation of Modulatory Activities of *Lactobacillus crispatus* Strains in the Context of the Vaginal Microbiota. *Microbiology Spectrum*. 2022;10: e02733-21. doi:10.1128/spectrum.02733-21
43. Khan S, Voordouw MJ, Hill JE. Competition Among *Gardnerella* Subgroups From the Human Vaginal Microbiome. *Frontiers in Cellular and Infection Microbiology*. 2019;9. Available: <https://www.frontiersin.org/articles/10.3389/fcimb.2019.00374>

44. Vet S, Buyl S de, Faust K, Danckaert J, Gonze D, Gelens L. Bistability in a system of two species interacting through mutualism as well as competition: Chemostat vs. Lotka-Volterra equations. *PLOS ONE*. 2018;13: e0197462. doi:10.1371/journal.pone.0197462
45. Simoes JA, Hashemi FB, Aroutcheva AA, Heimler I, Spear GT, Shott S, et al. Human Immunodeficiency Virus Type 1 Stimulatory Activity by *Gardnerella vaginalis*: Relationship to Biotypes and Other Pathogenic Characteristics. *The Journal of Infectious Diseases*. 2001;184: 22–27.
46. Anderson DJ, Marathe J, Pudney J. The Structure of the Human Vaginal Stratum Corneum and its Role in Immune Defense. *Am J Reprod Immunol*. 2014;71: 618–623. doi:10.1111/aji.12230
47. Mirmonsef P, Hotton AL, Gilbert D, Gioia CJ, Maric D, Hope TJ, et al. Glycogen Levels in Undiluted Genital Fluid and Their Relationship to Vaginal pH, Estrogen, and Progesterone. *PLOS ONE*. 2016;11: e0153553. doi:10.1371/journal.pone.0153553
48. Mirmonsef P, Hotton AL, Gilbert D, Burgad D, Landay A, Weber KM, et al. Free Glycogen in Vaginal Fluids Is Associated with *Lactobacillus* Colonization and Low Vaginal pH. *PLoS One*. 2014;9. doi:10.1371/journal.pone.0102467
49. Lacroix G, Gouyer V, Gottrand F, Desseyn J-L. The Cervicovaginal Mucus Barrier. *Int J Mol Sci*. 2020;21: 8266. doi:10.3390/ijms21218266
50. France M, Alizadeh M, Brown S, Ma B, Ravel J. Towards a deeper understanding of the vaginal microbiota. *Nat Microbiol*. 2022;7: 367–378. doi:10.1038/s41564-022-01083-2
51. Hill DR, Brunner ME, Schmitz DC, Davis CC, Flood JA, Schlievert PM, et al. In vivo assessment of human vaginal oxygen and carbon dioxide levels during and post menses. *Journal of Applied Physiology*. 2005;99: 1582–1591. doi:10.1152/jappphysiol.01422.2004
52. O’Hanlon DE, Lanier BR, Moench TR, Cone RA. Cervicovaginal fluid and semen block the microbicidal activity of hydrogen peroxide produced by vaginal lactobacilli. *BMC Infect Dis*. 2010;10: 1–8. doi:10.1186/1471-2334-10-120
53. O’Hanlon DE, Moench TR, Cone RA. Vaginal pH and microbicidal lactic acid when lactobacilli dominate the microbiota. *PLoS ONE*. 2013;8: e80074. doi:10.1371/journal.pone.0080074
54. O’Hanlon DE, Moench TR, Cone RA. In vaginal fluid, bacteria associated with bacterial vaginosis can be suppressed with lactic acid but not hydrogen peroxide. *BMC Infect Dis*. 2011;11: 200. doi:10.1186/1471-2334-11-200
55. Atassi F, Brassart D, Grob P, Graf F, Servin AL. *Lactobacillus* strains isolated from the vaginal microbiota of healthy women inhibit *Prevotella bivia* and *Gardnerella vaginalis* in coculture and cell culture. *FEMS Immunol Med Microbiol*. 2006;48: 424–432. doi:10.1111/j.1574-695X.2006.00162.x

56. Atassi F, Pho Viet Ahn DL, Lievin-Le Moal V. Diverse Expression of Antimicrobial Activities Against Bacterial Vaginosis and Urinary Tract Infection Pathogens by Cervicovaginal Microbiota Strains of *Lactobacillus gasseri* and *Lactobacillus crispatus*. *Front Microbiol.* 2019;10. doi:10.3389/fmicb.2019.02900
57. van der Veer C, Hertzberger RY, Bruisten SM, Tytgat HLP, Swanenburg J, de Kat Angelino-Bart A, et al. Comparative genomics of human *Lactobacillus crispatus* isolates reveals genes for glycosylation and glycogen degradation: implications for in vivo dominance of the vaginal microbiota. *Microbiome.* 2019;7. doi:10.1186/s40168-019-0667-9
58. Jenkins DJ, Woolston BM, Hood-Pishchany MI, Pelayo P, Konopaski AN, Quinn Peters M, et al. Bacterial amylases enable glycogen degradation by the vaginal microbiome. *Nat Microbiol.* 2023; 1–12. doi:10.1038/s41564-023-01447-2
59. Castro J, Henriques A, Machado A, Henriques M, Jefferson KK, Cerca N. Reciprocal Interference between *Lactobacillus* spp. and *Gardnerella vaginalis* on Initial Adherence to Epithelial Cells. *Int J Med Sci.* 2013;10: 1193–1198. doi:10.7150/ijms.6304
60. Nilsen T, Swedek I, Lagenaur LA, Parks TP. Novel Selective Inhibition of *Lactobacillus iners* by *Lactobacillus*-Derived Bacteriocins. *Appl Environ Microbiol.* 2020;86. doi:10.1128/AEM.01594-20
61. Bloom SM, Mafunda NA, Woolston BM, Hayward MR, Frempong JF, Abai AB, et al. Cysteine dependence of *Lactobacillus iners* is a potential therapeutic target for vaginal microbiota modulation. *Nat Microbiol.* 2022;7: 434–450. doi:10.1038/s41564-022-01070-7
62. France MT, Mendes-Soares H, Forney LJ. Genomic Comparisons of *Lactobacillus crispatus* and *Lactobacillus iners* Reveal Potential Ecological Drivers of Community Composition in the Vagina. *Appl Environ Microbiol.* 2016;82: 7063–7073. doi:10.1128/AEM.02385-16
63. Ragaliauskas T, Plečkaitytė M, Jankunec M, Labanauskas L, Baranauskiene L, Valincius G. Inerolysin and vaginolysin, the cytolysins implicated in vaginal dysbiosis, differently impair molecular integrity of phospholipid membranes. *Sci Rep.* 2019;9: 10606. doi:10.1038/s41598-019-47043-5
64. Rampersaud R, Planet PJ, Randis TM, Kulkarni R, Aguilar JL, Lehrer RI, et al. Inerolysin, a cholesterol-dependent cytolysin produced by *Lactobacillus iners*. *J Bacteriol.* 2011;193: 1034–1041. doi:10.1128/JB.00694-10
65. Kim H, Kim T, Kang J, Kim Y, Kim H. Is *Lactobacillus* Gram-Positive? A Case Study of *Lactobacillus iners*. *Microorganisms.* 2020;8: 969. doi:10.3390/microorganisms8070969
66. Nunn KL, Forney LJ. Unraveling the Dynamics of the Human Vaginal Microbiome. *Yale J Biol Med.* 2016;89: 331–337.

67. Fredricks DN, Fiedler TL, Thomas KK, Mitchell CM, Marrazzo JM. Changes in Vaginal Bacterial Concentrations with Intravaginal Metronidazole Therapy for Bacterial Vaginosis as Assessed by Quantitative PCR. *J Clin Microbiol.* 2009;47: 721–726. doi:10.1128/JCM.01384-08
68. Srinivasan S, Liu C, Mitchell CM, Fiedler TL, Thomas KK, Agnew KJ, et al. Temporal Variability of Human Vaginal Bacteria and Relationship with Bacterial Vaginosis. *PLOS ONE.* 2010;5: e10197. doi:10.1371/journal.pone.0010197
69. Castro J, Jefferson KK, Cerca N. Genetic Heterogeneity and Taxonomic Diversity among *Gardnerella* Species. *Trends in Microbiology.* 2020;28: 202–211. doi:10.1016/j.tim.2019.10.002
70. Gelber SE, Aguilar JL, Lewis KLT, Ratner AJ. Functional and phylogenetic characterization of Vaginolysin, the human-specific cytolysin from *Gardnerella vaginalis*. *J Bacteriol.* 2008;190: 3896–3903. doi:10.1128/JB.01965-07
71. Yeoman CJ, Yildirim S, Thomas SM, Durkin AS, Torralba M, Sutton G, et al. Comparative Genomics of *Gardnerella vaginalis* Strains Reveals Substantial Differences in Metabolic and Virulence Potential. *PLOS ONE.* 2010;5: e12411. doi:10.1371/journal.pone.0012411
72. Rosca AS, Castro J, Sousa LGV, França A, Vanechoutte M, Cerca N. In vitro interactions within a biofilm containing three species found in bacterial vaginosis (BV) support the higher antimicrobial tolerance associated with BV recurrence. *Journal of Antimicrobial Chemotherapy.* 2022; dkac155. doi:10.1093/jac/dkac155
73. Castro J, Rosca AS, Cools P, Vanechoutte M, Cerca N. *Gardnerella vaginalis* Enhances *Atopobium vaginae* Viability in an in vitro Model. *Front Cell Infect Microbiol.* 2020;10: 83. doi:10.3389/fcimb.2020.00083
74. Pybus V, Onderdonk AB. Evidence for a commensal, symbiotic relationship between *Gardnerella vaginalis* and *Prevotella bivia* involving ammonia: potential significance for bacterial vaginosis. *J Infect Dis.* 1997;175: 406–413. doi:10.1093/infdis/175.2.406
75. Borgogna J-LC, Shardell MD, Grace SG, Santori EK, Americus B, Li Z, et al. Biogenic Amines Increase the Odds of Bacterial Vaginosis and Affect the Growth and Lactic Acid Production by Vaginal *Lactobacillus* spp. *Appl Environ Microbiol.* 2021 [cited 10 Mar 2021]. doi:10.1128/AEM.03068-20
76. Cruden DL, Galask RP. Reduction of Trimethylamine Oxide to Trimethylamine by *Mobiluncus* Strains Isolated from Patients with Bacterial Vaginosis. *Microbial Ecology in Health and Disease.* 1988;1: 95–100. doi:10.3109/08910608809140187
77. Bradshaw CS, Sobel JD. Current Treatment of Bacterial Vaginosis-Limitations and Need for Innovation. *J Infect Dis.* 2016;214 Suppl 1: S14-20. doi:10.1093/infdis/jiw159

78. Thurman AR, Kimble T, Herold B, Mesquita PMM, Fichorova RN, Dawood HY, et al. Bacterial Vaginosis and Subclinical Markers of Genital Tract Inflammation and Mucosal Immunity. *AIDS Research and Human Retroviruses*. 2015;31: 1139–1152. doi:10.1089/aid.2015.0006
79. Bradshaw CS, Morton AN, Hocking J, Garland SM, Morris MB, Moss LM, et al. High Recurrence Rates of Bacterial Vaginosis over the Course of 12 Months after Oral Metronidazole Therapy and Factors Associated with Recurrence. *J Infect Dis*. 2006;193: 1478–1486. doi:10.1086/503780
80. Ma L, Su J, Su Y, Sun W, Zeng Z. Probiotics administered intravaginally as a complementary therapy combined with antibiotics for the treatment of bacterial vaginosis: a systematic review protocol. *BMJ Open*. 2017;7: e019301. doi:10.1136/bmjopen-2017-019301
81. Ferris DG, Litaker MS, Woodward L, Mathis D, Hendrich J. Treatment of bacterial vaginosis: a comparison of oral metronidazole, metronidazole vaginal gel, and clindamycin vaginal cream. *J Fam Pract*. 1995;41: 443–449.
82. Koumans EH, Markowitz LE, Hogan V, CDC BV Working Group. Indications for Therapy and Treatment Recommendations for Bacterial Vaginosis in Nonpregnant and Pregnant Women: A Synthesis of Data. *Clinical Infectious Diseases*. 2002;35: S152–S172. doi:10.1086/342103
83. Oduyebo OO, Anorlu RI, Ogunsola FT. The effects of antimicrobial therapy on bacterial vaginosis in non-pregnant women. *Cochrane Database of Systematic Reviews*. 2009 [cited 1 Feb 2023]. doi:10.1002/14651858.CD006055.pub2
84. Nagaraja P. Antibiotic resistance of *Gardnerella vaginalis* in recurrent bacterial vaginosis. *Indian J Med Microbiol*. 2008;26: 155–157. doi:10.4103/0255-0857.40531
85. Ferris MJ, Maszta A, Aldridge KE, Fortenberry JD, Fidel PL, Martin DH. Association of *Atopobium vaginae*, a recently described metronidazole resistant anaerobe, with bacterial vaginosis. *BMC Infectious Diseases*. 2004;4: 5. doi:10.1186/1471-2334-4-5
86. De Backer E, Verhelst R, Verstraelen H, Claeys G, Verschraegen G, Temmerman M, et al. Antibiotic susceptibility of *Atopobium vaginae*. *BMC Infectious Diseases*. 2006;6: 51. doi:10.1186/1471-2334-6-51
87. Li T, Zhang Z, Wang F, He Y, Zong X, Bai H, et al. Antimicrobial Susceptibility Testing of Metronidazole and Clindamycin against *Gardnerella vaginalis* in Planktonic and Biofilm Formation. *Can J Infect Dis Med Microbiol*. 2020;2020: 1361825. doi:10.1155/2020/1361825
88. Petrina MAB, Cosentino LA, Rabe LK, Hillier SL. Susceptibility of bacterial vaginosis (BV)-associated bacteria to secnidazole compared to metronidazole, tinidazole and clindamycin. *Anaerobe*. 2017;47: 115–119. doi:10.1016/j.anaerobe.2017.05.005

89. Dingsdag SA, Hunter N. Metronidazole: an update on metabolism, structure–cytotoxicity and resistance mechanisms. *J Antimicrob Chemother.* 2018;73: 265–279. doi:10.1093/jac/dkx351
90. Müller M. Mode of action of metronidazole on anaerobic bacteria and protozoa. *Surgery.* 1983;93: 165–171.
91. Edwards DI, Thompson EJ, Tomusange J, Shanson D. Inactivation of metronidazole by aerobic organisms. *J Antimicrob Chemother.* 1979;5: 315–316. doi:10.1093/jac/5.3.315
92. Muzny CA, Schwebke JR. Biofilms: An Underappreciated Mechanism of Treatment Failure and Recurrence in Vaginal Infections. *Clin Infect Dis.* 2015;61: 601–606. doi:10.1093/cid/civ353
93. Latham-Cork HC, Walker KF, Thornton JG, Gunnarsson OS, Säfholm A, Cardell M, et al. A novel non-antimicrobial treatment of bacterial vaginosis: An open label two-private centre study. *Eur J Obstet Gynecol Reprod Biol.* 2021;256: 419–424. doi:10.1016/j.ejogrb.2020.11.059
94. Marrazzo JM, Dombrowski JC, Wierzbicki MR, Perlowski C, Pontius A, Dithmer D, et al. Safety and Efficacy of a Novel Vaginal Anti-infective, TOL-463, in the Treatment of Bacterial Vaginosis and Vulvovaginal Candidiasis: A Randomized, Single-blind, Phase 2, Controlled Trial. *Clin Infect Dis.* 2019;68: 803–809. doi:10.1093/cid/ciy554
95. Gottschick C, Deng Z-L, Vital M, Masur C, Abels C, Pieper DH, et al. Treatment of biofilms in bacterial vaginosis by an amphoteric tenside pessary-clinical study and microbiota analysis. *Microbiome.* 2017;5: 119. doi:10.1186/s40168-017-0326-y
96. Gottschick C, Szafranski SP, Kunze B, Sztajer H, Masur C, Abels C, et al. Screening of Compounds against *Gardnerella vaginalis* Biofilms. *PLOS ONE.* 2016;11: e0154086. doi:10.1371/journal.pone.0154086
97. pHyph. In: Gedeo Biotech [Internet]. [cited 8 Mar 2023]. Available: <https://gedeabiotech.com/phyph>
98. Plummer EL, Bradshaw CS, Doyle M, Fairley CK, Murray GL, Bateson D, et al. Lactic acid-containing products for bacterial vaginosis and their impact on the vaginal microbiota: A systematic review. *PLoS One.* 2021;16: e0246953. doi:10.1371/journal.pone.0246953
99. Wu S, Hugerth LW, Schuppe-Koistinen I, Du J. The right bug in the right place: opportunities for bacterial vaginosis treatment. *npj Biofilms Microbiomes.* 2022;8: 1–11. doi:10.1038/s41522-022-00295-y
100. Lev-Sagie A, Goldman-Wohl D, Cohen Y, Dori-Bachash M, Leshem A, Mor U, et al. Vaginal microbiome transplantation in women with intractable bacterial vaginosis. *Nature Medicine.* 2019;25: 1500–1504. doi:10.1038/s41591-019-0600-6

101. Chetwin E, Manhanzva MT, Abrahams AG, Froissart R, Gamiendien H, Jaspan H, et al. Antimicrobial and inflammatory properties of South African clinical *Lactobacillus* isolates and vaginal probiotics. *Scientific Reports*. 2019;9: 1917. doi:10.1038/s41598-018-38253-4
102. Lagenaur LA, Hemmerling A, Chiu C, Miller S, Lee PP, Cohen CR, et al. Connecting the Dots: Translating the Vaginal Microbiome Into a Drug. *J Infect Dis*. 2020;223: S296–S306. doi:10.1093/infdis/jiaa676
103. Armstrong E, Hemmerling A, Miller S, Burke KE, Newmann SJ, Morris SR, et al. Sustained effect of LACTIN-V (*Lactobacillus crispatus* CTV-05) on genital immunology following standard bacterial vaginosis treatment: results from a randomised, placebo-controlled trial. *The Lancet Microbe*. 2022;3: e435–e442. doi:10.1016/S2666-5247(22)00043-X
104. Cohen CR, Wierzbicki MR, French AL, Morris S, Newmann S, Reno H, et al. Randomized Trial of Lactin-V to Prevent Recurrence of Bacterial Vaginosis. *New England Journal of Medicine*. 2020;382: 1906–1915. doi:10.1056/NEJMoa1915254
105. Laue C, Papazova E, Liesegang A, Pannenbeckers A, Arendarski P, Linnerth B, et al. Effect of a yoghurt drink containing *Lactobacillus* strains on bacterial vaginosis in women - a double-blind, randomised, controlled clinical pilot trial. *Benef Microbes*. 2018;9: 35–50. doi:10.3920/BM2017.0018
106. Heczko PB, Tomusiak A, Adamski P, Jakimiuk AJ, Stefański G, Mikołajczyk-Cichońska A, et al. Supplementation of standard antibiotic therapy with oral probiotics for bacterial vaginosis and aerobic vaginitis: a randomised, double-blind, placebo-controlled trial. *BMC Womens Health*. 2015;15: 115. doi:10.1186/s12905-015-0246-6
107. Russo R, Karadja E, De Seta F. Evidence-based mixture containing *Lactobacillus* strains and lactoferrin to prevent recurrent bacterial vaginosis: a double blind, placebo controlled, randomised clinical trial. *Benef Microbes*. 2019;10: 19–26. doi:10.3920/BM2018.0075
108. Vujic G, Jajac Knez A, Despot Stefanovic V, Kuzmic Vrbanovic V. Efficacy of orally applied probiotic capsules for bacterial vaginosis and other vaginal infections: a double-blind, randomized, placebo-controlled study. *Eur J Obstet Gynecol Reprod Biol*. 2013;168: 75–79. doi:10.1016/j.ejogrb.2012.12.031
109. Anukam KC, Osazuwa E, Osemene GI, Ehigiagbe F, Bruce AW, Reid G. Clinical study comparing probiotic *Lactobacillus* GR-1 and RC-14 with metronidazole vaginal gel to treat symptomatic bacterial vaginosis. *Microbes Infect*. 2006;8: 2772–2776. doi:10.1016/j.micinf.2006.08.008
110. Martin DH, Marrazzo JM. The Vaginal Microbiome: Current Understanding and Future Directions. *The Journal of Infectious Diseases*. 2016;214: S36–S41. doi:10.1093/infdis/jiw184

111. Mahajan G, Doherty E, To T, Sutherland A, Grant J, Junaid A, et al. Vaginal microbiome-host interactions modeled in a human vagina-on-a-chip. *Microbiome*. 2022;10: 1–18. doi:10.1186/s40168-022-01400-1
112. Faith JJ, Guruge JL, Charbonneau M, Subramanian S, Seedorf H, Goodman AL, et al. The long-term stability of the human gut microbiota. *Science*. 2013;341: 1237439. doi:10.1126/science.1237439
113. Oh J, Byrd AL, Park M, Kong HH, Segre JA. Temporal Stability of the Human Skin Microbiome. *Cell*. 2016;165: 854–866. doi:10.1016/j.cell.2016.04.008
114. Song SD, Acharya KD, Zhu JE, Deveney CM, Walther-Antonio MRS, Tetel MJ, et al. Daily Vaginal Microbiota Fluctuations Associated with Natural Hormonal Cycle, Contraceptives, Diet, and Exercise. *mSphere*. 2020;5. doi:10.1128/mSphere.00593-20
115. Ravel J, Brotman RM, Gajer P, Ma B, Nandy M, Fadrosh DW, et al. Daily temporal dynamics of vaginal microbiota before, during and after episodes of bacterial vaginosis. *Microbiome*. 2013;1: 1–6. doi:10.1186/2049-2618-1-29
116. Costello EK, Lauber CL, Hamady M, Fierer N, Gordon JI, Knight R. Bacterial Community Variation in Human Body Habitats Across Space and Time. *Science*. 2009;326: 1694–1697. doi:10.1126/science.1177486
117. Tamashiro R, Strange L, Schnackenberg K, Santos J, Gadalla H, Zhao L, et al. Stability of healthy subgingival microbiome across space and time. *Sci Rep*. 2021;11: 23987. doi:10.1038/s41598-021-03479-2
118. Dewhirst FE, Chen T, Izard J, Paster BJ, Tanner ACR, Yu W-H, et al. The Human Oral Microbiome. *Journal of Bacteriology*. 2010;192: 5002–5017. doi:10.1128/JB.00542-10
119. Flores GE, Caporaso JG, Henley JB, Rideout JR, Domogala D, Chase J, et al. Temporal variability is a personalized feature of the human microbiome. *Genome Biol*. 2014;15: 531. doi:10.1186/s13059-014-0531-y
120. Skowron K, Bauza-Kaszewska J, Kraszewska Z, Wiktorczyk-Kapischke N, Grudlewska-Buda K, Kwiecińska-Piróg J, et al. Human Skin Microbiome: Impact of Intrinsic and Extrinsic Factors on Skin Microbiota. *Microorganisms*. 2021;9: 543. doi:10.3390/microorganisms9030543
121. Ross AA, Müller KM, Weese JS, Neufeld JD. Comprehensive skin microbiome analysis reveals the uniqueness of human skin and evidence for phyllosymbiosis within the class Mammalia. *Proceedings of the National Academy of Sciences*. 2018;115: E5786–E5795. doi:10.1073/pnas.1801302115
122. Man WH, de Steenhuijsen Piters WAA, Bogaert D. The microbiota of the respiratory tract: gatekeeper to respiratory health. *Nat Rev Microbiol*. 2017;15: 259–270. doi:10.1038/nrmicro.2017.14

123. Carney SM, Clemente JC, Cox MJ, Dickson RP, Huang YJ, Kitsios GD, et al. Methods in Lung Microbiome Research. *Am J Respir Cell Mol Biol.* 2020;62: 283–299. doi:10.1165/rcmb.2019-0273TR
124. Yi X, Gao J, Wang Z. The human lung microbiome—A hidden link between microbes and human health and diseases. *iMeta.* 2022;1: e33. doi:10.1002/imt2.33
125. Rivera AJ, Frank JA, Stumpf R, Salyers AA, Wilson BA, Olsen GJ, et al. Differences between the normal vaginal bacterial community of baboons and that of humans. *Am J Primatol.* 2011;73: 119–126. doi:10.1002/ajp.20851
126. Yildirim S, Yeoman CJ, Janga SC, Thomas SM, Ho M, Leigh SR, et al. Primate vaginal microbiomes exhibit species specificity without universal *Lactobacillus* dominance. *ISME J.* 2014;8: 2431–2444. doi:10.1038/ismej.2014.90
127. Holm JB, France MT, Ma B, McComb E, Robinson CK, Mehta A, et al. Comparative Metagenome-Assembled Genome Analysis of “*Candidatus Lachnocurva vaginae*”, Formerly Known as Bacterial Vaginosis-Associated Bacterium–1 (BVAB1). *Frontiers in Cellular and Infection Microbiology.* 2020;10. Available: <https://www.frontiersin.org/articles/10.3389/fcimb.2020.00117>
128. Yang E, Fan L, Yan J, Jiang Y, Doucette C, Fillmore S, et al. Influence of culture media, pH and temperature on growth and bacteriocin production of bacteriocinogenic lactic acid bacteria. *AMB Express.* 2018;8: 10. doi:10.1186/s13568-018-0536-0
129. Miller EA, Beasley DE, Dunn RR, Archie EA. Lactobacilli Dominance and Vaginal pH: Why is the Human Vaginal Microbiome Unique? *Front Microbiol.* 2016;7. doi:10.3389/fmicb.2016.01936
130. Friedman J, Alm EJ. Inferring Correlation Networks from Genomic Survey Data. *PLOS Computational Biology.* 2012;8: e1002687. doi:10.1371/journal.pcbi.1002687
131. Kurtz ZD, Müller CL, Miraldi ER, Littman DR, Blaser MJ, Bonneau RA. Sparse and Compositionally Robust Inference of Microbial Ecological Networks. *PLOS Computational Biology.* 2015;11: e1004226. doi:10.1371/journal.pcbi.1004226
132. Grieves M, Vickers J. Digital Twin: Mitigating Unpredictable, Undesirable Emergent Behavior in Complex Systems. In: Kahlen F-J, Flumerfelt S, Alves A, editors. *Transdisciplinary Perspectives on Complex Systems: New Findings and Approaches.* Cham: Springer International Publishing; 2017. pp. 85–113. doi:10.1007/978-3-319-38756-7_4
133. Rahmim A, Brosch-Lenz J, Fele-Paranj A, Yousefirizi F, Soltani M, Uribe C, et al. Theranostic digital twins for personalized radiopharmaceutical therapies: Reimagining theranostics via computational nuclear oncology. *Frontiers in Oncology.* 2022;12. Available: <https://www.frontiersin.org/articles/10.3389/fonc.2022.1062592>

134. Ardila D, Kiraly AP, Bharadwaj S, Choi B, Reicher JJ, Peng L, et al. End-to-end lung cancer screening with three-dimensional deep learning on low-dose chest computed tomography. *Nat Med.* 2019;25: 954–961. doi:10.1038/s41591-019-0447-x
135. Filippo MD, Damiani C, Vanoni M, Maspero D, Mauri G, Alberghina L, et al. Single-cell Digital Twins for Cancer Preclinical Investigation. In: Nagrath D, editor. *Metabolic Flux Analysis in Eukaryotic Cells: Methods and Protocols.* New York, NY: Springer US; 2020. pp. 331–343. doi:10.1007/978-1-0716-0159-4_15
136. Niederer SA, Aboelkassem Y, Cantwell CD, Corrado C, Coveney S, Cherry EM, et al. Creation and application of virtual patient cohorts of heart models. *Philosophical Transactions of the Royal Society A: Mathematical, Physical and Engineering Sciences.* 2020;378: 20190558. doi:10.1098/rsta.2019.0558
137. Mazumder O, Roy D, Bhattacharya S, Sinha A, Pal A. Synthetic PPG generation from haemodynamic model with baroreflex autoregulation: a Digital twin of cardiovascular system. 2019 41st Annual International Conference of the IEEE Engineering in Medicine and Biology Society (EMBC). 2019. pp. 5024–5029. doi:10.1109/EMBC.2019.8856691
138. An in silico twin for epicardial augmentation of the failing heart - Hirschvogel - 2019 - International Journal for Numerical Methods in Biomedical Engineering - Wiley Online Library. [cited 3 Oct 2023]. Available: <https://onlinelibrary-wiley-com.proxy.lib.umich.edu/doi/10.1002/cnm.3233>
139. Corral-Acero J, Margara F, Marciniak M, Rodero C, Loncaric F, Feng Y, et al. The ‘Digital Twin’ to enable the vision of precision cardiology. *European Heart Journal.* 2020;41: 4556–4564. doi:10.1093/eurheartj/ehaa159
140. Laubenbacher R, Sluka JP, Glazier JA. Using digital twins in viral infection. *Science.* 2021;371: 1105–1106. doi:10.1126/science.abf3370
141. Laubenbacher R, Niarakis A, Helikar T, An G, Shapiro B, Malik-Sheriff RS, et al. Building digital twins of the human immune system: toward a roadmap. *npj Digit Med.* 2022;5: 1–5. doi:10.1038/s41746-022-00610-z
142. Cen S, Gebregziabher M, Moazami S, Azevedo CJ, Pelletier D. Toward precision medicine using a “digital twin” approach: modeling the onset of disease-specific brain atrophy in individuals with multiple sclerosis. *Sci Rep.* 2023;13: 16279. doi:10.1038/s41598-023-43618-5
143. Wickramasinghe N, Ulapane N, Andargoli A, Ossai C, Shuakat N, Nguyen T, et al. Digital twins to enable better precision and personalized dementia care. *JAMIA Open.* 2022;5: ooac072. doi:10.1093/jamiaopen/ooac072
144. Voigt I, Inojosa H, Dillenseger A, Haase R, Akgün K, Ziemssen T. Digital Twins for Multiple Sclerosis. *Frontiers in Immunology.* 2021;12. Available: <https://www.frontiersin.org/articles/10.3389/fimmu.2021.669811>

145. Moingeon P, Chenel M, Rousseau C, Voisin E, Guedj M. Virtual patients, digital twins and causal disease models: Paving the ground for in silico clinical trials. *Drug Discovery Today*. 2023;28: 103605. doi:10.1016/j.drudis.2023.103605
146. Benedict KF, Lauffenburger DA. Insights into proteomic immune cell signaling and communication via data-driven modeling. *Curr Top Microbiol Immunol*. 2013;363: 201–233. doi:10.1007/82_2012_249
147. Zhou Y-H, Gallins P. A Review and Tutorial of Machine Learning Methods for Microbiome Host Trait Prediction. *Front Genet*. 2019;0. doi:10.3389/fgene.2019.00579
148. Noël-Romas L, Perner M, Molatlhegi R, Zuend CF, Mabhula A, Hoger S, et al. Vaginal microbiome-hormonal contraceptive interactions associate with the mucosal proteome and HIV acquisition. *PLOS Pathogens*. 2020;16: e1009097. doi:10.1371/journal.ppat.1009097
149. Liu J, Luo M, Zhang Y, Cao G, Wang S. Association of high-risk human papillomavirus infection duration and cervical lesions with vaginal microbiota composition. *Ann Transl Med*. 2020;8: 1161. doi:10.21037/atm-20-5832
150. Janes KA, Chandran PL, Ford RM, Lazzara MJ, Papin JA, Peirce SM, et al. An engineering design approach to systems biology. *Integr Biol (Camb)*. 2017;9: 574–583. doi:10.1039/c7ib00014f
151. Machado D, Costa RS, Rocha M, Ferreira EC, Tidor B, Rocha I. Modeling formalisms in Systems Biology. *AMB Expr*. 2011;1: 1–14. doi:10.1186/2191-0855-1-45
152. Oberhardt MA, Palsson BØ, Papin JA. Applications of genome-scale metabolic reconstructions. *Molecular Systems Biology*. 2009;5: 320. doi:10.1038/msb.2009.77
153. An G, Mi Q, Dutta-Moscato J, Vodovotz Y. Agent-based models in translational systems biology. *WIREs Systems Biology and Medicine*. 2009;1: 159–171. doi:10.1002/wsbm.45
154. Kindschuh WF, Baldini F, Liu MC, Liao J, Meydan Y, Lee HH, et al. Preterm birth is associated with xenobiotics and predicted by the vaginal metabolome. *Nat Microbiol*. 2023;8: 246–259. doi:10.1038/s41564-022-01293-8
155. Truong VT, Baverel PG, Lythe GD, Vicini P, Yates JWT, Dubois VFS. Step-by-step comparison of ordinary differential equation and agent-based approaches to pharmacokinetic-pharmacodynamic models. *CPT Pharmacometrics Syst Pharmacol*. 2022;11: 133–148. doi:10.1002/psp4.12703
156. Wang W, Hallow K, James D. A Tutorial on RxODE: Simulating Differential Equation Pharmacometric Models in R. *CPT: Pharmacometrics & Systems Pharmacology*. 2016;5: 3–10. doi:10.1002/psp4.12052
157. Nielsen EI, Cars O, Friberg LE. Pharmacokinetic/Pharmacodynamic (PK/PD) Indices of Antibiotics Predicted by a Semimechanistic PKPD Model: a Step toward Model-Based

- Dose Optimization ∇ . *Antimicrob Agents Chemother.* 2011;55: 4619–4630.
doi:10.1128/AAC.00182-11
158. Coyte KZ, Schluter J, Foster KR. The ecology of the microbiome: Networks, competition, and stability. *Science.* 2015;350: 663–666. doi:10.1126/science.aad2602
 159. Stein RR, Bucci V, Toussaint NC, Buffie CG, Räscher G, Pamer EG, et al. Ecological modeling from time-series inference: insight into dynamics and stability of intestinal microbiota. *PLoS Comput Biol.* 2013;9: e1003388. doi:10.1371/journal.pcbi.1003388
 160. Lahti L, Salojärvi J, Salonen A, Scheffer M, de Vos WM. Tipping elements in the human intestinal ecosystem. *Nat Commun.* 2014;5: 4344. doi:10.1038/ncomms5344
 161. Vos MGJ de, Zagorski M, McNally A, Bollenbach T. Interaction networks, ecological stability, and collective antibiotic tolerance in polymicrobial infections. *PNAS.* 2017;114: 10666–10671. doi:10.1073/pnas.1713372114
 162. Gibson TE, Bashan A, Cao H-T, Weiss ST, Liu Y-Y. On the Origins and Control of Community Types in the Human Microbiome. *PLOS Computational Biology.* 2016;12: e1004688. doi:10.1371/journal.pcbi.1004688
 163. Ho P-Y, Good BH, Huang KC. Competition for fluctuating resources reproduces statistics of species abundance over time across wide-ranging microbiotas. Segata N, Garrett WS, Gibbons S, editors. *eLife.* 2022;11: e75168. doi:10.7554/eLife.75168
 164. Peebles K, Velloza J, Balkus JE, McClelland RS, Barnabas RV. High Global Burden and Costs of Bacterial Vaginosis: A Systematic Review and Meta-Analysis. *Sex Transm Dis.* 2019;46: 304–311. doi:10.1097/OLQ.0000000000000972
 165. Bradshaw CS, Brotman RM. Making inroads into improving treatment of bacterial vaginosis - striving for long-term cure. *BMC Infect Dis.* 2015;15: 292. doi:10.1186/s12879-015-1027-4
 166. Xiao B, Wu C, Song W, Niu X, Qin N, Liu Z, et al. Association Analysis on Recurrence of Bacterial Vaginosis Revealed Microbes and Clinical Variables Important for Treatment Outcome. *Front Cell Infect Microbiol.* 2019;9. doi:10.3389/fcimb.2019.00189
 167. Wang B, Xiao BB, Shang CG, Wang K, Na RS, Nu XX, et al. Molecular analysis of the relationship between specific vaginal bacteria and bacterial vaginosis metronidazole therapy failure. *Eur J Clin Microbiol Infect Dis.* 2014;33: 1749–1756. doi:10.1007/s10096-014-2128-5
 168. Zhou X, Brotman RM, Gajer P, Abdo Z, Schüette U, Ma S, et al. Recent Advances in Understanding the Microbiology of the Female Reproductive Tract and the Causes of Premature Birth. In: *Infectious Diseases in Obstetrics and Gynecology* [Internet]. 2010 [cited 13 Jan 2020]. doi:10.1155/2010/737425

169. Ferreira CST, Donders GG, Parada CMG de L, Tristão A da R, Fernandes T, da Silva MG, et al. Treatment failure of bacterial vaginosis is not associated with higher loads of *Atopobium vaginae* and *Gardnerella vaginalis*. *Journal of Medical Microbiology*. 2017;66: 1217–1224. doi:10.1099/jmm.0.000561
170. Tamarelle J, Ma B, Gajer P, Humphrys MS, Terplan M, Mark KS, et al. Non-optimal vaginal microbiota after azithromycin treatment for *Chlamydia trachomatis* infection. *J Infect Dis*. 2019. doi:10.1093/infdis/jiz499
171. Vaneechoutte M. *Lactobacillus iners*, the unusual suspect. *Res Microbiol*. 2017;168: 826–836. doi:10.1016/j.resmic.2017.09.003
172. Faust K, Lahti L, Gonze D, de Vos WM, Raes J. Metagenomics meets time series analysis: unraveling microbial community dynamics. *Curr Opin Microbiol*. 2015;25: 56–66. doi:10.1016/j.mib.2015.04.004
173. Lugo-Martinez J, Ruiz-Perez D, Narasimhan G, Bar-Joseph Z. Dynamic interaction network inference from longitudinal microbiome data. *Microbiome*. 2019;7: 54. doi:10.1186/s40168-019-0660-3
174. Brotman RM, Ravel J, Cone RA, Zenilman JM. Rapid fluctuation of the vaginal microbiota measured by Gram stain analysis. *Sexually Transmitted Infections*. 2010;86: 297–302. doi:10.1136/sti.2009.040592
175. Tally FP, Goldin BR, Sullivan N, Johnston J, Gorbach SL. Antimicrobial activity of metronidazole in anaerobic bacteria. *Antimicrobial Agents and Chemotherapy*. 1978;13: 460–465. doi:10.1128/AAC.13.3.460
176. Church DL, Rabin HR, Lalshley EJ. Role of hydrogenase 1 of *Clostridium pasteurianum* in the reduction of metronidazole. *Biochemical Pharmacology*. 1988;37: 1525–1534. doi:10.1016/0006-2952(88)90014-7
177. Edwards DI. Mechanisms of selective toxicity of metronidazole and other nitroimidazole drugs. *Br J Vener Dis*. 1980;56: 285–290.
178. Ralph ED, Clarke DA. Inactivation of Metronidazole by Anaerobic and Aerobic Bacteria. *Antimicrob Agents Chemother*. 1978;14: 377–383.
179. Koch RL, Chrystal EJ, Beaulieu BB, Goldman P. Acetamide--a metabolite of metronidazole formed by the intestinal flora. *Biochem Pharmacol*. 1979;28: 3611–3615. doi:10.1016/0006-2952(79)90407-6
180. Regoes RR, Wiuff C, Zappala RM, Garner KN, Baquero F, Levin BR. Pharmacodynamic functions: a multiparameter approach to the design of antibiotic treatment regimens. *Antimicrob Agents Chemother*. 2004;48: 3670–3676. doi:10.1128/AAC.48.10.3670-3676.2004

181. Meredith HR, Andreani V, Ma HR, Lopatkin AJ, Lee AJ, Anderson DJ, et al. Applying ecological resistance and resilience to dissect bacterial antibiotic responses. *Science Advances*. 2018;4: eaau1873. doi:10.1126/sciadv.aau1873
182. Ings RM, McFadzean JA, Ormerod WE. The mode of action of metronidazole in *Trichomonas vaginalis* and other micro-organisms. *Biochem Pharmacol*. 1974;23: 1421–1429. doi:10.1016/0006-2952(74)90362-1
183. Davis B, Glover DD, Larsen B. Analysis of metronidazole penetration into vaginal fluid by reversed-phase high-performance liquid chromatography. *American Journal of Obstetrics & Gynecology*. 1984;149: 802–803. doi:10.5555/uri:pii:0002937884901303
184. Brooks JP, Buck GA, Chen G, Diao L, Edwards DJ, Fettweis JM, et al. Changes in vaginal community state types reflect major shifts in the microbiome. *Microb Ecol Health Dis*. 2017;28. doi:10.1080/16512235.2017.1303265
185. Simoes JA, Aroutcheva AA, Shott S, Faro S. Effect of metronidazole on the growth of vaginal lactobacilli in vitro. *Infect Dis Obstet Gynecol*. 2001;9: 41–45. doi:10.1155/S1064744901000072
186. De Backer E, Verhelst R, Verstraelen H, Claeys G, Verschraegen G, Temmerman M, et al. Antibiotic susceptibility of *Atopobium vaginae*. *BMC Infect Dis*. 2006;6: 51. doi:10.1186/1471-2334-6-51
187. Anukam KC, Reid G. Effects of metronidazole on growth of *Gardnerella vaginalis* ATCC 14018, probiotic *Lactobacillus rhamnosus* GR-1 and vaginal isolate *Lactobacillus plantarum* KCA. *Microbial Ecology in Health and Disease*. 2008;20: 48–52. doi:10.1080/08910600701837964
188. Buffie CG, Jarchum I, Equinda M, Lipuma L, Gobourne A, Viale A, et al. Profound Alterations of Intestinal Microbiota following a Single Dose of Clindamycin Results in Sustained Susceptibility to *Clostridium difficile*-Induced Colitis. *Infect Immun*. 2012;80: 62–73. doi:10.1128/IAI.05496-11
189. Deng Z-L, Gottschick C, Bhujji S, Masur C, Abels C, Wagner-Döbler I. Metatranscriptome Analysis of the Vaginal Microbiota Reveals Potential Mechanisms for Protection against Metronidazole in Bacterial Vaginosis. *mSphere*. 2018;3. doi:10.1128/mSphereDirect.00262-18
190. Brook I. Inoculum Effect. *Rev Infect Dis*. 1989;11: 361–368. doi:10.1093/clinids/11.3.361
191. Xiao B, Niu X, Han N, Wang B, Du P, Na R, et al. Predictive value of the composition of the vaginal microbiota in bacterial vaginosis, a dynamic study to identify recurrence-related flora. *Sci Rep*. 2016;6. doi:10.1038/srep26674
192. Verwijs MC, Agaba SK, Darby AC, Wijgert JHHM van de. Impact of oral metronidazole treatment on the vaginal microbiota and correlates of treatment failure. *American Journal of Obstetrics & Gynecology*. 2020;222: 157.e1-157.e13. doi:10.1016/j.ajog.2019.08.008

193. Allee WC. Principles of animal ecology,. Philadelphia: Saunders Co.; 1949.
194. Goswami M, Bhattacharyya P, Tribedi P. Allee effect: the story behind the stabilization or extinction of microbial ecosystem. Arch Microbiol. 2017;199: 185–190. doi:10.1007/s00203-016-1323-4
195. May R. Stability and Complexity in Model Ecosystems. 2001. Available: <https://press.princeton.edu/books/paperback/9780691088617/stability-and-complexity-in-model-ecosystems>
196. Medlock GL, Carey MA, McDuffie DG, Mundy MB, Giallourou N, Swann JR, et al. Inferring Metabolic Mechanisms of Interaction within a Defined Gut Microbiota. Cell Syst. 2018;7: 245-257.e7. doi:10.1016/j.cels.2018.08.003
197. Momeni B, Xie L, Shou W. Lotka-Volterra pairwise modeling fails to capture diverse pairwise microbial interactions. Levin B, editor. eLife. 2017;6: e25051. doi:10.7554/eLife.25051
198. Goldford JE, Lu N, Bajić D, Estrela S, Tikhonov M, Sanchez-Gorostiaga A, et al. Emergent simplicity in microbial community assembly. Science. 2018;361: 469–474. doi:10.1126/science.aat1168
199. McKendrick AG, Pai MK. XLV.—The Rate of Multiplication of Micro-organisms: A Mathematical Study. Proceedings of the Royal Society of Edinburgh. 1912;31: 649–653. doi:10.1017/S0370164600025426
200. Marino S, Hogue IB, Ray CJ, Kirschner DE. A Methodology For Performing Global Uncertainty And Sensitivity Analysis In Systems Biology. J Theor Biol. 2008;254: 178–196. doi:10.1016/j.jtbi.2008.04.011
201. Narikawa S. Distribution of metronidazole susceptibility factors in obligate anaerobes. J Antimicrob Chemother. 1986;18: 565–574. doi:10.1093/jac/18.5.565
202. Guillén H, Curiel JA, Landete JM, Muñoz R, Herraiz T. Characterization of a Nitroreductase with Selective Nitroreduction Properties in the Food and Intestinal Lactic Acid Bacterium *Lactobacillus plantarum* WCFS1. J Agric Food Chem. 2009;57: 10457–10465. doi:10.1021/jf9024135
203. Altschul SF, Koonin EV. Iterated profile searches with PSI-BLAST--a tool for discovery in protein databases. Trends Biochem Sci. 1998;23: 444–447. doi:10.1016/s0968-0004(98)01298-5
204. Juárez Tomás MS, Ocaña VS, Wiese B, Nader-Macías ME. Growth and lactic acid production by vaginal *Lactobacillus acidophilus* CRL 1259, and inhibition of uropathogenic *Escherichia coli*. J Med Microbiol. 2003;52: 1117–1124. doi:10.1099/jmm.0.05155-0

205. Gause GF. Experimental Demonstration of Volterra's Periodic Oscillations in the Numbers of Animals. *Journal of Experimental Biology*. 1935;12: 44–48.
206. Jackman CM, Deans KW, Forney LJ, Lin XN. Microdroplet co-cultivation and interaction characterization of human vaginal bacteria. *Int Bio (Cam)*. 2019;11: 69–78. doi:10.1093/intbio/zyz006
207. CDC - STD Treatment. 8 Sep 2020 [cited 16 Oct 2020]. Available: <https://www.cdc.gov/std/treatment/default.htm>
208. McKinnon LR, Achilles SL, Bradshaw CS, Burgener A, Crucitti T, Fredricks DN, et al. The Evolving Facets of Bacterial Vaginosis: Implications for HIV Transmission. *AIDS Res Hum Retroviruses*. 2019;35: 219–228. doi:10.1089/aid.2018.0304
209. Campisciano G, Florian F, D'Eustacchio A, Stanković D, Ricci G, Seta FD, et al. Subclinical alteration of the cervical–vaginal microbiome in women with idiopathic infertility. *Journal of Cellular Physiology*. 2017;232: 1681–1688. doi:10.1002/jcp.25806
210. Myer L, Denny L, Telerant R, Souza M de, Wright TC, Kuhn L. Bacterial vaginosis and susceptibility to HIV infection in South African women: a nested case-control study. *J Infect Dis*. 2005;192: 1372–1380. doi:10.1086/462427
211. Hirota M, Holmgren M, Van Nes EH, Scheffer M. Global Resilience of Tropical Forest and Savanna to Critical Transitions. *Science*. 2011;334: 232–235. doi:10.1126/science.1210657
212. Scheffer M, Hosper SH, Meijer M-L, Moss B, Jeppesen E. Alternative equilibria in shallow lakes. *Trends in Ecology & Evolution*. 1993;8: 275–279. doi:10.1016/0169-5347(93)90254-M
213. Witkin SS, Mendes-Soares H, Linhares IM, Jayaram A, Ledger WJ, Forney LJ. Influence of vaginal bacteria and D- and L-lactic acid isomers on vaginal extracellular matrix metalloproteinase inducer: implications for protection against upper genital tract infections. *mBio*. 2013;4: e00460-13. doi:10.1128/mBio.00460-13
214. Munoz AR. Markov-Based Model of Cervicovaginal Bacterial Dynamics Predicts Community Equilibrium States in Young South African Women. 2018 [cited 1 Jul 2021]. Available: <https://dash.harvard.edu/handle/1/38811553>
215. Estrela S, Brown SP. Community interactions and spatial structure shape selection on antibiotic resistant lineages. *PLoS Comput Biol*. 2018;14. doi:10.1371/journal.pcbi.1006179
216. Parijs I, Steenackers HP. Competitive inter-species interactions underlie the increased antimicrobial tolerance in multispecies brewery biofilms. *ISME J*. 2018;12: 2061–2075. doi:10.1038/s41396-018-0146-5

217. Schuyler JA, Mordechai E, Adelson ME, Sobel JD, Gyax SE, Hilbert DW. Identification of intrinsically metronidazole-resistant clades of *Gardnerella vaginalis*. *Diagnostic Microbiology and Infectious Disease*. 2016;84: 1–3. doi:10.1016/j.diagmicrobio.2015.10.006
218. Bucci V, Tzen B, Li N, Simmons M, Tanoue T, Bogart E, et al. MDSINE: Microbial Dynamical Systems INference Engine for microbiome time-series analyses. *Genome Biol*. 2016;17: 121. doi:10.1186/s13059-016-0980-6
219. Remien CH, Eckwright MJ, Ridenhour BJ. Structural identifiability of the generalized Lotka-Volterra model for microbiome studies. *R Soc Open Sci*. 2021;8: 201378. doi:10.1098/rsos.201378
220. Gustin AT, Thurman AR, Chandra N, Schifanella L, Alcaide M, Fichorova R, et al. Recurrent bacterial vaginosis following metronidazole treatment is associated with microbiota richness at diagnosis. *Am J Obstet Gynecol*. 2022;226: 225.e1-225.e15. doi:10.1016/j.ajog.2021.09.018
221. Mayer BT, Srinivasan S, Fiedler TL, Marrazzo JM, Fredricks DN, Schiffer JT. Rapid and Profound Shifts in the Vaginal Microbiota Following Antibiotic Treatment for Bacterial Vaginosis. *J Infect Dis*. 2015;212: 793–802. doi:10.1093/infdis/jiv079
222. Aguin T, Akins RA, Sobel JD. High-Dose Vaginal Maintenance Metronidazole for Recurrent Bacterial Vaginosis: A Pilot Study. *Sexually Transmitted Diseases*. 2014;41: 290–291. doi:10.1097/OLQ.0000000000000123
223. Reichman O, Akins R, Sobel JD. Boric Acid Addition to Suppressive Antimicrobial Therapy for Recurrent Bacterial Vaginosis. *Sexually Transmitted Diseases*. 2009;36: 732–734. doi:10.1097/OLQ.0b013e3181b08456
224. Schwebke J, Carter B, Waldbaum A, Price C, Castellarnau A, Paull J, et al. Results of a phase 3, randomized, double-blind, placebo-controlled study to evaluate the efficacy and safety of astodrimer gel for prevention of recurrent bacterial vaginosis. *American Journal of Obstetrics and Gynecology*. 2019;221: 672–673. doi:10.1016/j.ajog.2019.10.087
225. Surapaneni S, Akins R, Sobel JD. Recurrent Bacterial Vaginosis: An Unmet Therapeutic Challenge. Experience With a Combination Pharmacotherapy Long-Term Suppressive Regimen. *Sex Transm Dis*. 2021;48: 761–765. doi:10.1097/OLQ.0000000000001420
226. Boskey ER, Telsch KM, Whaley KJ, Moench TR, Cone RA. Acid Production by Vaginal Flora In Vitro Is Consistent with the Rate and Extent of Vaginal Acidification. *Infect Immun*. 1999;67: 5170–5175.
227. Macklaim JM, Fernandes AD, Di Bella JM, Hammond J-A, Reid G, Gloor GB. Comparative meta-RNA-seq of the vaginal microbiota and differential expression by *Lactobacillus iners* in health and dysbiosis. *Microbiome*. 2013;1: 12. doi:10.1186/2049-2618-1-12

228. Antonio MAD, Meyn LA, Murray PJ, Busse B, Hillier SL. Vaginal colonization by probiotic *Lactobacillus crispatus* CTV-05 is decreased by sexual activity and endogenous Lactobacilli. *J Infect Dis*. 2009;199: 1506–1513. doi:10.1086/598686
229. Dubinkina V, Fridman Y, Pandey PP, Maslov S. Multistability and regime shifts in microbial communities explained by competition for essential nutrients. Shou W, Baldwin IT, Shou W, editors. *eLife*. 2019;8: e49720. doi:10.7554/eLife.49720
230. Tomás MSJ, Nader-Macías ME. Effect of a medium simulating vaginal fluid on the growth and expression of beneficial characteristics of potentially probiotic lactobacilli. *Communicating Current Research and Educational Topics and Trends in Applied Microbiology*,. 2007; 8.
231. Shishpal P, Patel V, Singh D, Bhor VM. pH Stress Mediated Alteration in Protein Composition and Reduction in Cytotoxic Potential of *Gardnerella vaginalis* Membrane Vesicles. *Front Microbiol*. 2021;12: 723909. doi:10.3389/fmicb.2021.723909
232. Breshears LM, Edwards VL, Ravel J, Peterson ML. *Lactobacillus crispatus* inhibits growth of *Gardnerella vaginalis* and *Neisseria gonorrhoeae* on a porcine vaginal mucosa model. *BMC Microbiol*. 2015;15. doi:10.1186/s12866-015-0608-0
233. Agnew KJ, Hillier SL. The effect of treatment regimens for vaginitis and cervicitis on vaginal colonization by lactobacilli. *Sex Transm Dis*. 1995;22: 269–273. doi:10.1097/00007435-199509000-00001
234. Ahrens P, Andersen LO, Lilje B, Johannesen TB, Dahl EG, Baig S, et al. Changes in the vaginal microbiota following antibiotic treatment for *Mycoplasma genitalium*, *Chlamydia trachomatis* and bacterial vaginosis. *PLoS One*. 2020;15: e0236036. doi:10.1371/journal.pone.0236036
235. Gosmann C, Anahtar MN, Handley SA, Farcasanu M, Abu-Ali G, Bowman BA, et al. *Lactobacillus*-Deficient Cervicovaginal Bacterial Communities Are Associated with Increased HIV Acquisition in Young South African Women. *Immunity*. 2017;46: 29–37. doi:10.1016/j.immuni.2016.12.013
236. Shannon B, Yi TJ, Perusini S, Gajer P, Ma B, Humphrys MS, et al. Association of HPV infection and clearance with cervicovaginal immunology and the vaginal microbiota. *Mucosal Immunology*. 2017;10: 1310–1319. doi:10.1038/mi.2016.129
237. Brown RG, Al-Memar M, Marchesi JR, Lee YS, Smith A, Chan D, et al. Establishment of vaginal microbiota composition in early pregnancy and its association with subsequent preterm prelabor rupture of the fetal membranes. *Translational Research*. 2019;207: 30–43. doi:10.1016/j.trsl.2018.12.005
238. Sobel JD, Ferris D, Schwebke J, Nyirjesy P, Wiesenfeld HC, Peipert J, et al. Suppressing antibacterial therapy with 0.75% metronidazole vaginal gel to prevent recurrent bacterial vaginosis. *American Journal of Obstetrics and Gynecology*. 2006;194: 1283–1289. doi:10.1016/j.ajog.2005.11.041

239. Dausset C, Patrier S, Gajer P, Thorat C, Lenglet Y, Cardot J-M, et al. Comparative phase I randomized open-label pilot clinical trial of Gynophilus® (Lcr regenerans®) immediate release capsules versus slow release muco-adhesive tablets. *Eur J Clin Microbiol Infect Dis*. 2018;37: 1869–1880. doi:10.1007/s10096-018-3321-8
240. Happel A-U, Singh R, Mitchev N, Mlisana K, Jaspan HB, Barnabas SL, et al. Testing the regulatory framework in South Africa – a single-blind randomized pilot trial of commercial probiotic supplementation to standard therapy in women with bacterial vaginosis. *BMC Infect Dis*. 2020;20: 1–13. doi:10.1186/s12879-020-05210-4
241. Mastromarino P, Macchia S, Meggiorini L, Trinchieri V, Mosca L, Perluigi M, et al. Effectiveness of Lactobacillus-containing vaginal tablets in the treatment of symptomatic bacterial vaginosis. *Clinical Microbiology and Infection*. 2009;15: 67–74. doi:10.1111/j.1469-0691.2008.02112.x
242. van de Wijgert JHHM, Verwijs MC, Agaba SK, Bronowski C, Mwambarangwe L, Uwineza M, et al. Intermittent Lactobacilli-containing Vaginal Probiotic or Metronidazole Use to Prevent Bacterial Vaginosis Recurrence: A Pilot Study Incorporating Microscopy and Sequencing. *Sci Rep*. 2020;10: 3884. doi:10.1038/s41598-020-60671-6
243. Lee CY, Diegel J, France MT, Ravel J, Arnold KB. Evaluation of vaginal microbiome equilibrium states identifies microbial parameters linked to resilience after menses and antibiotic therapy. *PLOS Computational Biology*. 2023;19: e1011295. doi:10.1371/journal.pcbi.1011295
244. Tachedjian G, Aldunate M, Bradshaw CS, Cone RA. The role of lactic acid production by probiotic Lactobacillus species in vaginal health. *Research in Microbiology*. 2017;168: 782–792. doi:10.1016/j.resmic.2017.04.001
245. Turovskiy Y, Ludescher RD, Aroutcheva AA, Faro S, Chikindas ML. Lactocin 160, a Bacteriocin Produced by Vaginal Lactobacillus rhamnosus, Targets Cytoplasmic Membranes of the Vaginal Pathogen, Gardnerella vaginalis. *Probiotics Antimicrob Proteins*. 2009;1: 67–74. doi:10.1007/s12602-008-9003-6
246. Blackburn TM, Pyšek P, Bacher S, Carlton JT, Duncan RP, Jarošík V, et al. A proposed unified framework for biological invasions. *Trends Ecol Evol*. 2011;26: 333–339. doi:10.1016/j.tree.2011.03.023
247. Kurkjian HM, Akbari MJ, Momeni B. The impact of interactions on invasion and colonization resistance in microbial communities. *PLOS Computational Biology*. 2021;17: e1008643. doi:10.1371/journal.pcbi.1008643
248. DiGiulio DB, Callahan BJ, McMurdie PJ, Costello EK, Lyell DJ, Robaczewska A, et al. Temporal and spatial variation of the human microbiota during pregnancy. *PNAS*. 2015;112: 11060–11065.
249. Fettweis JM, Brooks JP, Serrano MG, Sheth NU, Girerd PH, Edwards DJ, et al. Differences in vaginal microbiome in African American women versus women of

- European ancestry. *Microbiology (Reading)*. 2014;160: 2272–2282.
doi:10.1099/mic.0.081034-0
250. Klebanoff MA, Nansel TR, Brotman RM, Zhang J, Yu K-F, Schwebke JR, et al. Personal hygienic behaviors and bacterial vaginosis. *Sex Transm Dis*. 2010;37: 94–99.
doi:10.1097/OLQ.0b013e3181bc063c
251. Monod J. The growth of bacterial cultures. *Annu Rev Microbiol*. 1949;3: 371–394.
doi:10.1146/annurev.mi.03.100149.002103
252. GOEL NS, MAITRA SC, MONTROLL EW. On the Volterra and Other Nonlinear Models of Interacting Populations. *Rev Mod Phys*. 1971;43: 231–276.
doi:10.1103/RevModPhys.43.231
253. May RM. Stability in multispecies community models. *Mathematical Biosciences*. 1971;12: 59–79. doi:10.1016/0025-5564(71)90074-5
254. Mollin A, Katta M, Sobel JD, Akins RA. Association of key species of vaginal bacteria of recurrent bacterial vaginosis patients before and after oral metronidazole therapy with short- and long-term clinical outcomes. *PLOS ONE*. 2022;17: e0272012.
doi:10.1371/journal.pone.0272012
255. Zhou R, Lu J, Wang J, Xiao B. Vaginal *Lactobacillus iners* abundance is associated with outcome in antibiotic treatment of bacterial vaginosis and capable of inhibiting *Gardnerella*. *Frontiers in Cellular and Infection Microbiology*. 2022;12. Available: <https://www.frontiersin.org/articles/10.3389/fcimb.2022.1033431>
256. Turner E, Sobel JD, Akins RA. Prognosis of recurrent bacterial vaginosis based on longitudinal changes in abundance of *Lactobacillus* and specific species of *Gardnerella*. *PLoS One*. 2021;16: e0256445. doi:10.1371/journal.pone.0256445
257. Armstrong E, Hemmerling A, Joag V, Huibner S, Kulikova M, Crawford E, et al. Treatment Success Following Standard Antibiotic Treatment for Bacterial Vaginosis Is Not Associated With Pretreatment Genital Immune or Microbial Parameters. *Open Forum Infectious Diseases*. 2023;10: ofad007. doi:10.1093/ofid/ofad007
258. Castro J, Machado D, Cerca N. Unveiling the role of *Gardnerella vaginalis* in polymicrobial Bacterial Vaginosis biofilms: the impact of other vaginal pathogens living as neighbors. *The ISME Journal*. 2019;13: 1306–1317. doi:10.1038/s41396-018-0337-0
259. Hoiby N, Bjarnsholt T, Givskov M, Molin S, Ciofu O. Antibiotic resistance of bacterial biofilms. *Int J Antimicrob Agents*. 2010;35: 322–332.
doi:10.1016/j.ijantimicag.2009.12.011
260. Patterson JL, Girerd PH, Karjane NW, Jefferson KK. Effect of biofilm phenotype on resistance of *Gardnerella vaginalis* to hydrogen peroxide and lactic acid. *Am J Obstet Gynecol*. 2007;197: 170.e1–7. doi:10.1016/j.ajog.2007.02.027

261. Scheffer M, Carpenter SR. Catastrophic regime shifts in ecosystems: linking theory to observation. *Trends in Ecology & Evolution*. 2003;18: 648–656. doi:10.1016/j.tree.2003.09.002
262. Nyström M, Folke C, Moberg F. Coral reef disturbance and resilience in a human-dominated environment. *Trends in Ecology & Evolution*. 2000;15: 413–417. doi:10.1016/S0169-5347(00)01948-0
263. Scheffer M, Szabó S, Gragnani A, van Nes EH, Rinaldi S, Kautsky N, et al. Floating plant dominance as a stable state. *Proceedings of the National Academy of Sciences*. 2003;100: 4040–4045. doi:10.1073/pnas.0737918100
264. Gonze D, Lahti L, Raes J, Faust K. Multi-stability and the origin of microbial community types. *The ISME Journal*. 2017;11: 2159–2166. doi:10.1038/ismej.2017.60
265. Wright ES, Gupta R, Vetsigian KH. Multi-stable bacterial communities exhibit extreme sensitivity to initial conditions. *FEMS Microbiology Ecology*. 2021;97: fiab073. doi:10.1093/femsec/fiab073
266. Tropini C, Moss EL, Merrill BD, Ng KM, Higginbottom SK, Casavant EP, et al. Transient Osmotic Perturbation Causes Long-Term Alteration to the Gut Microbiota. *Cell*. 2018;173: 1742-1754.e17. doi:10.1016/j.cell.2018.05.008
267. McCracken JM, Calderon GA, Robinson AJ, Sullivan CN, Cosgriff-Hernandez E, Hakim JCE. Animal Models and Alternatives in Vaginal Research: a Comparative Review. *Reprod Sci*. 2021;28: 1759–1773. doi:10.1007/s43032-021-00529-y
268. Gadkar K, Kirouac D, Mager D, van der Graaf P, Ramanujan S. A Six-Stage Workflow for Robust Application of Systems Pharmacology. *CPT: Pharmacometrics & Systems Pharmacology*. 2016;5: 235–249. doi:10.1002/psp4.12071
269. Allen R, Rieger T, Musante C. Efficient Generation and Selection of Virtual Populations in Quantitative Systems Pharmacology Models. *CPT Pharmacometrics Syst Pharmacol*. 2016;5: 140–146. doi:10.1002/psp4.12063
270. Rodríguez-Gascón A, Solinís MÁ, Isla A. The Role of PK/PD Analysis in the Development and Evaluation of Antimicrobials. *Pharmaceutics*. 2021;13: 833. doi:10.3390/pharmaceutics13060833
271. Cheng Y, Straube R, Alnaif AE, Huang L, Leil TA, Schmidt BJ. Virtual Populations for Quantitative Systems Pharmacology Models. In: Bai JPF, Hur J, editors. *Systems Medicine*. New York, NY: Springer US; 2022. pp. 129–179. doi:10.1007/978-1-0716-2265-0_8
272. Pino A, Bartolo E, Caggia C, Cianci A, Randazzo CL. Detection of vaginal lactobacilli as probiotic candidates. *Sci Rep*. 2019;9: 3355. doi:10.1038/s41598-019-40304-3

273. Ravel J, Brotman RM. Translating the vaginal microbiome: gaps and challenges. *Genome Medicine*. 2016;8: 35. doi:10.1186/s13073-016-0291-2
274. Liao C, Wang T, Maslov S, Xavier JB. Modeling microbial cross-feeding at intermediate scale portrays community dynamics and species coexistence. *PLOS Computational Biology*. 2020;16: e1008135. doi:10.1371/journal.pcbi.1008135
275. Navarro S, Abla H, Delgado B, Colmer-Hamood JA, Ventolini G, Hamood AN. Glycogen availability and pH variation in a medium simulating vaginal fluid influence the growth of vaginal *Lactobacillus* species and *Gardnerella vaginalis*. *BMC Microbiology*. 2023;23: 186. doi:10.1186/s12866-023-02916-8
276. Bhandari P, Tingley J, Abbott DW, Hill JE. Glycogen-Degrading Activities of Catalytic Domains of α -Amylase and α -Amylase-Pullulanase Enzymes Conserved in *Gardnerella* spp. from the Vaginal Microbiome. *J Bacteriol*. 2023;205: e0039322. doi:10.1128/jb.00393-22
277. Spear GT, French AL, Gilbert D, Zariffard MR, Mirmonsef P, Sullivan TH, et al. Human α -amylase Present in Lower-Genital-Tract Mucosal Fluid Processes Glycogen to Support Vaginal Colonization by *Lactobacillus*. *The Journal of Infectious Diseases*. 2014;210: 1019–1028. doi:10.1093/infdis/jiu231
278. Nelson TM, Borgogna J-LC, Brotman RM, Ravel J, Walk ST, Yeoman CJ. Vaginal biogenic amines: biomarkers of bacterial vaginosis or precursors to vaginal dysbiosis? *Front Physiol*. 2015;6: 253. doi:10.3389/fphys.2015.00253
279. Vitali B, Cruciani F, Picone G, Parolin C, Donders G, Laghi L. Vaginal microbiome and metabolome highlight specific signatures of bacterial vaginosis. *Eur J Clin Microbiol Infect Dis*. 2015;34: 2367–2376. doi:zh
280. Rose WA, McGowin CL, Spagnuolo RA, Eaves-Pyles TD, Popov VL, Pyles RB. Commensal bacteria modulate innate immune responses of vaginal epithelial cell multilayer cultures. *PLoS One*. 2012;7: e32728. doi:10.1371/journal.pone.0032728
281. Ma B, Forney LJ, Ravel J. The vaginal microbiome: rethinking health and diseases. *Annu Rev Microbiol*. 2012;66: 371–389. doi:10.1146/annurev-micro-092611-150157
282. Amabebe E, Anumba DOC. Mechanistic Insights into Immune Suppression and Evasion in Bacterial Vaginosis. *Curr Microbiol*. 2022;79: 84. doi:10.1007/s00284-022-02771-2
283. Faught BM, Reyes S. Characterization and Treatment of Recurrent Bacterial Vaginosis. *Journal of Women's Health*. 2019;28: 1218–1226. doi:10.1089/jwh.2018.7383
284. Gottschick C, Szafranski SP, Kunze B, Sztajer H, Masur C, Abels C, et al. Screening of Compounds against *Gardnerella vaginalis* Biofilms. *PLoS One*. 2016;11: e0154086. doi:10.1371/journal.pone.0154086

285. Hardy L, Jespers V, Dahchour N, Mwambarangwe L, Musengamana V, Vaneechoutte M, et al. Unravelling the Bacterial Vaginosis-Associated Biofilm: A Multiplex Gardnerella vaginalis and Atopobium vaginae Fluorescence In Situ Hybridization Assay Using Peptide Nucleic Acid Probes. *PLoS One*. 2015;10. doi:10.1371/journal.pone.0136658
286. Venturelli OS, Carr AC, Fisher G, Hsu RH, Lau R, Bowen BP, et al. Deciphering microbial interactions in synthetic human gut microbiome communities. *Mol Syst Biol*. 2018;14: e8157. doi:10.15252/msb.20178157
287. Goltsman DSA, Sun CL, Proctor DM, DiGiulio DB, Robaczewska A, Thomas BC, et al. Metagenomic analysis with strain-level resolution reveals fine-scale variation in the human pregnancy microbiome. *Genome Res*. 2018;28: 1467–1480. doi:10.1101/gr.236000.118
288. Segel LA. *Mathematical Models in Biology* (Leah Edelstein-Keshet). *SIAM Rev*. 1988;30: 679–680. doi:10.1137/1030168
289. MacArthur R. Species packing and competitive equilibrium for many species. *Theoretical Population Biology*. 1970;1: 1–11. doi:10.1016/0040-5809(70)90039-0
290. Biggs MB, Medlock GL, Moutinho TJ, Lees HJ, Swann JR, Kolling GL, et al. Systems-level metabolism of the altered Schaedler flora, a complete gut microbiota. *ISME J*. 2017;11: 426–438. doi:10.1038/ismej.2016.130
291. Magnúsdóttir S, Heinken A, Kutt L, Ravcheev DA, Bauer E, Noronha A, et al. Generation of genome-scale metabolic reconstructions for 773 members of the human gut microbiota. *Nat Biotechnol*. 2017;35: 81–89. doi:10.1038/nbt.3703
292. Singh R, Dutta A, Bose T, Mande SS. A compendium of predicted growths and derived symbiotic relationships between 803 gut microbes in 13 different diets. *Curr Res Microb Sci*. 2022;3: 100127. doi:10.1016/j.crmicr.2022.100127
293. Baldini F, Heinken A, Heirendt L, Magnusdottir S, Fleming RMT, Thiele I. The Microbiome Modeling Toolbox: from microbial interactions to personalized microbial communities. *Bioinformatics*. 2019;35: 2332–2334. doi:10.1093/bioinformatics/bty941
294. Heinken A, Hertel J, Acharya G, Ravcheev DA, Nyga M, Okpala OE, et al. Genome-scale metabolic reconstruction of 7,302 human microorganisms for personalized medicine. *Nat Biotechnol*. 2023; 1–12. doi:10.1038/s41587-022-01628-0
295. Zhuang K, Izallalen M, Mouser P, Richter H, Risso C, Mahadevan R, et al. Genome-scale dynamic modeling of the competition between *Rhodospirillum rubrum* and *Geobacter* in anoxic subsurface environments. *The ISME Journal*. 2011;5: 305–316. doi:10.1038/ismej.2010.117
296. Khazaei T, Williams RL, Bogatyrev SR, Doyle JC, Henry CS, Ismagilov RF. Metabolic multistability and hysteresis in a model aerobe-anaerobe microbiome community. *Science Advances*. 6: eaba0353. doi:10.1126/sciadv.aba0353

297. Brunner JD, Chia N. Metabolic Model-based Ecological Modeling for Probiotic Design. arXiv; 2022. doi:10.48550/arXiv.2210.03198
298. Huang S, Jiang S, Huo D, Allaband C, Estaki M, Cantu V, et al. Candidate probiotic *Lactiplantibacillus plantarum* HNU082 rapidly and convergently evolves within human, mice, and zebrafish gut but differentially influences the resident microbiome. *Microbiome*. 2021;9: 1–17. doi:10.1186/s40168-021-01102-0
299. Battaglioli EJ, Hale VL, Chen J, Jeraldo P, Ruiz-Mojica C, Schmidt BA, et al. *Clostridioides difficile* uses amino acids associated with gut microbial dysbiosis in a subset of patients with diarrhea. *Sci Transl Med*. 2018;10: eaam7019. doi:10.1126/scitranslmed.aam7019
300. Maldonado-Gómez MX, Martínez I, Bottacini F, O’Callaghan A, Ventura M, van Sinderen D, et al. Stable Engraftment of *Bifidobacterium longum* AH1206 in the Human Gut Depends on Individualized Features of the Resident Microbiome. *Cell Host Microbe*. 2016;a: 515–526. doi:10.1016/j.chom.2016.09.001
301. Dillard LR, Glass EM, Lewis AL, Thomas-White K, Papin JA. Metabolic Network Models of the *Gardnerella* Pangenome Identify Key Interactions with the Vaginal Environment. *mSystems*. 2022;8: e00689-22. doi:10.1128/msystems.00689-22
302. Shirsat N, Mohd A, Whelan J, English NJ, Glennon B, Al-Rubeai M. Revisiting Verhulst and Monod models: analysis of batch and fed-batch cultures. *Cytotechnology*. 2015;67: 515–530. doi:10.1007/s10616-014-9712-5
303. Hertzberger R, Himschoot L, Bruisten S, Steenbergen L, Lewis W, Cools P, et al. Bacterial vaginosis is associated with increased amylolytic activity. 2023. doi:10.1101/2023.01.28.526025
304. Marsland R, Cui W, Mehta P. A minimal model for microbial biodiversity can reproduce experimentally observed ecological patterns. *Sci Rep*. 2020;10: 3308. doi:10.1038/s41598-020-60130-2
305. Anahtar MN, Byrne EH, Doherty KE, Bowman BA, Yamamoto HS, Soumillon M, et al. Cervicovaginal Bacteria Are a Major Modulator of Host Inflammatory Responses in the Female Genital Tract. *Immunity*. 2015;42: 965–976. doi:10.1016/j.immuni.2015.04.019
306. Iguchi T, Uchima FD, Ostrander PL, Bern HA. Growth of normal mouse vaginal epithelial cells in and on collagen gels. *Proc Natl Acad Sci U S A*. 1983;80: 3743–3747.
307. Pleckaityte M. Cholesterol-Dependent Cytolysins Produced by Vaginal Bacteria: Certainties and Controversies. *Frontiers in Cellular and Infection Microbiology*. 2020;9. Available: <https://www.frontiersin.org/articles/10.3389/fcimb.2019.00452>
308. Castro J, França A, Bradwell KR, Serrano MG, Jefferson KK, Cerca N. Comparative transcriptomic analysis of *Gardnerella vaginalis* biofilms vs. planktonic cultures using RNA-seq. *npj Biofilms Microbiomes*. 2017;3: 1–7. doi:10.1038/s41522-017-0012-7

309. Castro J, Martins AP, Rodrigues ME, Cerca N. *Lactobacillus crispatus* represses vaginolysin expression by BV associated *Gardnerella vaginalis* and reduces cell cytotoxicity. *Anaerobe*. 2018;50: 60–63. doi:10.1016/j.anaerobe.2018.01.014
310. Happel A-U, Kullin B, Gamielien H, Wentzel N, Zauchenberger CZ, Jaspan HB, et al. Exploring potential of vaginal *Lactobacillus* isolates from South African women for enhancing treatment for bacterial vaginosis. *PLoS Pathog*. 2020;16: e1008559. doi:10.1371/journal.ppat.1008559
311. Juárez Tomás MS, Ocaña VS, Wiese B, Nader-Macías ME. Growth and lactic acid production by vaginal *Lactobacillus acidophilus* CRL 1259, and inhibition of uropathogenic *Escherichia coli*. *J Med Microbiol*. 2003;52: 1117–1124. doi:10.1099/jmm.0.05155-0
312. Santos CMA, Pires MCV, Leão TL, Hernández ZP, Rodriguez ML, Martins AKS, et al. Selection of *Lactobacillus* strains as potential probiotics for vaginitis treatment. *Microbiology*. 2016;162: 1195–1207. doi:10.1099/mic.0.000302
313. Abdelmaksoud AA, Koparde VN, Sheth NU, Serrano MG, Glascock AL, Fettweis JM, et al. Comparison of *Lactobacillus crispatus* isolates from *Lactobacillus*-dominated vaginal microbiomes with isolates from microbiomes containing bacterial vaginosis-associated bacteria. *Microbiology*. 2016;162: 466–475. doi:10.1099/mic.0.000238
314. De Gregorio PR, Tomás MSJ, Terraf MCL, Nader-Macías MEF. In vitro and in vivo effects of beneficial vaginal lactobacilli on pathogens responsible for urogenital tract infections. *J Med Microbiol*. 2014;63: 685–696. doi:10.1099/jmm.0.069401-0
315. Passos FV, Fleming HP, Ollis DF, Hassan HM, Felder RM. Modeling the specific growth rate of *Lactobacillus plantarum* in cucumber extract. *Appl Microbiol Biotechnol*. 1993;40: 143–150. doi:10.1007/BF00170443
316. Hertzberger R, Himschoot L, Bruisten S, Steenbergen L, Lewis W, Cools P, et al. Bacterial vaginosis is associated with increased amylolytic activity. *bioRxiv*; 2023. p. 2023.01.28.526025. doi:10.1101/2023.01.28.526025
317. O’Hanlon DE, Gajer P, Brotman RM, Ravel J. Asymptomatic Bacterial Vaginosis Is Associated With Depletion of Mature Superficial Cells Shed From the Vaginal Epithelium. *Frontiers in Cellular and Infection Microbiology*. 2020;10. Available: <https://www.frontiersin.org/articles/10.3389/fcimb.2020.00106>
318. Nielsen EI, Viberg A, Löwdin E, Cars O, Karlsson MO, Sandström M. Semimechanistic Pharmacokinetic/Pharmacodynamic Model for Assessment of Activity of Antibacterial Agents from Time-Kill Curve Experiments. *Antimicrob Agents Chemother*. 2007;51: 128–136. doi:10.1128/AAC.00604-06
319. Wanner O, Reichert P. Mathematical modeling of mixed-culture biofilms. *Biotechnol Bioeng*. 1996;49: 172–184. doi:10.1002/(SICI)1097-0290(19960120)49:2<172::AID-BIT6>3.0.CO;2-N